Die Rolle von Chemokinen
bei der Rekrutierung von Leukozyten
durch die Blut-Hirn-Schranke

Carsten Alt

aus Friedberg / Hessen

From the

Max-Planck Institute for Clinical and Physiological Research /

Kerckhoff Institute, Bad Nauheim

Director: Prof. Dr. Werner Risau †

and

Max-Planck Institute for Vascular Biology, Münster

Director: Prof. Dr. Dietmar Vestweber

The Role of Chemokines

in Leukocyte Recruitment

across the Blood-Brain Barrier

Inaugural-Dissertation to obtain the degree of Doctor of Human Biology

submitted to the Faculty of Medicine at the Philipps-University Marburg by

Carsten Alt

from Friedberg / Hessen

Marburg 2003

iv

Contents

Chapter 1

Introduction

The highly sophisticated network of cooperating neurons within the central nervous system (CNS) requires stringent homeostasis of its environment for proper function. This homeostasis is maintained by the endothelial blood-brain barrier (BBB), which protects the CNS from the changing milieu of the bloodstream by strictly limiting passage of molecules and cells. However, another highly sophisticated network of cells, which composes the immune system, requires trafficking of its cellular components through the whole organism to guarantee immunosurveillance. Trafficking of lymphocytes from the bloodstream into tissues is not random, but strictly regulated. Taken together, the necessity of stringent regulation of the CNS micromilieu on the one hand and immunosurveillance on the other hand suggests unique mechanisms for lymphocyte recruitment across the endothelial BBB into the CNS.

1.1 The blood-brain barrier

Normal function of neurons within the brain and spinal cord requires a homeostatic microenvironment, which is maintained by the blood-brain barrier. However, the high metabolic needs of CNS tissue demand a close connection to the bloodstream to mediate transport of nutrients into the CNS and toxic metabolites out of the CNS.

The barrier between the blood and the brain was discovered in the early 20th century. Paul Ehrlich described the way in which intravenously injected dyes could be detected in all organs but the CNS (Ehrlich, 1904). However, while he interpreted these findings as a lack of affinity of the CNS for these dyes, his fellow

researcher Goldmann modified the experiment and injected the same dyes into the cerebrospinal fluid. In that way, CNS tissue was stained while peripheral organs kept unstained (Goldmann, 1913). Goldmann concluded that there must be a dye-impermeable blood-brain barrier, which also serves as a functional brain-blood barrier. Although this compartmentalization of the brain was described that early, decades passed before Reese and Karnovsky could structurally describe the BBB (Reese and Karnovsky, 1967). Enhancing the procedures established by Ehrlich and Goldmann, they injected horseradish peroxidase intravenously, which could be visualized by electron microscopy. Diffusion of horseradish peroxidase from the bloodstream into the CNS was limited by special endothelial cell-to-cell contacts, the tight junctions (TJ). Therefore, interendothelial TJ are the morphological correlate of the BBB. In addition, BBB endothelial cells contain few if any pinocytotic vesicles, thereby strictly limiting diffusion of hydrophilic substances from the bloodstream to the CNS parenchyma and vice versa, which results in a high transelectrical resistance (Crone and Olesen, 1982). However, specialized transport mechanisms guarantee specific exchange of metabolites between the bloodstream and the CNS parenchyma.

TJ at the blood-brain barrier endothelium have been demonstrated to be more complex than TJ of other endothelial cells in the body. While complexity of the strands is one feature of the tight junctional network, association of the TJ particles with the protoplasmic leaflet (P-face) or the exoplasmic leaflet (E-face) of the membrane is another criterion to correlate their morphology and physiology. TJ particles of BBB endothelial cells remain mostly at the P-face, in contrast to other endothelial cells (Wolburg et al., 1994). This suggests a special cytoplasmic anchorage of TJ associated proteins to the cytoskeleton. Occludin and claudins seem to be specifically located within TJ particles (Tsukita and Furuse, 1998; Morita et al., 1999). Of the to-date more than 20 members of the claudin gene-family, claudin-3 and claudin-5 are localized within human and mouse endothelial cells within the CNS (Wolburg et al., 2003). Functionally, loss of claudin-5 has recently been shown to result in size-selective loosening of the BBB *in vivo*, suggesting a loss of TJ consistency (Nitta et al., 2003).

Development of the cerebral vascular system begins by vasculogenesis when mesodermally originating angioblasts enter the head region and form the perineural
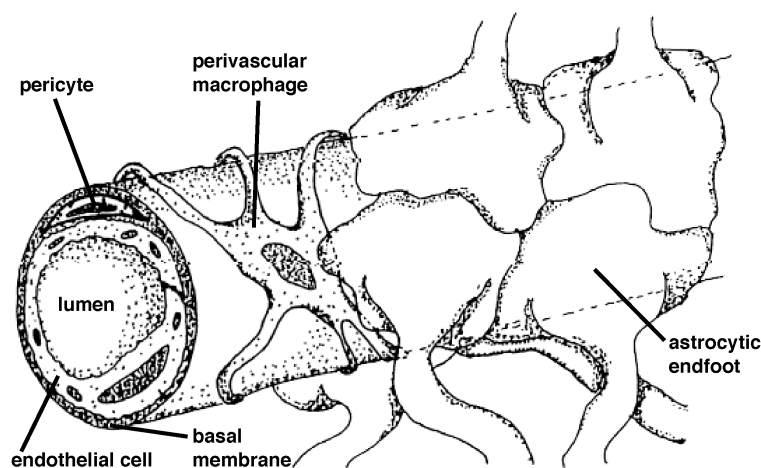
Figure 1.1.1: Cellular components of the blood-brain barrier (modified from Engelhardt et al., 1997)

plexus. Perineural plexus-derived vascular sprouts grow into the developing neuroectoderm, which is called angiogenesis (Risau and Wolburg, 1990). Therefore, BBB endothelial cells are mesodermally and not neuroectodermally derived. Transplantation studies have demonstrated, that vessels derived from the coelomic cavity, when growing in an embryonic ectopic brain transplant, gain BBB characteristics (Stewart and Wiley, 1981). Thus, development of BBB characteristics in endothelial cells is not pre-determined but rather induced by surrounding neuroectoderm. Additionally, culture of BBB endothelial cells *in vitro* results in loss of specific BBB properties. Therefore, an interaction between endothelial cells and surrounding CNS parenchyma is necessary for BBB maintenance (Figure 1.1.1). Despite these findings, factors which are involved in either BBB development or maintenance could not be identified yet. Also remaining unsolved is the question of which cell type or combination of cell types within the neuroectoderm induces BBB characteristics in endothelium. There are several potential candidates. BBB endothelial cells are surrounded by a basal membrane containing a large number of pericytes most likely being required for vessel maturation (Sims, 1986; Lindahl et al., 1997). Additionally, this basal membrane is nearly completely covered by astrocytic endfeet. This close proximity as well as the temporal correlation of astrocytic vascular sheet formation and BBB permeability development suggests an important role of astrocytes in BBB development. This is underlined by the fact that coculture models of endothelial cells and astrocytes *in vitro* improve blood-brain barrier character-

istics compared to endothelial monocultures (Cecchelli et al., 1999). Furthermore, microglial cells or macrophages located within the perivascular space (Hickey and Kimura, 1988) have been reported to be able to phagocytose and present antigen after activation (Rieske et al., 1989). Therefore, they have been suggested to form a second line of defense within the CNS, while a possible role in differentiation and maintenance of the BBB characteristics has not been elucidated yet. In conclusion, the BBB is formed by endothelial cells. However, although their interactions with the surrounding parenchyma is required for its development and maintenance, open questions remain about the molecular means of these interactions.

1.2   Multiple sclerosis and experimental autoimmune encephalomyelitis

Because of the presence of the BBB, the absence of lymphatic vessels and the lack of antigen-presentation, the CNS is considered as an immunoprivileged organ. The first to describe this functionality was Sir Peter Medawar, who showed that allogenic, ectopic tissue transplants were not rejected for long periods of time after transplantation into the CNS, while they were rejected quickly after transplantation into other organs (Medawar, 1948). Under physiological conditions, lymphocyte entry across the BBB into the CNS is low, but has been described for activated T cells which are able to access the CNS parenchyma in Lewis rats disregarding their antigen specificity *in vivo* (Wekerle et al., 1986; Hickey et al., 1991). During viral infection of cells within the CNS, recruitment of mononuclear cells into the CNS has been described (Griffin et al., 1992). Therefore, immune cells readily gain access to the CNS under pathological conditions, which can also be seen during inflammatory diseases of the CNS, such as multiple sclerosis (MS).

MS is an inflammatory demyelinating disease of the CNS during which mononuclear cells gain access to the CNS parenchyma (Martin and McFarland, 1995). Although MS was first described around 1835 (Cruveilhier, 1830 – 1842), its etiology is still unknown. It has been suggested that specific genetic predisposition and a viral infection during childhood are a prerequisite to trigger disease during adulthood by additional infections and environmental factors (Sibley et al., 1985; Poser, 1994). MS disease courses are classified to be either relapsing-remitting, progressive-remitting,

secondary-progressive or primary-progressive. MS therapy either targets symptoms to increase life quality or to globally modulate immune functions with either corticoids, interferon-β or copolymer 1 (Beck et al., 1992; Jacobs et al., 1995; Johnson et al., 1995). Besides these treatments with general immunomodulatory effects, there is hope that future therapeutics will more directly modulate MS pathogenesis. Clinical trials with humanized antibodies against α_4-integrin are currently ongoing (Miller et al., 2003). Such reagents could be developed using the animal model for MS best known today, experimental autoimmune encephalomyelitis (EAE).

EAE is an inflammatory disease of the CNS causing focal areas of inflammation within the CNS, which are called perivascular infiltrates or inflammatory cuffs (Levine, 1974). The disease is accompanied by edema formation and demyelination of the CNS resulting in an ascending paralysis (Martin and McFarland, 1995). EAE was first described in the late 19th century, when Louis Pasteur used inactivated rabies virus particles purified from rabbit brains to develop a vaccination therapy against rabies, which resulted in lethal neuroparalytic complications (Pasteur, 1885). The same disease could be induced by injecting brain preparations from healthy rabbits into monkeys (Rivers et al., 1933), thereby proving that brain tissue contaminations in the rabies virus particle purifications were able to induce EAE. Addition of adjuvant removed the necessity for multiple injections and markedly reduced the time till onset of disease (Kabat et al., 1947). Later on, analysis of different fractions of spinal cord homogenate allowed identification of myelin basic protein (MBP) as the first autoantigen being usable for induction of EAE (Laatsch et al., 1962). Additionally, myelin oligodendrocytic glycoprotein (MOG) as well as proteolipid protein (PLP) were identified to be encephalitogenic (Zamvil and Steinman, 1990; Linington et al., 1993). Specific peptides of these proteins were identified as the encephalitogenic agents (Tuohy et al., 1989; Adelmann et al., 1995). Whereas all these molecules are constituents of the myelin sheets being formed by oligodendrocytes, injection of astrocytic S100β protein did also result in a disease resembling EAE (Kojima et al., 1994). While active immunization of animals with encephalitogenic autoantigens causes active EAE (aEAE), transfer of T lymphocytes from EAE afflicted rats into untreated syngeneic animals caused transfer EAE (tEAE), but serumtransfusion did not propagate the disease (Paterson, 1960). Later experiments established MBP antigen specific T cell lines from rat *in vitro*, which could be

used to induce EAE in healthy syngeneic animals (Ben-Nun et al., 1981). Therefore, EAE is mediated by T cells, which were further characterized to be $CD4^+$ $CD8^-$ T_H1 lymphoblasts. EAE can only be induced in specific susceptible animal strains, indicating the necessity for a specific genetic background. While basic mechanisms of EAE in different susceptible animal strains are the same, there are specific differences as well. On the one hand, in C57Bl/6 mice, EAE is induced by a peptide of myelin oligodendrocytic glycoprotein (MOG^{35-55}) leading to massive demyelination and resulting in a chronic relapsing/remitting disease course. On the other hand, in SJL/N mice, induction of EAE with a short peptide of proteolipid protein ($PLP^{139-151}$) results in little demyelination and a mostly monophasic clinical behavior. It has been hypothesized that these different EAE models resemble different features of MS (Wekerle et al., 1994), making each model a useful tool for investigation of the disease.

Only freshly *in vitro* activated T lymphoblasts are able to induce tEAE. The question, where T lymphocytes are activated *in vivo*, could not be answered yet. As inflammatory processes during EAE are limited to the CNS, it is suggestive, that antigen-presentation is performed by BBB endothelial cells themselves, so that T lymphocytes are locally activated and can migrate from the bloodstream across the endothelial BBB into the CNS parenchyma. However, although BBB endothelial cells are competent to present antigen, they are unable to fully activate T lymphocytes (Risau et al., 1990). Therefore, firsthand involvement of antigen presentation in recruitment of T cells across the endothelial BBB is improbable. More likely, specific adhesion and signaling molecules at the endothelial BBB are meaningful for the recruitment of lymphoblasts from the bloodstream across the endothelial BBB into the CNS parenchyma. Additionally, TJ molecules, such as claudins, may be relevant for leukocyte recruitment into the CNS, as claudin-3 is lost from endothelial TJ during EAE pathogenesis (Wolburg et al., 2003). However, as encephalitogenic T cells appear to migrate instead through the endothelial cells, they should therefore not require TJ modifications (Wolburg et al., 2003 - in press -). Nevertheless, TJ modifications might be involved in the recruitment of secondary inflammatory cells such as macrophages.
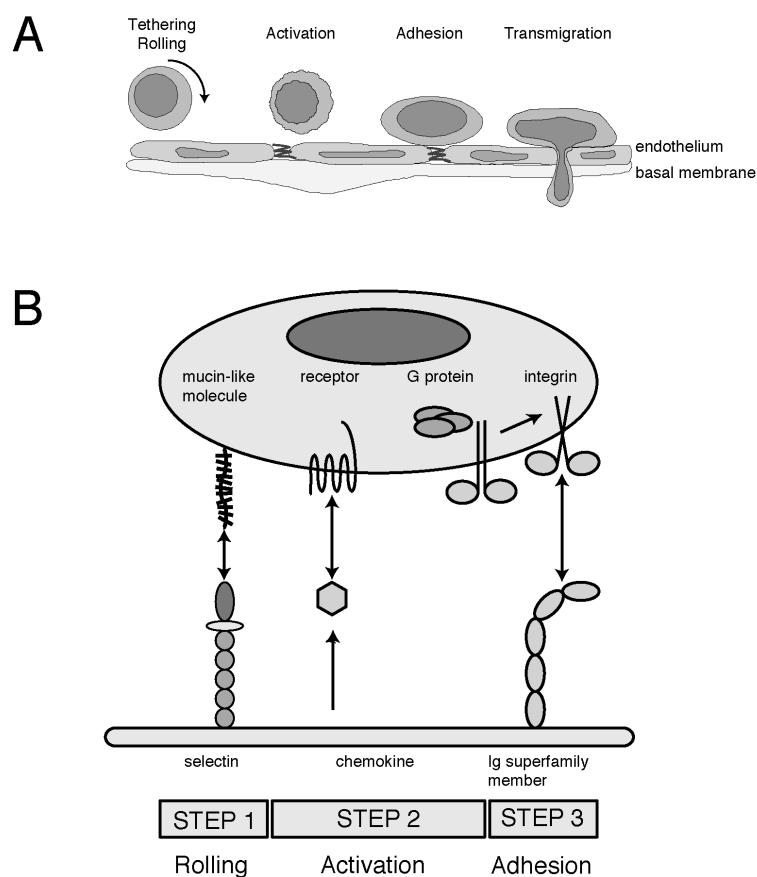
Figure 1.3.1: Schematic description of the multistep model. A: Steps involved in leukocyte-endothelial interactions. B: Molecules involved in the cascade (modified from Butcher, 1991; Springer, 1994)

1.3   Multi-step model

Lymphocytes extravasate from the bloodstream mainly across postcapillary venules into parenchymal tissue. This extravasation is not random but rather well-regulated by a successive cascade of molecular interactions described as the multi-step model (Butcher, 1991; Springer, 1994). Therefore, only if leukocytes and endothelial cells have the correct combination of ligands and receptors on their respective surfaces, a full cascade of leukocyte-endothelial interactions can take place in four sequential steps: Tethering/Rolling, Activation, Adhesion and Transmigration, resulting in recruitment of the leukocyte from the bloodstream into the parenchyma (Figure 1.3.1).

Initial transient contact of circulating leukocytes with the vascular wall is generally mediated by adhesion molecules of the selectin family and their respective carbohydrate ligands, which are located on microvilli / cell protrusions on the surface of the leukocytes. Selectins are able to interact via their lectin domain

with their respective ligands on the endothelial surface and consequently deceler-
ate the leukocytes, resulting in rolling of the leukocyte along the vascular wall.
Leukocyte-selectin (L-selectin) is expressed by leukocytes, while endothelial- and
platelet-selectin (E- and P-selectin) can be expressed on inflamed endothelial cells.
Next, chemokines being presented on the endothelial cells can bind to their respec-
tive seven-transmembrane spanning receptors / serpentine receptors / G protein
coupled receptors on the leukocytes. This interaction is followed by pertussis toxin
sensitive $G_{\alpha i}$-mediated inside-out signaling, which results in activation of the inte-
grins on the leukocyte surface by increase of their affinity to their ligands due to
conformational changes and potentially additional increase in integrin avidity by
clustering (Takagi et al., 2002). Integrins are heterodimers consisting of an α- and
β-subunit. Once activated, integrins mediate firm adhesion of the leukocyte to their
immunoglobulin (Ig)-superfamily ligands located on the endothelial cells. After firm
adhesion, leukocytes can transmigrate through the vessel wall into the parenchymal
tissue. This transmigration is as well mediated by integrins and Ig superfamily
ligands, like ICAM-1, PECAM-1, JAM-1 or CD99.

1.4   Chemokines and chemokine receptors

The first chemokine to be functionally described was interleukin-8 (IL-8) which is
secreted by monocytes and has chemotactic activity on neutrophilic granulocytes
(Walz et al., 1987; Yoshimura et al., 1987; Schroder et al., 1987). Therefore, this
molecule was termed a <u>chemo</u>tactic cyto<u>kine</u> or in short, chemokine. Later on, more
and more chemokines were identified by their chemotactic activity. Chemokines
are about 8 – 12 kDa in size consisting of about 90 – 130 amino acids. Molecular
cloning of these proteins helped to identify a common structural motif. Four highly
conserved cysteine residues form two disulfide bridges between the first and third as
well as the second and fourth cysteine respectively. The number of amino acids in
between the first and second cysteine defines chemokine subfamilies (Figure 1.4.1).
Identification of chemokines by their functional, chemotactic properties led to several
names for certain chemokines. This generated a lot of confusion and urged the need
of getting a consistent nomenclature. Therefore, chemokines were named according
to their subfamilies either CXC, CC, XC or CX3C supplemented with an L for

CXCL8 / IL-8

CCL5 / RANTES
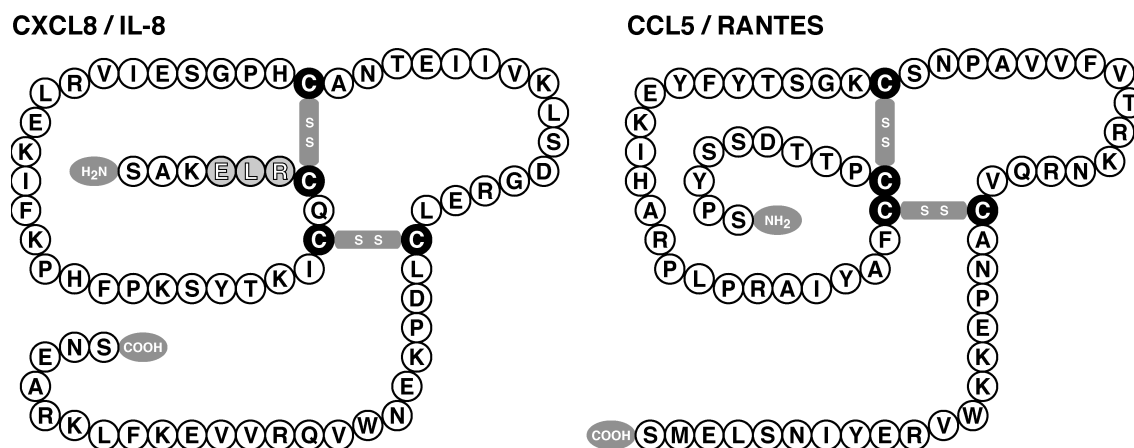
Figure 1.4.1: Schematic description of two exemplary members of the CXC and CC chemokine subfamilies (modified from Hughes and Yeager, 1999)

ligand and a number according to the timepoint when the human homolog was cloned (Table 1.4.1).

CXCL8 / IL-8 belongs to the CXC- or α-chemokine subfamily which contains exactly one amino acid in between the first and second cystein residue (Figure 1.4.1). Additionally, most CXC chemokines contain an N-terminal ELR motif, consisting of glutaminic acid (E), leucin (L) and arginine (R). These ELR motif containing chemokines like CXCL8 and CXCL1 / Groα preferentially chemoattract neutrophilic granulocytes (Moser et al., 1990; Schroder et al., 1990). In contrast, non-ELR motif containing CXC chemokines mainly attract activated T cells. Expression of such a chemokine, CXCL10 / interferon-γ-inducible protein 10 (IP-10) was described to be detectable in fibroblasts, mononuclear cells, endothelial cells and lymphocytes *in vitro* (Luster et al., 1985). Additional studies reported it to be expressed in kidney, liver and spleen after systemic application of IFN-γ *in vivo*. Besides CXCL10, CXCL9 / monokine-induced by interferon-γ (IFN-γ; MIG) is another non-ELR motif containing chemokine (Farber, 1990). It is functionally related to CXCL10, as it binds to the same chemokine receptor (Loetscher et al., 1996). A third non-ELR chemokine, CXCL12 / stromal cell derived factor 1 (SDF-1), chemoattracts T cells as well; however, it appears to be rather unusual, as it has been described to be constitutively expressed in many organs (Tashiro et al., 1993; Bleul et al., 1996).

The first and second cysteine residues of the CC- or β-chemokine subfamily members are directly linked (Figure 1.4.1). CCL2 / monocyte chemoattractant protein 1 (MCP-1) chemoattracts monocytes, CD4^{+} and CD8^{+} T cells, but does not

systematic name	human ligand	mouse ligand	receptors
CXCL1	GROα/MGSA-α	GRO/KC?	CXCR2 > CXCR1
CXCL2	GROβ/MGSA-β/MIP-2	GRO/KC?	CXCR2
CXCL3	GROγ/MGSA-γ	GRO/KC?	CXCR2
CXCL4	PF4	PF4	unknown
CXCL5	ENA-78	LIX?	CXCR2
CXCL6	GCP-2	CKα-3	CXCR1, CXCR2
CXCL7	NAP-2	unknown	CXCR2
CXCL8	IL-8	unknown	CXCR1, CXCR2
CXCL9	MIG	MIG	CXCR3
CXCL10	IP-10	IP-10	CXCR3
CXCL11	I-TAC	unknown	CXCR3
CXCL12	SDF-1α/β	SDF-1	CXCR4
CXCL13	BLC/BCA-1	BLC/BCA-1	CXCR5
CXCL14	BRAK/bolekine	BRAK	unknown
(CXCL15)	unknown	Lungkine	unknown
CCL1	I-309	TCA-3, P500	CCR8
CCL2	MCP-1/MCAF	JE?	CCR2
CCL3	MIP-1α/LD78α	MIP-1α	CCR1, CCR5
CCL4	MIP-1β	MIP-1β	CCR5
CCL5	RANTES	RANTES	CCR1, CCR3, CCR5
(CCL6)	unknown	C10, MRP-1	unknown
CCL7	MCP-3	MARC?	CCR1, CCR2, CCR3
CCL8	MCP-2	MCP-2?	CCR3
(CCL9/10)	MRP-2, CCF18	MIP-1γ	unknown
CCL11	Eotaxin	Eotaxin	CCR3
(CCL12)	unknown	MCP-5	CCR2
CCL13	MCP-4	unknown	CCR2, CCR3
CCL14	HCC-1	unknown	CCR1
CCL15	HCC-2/Lkn-1/MIP-1d	unknown	CCR1, CCR3
CCL16	HCC-4/LEC	LCC-1	CCR1
CCL17	TARC	TARC	CCR4
CCL18	DC-CK1/PARC AMAC-1	unknown	unknown
CCL19	MIP-3β/ELC/exodus-3	MIP-3β/ELC/exodus-3	CCR7
CCL20	MIP-3α/LARC/exodus-1	MIP-3α/LARC/exodus-1	CCR6
CCL21	6Ckine/SLC/exodus-2	6Ckine/SLC/exodus-2/TCA-4	CCR7
CCL22	MDC/STCP-1	ABCD-1	CCR4
CCL23	MPIF-1	unknown	CCR1
CCL24	MPIF-2/Eotaxin-2	unknown	CCR3
CCL25	TECK	TECK	CCR9
CCL26	Eotaxin-3	unknown	CCR3
CCL27	CTACK/ILC	ALP/CTACK/ILC ESkine	CCR10
XCL1	Lymphotactin/SCM-1α/ATAC	Lymphotactin	XCR1
XCL2	SCM-1β	unknown	XCR1
CX3CL1	Fractalkine	Neurotactin	CX3CR1

Table 1.4.1: Systematic nomenclature for CXC, CC, C and CX3C chemokines. Listed are systemic names and names which have been used for a particular chemokine before. Question marks indicate if listed mouse chemokines may not correspond to the listed human ligand. Additionally, main receptors for each chemokine are listed. Systematic names in brackets indicates that no human homolog has been identified. (modified from Zlotnik and Yoshie, 2000).

chemoattract neutrophilic granulocytes or B cells (Valente et al., 1988; Carr et al., 1994). Additionally, it has been described to increase integrin affinity on T lymphocytes (Carr et al., 1996). CCL3 / macrophage inflammatory protein 1α (MIP-1α) and CCL4 / macrophage inflammatory protein 1β (MIP-1β) were isolated from lipopolysaccharide (LPS) treated monocytes (Wolpe et al., 1988; Sherry et al., 1988). CCL3 is a more potent chemoattractant and preferentially chemoattracts CD4$^+$ T cells as compared to CCL4 which mainly chemoattracts CD8$^+$ T lymphocytes (Fahey et al., 1992; Taub et al., 1993). CCL5 / regulated upon activation normal T cell expressed and secreted (RANTES) is expressed by T cells and eosinophils (Schall et al., 1988; Lim et al., 1996) and chemoattracts CD4$^+$ and CD8$^+$ T lymphocytes, eosinophilic and basophilic granulocytes and Natural Killer (NK) cells (Roth et al., 1995; Rot et al., 1992; Kuna et al., 1992; Taub et al., 1995). CCL6 / C10 expression was described in differentiated hematopoietic progenitor cells, macrophages and T cells *in vitro* and to chemoattract macrophages (Kleinerman et al., 1984; Orlofsky et al., 1991, 1994; Berger et al., 1996). CCL11 / eotaxin chemoattracts eosinophilic granulocytes and T$_H$2 lymphocytes (Griffiths-Johnson et al., 1993; Sallusto et al., 1997). CCL19 / Epstein-Barr-induced 1 ligand chemokine (ELC) is expressed by lymph node dendritic cells within the T cell zones and then transported to the high endothelial venules, where it chemoattracts naïve T cells (Yoshida et al., 1997; Ngo et al., 1998; Baekkevold et al., 2001). CCL21 / secondary lymphoid chemokine (SLC) / 6CKine / thymus-derived chemotactic agent 4 (TCA-4) recruits naïve T cells to the lymph nodes as well; however, it is expressed and presented by endothelial cells themselves (Gunn et al., 1998). While both, CCL19 and CCL21 bind to the same chemokine receptor, CCR7, this binding has been described to result in different effects, as CCL19 binding, but not CCL21 binding, results in internalization of CCR7 (Bardi et al., 2001). Additionally, murine CCL21 binds to the chemokine receptor CXCR3 (Soto et al., 1998). CCL22 / macrophage derived chemokine (MDC) / activated B cell derived chemokine (ABCD-1) has been described to be expressed by macrophages and chemoattract dendritic cells, macrophages and NK cells *in vitro* (Godiska et al., 1997) while the mouse homolog appears to chemoattract activated T cells (Schaniel et al., 1998, 1999a,b).

XCL1 / lymphotactin, which is a potent chemoattractant for lymphocytes, does not fit into either of these two subfamilies, as it only contains two cysteine residues

representing the second and fourth cysteine as compared to CXC- or CC-chemokines (Houck and Chang, 1977; Kelner et al., 1994). Therefore, XCL1 constitutes the C- or γ-chemokine subfamily.

Another very special chemokine is CX3CL1 / fractalkine / neurotactin (Bazan et al., 1997; Pan et al., 1997). As its first and second cysteine residue are separated by three amino acids, it is assigned to the CX3C- or δ-chemokine subfamily. Furthermore, CX3CL1 is membrane-bound via a mucin stalk and can be shed off the membrane to become soluble.

While this classification in CXC-, CC-, C- and CX3C-subfamilies is based on the structural properties of chemokines, they can also be divided into functional groups. There are so-called lymphoid, constitutive or homeostatic chemokines, like CXCL12, CCL19, CCL21, which are constitutively expressed in lymphoid organs. In contrast, inducible or inflammatory chemokines are induced during inflammation.

IL-8 and platelet-factor 4 (PF4) were the first chemokines to be structurally analyzed. Monomeric chemokines consist of an N-terminal loop, three antiparallel β-sheets and a C-terminal α-helix. IL-8 forms homodimers and PF4 tetramers, which resemble a dimeric IL-8 dimer (Clore et al., 1990; Baldwin et al., 1991). The question of whether monomers, dimers or tetramers are biologically active, remains controversial. While physiologic chemokine concentrations are in nanomolar ranges (Burrows et al., 1994), chemokine dimer dissociation constants are in micromolar ranges, suggesting chemokine monomers to be the physiologically relevant form. This is emphasized as modified IL-8, which is no longer able to dimerize, maintains its chemotactic activity *in vitro* (Rajarathnam et al., 1994). However, recently it was described that dimerization of chemokines as well as their ability to bind proteoglycans is required to maintain their biologic activity *in vivo* (Proudfoot et al., 2003). Therefore, it has been suggested that chemokine binding to proteoglycans locally increases chemokine concentration and thereby results in dimerization.

Besides their chemotactic activity, chemokines have been suggested to be involved in additional biological effector functions, like T_H1/T_H2 development, angiogenesis/angiostasis, metastasis, cell recruitment, inflammation, lymphoid organ development, lymphoid trafficking and wound healing (reviewed in Rossi and Zlotnik, 2000).

Chemokines bind to chemokine receptors, which are named CXCR1 – CXCR5,

CCR1 – CCR10, XCR1 and CX3CR1 according to their ligand subfamilies. Chemokine – chemokine receptor binding is very promiscuous, as chemokines may bind to different receptors and chemokine receptors bind different chemokines. Therefore, it is often not possible to assign distinct receptor ligand pairs. In general, chemokine binding to its receptor results in a $G_{\alpha i}$-mediated, pertussis-toxin sensitive signaling pathway which leads to Ca^{2+} influx and chemotaxis (Rollins et al., 1991). On the other hand, via arrestin signaling pathways, chemokine receptor internalization is induced to limit chemokine signaling.

Besides known chemokine receptors, there are a lot of orphan receptors with a high homology to chemokine receptors. However, their ligands have not been identified yet, so they are not termed chemokine receptors. Two very special chemokine receptors are Duffy antigen / receptor for chemokines (DARC) and D6. These are two atypical chemokine receptors, as they unspecifically bind chemokines of the CXC- and CC-subfamilies and additionally lack the typical chemokine receptor intracellular signal transducing domains. Therefore they do not induce functional responses like Ca^{2+}-influx or chemotaxis. DARC is a blood group antigen and therefore largely expressed on erythrocytes. Additionally, upregulation of DARC on BBB endothelial cells during EAE pathogenesis was first observed by us (Alt, 1999), strongly suggesting a special role during EAE pathogenesis. DARC might act as a sink to remove chemokines from the bloodstream, it might present chemokines on the luminal surface of the endothelium and thereby facilitate ligand binding or it might be involved in active transcytosis of chemokines from the CNS parenchymal tissue across the endothelial BBB onto the luminal surface of the endothelial cells.

1.5   Chemokine involvement in EAE

Several chemokines have been described to be expressed in CNS tissue of EAE afflicted animals. Godiska et al. performed reverse transcription - polymerase chain reactions (RT-PCR) and Northern hybridizations, thereby reporting expression of CXCL1, CXCL10, CCL1, CCL2, CCL3, CCL4, CCL5 and CCL7 in spinal cord preparations of SJL mice afflicted with EAE (Godiska et al., 1995). They described CXCL12 to be expressed in spinal cord preparations of healthy and EAE afflicted mice, while they could detect neither CCL6 nor CXCL2. Expression of CXCL10

and CCL2 was reported in astrocytes of SJL mice afflicted with EAE (Ransohoff et al., 1993), while expression of CCL3 and CCL4 was described in inflammatory cells, microglial cells and astrocytes of Lewis rats afflicted with EAE (Miyagishi et al., 1997). Thus, different chemokines have been reported to be expressed during EAE in the CNS; however, none of them has been shown to be expressed by the BBB endothelial cells themselves. Karpus et al. reported that pretreatment with polyclonal CCL3 but not CCL2 antisera protected SJL mice from transfer EAE and reduced the number of inflammatory cells within the spinal cord, while administration of this antiserum additionally ameliorated an ongoing disease (Karpus et al., 1995). However, whereas application of polyclonal antiserum against CCL2 but not CCL5 could ameliorate the EAE relapse in SJL mice, it had no effect on the acute phase of disease (Kennedy et al., 1998). Although these studies suggest an important role of CCL2 and CCL3 in the pathogenesis of EAE, their exact mechanistic role in EAE pathogenesis is not clear. CNS specific expression of CCL6 was shown to induce leukocyte infiltration into the CNS (Asensio et al., 1999). In contrast to this, absence of CCL2 was shown to lead to amelioration of EAE, while absence of its receptor CCR2 inhibits onset of the disease (Fife et al., 2000; Izikson et al., 2000; Huang et al., 2001). Lack of CCR1, which is a receptor for both, CCL5 and CCL7, has been described to result in less severe EAE (Rottman et al., 2000). However, absence of CCR5, an additional receptor for CCL5 was shown to have no influence EAE pathogenesis (Tran et al., 2000). This suggests that lack of CCR5 can be compensated by CCL5 binding to CCR1, while lack of CCR1 results in lack of CCL5 and CCL7 binding which cannot be compensated. Although several of these studies describe an important role of chemokines during EAE pathogenesis, it has not been investigated yet, if these chemokines are involved in recruitment of encephalitogenic T cells from the bloodstream across the endothelial blood-brain barrier into the CNS parenchyma or if they have different effector functions. None of these chemokines has been reported to be expressed by BBB endothelial cells themselves.

1.6   The aim of this study

Aim of this study was the identification of chemokines which are involved in lymphocyte recruitment from the bloodstream across the endothelial BBB into the brain parenchyma. For chemokines to be involved in this process, they have to be either expressed by BBB endothelial cells themselves or would require a yet unknown transport mechanism from the brain parenchyma across the endothelial BBB to the luminal surface of the endothelial cells. Preliminary results from earlier studies had pointed out the possibility that CCL21 and therefore lymphoid chemokines might be involved in this process (Alt, 1999). Hence, expression of lymphoid chemokines and inflammatory chemokines which had been reported to be involved in EAE pathogenesis or lymphocyte recruitment, was analyzed by *in situ* hybridization. Chemokines which could be detected as being expressed by BBB endothelial cells themselves were to be analyzed in more detail by immunohistochemistry and immunoblot. Additional studies had to evaluate chemokine receptor expression on encephalitogenic T cells, while functional relevance of the findings was subject to transmigration and frozen-section assays *in vitro*. Application of intravital fluorescence videomicroscopy in cooperation with Dr. Peter Vajkoczy (Klinikum Mannheim, University of Heidelberg) should prove involvement of these chemokines in T lymphoblast recruitment across the endothelial BBB *in vivo*.

Furthermore, involvement of so far not known chemokines and receptors possibly being involved in lymphocyte recruitment across the endothelial BBB was addressed by three different technical approaches targeting two different tissues in cooperation with Astra-Zeneca (Södertälje, Sweden). Gene array, subtractive suppression hybridization and proteomics analysis were applied either to compare cerebral microvessels from EAE-afflicted mice with healthy control mice or to compare encephalitogenic with non-encephalitogenic T cells. Results should be analyzed by extensive gene bank searches to identify possible targets for further investigation.

The Duffy antigen / receptor for chemokines (DARC) is a potential transporter of chemokines across the endothelial BBB. By use of DARC-deficient mice, which were kindly provided by Antal Rot (Novartis, Vienna, Austria; Dawson et al. (2000)), a potential involvement of DARC in lymphocyte recruitment across the endothelial BBB should be analyzed *in vitro* and *in vivo*.

Chapter 2

Materials and Methods

2.0.1 Devices

ABI Prism 3700 DNA Analyzer . . . . Applied Biosystems, Darmstadt, Germany)

β-scintillation counter LS 6500 . . . . Beckman-Coulter, Unterschleißheim, Germany

Balance LC 4800 P . . . . Sartorius, Hamburg, Germany

Balance RC 210 D . . . . Sartorius, Karlsruhe, Germany

Binocular KL 1500 electronic . . . . Zeiss, Oberkochen, Germany

Cell Harvester . . . . Inotech, Dottikon, Switzerland

Centrifuge Biofuge Fresco . . . . Heraeus, Hanau, Germany

Centrifuge Biofuge Pico . . . . Heraeus, Hanau, Germany

Centrifuge 5415 C . . . . Eppendorf, Hamburg, Germany

Centrifuge 4K15 . . . . Sigma-Zentrifugen, Osterode, Germany

Centrifuge 4K15 C . . . . Sigma-Zentrifugen, Osterode, Germany

CO_2 incubator IR Autoflow . . . . Nuaire; Zapf, Sarstedt, Germany

Developing machine M35 X-OMAT . . . . Kodak, Stuttgart, Germany

Electrophoresis apparatus . . . . Peqlab, Erlangen, Germany

Gel chamber Mini-Sub Cell GT . . . . Bio-Rad, Munich, Germany

Gel chamber Sub-Cell GT . . . . Bio-Rad, Munich, Germany

Gel chamber Mini-Sub Cell Model 192 . Bio-Rad, Munich, Germany

Gel Dryer Model 583 . . . . Bio-Rad, Munich, Germany

Gene Amp PCR System 9700. . . . . Applied Biosystems, Darmstadt, Germany

Heating Block thermomixer 5436 . . . . . . Eppendorf, Hamburg, Germany

Heating Plate . . . . Medax, Kiel, Germany

Hybridization oven . . . . Bachofer, Reutlingen, Germany

Incubator B5060E . . . . Heraeus, Hanau, Germany

Laminar flow cabinet 425-400E . . . . Nuaire; Zapf, Sarstedt, Germany

Disperser Ultra-Turrax T25. . . . . IKA Labortechnik, Staufen, Germany

Microscope Axiophot . . . . Zeiss, Oberkochen, Germany

Microtome HM 500 OM . . . . Microm, Walldorf, Germany

Microwave oven Inverter . . . . Panasonic, Hamburg, Germany

Multi stepping pipet . . . . Eppendorf, Hamburg, Germany

pH meter pH 192 . . . . WTW, Weilheim, Germany

Phosphoimager BAS-2500 . . . . Fujifilm, Raytest, Straubenhardt, Germany

Pipetboy acu . . . . Integra Biosciences, Fernwald, Germany

Electronic pipettor Impact2 . . . . Matrix, Wehrheim, Germany

Power supply E 450 . . . . Consort, Turnhout, Belgium

Power supply E 455 . . . . Consort, Turnhout, Belgium

Shaking Incubator . . . . HT Infors, Bottmingen, Switzerland

UV-Systeme . . . . Intas, Göttingen, Germany

UV Screen 312 nm . . . . Bachofer, Reutlingen, Germany

UV/VIS Spectrometer Lambda Bio . . . . Perkin-Elmer, Munich-Neuried, Germany

Vortex-Genie 2 . . . . Scientific Industries, Bohemia, NY, USA

Water bath Julabo 7 A . . . .   Julabo, Seebach, Germany

Water bath Julabo SW 20 C . . . .   Julabo, Seebach, Germany

2.0.2   Expendable materials

Reaction tubes, 0.5 – 2.0 ml . . . .   Eppendorf, Hamburg, Germany

15 ml, 50 ml tubes . . . .   Greiner, Nürtingen, Germany

Tissue culture flasks . . . .   Costar, Bodenheim, Germany; Greiner,
                                                                        Nürtingen, Germany

Pipet tips . . . .   Greiner, Nürtingen, Germany

Sterile filters . . . .   Millipore,   Eschborn,   Germany;   Pall,
                                                                        Dreieich, Germany

Photofilm EPY64T . . . .   Kodak, Stuttgart, Germany

2.0.3   Chemicals

Chemicals were obtained in purity p. a. from BDBiosciences, Heidelberg, Germany;
Invitrogen, Karlsruhe, Germany; J. T. Baker, Deventer, The Netherlands; Merck,
Darmstadt, Germany; Riedel-de-Haen, Seelze, Germany; Roth, Karlsruhe, Germany
and Sigma, Deisenhofen, Germany.

2.0.4   Buffers and Solutions

Standard solutions were prepared using deionized, ultrafiltered and autoclaved tap
water. If not explicitly noted, pH was adjusted using hydrochloric acid or sodium
hydroxide solution.

2.1   Tissue culture

2.1.1   Tissue culture media and solutions

Supplements for tissue culture were obtained from Invitrogen (Karlsruhe, Germany),
PAA (Cölbe, Germany), PAN (Aidenbach, Germany) or Sigma (Deisenhofen, Ger-

many) unless otherwise noted. Supplements were either filtered sterile or autoclaved. All sera were heated before use (30 min, 56°C) to inactivate complement factors.

Cells were cultured under sterile conditions in a CO_2 incubator (NUAire; Zapf, Sarstedt, Germany) at 37°C, 7 % – 10 % CO_2 and 100 % humidity in tissue culture dishes (BDBiosciences Falcon, Heidelberg, Germany) or flasks (Greiner, Nürtingen, Germany).

2.1.1.0.1 Concanavalin A (ConA) medium

Cytokine producing splenocytes were grown in DMEM (4500 g/l glucose) supplemented with 1 % normal mouse serum (see 2.3.1.5), 4 mM L-glutamine, 1 mM sodium pyruvate, 1 % (v/v) MEM non-essential amino acids (100×), 100 U/ml penicillin, 100 μg/ml streptomycin and 0.05 mM β-mercaptoethanol.

2.1.1.0.2 Endothelioma medium

Endothelioma cell lines were cultured in DMEM (4500 g/l glucose) supplemented with 10 % fetal calf serum, 4 mM L-glutamine, 1 mM sodium pyruvate, 1 % (v/v) MEM non-essential amino acids (100×), 100 U/ml penicillin, 100 μg/ml streptomycin and 0.05 mM β-mercaptoethanol.

2.1.1.0.3 Migration assay medium (MAM)

Migration and chemotaxis assays were performed in DMEM (4500 g/l glucose) supplemented with 5 % calf serum, 4 mM L-glutamine and 25 mM HEPES.

2.1.1.0.4 Mouse brain endothelial (MBE) medium

Primary endothelial cells were grown in DMEM (4500 g/l glucose) supplemented with 10 % calf serum, 4 mM L-glutamine, 1 mM sodium pyruvate, 1 % (v/v) MEM non-essential amino acids (100×), 100 U/ml penicillin, 100 μg/ml streptomycin and 1 % retinal factor (see 2.1.4.6).

2.1.1.0.5 Phosphate-buffered saline (PBS)

PBS solution contained 137 mM NaCl, 2.7 mM KCl, 4.3 mM Na_2HPO_4 and 1.4 mM KH_2PO_4.

2.1.1.0.6 T cell (TC) medium

T cells were restimulated in RPMI-1640 supplemented with 10 % fetal calf

serum, 4 mM L-glutamine, 1 mM sodium pyruvate, 1 % (v/v) MEM non-essential amino acids (100×), 100 U/ml penicillin, 100 μg/ml streptomycin and 0.05 mM β-mercaptoethanol.

2.1.1.0.7 T cell growth factor (TCGF) medium

T cells were propagated in RPMI-1640 supplemented with 10 % fetal calf serum, 4 mM L-glutamine, 1 mM sodium pyruvate, 1 % (v/v) MEM non-essential amino acids (100×), 100 U/ml penicillin, 100 μg/ml streptomycin, 0.05 mM β-mercaptoethanol and 10 % – 20 % concanavalin A supernatant (see 2.1.3.8).

2.1.1.0.8 Washing buffer

Cells were washed in HBSS supplemented with 10 % FCS and 25 mM HEPES.

2.1.2 Primary cell preparation

2.1.2.1 Preparation of splenocytes

Mice were sacrificed by cervical dislocation. Spleens were taken out under sterile conditions while thoroughly removing connective and fatty tissue. Spleens were washed twice in washing buffer, cut up into small pieces and homogenized using a Dounce homogenizer with a large clearance pestle (Bellco Glass, NJ, USA). The cell suspension was filtered using a 100 μm nylon mesh and centrifuged (250 g, 10 min, RT). Erythrocytes were lysed as described (Boyle, 1968) with a prewarmed mixture of 9 volumes ACT I (155 mM NH_4Cl) and 1 volume ACT II (170 mM Tris-HCl pH 7.65) (2×10^7 cells/ml; 5 min, 37°C). Erylysis was stopped by dilution with washing buffer and centrifugation (250 g, 10 min, RT). Cells were filtered through a 100 μm nylon mesh again, washed twice, counted and used for experiments.

2.1.2.2 Preparation of lymphocytes

Mesenteric or peripheral lymph nodes were prepared, while connective and fatty tissue was thoroughly removed under sterile conditions. Lymph nodes were washed twice in washing buffer, cut into small pieces and homogenized using a Dounce homogenizer with a large clearance pestle (Bellco Glass, NJ, USA). Cell suspension was filtered through a 100 μm nylon mesh, centrifuged (250 g, 10 min, RT), filtered and washed again. Cells were counted and used for subsequent experiments.

2.1.2.3   Preparation of peripheral blood cells

Mice were anesthetized with isoflurane and blood was collected intracardially using a syringe, which contained 75 IU sodium-heparin in 100 μl PBS to avoid coagulation. Blood samples were diluted 2-fold in PBS, carefully applied on top of 4 ml ficoll gradient solution and centrifuged (1600 rpm, 20 min, RT, without brake). Cells were washed three times in HBSS/25 mM HEPES, counted and used for experiments.

2.1.3   T cell culture

2.1.3.1   Preparation of primary PLP specific T cell lines

PLP specific T cell lines were established from SJL/N mice, as their genetic background allows them to develop EAE. 50 μg PLP$^{139-151}$ (H_2N - H - C - L - G - K - W - L - G - H - P - D - K - F - $COOH$) solved in 50 μl PBS were emulsified with 50 μl complete Freund's adjuvant (CFA; incomplete Freund's adjuvant, Invitrogen, Karlsruhe, Germany supplemented with 4 mg/ml heat-inactivated organisms of *Mycobacterium tuberculosis*, BDBiosciences Difco, Heidelberg, Germany) by mixing with two interconnected syringes. Female SJL/N mice (Taconics, Ry, Denmark) were immunized with 100 μl emulgate by subcutaneous injection into the footpads. At day 15 after injection, mice were sacrificed by cervical dislocation and peripheral lymph nodes were prepared under sterile conditions. Lymph nodes were homogenized and filtered through a 100 μm nylon mesh to obtain a single cell suspension. 5×10^7 lymphocytes were cultured per 60 mm dish in 5 ml TC medium, supplemented with 10 μg/ml PLP$^{139-151}$. After three days, 1 ml TCGF medium was added and cells were cultured for one more day. Highly activated T lymphoblasts were then separated by density gradient centrifugation (see 2.1.3.3). In parallel, antigen specificity was checked (see 2.1.3.7).

2.1.3.2   Preparation of primary MOG specific T cell lines

MOG specific T cell lines were prepared from spleens of C57Bl/6 mice (Harlan-Winkelmann, Borchen, Germany). Mice were immunized with 200 μg MOG$^{35-55}$ (H_2N - M - E - V - G - W - Y - R - S - P - F - S - R - V - V - H - L - Y - R - N - G - K - $COOH$) in 50 ml PBS emulsified with 50 μl CFA subcutaneously in the footpads, hind legs and tail root. At day 15 after injection, mice were sacrificed

by cervical dislocation and lymph nodes and spleens were prepared under sterile conditions. Cells were homogenized and filtered through a 100 μm nylon mesh to obtain a single cell suspension. 5×10^7 cells were cultured per 60 mm dish in 5 ml TC medium, supplemented with 40 μg/ml MOG$^{35-55}$. After three days, 1 ml TCGF medium was added and cells were cultured for one more day. Highly activated T lymphoblasts were then separated by density gradient centrifugation (see 2.1.3.3). In parallel, antigen specificity was checked (see 2.1.3.7).

2.1.3.3   T lymphoblast separation by density gradient centrifugation

Highly activated T lymphoblasts were separated from resting T lymphocytes and cell debris by Ficoll density gradient centrifugation (Nycoprep; Nycomed, Oslo, Norway). Therefore, cells from about $1 - 2$ 60 mm dishes were collected, centrifuged (250 g, 10 min, RT) and resuspended in 3 ml HBSS / 25mM HEPES. This suspension was carefully put on top of 5 ml Nycoprep 1.077 A solution (density: 1.077 g/ml at 20°C; Nycomed, Oslo, Norway) and centrifuged (450 g, 20 min, RT, without brake). T lymphoblasts were collected from the interphase and washed three times with washing buffer. 3×10^6 cells were resuspended in 10 ml TCGF medium and plated per 100 mm dish.

2.1.3.4   Culture in IL-2 containing medium

T lymphoblasts were propagated in IL-2 containing TCGF medium for $8 - 10$ days. Therefore, they were regularly checked by microscopy and split or fed accordingly. Freshly activated T lymphoblasts were typically large and shaped like a tennis racket, while resting T lymphocytes were round and small. Once the majority of T cells had entered the resting phase, they had to be restimulated with their respective antigen.

2.1.3.5   Restimulation of antigen specific T cell lines

Resting T cells were restimulated with antigen presenting cells and their respective antigen. Therefore, syngeneic mice were sacrificed and their spleens were dissected under sterile conditions. Spleens were homogenized and filtered through a 100 μm nylon mesh to obtain a splenocyte single cell suspension. Cells were centrifuged (250 g, 10 min, RT) and resuspended in Washing Buffer. They were then sublethally irradiated (3000 rad, Strahlenzentrum University in Giessen / 45 Gy, University

of Münster, Germany) to avoid cell division. Irradiated splenocytes were filtered again through a 100 μm nylon mesh and washed in washing buffer. Per 60 mm dish, $1.5 - 2 \times 10^6$ resting T lymphocytes were plated together with $2.5 - 4 \times 10^7$ antigen presenting cells in 5 ml TC medium containing either 10 μg/ml PLP$^{139-151}$ or 50 μg/ml MOG$^{35-55}$. After two days, 1 ml TCGF medium was added per dish and after one more day, freshly activated T lymphoblasts were separated by density gradient centrifugation (see 2.1.3.3). In parallel, specific antigen response was tested (see 2.1.3.7).

2.1.3.6 Freezing and thawing of T cell lines

T cells were collected from about $3 - 5$ tissue culture dishes and centrifuged (250 g, 10 min, RT). Pelleted cells were resuspended in 1.5 ml freezing medium (RPMI-1640, 50 % (v/v) FCS, 10 % (v/v) DMSO), put into cryo tubes and slowly (about 1°C per minute) cooled down to -80°C in cryo freezing containers (Nalgene; Nunc, Wiesbaden, Germany). Frozen cells were kept at -80°C for two days and afterwards stored in gaseous liquid nitrogen. Cells were thawed rapidly, immediately resuspended in washing buffer and plated on tissue culture dishes in TCGF medium. Freezing and thawing advanced T cells into the resting phase.

2.1.3.7 T cell proliferation assay to detect antigen specificity

Antigen specific proliferation of encephalitogenic T cells was measured by ^{3}H-thymidin (^{3}H-dT) incorporation in presence of antigen presenting cells and different antigens. Therefore, 2×10^4 T cells were cultured together with 5×10^5 sublethally irradiated splenocytes as antigen presenting cells per well in U-shaped 96-well plates. Either 10 μg/ml PLP$^{139-151}$ or 40 μg/ml MOG$^{35-55}$ were added as specific antigen. 10 μg/ml purified protein derivate (PPD) from *Mycobacterium tuberculosis* or no antigen were added to check for unspecific proliferation. 2.5 μg/ml concanavalin A (Sigma, Deisenhofen, Germany) was added as a positive control. All values were determined in triplicates. After 54 h, 1 μCi ^{3}H-dT was added per well and cells were incubated for another 16 hours. During this period, ^{3}H-dT was incorporated into proliferating cells. Cell suspensions were aspirated with a cell harvester (Inotech, Dottikon, Switzerland) through glass fibre filters so that cells got stuck and were subsequently lysed with ddH$_2$O. Non-incorporated ^{3}H-dT was removed by thorough

washing. Glass fibre filters were dried (2 h, RT) and radioactivity was measured by β-liquid scintillation counting.

2.1.3.8   Preparation of Concanavalin A supernatant (ConAS)

Interleukin-2 (IL-2) containing Concanavalin A supernatant was prepared as follows. Spleens were dissected sterile from C3H mice (Harlan-Winkelmann, Borchen, Germany), homogenized and filtered through a 100 μm nylon mesh to obtain a single cell suspension. These cells were resuspended three times in Washing Buffer and centrifuged (250 g, 10 min, RT). Subsequently, splenocytes (10^7 cells/ml) were cultured in ConA medium for 24 hours. Supernatant was collected, stored at -20°C and its activity tested. Therefore, proliferation of 2×10^4 T cells / 200 μl TC medium dependent on either 50 %, 25 %, 12.5 %, 6.25 %, 3.125 % or 0 % ConAS was compared (see 2.1.3.7). A batch of tested ConAS was used as a control. All values were determined in triplicates. As a result, ConAS was typically used in concentrations ranging from 10 % – 20 %.

2.1.3.9   Fluorescent cell labeling

Cells were labeled using either 20 nM Cell Tracker Orange (CTrO; Molecular Probes, Eugene, OR, USA) or 20 nM Cell Tracker Green (CTrG; Molecular Probes, Eugene, OR, USA) in RPMI-1640 / 10 % FCS at 5×10^6 cells/ml and incubated at 37°C for 45 minutes as described (Hamann and Jonas, 1997). Cells were washed with 50 ml RPMI-1640 / 10 % FCS, centrifuged (250 g, 10 min, RT), 5×10^6 cells were plated in 10 ml RPMI-1640 / 10 % FCS per 100 mm tissue culture dish and incubated for 30 minutes at 37°C. Cells were harvested and centrifuged (250 g, 10 min, RT). Dead cells were removed by Nycodenz gradient centrifugation, applying 5×10^6 cells in 1 ml RPMI-1640 on top of 5 ml FCS which were on top of 3 ml Nycodenz. After centrifugation (10 min, 1200 rpm, RT, without brake), cells were collected and washed three times in washing buffer. Cells were counted and stored on ice for experiments.

2.1.4 Endothelial cell culture

2.1.4.1 Preparation of primary endothelial cells

2.1.4.1.1 by collagenase digestion

Brains of mice were prepared and stored on ice in buffer A (153 mM NaCl, 5.6 mM KCl, 2.3 mM $CaCl_2$, 2.6 mM $MgCl_2$, 15 mM HEPES, 1 % (v/v) bovine serum albumine (BSA), pH 7.4). Cerebellum and meninges were carefully removed. Cerebral hemispheres were washed twice with buffer A, cut into small pieces using two scalpels, resuspended in buffer A and centrifuged (250 g, 5 min, RT). The pellet was digested for 30 minutes at 37°C by addition of 1 volume collagenase type II (0.75 %; Biochrome, Berlin, Germany) and 1 volume buffer A (30 min, 37°C, shaking). Digestion was stopped by addition of 40 ml ice-cold buffer A and centrifugation (250 g, 10 min, 4°C). The pellet was carefully resuspended in 20 ml 25 % BSA / PBS and centrifuged (1000 g, 20 min, 4°C) to separate myelin components. Myelin and BSA were decanted and the centrifugation tube thoroughly dried. Pelleted microvessels were carefully resuspended in PBS avoiding any backflow of BSA. Then, cells were either plated on collagen-coated 35 mm tissue culture dishes (see 2.1.4.3) or washed and shock-frozen for gene array (see 2.4.7) or proteomic analysis (see 2.5.7).

2.1.4.1.2 by mechanic separation

Brains of mice were dissected, stored in ice-cold PBS and cerebellum and meninges were carefully removed. Tissue was washed twice with PBS and homogenized using a Dounce homogenizer (Bellco Glass, NJ, USA) with a large clearance pestle. Cell suspension was filtered through a 180 μm nylon mesh, which had been straddled over a beaker and the nylon mesh was washed with PBS. The filtrate was homogenized again, using a small clearance pestle, filtered through a 63 μm nylon mesh and washed again with PBS. Thereby, microvessels got stuck on the nylon mesh and were collected for further experiments.

2.1.4.2 Retroviral infection of primary endothelial cell lines

Primary endothelial cell lines were prepared as described above (see 2.1.4.1.1), cultured over night and then transformed by infection with polyoma middle T oncogene (pymT) transducing recombinant retrovirus. This virus was produced by GP+E86

cells (see 2.1.5) and additionally contained a neomycin resistance gene locus. Virus containing supernatant of these cells had been collected freshly, filter sterilized (0.45 μm) and supplemented with 8 μg/ml polybrene (hexadimethin bromid; Sigma, Deisenhofen, Germany). Endothelial cells were washed twice with PBS, and 2 ml supernatant were added per 35 mm tissue culture dish. This procedure was repeated after 24 hours. 48 hours after virus infection, cells were washed again with PBS and MBE medium was added.

2.1.4.3   Culture of transfected endothelial cells

Transfected endothelial cells were grown on tissue culture dishes or flasks which had been coated with collagen (1:20 in PBS from stock solution: 2.76 mg/ml) for at least one hour and washed twice with PBS just before use. These cells were cultured in MBE medium supplemented with 1 μg/ml G418 until pure endothelioma cell lines were established. They were grown to confluency and then split 4-fold. Therefore, they were washed with PBS/5mM EDTA and digested with 0.05 % Trypsin/EDTA (Invitrogen, Karlsruhe, Germany). Subsequently, cells were centrifuged (250 g, 10 min, RT). Pelleted cells were resuspended in MBE medium and seeded onto new collagen dishes. Once pure endothelioma cultures were established, cells were grown in endothelioma medium on uncoated tissue culture flasks.

2.1.4.4   Culture of endothelioma cell lines

Brain endothelioma cell line 5 (bEnd5) was used as a model system representing wildtype endothelial cells, regarding its generic adhesion molecule expression pattern (Reiss et al., 1998). It had been established by polyoma middle T oncogene expression (pymT) in primary brain microvessels freshly prepared from BALB/c mice (Kiefer et al., 1994; Wagner and Risau, 1994). bEnd5 cells were grown in endothelioma medium to confluency and split 4-fold about every 2 – 3 weeks as described above (see 2.1.4.3). Endothelioma cells were used in experiments during passage 10 to 25.

2.1.4.5   Freezing and thawing of endothelioma cell lines

Endothelioma cells were detached and spun down as described (see 2.1.4.4). Cell pellets were resuspended in freezing medium (DMEM / 30 % (v/v) FCS / 10 % (v/v)

DMSO), put into cryo tubes (Greiner, Nürtingen, Germany) and gently cooled down in Cryo Freezing Containers (Nalgene; Nunc, Wiesbaden, Germany) about 1°C/min to -80°C. They were stored for 2 days at -80°C and then transferred to gaseous liquid nitrogen storage conditions (-179°C). Cells were thawed rapidly, washed in Washing buffer and seeded in tissue culture flasks in endothelioma medium.

2.1.4.6   Preparation of retinal factor

Retinal factor containing endothelial growth factors was prepared as described (D'Amore and Klagsbrun, 1984). Retinas were dissected from 25 bovine eyes (slaughterhouse, Hamm-Uentrop, Germany) and incubated in 25 ml PBS at 4°C over night. After extraction, insoluble components were removed by two successive centrifugation steps (5000 g, 30 min, RT; 30000 g, 30 min, RT). Supernatant was stored in aliquots at -20°C.

2.1.5   GP+E86 cell culture

Virus was produced by GP+E86 cells, which are modified 3T3 fibroblasts. This is a retroviral packaging cell line containing parts of the polyoma virus on two different plasmids (Markowitz et al., 1988). In this present study, the cell line GPE-pymT-neo was used, which produced an ectopic retrovirus, containing the pymT gene as well as a neomycin resistance gene (Williams et al., 1988, 1989). Transfection experiments with established fibroblast cell lines could show, that pymT is the transforming gene of polyoma virus (Treisman et al., 1981) and preferably transforms endothelial cells. GPE-pymT-neo fibroblasts were grown to confluency in endothelioma medium, and then split 5- to 10-fold. For production of virus containing supernatant, GPE-pymT-neo were grown to subconfluency and supernatant was used as described (see 2.1.4.2).

2.1.6   Chemotaxis assay

Chemotaxis assays were performed slightly modified as described (Siveke and Hamann, 1998). Transwell culture inserts (diameter 6.5 mm; pore size 5 μm; Costar, Bodenheim, Germany) were put into a 24-well plate. These inserts were coated with 10 μg/ml fibronectin (Roche, Mannheim, Germany) for 1 hour at 37°C in 7 % CO_2

and air-dried (2 h, RT). Chemokines were diluted in migration assay medium and added in triplicates to the lower chamber in a final volume of 600 μl. 10^5 lymphocytes were added to the upper chamber in 100 μl MAM and chemotaxis assays were incubated (2 h, 37°C, 7 % CO_2). Cells were analyzed by phase contrast microscopy. 500 μl cell suspension were collected from the lower chamber, 20-fold diluted in CASYton (Schärfe System, Reutlingen, Germany) and cell numbers were determined using a CASY TT cell counter (Schärfe System, Reutlingen, Germany).

2.1.7   Transmigration assay

Transmigration of lymphocytes was assayed as described (Rohnelt et al., 1997) Therefore, a two-chamber system was used (see 2.1.6). Filters were coated with 100 μl laminin solution (50 μg/ml; Roche, Mannheim, Germany) for 30 min at room temperature. Unbound laminin solution was aspirated and filter inserts were air-dried (1 h, RT). Then, 4×10^4 endothelioma cells were plated onto the filter inserts and cultured for two days until confluency. Optionally, endothelioma cells were stimulated for 16 hours with TNF-α (5nM; Cell Concept, Freiburg, Germany). Chemokines were added in 600 μl MAM into the lower chamber, 10^5 lymphocytes were added in 100 μl MAM into the upper chamber and cells were incubated (4 h, 37°C, 7 % CO_2). During this time lymphocytes spontaneously migrated through the endothelial monolayer. Afterwards, filter inserts were removed, 500 μl of the cell suspension from the lower chamber were 20-fold diluted in CASYton and cell numbers was measured using a CASY TT cell counter. Filter inserts were washed with cold PBS, fixed for 2 hours in formalin gas phase, stained with 2.6 % (v/v) Giemsa, air-dried over night and mounted. Endothelial monolayer confluency was analyzed by light microscopy. All values were determined in triplicates.

2.1.8   Frozen section assay

Frozen section assays using a modified version of the original Stamper-Woodruff protocol (Stamper and Woodruff, 1976) were performed as described before (Steffen et al., 1994). Brain sections from mice afflicted with EAE were freshly cut and air-dried (2 h, RT).

Meanwhile, T lymphocytes were either desensitized by preincubation with high

chemokine concentrations (10 μg/ml; 30 min, 37°C) or pretreated with pertussis toxin (Sigma, Deisenhofen, Germany) followed by washing 3 times in washing buffer as described (Warnock et al., 1998). 10^6 encephalitogenic T lymphocytes were applied per cryo section under rotation (30 min, RT). Alternatively, brain sections were preincubated with blocking chemokine antibodies or normal goat IgG (100 μg/ml) as a control for 30 minutes. 10^6 untreated encephalitogenic T lymphocytes were applied per section (30 min, RT).

Slides were extremely gently put upside-down into 2.5 % glutaraldehyde on ice, fixed for 2 hours, washed twice in PBS and counterstained (0.5 % toluidine blue, 20 % ethanol). Sections were analyzed by counting the number of T lymphocytes specifically bound to cerebral vessels.

2.1.9 Cytospin

Cytospins of T lymphoblasts were performed in a Cytospin 3 (Thermo Shandon, PA, USA). PLP-specific T lymphoblasts (2×10^5) were suspended in 50 μl RPMI-1640 / 20 % FCS, placed in one cytocentrifuge assembly funnel and centrifuged at 700 rpm for 5 min exactly according to the manufacturer's protocol. Slides were air-dried over night, fixed with acetone and stained as described (see 2.3.3).

2.1.10 Flow cytometry

2.1.10.1 Analysis of cell surface epitopes by antibody binding

Flow cytometry was used for phenotypic analysis of endothelial cells and T cells. Adhering cells were detached by incubation in HBSS / 25mM HEPES / 5mM EDTA, resuspended in washing buffer and centrifuged (250 g, 10 min, RT). Suspension cells were collected and centrifuged (250 g, 10 min, RT). Cells were then resuspended in flow cytometry (FC) buffer (PBS / 2.5 % (v/v) CS / 0.1 % NaN$_3$) and 10^5 cells were added per well in a 96-well U-shaped microtiter plate on ice. Cells were washed twice in FC buffer and incubated for 30 minutes in 100 μl primary antibody solution. This was either hybridoma cell supernatant or purified antibodies diluted in PBS (10 μg/ml). Then, cells were washed twice in 200 μl FC buffer and centrifuged (300 g, 3 min, 4°C). Cells were incubated with phycoerythrin (PE)-conjugated goat-anti-rat IgG (10 μg/ml; Jackson Laboratories; Dianova, Hamburg, Germany) which had

been preincubated with 10 % NMS (see 2.3.1.5) to block unspecific binding. After washing twice, like described before, cells were fixed in 1 % PFA/PBS and analyzed by FACScan and CellQuest software (BDBiosciences, Heidelberg, Germany).

2.1.10.2   Analysis of cell surface sugar epitopes by lectin binding

Carbohydrate structures were detected by there binding to biotin-conjugated lectin molecules (see 2.3.1.4). These were used instead of primary antibodies (see 2.1.10.1) and were detected using PE-conjugated streptavidin (1:500; Jackson; Dianova, Hamburg, Germany).

2.1.10.3   Detection of fluorescently labeled cells

Cells which had been labeled with CellTrackerGreen (see 2.1.3.9) were detected by flow cytometrical analysis. These cells were additionally stained as described (see 2.1.10.1). Therefore, a maximum of 10^7 cells were stained per ml antibody solution.

2.2   Animal models

2.2.1   Experimental autoimmune encephalomyelitis

2.2.1.1   active EAE in SJL/N mice

Induction of active EAE in SJL/N mice was essentially done as described in great detail before (Engelhardt et al., 1998; Laschinger and Engelhardt, 2000). SJL/N mice (Taconic, Ry, Denmark) were immunized subcutaneously into the footpads with 50 μg PLP$^{139-151}$ (Thermo Electron Corporation, Egelsbach, Germany) in CFA. One and three days after immunization, 3×10^9 heat-inactivated organisms of *Bordetella pertussis* were injected intravenously (kindly provided by Dr. Blackolb, Chiron-Behring, Marburg, Germany). Weight and clinical disease were checked daily and scored as follows:

    0.5 limp tail
      1 hind leg weakness
      2 hind leg paralysis
      3 hind leg paraparesis and incontinence
      4 death

A schematic overview is given in Figure 2.2.1.
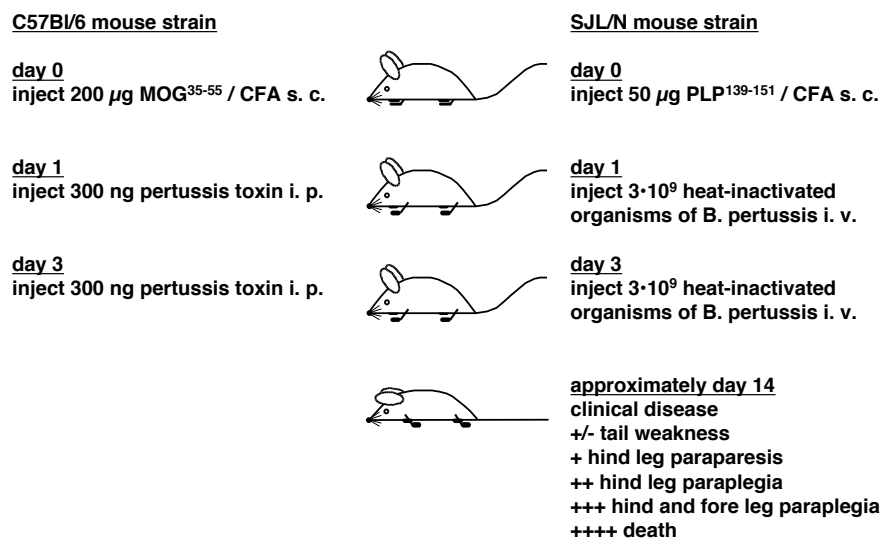
Figure 2.2.1: active EAE in C57Bl/6 and SJL/N mice

2.2.1.2   active EAE in C57Bl/6 mice

C57Bl/6 mice were immunized subcutaneously with 200 μg MOG$^{35-55}$; Thermo Electron Corporation, Egelsbach, Germany) in complete Freund's adjuvant (see 2.2.1.1) subcutaneously in the footpads, hind legs and tailroot. One and three days after immunization, 300 ng pertussis toxin were applied intraperitoneally (Sigma, Deisenhofen, Germany). Weight and clinical disease were checked daily and scored (see 2.2.1.1). A schematic overview is given in Figure 2.2.1.

2.2.1.3   transfer EAE

Established antigen specific T cell lines (see 2.1.3) were tested for their ability to induce EAE in syngeneic recipient mice. Therefore, 3×10^6 freshly activated T lymphoblasts were in PBS and injected i. v. into 8 – 12 week old syngeneic recipient mice (day 1). Weight and clinical disease score was measured daily and scored as described above (see 2.2.1.1). Typically, first signs of clinical disease appeared around day 5 – 7 after immunization.

2.2.2   Intravital microscopy

2.2.2.1   Preparation of the spinal cord window

Preparation of the spinal cord window was done by Dr. Peter Vajkoczy (Klinikum
Mannheim at the University of Heidelberg, Germany) as described (Vajkoczy et al.,
2001). 15 – 20 week old female SJL/N mice were anesthetized by injection of
2.5 mg/kg ketamine and 7.5 mg/kg xylazine subcutaneously. A polyethylene
catheter (PE-10) was inserted into the right common carotid artery of a thermo-
controlled mouse placed on a heating pad, to allow systemic administration of flu-
orescent markers and injection of cells. Then, the animal was turned to the prone
position so that the head could be fixed in a stereotactic rodent head holder. After
a 3 – 4 cm midline skin incision, paravertebral musculature was detached from the
cervical spinous processes and retracted laterally, so that the vertebral laminae were
exposed. Microsurgical techniques were used to perform a laminectomy of C1 –
C7. The dura was opened over the dorsal spinal cord while taking care to avoid
trauma to the parenchyma and the spinal cord microvasculature. Dehydration was
prevented and ambient oxygen excluded by covering the site with an impermeable
transparent membrane. Mice which had been traumatized during surgery or devel-
oped signs of acute inflammation such as distorted vessels, hyperemia or stagnant
blood flow, were excluded from the experiments.

2.2.2.2   Intravital fluorescence videomicroscopy

The animals remained within the stereotactic head holder which was transferred to
the microscope stage to perform intravital fluorescence videomicroscopy. Therefore,
epiillumination techniques were applied using a modified Axiotech Vario microscope
(Attoarc; Zeiss, Oberkochen, Germany) with a 100 W mercury lamp emitting an
adjustable light intensity, being attached to a combined blue (450 – 490 nm) and
green (520 – 570 nm) filter block (Zeiss, Oberkochen, Germany). Observations were
made using $3.2\times$ long-distance, $10\times$ long-distance and $20\times$ water immersion working
objectives (Zeiss, Oberkochen, Germany), which resulted in magnifications of $50\times$,
$200\times$ and $400\times$. Microscopic images were recorded using a low-light level charged
coupled device video camera with an optional image intensifier for weak fluorescence
(Kappa Opto-Electronics, Gleichen, Germany), which were transferred to an S-VHS

videosystem (Panasonic, Hamburg, Germany) for slow-motion off-line evaluation.

100 μl 2 % FITC-conjugated dextrane (MW = 150,000; Sigma, Deisenhofen, Germany) were injected to visualize spinal cord microvasculature by contrast enhancement using blue-light epiillumination. Approximately 1 min after injection, FITC-conjugated dextrane was equally distributed within the vascular system. Simultaneously, CTrO-labeled T cell blasts (see 2.1.3.9) were injected and visualized within the spinal cord microcirculation using greenlight epiillumination. By combination of these two fluorescent markers with distinct excitation wavelengths, CTrO-labeled T cell blasts could be localized with respect to FITC-stained vessel luminae. After visualization of spinal cord microvasculature by FITC-conjugated dextrane, 3×10^6 CTrO-labeled PLP-specific T cell blasts were injected in aliquots of 100 μl, containing 10^6 T cells each. Their interaction with the endothelium was observed for 60 seconds within the spinal cord capillary bed and postcapillary venules (20 – 60 μm) of three different regions of interest. In contrast to this, T cell blast/endothelial interaction within precapillary arterioles could not be visualized by intravital fluorescence videomicroscopy due to the architecture of the spinal cord microvasculature, as precapillary arterioles are located deep in the spinal cord parenchyma. Permanent T lymphoblast adhesion to spinal cord microvasculature was assessed by scanning 10 minutes, 1 hour, and 2 hours after cell injection and is expressed as the number of both adherent and plugging T lymphoblasts per region of interest (mm^2).

2.2.2.3   Intravital microscopic image analysis

Spinal cord microcirculation was quantitatively analyzed by measuring the diameter d of postcapillary venules and the velocity v of nonadherent T lymphoblasts. The highest cell velocity per vessel segment, v_{max}, was used to calculate the mean blood flow velocity v_{mean} as described previously: $v_{mean} = v_{max}/(2 - \epsilon^2)$ ($\mu m/s$) (Ley and Gaehtgens, 1991). ϵ is the ratio of T lymphoblast diameter to vessel diameter d. Using Hagen-Poiseuille's law, the wall shear rate γ was estimated as $\gamma = 8 \times v_{mean}/d$ (s^{-1}) (Ley and Gaehtgens, 1991). Shear stress (τ) was approximated $\tau = \lambda \times 0.025 poise$ (dyn/cm^2) (Von Andrian et al., 1992). Assuming a parabolic velocity profile in the microvessel, nonpermanently adherent T lymphoblasts were further categorized (Ley and Gaehtgens, 1991). Therefore, the veloc-

ity v_{crit} of an idealized noninteracting cell traveling at the vessel wall was calculated as $v_{crit} = v_{mean} \times \epsilon \times (2 - \epsilon)$. This means, that the normalized velocity v_{norm} of an individual cell, which was defined as the ratio $v_{norm} = v/v_{crit}$ is an indicator if an individual cell was interacting with the vessel wall. If this ratio v_{norm} was smaller than 1, the individual cell was traveling below v_{crit} and therefore regarded as a cell interacting with the vessel wall. If v_{norm} was larger than 1, the individual cell was traveling with a velocity higher than v_{crit} and therefore regarded as not interacting with the vessel wall (Ley and Gaehtgens, 1991; Robert et al., 1999). Looking at the capillary network, plugging T lymphoblasts were defined as cells that did not move and obviously blocked the capillary lumen, as evident by induction blood flow stasis in the corresponding vascular segment.

2.2.2.4 Detection of T lymphoblasts in the spinal cord by immunofluorescence

T lymphoblasts were detected in the spinal cord by immunofluorescence to distinguish localization within or outside the blood vessels. Therefore, mice were perfused with 1 % paraformaldehyde in PBS 6 hours after injection of the PLP-specific T cell blasts. Spinal cords were prepared as described (see 2.3.2). Serial longitudinal 6 μm cryosections of the spinal cords were cut, air-dried overnight and fixed in acetone (10 min, -20°C). CTrO-labeled T lymphoblasts were detected by immunofluorescence microscopy. Localization of CTrO-labeled T lymphoblasts could only be judged after visualization of vessels by immunofluorescence with an endothelial cell specific antibody. Therefore, the vessels were stained with the monoclonal antibody MJ7/18 (see 2.3.1.1), followed by a FITC-labeled goat-anti-rat antiserum (Jackson; Dianova, Hamburg, Germany), mounted and immediately analyzed (see 2.3.4). The number of cells within or outside of vessels were counted manually. Serial sections had to be analyzed to carefully determine if a CTrO-labeled T lymphoblast is located within a spinal cord microvessel or has already migrated into the brain parenchyma.

2.3 Morphological methods

2.3.1 Reagents

2.3.1.1 Monoclonal antibodies

Tissue culture supernatants of the following rat-anti-mouse hybridoma cells were either used directly or as purified monoclonal antibodies for flow cytometry, immunohistochemistry or immunofluorescence (see 2.1.10, 2.3.3, 2.3.4).

antibody	antigen	isotype	source	reference
10E9.6	E-selectin	IgG2a	BDBiosciences, Heidelberg, Germany	Bosse and Vestweber (1994)
11D4	VE-Cadherin	IgG2a	D. Vestweber, Münster, Germany	Gotsch et al. (1997)
25ZC7	ICAM-1	IgG2a	D. Vestweber, Münster, Germany	Steffen et al. (1996)
3C4	ICAM-2	IgG2a	BDBiosciences, Heidelberg, Germany	Xu et al. (1996)
4RA10	PSGL-1	IgG1	D. Vestweber, Münster, Germany	Pendl et al. (2002)
9B5	human CD44	IgG2a	E. C. Butcher, Stanford, CA, USA	Jalkanen et al. (1986)
9DB3	VCAM-1	IgG2a	D. Vestweber, Münster, Germany	Hahne et al. (1994)
BV11	JAM-A	IgG2b	E. Dejana, Milano, Italy	Del Maschio et al. (1999)
GK1.5	CD4	IgG2b	ATCC, Rockville, MD, USA	Wilde et al. (1983)
Lyt-2	CD8	IgG2a	ATCC, Rockville, MD, USA	ATCC, Rockville, MD, USA
M1/70	α_M-integrin	IgG2b	ATCC, Rockville, MD, USA	ATCC, Rockville, MD, USA
M1/9	CD45	IgG2a	ATCC, Rockville, MD, USA	Springer et al. (1978)
Mec13.3	PECAM-1	IgG2a	ATCC, Rockville, MD, USA	Vecchi et al. (1994)
MECA32	MECA32 antigen	IgG2a	E. C. Butcher, Stanford, CA, USA	Hallmann et al. (1995)
MECA367	MAdCAM-1	IgG2a	ATCC, Rockville, MD, USA	Briskin et al. (1993)
MECA79	PNAd	IgM	E. C. Butcher, Stanford, CA, USA	Streeter et al. (1988)
Mel-14	L-selectin	IgG2a	E. C. Butcher, Stanford, CA, USA	Gallatin et al. (1983)
M1/70	$\alpha_M\beta_2$-integrin	IgG2b	ATCC, Rockville, MD, USA	Springer et al. (1978)
MJ7/18	Endoglin	IgG2a	E. C. Butcher, Stanford, CA, USA	Ge and Butcher (1994)
RA3-6B2	CD45R / B220	IgG2a	BDBiosciences, Heidelberg, Germany	Coffman (1982)
RB40	P-selectin	IgG1	D. Vestweber, Münster, Germany	Bosse and Vestweber (1994)
RB6-8C5	Gr-1	IgG2b	BDBiosciences, Heidelberg, Germany	Fleming et al. (1993)
UZ4	E-selectin	IgM	R. Hallmann, Erlangen, Germany	Hammel et al. (2001)
V3C10	ICAM-2	IgG2a	D. Vestweber, Münster, Germany	unpublished
7-188	VAP-1	IgG2b	S. Jalkanen, Turku, Finland	unpublished

2.3.1.2   Polyclonal antisera

serum	antigen	species	source	dilution
AF880	mouse CCL19	goat	R&D, Wiesbaden, Germany	10–20 μg/ml
AF457	mouse CCL21	goat	R&D, Wiesbaden, Germany	10–20 μg/ml
P114	mouse CCL21	rabbit	Peprotech, London, UK	10 μg/ml
A-19	mouse CCR7	goat	Santa Cruz, Heidelberg, Germany	20 μg/ml
Y-16	mouse CXCR3	goat	Santa Cruz, Heidelberg, Germany	20 μg/ml
C-16	mouse $G_{\beta 2}$	rabbit	Santa Cruz, Heidelberg, Germany	10 μg/ml
C-20	human RACK1	goat	Santa Cruz, Heidelberg, Germany	10 μg/ml
F-16	human hnRNP A2/B1	goat	Santa Cruz, Heidelberg, Germany	10 μg/ml

2.3.1.3   Secondary antisera

Polyclonal secondary antisera used in this present work are listed with their respective antigen specificity, conjugates, used dilution and the source they were obtained from.

species	antigen	conjugate	dilution	source
goat	rabbit IgG	biotin	1 drop / 10 ml PBS (2 % GNS; 2 % MNS)	Vector; Linaris, Wertheim, Germany
donkey	goat IgG	biotin	1:1000 in PBS	Jackson Laboratories; Dianova, Hamburg, Germany
goat	rat IgG	biotin	1 drop / 10 ml PBS (2 % GNS; 2 % MNS)	Vector; Linaris, Wertheim, Germany
goat F(ab')$_2$	rat IgG	FITC	1:200 / in PBS (2 % MNS)	Jackson Laboratories; Dianova, Hamburg, Germany
goat F(ab')$_2$	rat IgG	PE	1:200 / in PBS (2 % MNS)	Biosource; Camarillo, CA, USA

2.3.1.4 Lectins

Lectins are listed with their preferred binding specificity and their concentrations (conc.) used in this present work.

lectin	preferred binding specificity	conc.
Maackia amurensis lectin II	(α-2,3)-sialylgalactose residues	10 μg/ml
Sambucus nigra lectin	(α-2,6)-sialylgalactose residues	10 μg/ml
Griffonia simplicifolia lectin I	α-galactose residues	10 μg/ml

2.3.1.5 Normal mouse serum preparation

Normal mouse serum was prepared from healthy mice. Therefore, mice were anesthetized and blood was taken intracardially. Blood samples were collected at room temperature, incubated at 37°C for 15 minutes, put on ice for 5 minutes and centrifuged (3200 g, 10 min, 4°C). Serum was stored at -20°C.

2.3.1.6 Preparation of Mowiol solution

Mowiol solution was used as a mounting medium to prevent bleaching of fluorescent dyes and was prepared as follows. 6 g glycerol and 2.4 g Mowiol type 4-88 were stirred in a 50 ml tube. 6 ml ddH$_2$O were added and mixed on a rotary shaker for 2 hours. 12 ml 200 mM Tris-HCl pH 8.5 were added and incubated for 10 minutes at 50°C. After cooling down to room temperature, it was centrifuged (5000 rpm, 15 min). Pellet was discarded and supernatant stored at -20°C.

2.3.1.7 Preparation of silanized slides

Slides (Marienfeld; VWR, Darmstadt, Germany) were silanized to prevent detachment of tissue sections. Therefore, they were degreased for 5 minutes in acetone and coated for 5 minutes with 2 % 3-aminopropyltriethoxysilane (TESPA) in acetone. Then, they were washed three times for 5 minutes in acetone and air-dried for at least 1 hour.

2.3.2   Tissue preparation and sectioning

Mice were anesthetized with isoflurane (CuraMED, Karlsruhe, Germany) and intra-cardially perfused with either ice-cold sterile PBS or ice-cold filtered 1 % PFA in PBS. Then, tissues were taken out and embedded in Tissue-Tek (Sakura Finetek; Vogel, Gießen, Germany) in cryo-molds (Miles Inc; Vogel, Gießen, Germany) and slowly frozen in isopentane, which had been cooled down with dry-ice. Tissues were stored at -80°C. Before sectioning, tissue blocks were warmed-up to -20°C for 30 minutes and frozen onto the blockholder with Tissue-Tek. Block temperature was -16°C. 6 μm sections were prepared and collected on silanized slides (see 2.3.1.7). Sections were dried for 14 – 16 hours at room temperature and fixed in acetone (10 min, -20°C). After drying for 30 minutes at room temperature, they were either directly used or stored in presence of silicagel at -20°C.

2.3.3   Immunohistochemistry

For immunohistochemical staining, slides were either used directly after fixation with acetone, or thawed on silicagel (30 min, RT), fixed in acetone (10 min, -20°C) and air-dried (30 min, RT). Sections were delimited using a PAP pen (DakoCytomation, Hamburg, Germany) to reduce the amount solution needed to completely cover the section. Volume ranged from 50 – 100 μl per section. Slides were hydrated with PBS for 5 minutes in a humid chamber and unspecific binding sites were blocked by 15 min treatment with normal serum, whose originating species depended on the primary antibody used (Table 2.3.2). Serum was removed and primary antibody (see 2.3.1.1 and 2.3.1.2) was added (30 min, RT). Sections were washed for 1 min with PBS and for 5 min PBST (PBS/0.1 % Tween 20). Meanwhile, the secondary antibody was preincubated with normal mouse serum for 30 minutes (Table 2.3.2) and then applied to the sections for 30 minutes. Sections were washed as before and incubated with SA/HRP (VectorStain Kit; Vector; Linaris, Wertheim, Germany) for 30 minutes. After additional washing, 3-amino-ethyl-carbazol (AEC Kit; Vector; Linaris, Wertheim, Germany) was added and incubated for 5 – 10 minutes until staining became detectable by light microscopy. Sections were washed, counterstained with hematoxyline, Gill I (Sigma, Deisenhofen, Germany) for 30 seconds and mounted with Aquatex (Merck, Darmstadt, Germany). Sections were analyzed

by bright field microscopy.

primary antibody species	blocking reagent	secondary antibody
rabbit	NGS	goat-anti-rabbit
goat	NRbS	donkey-anti-goat
rat	90 % NGS / 10 % NRbS	goat-anti-rat

Table 2.3.2: For immunohistochemical stainings, blocking reagent and secondary antibody were chosen depending on the origin of the primary antibody.

2.3.4 Immunofluorescence

For immunofluorescent staining of histological sections, sections were treated as described until primary antibody was applied and sections were washed (see 2.3.3). A secondary antibody directly conjugated to a chromophore (see 2.3.1.3) was preincubated with 2 % NMS and 2 % NGS in PBS to block unspecific binding. Sections were incubated light-protected with this antibody (30 min, RT) and washed with PBS (1 min, RT) and PBST (5 min, RT). Then, slides were mounted with Mowiol solution (see 2.3.1.6) and analyzed by fluorescent light microscopy.

Alternatively, biotinylated lectins (see 2.3.1.4) were used instead of the primary antibodies and detected with Cy3-conjugated strepatividin instead of the secondary antibody. As a control, sections were pretreated with *Clostridium perfringens*-derived sialidase (acylneuraminyl hydrolase EC 3.2.1.18) in 50 mM sodiumacetate pH 4.5 / 100 μg/ml BSA for 2 hours, to remove (α-2,3)-sialylgalactose residues.

2.3.5 *In situ* hybridization

While performing this method, strict usage of gloves and careful cleaning of work spaces with 70 % ethanol was substantial. Glass ware was either baked or treated with 0.1 % sodium hydroxide solution to prevent RNAse contaminations.

2.3.5.1 Buffers and solutions

2.3.5.1.1 Transcription buffer

In vitro transcription was performed in transcription buffer containing 40 mM Tris-HCl pH 8.0, 8 mM $MgCl_2$, 50 mM NaCl and 2 mM spermidin.

2.3.5.1.2   Pronase self-digestion

Pronase (Roche, Mannheim, Germany) was carefully solved in pronase buffer (50 mM Tris-HCl pH 7.5, 5 mM EDTA) and inactivated by self-digestion for 4 hours at 37°C. Aliquots were stored at -20°C.

2.3.5.1.3   Hybridization buffer

Hybridization buffer was prepared and stored in aliquots at -80°C.

10 %	dextrane sulfate
50 %	formamide
10 mM	Tris-HCl pH 7.5
10 mM	sodiumphosphate pH 6.8
5 mM	EDTA
2 ×	SSC (3 M NaCl, 0.3 M sodiumcitrate pH 7.0)
150 μg/ml	yeast tRNA
100 mM	UTP

Hybridization buffer was stored at -80°C. Before use, 1 % (v/v) each of 100 mM ADPβS, 1 mM ATPγS, 1 M DTT and 1 M β-mercaptoethanol were added.

2.3.5.2   Pretreatment of slides

Slides (Marienfeld; VWR, Darmstadt, Germany) were cleaned with 70 % ethanol and baked at 180°C for 6 hours. Afterwards, they were coated with TESPA as described to prevent detachment of tissue sections (see 2.3.1.7). Slides were protected from dust and stored at room temperature until use.

2.3.5.3   Tissue section preparation

Tissues were prepared from mice, which had been perfused with 1 % PFA/PBS (see 2.3.2) and 10 μm sections were prepared. These sections were air-dried on a heating plate (5 min, 50°C), fixed in 4 % PFA / PBS (20 min, RT), washed in PBS (5 min, RT) and dehydrated in ethanol (30 %, 60 %, 80 %, 95 %, 100 %) for 2 minutes each. Slides were air-dried dust-covered for 1 hour and stored in presence of silicagel at -80°C.

2.3.5.4   RNA probe preparation

2.3.5.4.1   DNA-linearizing

cDNA inserts had to be located in plasmids containing promoters for two different RNA polymerases. Plasmids were linearized using either of two different restriction enzymes in such a way, that transcription stopped after transcribing the insert cDNA. Therefore, 5 μg DNA were digested with 20 U restriction endonuclease in a total volume of 50 μl for 2 hours. Complete linearization was tested by agarose gel electrophoresis of 2 μl (see 2.4.2.6) and subsequently, DNA was purified using the Qiagen MinElute PCR purification kit (Qiagen, Hilden, Germany). Therefore, samples were mixed with 5 volumes buffer PB (recipe not provided by the manufacturer) and applied to MinElute columns, so that DNA could bind to the columns. Columns were centrifuged (13000 rpm, 1 min, RT) and flowthrough was discarded. Columns were washed with 750 μl PE (recipe not provided by the manufacturer) and centrifuged twice (13000 rpm, 1 min, RT) to thoroughly wash and dry the columns. They were put into new microcentrifuge tubes, 10 μl prewarmed ddH$_2$O were added, incubated for 1 min and centrifuged (13000 rpm, 1 min, RT). 0.5 μl solution were analyzed on the same agarose gel like used before, comparing it with the previously tested probe to check DNA loss. Linearized DNA samples were stored at -20°C until use.

2.3.5.4.2   *In vitro* transcription

^{35}S labeled RNA samples were prepared by *in vitro* transcription using the following reaction mix.

2.0 μl   10× transcription buffer (Stratagene, Amsterdam, The Netherlands)

1.0 μl   template DNA (500 ng/μl)

1.0 μl   100 mM DTT

0.5 μl   RNAguard (37.3 U/μl; Amersham Biosciences, Freiburg, Germany)

0.5 μl   10 mM ATP, CTP, GTP (Amersham Biosciences, Freiburg, Germany)

4.5 μl ^{35}S-UTPαS (10 μCi/μl; Amersham Biosciences, Freiburg, Germany)

0.7 μl   RNA polymerase (10 U/μl; Stratagene, Amsterdam, The Netherlands)

Reaction mixes were incubated for 90 minutes at 37°C. Subsequently, template DNA was digested with RNAse-free DNAse I (Roche, Mannheim, Germany) in

10 mM MgCl$_2$ (10 min, 37°C). RNA was purified by affinity chromatography using a PCR purification kit (Qiagen, Hilden, Germany). Therefore, 5 volumes buffer PB were added and mixed. Probes were applied to PCR purification columns and centrifuged (13000 rpm, 1 min, RT). Columns were washed with 750 μl PE and centrifuged twice (13000 rpm, 1 min, RT). 50 μl ddH$_2$O were added, incubated for 1 minute and RNA was eluted by centrifugation (13000 rpm, 1 min, RT).

2.3.5.4.3   Alkaline hydrolyzis

RNA probes which exceeded 500 bp in size had to be hydrolyzed to guarantee specific binding. Duration of hydrolyzis was dependent on the size of the RNA probe, meaning 1 min hydrolysis being necessary per 200 bp RNA probe length, i. e. 5 min hydrolysis for a 1000 bp probe. Probes were diluted in a total volume of 100 μl ddH$_2$O. Alkaline hydrolysis was performed on ice by addition of a tenth volume 2 M sodiumhydroxide solution and stopped by neutralization with a tenth volume of 2 M acetic acid. RNA was precipitated by addition of 4 μl tRNA (50 mg/ml; Roche, Mannheim, Germany), 50 μl 6 M ammonium acetate and 500 μl 100 % ethanol at -20°C for at least 60 minutes. Then, samples were centrifuged (13000 rpm, 30 min, RT) and supernatant was carefully removed. Precipitates were air-dried and solubilized in 50 μl ddH$_2$O.

2.3.5.4.4   Detection of RNA probe activity

50 μl RNA probe solution was supplemented with 50 μl formamide and 1 μl 1 M DTT. 1 μl of this solution was diluted in 2 ml scintillation liquid (Lumasafe; Lumac LSC, Groningen, The Netherlands) and radioactivity was measured by β-scintillation counting (LS-6500; Beckman-Coulter, Unterschleißheim, Germany). Probes were either used directly or stored at -20°C for up to 1 week.

2.3.5.5   Hybridization

Slides were transferred to room temperature in presence of silicagel for at least 1 hour to thaw from -80°C. Then, sections were pretreated for RNA probe hybridization at room temperature unless otherwise stated. Therefore, they were hydrated in ddH$_2$O (1 min), incubated in 2$\times$ SSC (3 M NaCl, 0.3 M sodiumcitrate pH 7.0; 30 min, 70°C) and washed in ddH$_2$O (1 min). Subsequently, they were digested with pronase

(40 μg/ml; see 2.3.5.1.2) in pronasebuffer (50 mM Tris-HCl pH 7.5, 5 mM EDTA) for 10 min, digestion was stopped in 0.2 % glycine (30 s) and washed in PBS (30 s). Sections were fixed with freshly prepared 4 % PFA/PBS (20 min, RT), washed in PBS (3 min), treated with 0.25 % acetic anhydride in 0.1 M triethanolamine and washed with PBS again (2 min). Sections were dehydrated with ascending concentration of ethanol (30 %, 60 %, 80 %, 95 %, 100 %; 2 min each) and air-dried for 1 hour. Slides were prewarmed in a hybridization oven at 60°C in 50 % formamide humid chambers, while radioactively labeled RNA probes were diluted in hybridization buffer to 25000 cpm/μl. Probes were denaturated (2 min, 95°C) and immediately applied to the sections. Sections were covered with parafilm (American National Can; VWR, Darmstadt, Germany). Once all probes were applied, slides were incubated for 10 minutes at 60°C. Then the hybridization oven was set to 48°C, so that temperature would slowly decrease over night. Hybridization was performed for 14 – 16 hours.

2.3.5.6 Washing

Sections were washed in washing buffer (50 % formamide, 2× SSC, 10 mM β-mercaptoethanol) while steadily shaking (3 – 4 h, 37°C) until parafilms floated off. Then, they were washed in RNAse buffer (500 mM NaCl, 10 mM Tris-HCl pH 7.5, 1 mM EDTA) for 20 minutes at 37°C, single strand RNA was digested in RNAse buffer supplemented with 20 μg/ml RNAse (Roche, Mannheim, Germany; 20 min, 37°C) and sections were washed again in RNAse buffer (20 min, 37°C). Subsequently, they were washed in washing buffer, supplemented with 5 mM DTT for 16 – 18 hours. Then sections were dehydrated in ascending concentrations of ethanol (30 %, 60 %, 80 %, 95 %, 100 %; 2 min each) and air-dried.

2.3.5.7 Exposition

Slides were exposed on a high resolution phosphoimager screen (Fujifilm; Raytest, Straubenhardt, Germany). Screen was analyzed after 24 hours to evaluate signal intensity and thereby estimate the subsequent exposure time. Exposure times usually ranged from 2 – 6 weeks. In a darkroom, photoemulsion NTB-2 (Kodak, Stuttgart, Germany) was emulsified in an equal amount of water, warmed to 42°C and 190 μl emulsion were applied per slide. Slides were air-dried for 3 – 4 hours and then stored

lightprotected in presence of silicagel at 4°C.

2.3.5.8   Development and counterstain

After 2 – 6 weeks, slides were warmed to room temperature for 1 hour. In darkroom, they were developed in Kodak D19 developer solution for 3 minutes. Developing reaction was stopped 1 % acetic acid for 30 secs and fixed in 30 % sodium thiosulfate for 3 minutes. Slides were washed for 15 minutes with tap water, counterstained with 0.2 % toluidine blue in 0.2 M sodiumacetate pH 4.2 for 3 minutes, washed in tap water, destained in PBS, desalted with ddH$_2$O, air-dried for 1 hour and mounted with entellan (Merck, Darmstadt, Germany).

2.3.5.9   Analysis

Sections were analyzed by dark and bright field microscopy.

2.4   Molecular Biology

2.4.1   Buffers and Solutions

2.4.1.1   Restriction endonuclease buffers

Restriction endonuclease buffers were purchased from New England Biolabs (Schwalbach, Germany).

2.4.1.1.1   NEBuffer 1 (yellow)

NEBuffer 1 contained 10 mM Bis Tris Propane-HCl, 10 mM MgCl$_2$ and 1 mM dithiothreitol (pH 7.0 at 25°C).

2.4.1.1.2   NEBuffer 2 (blue)

NEBuffer 2 contained 250 mM NaCl, 10 mM Tris-HCl, 10 mM MgCl$_2$ and 1 mM dithiothreitol (pH 7.9 at 25°C).

2.4.1.1.3   NEBuffer 3 (red)

NEBuffer 3 contained 100 mM NaCl, 50 mM Tris-HCl, 10 mM MgCl$_2$ and 1 mM dithiothreitol (pH 7.9 at 25°C).

2.4.1.1.4 NEBuffer 4 (green)

NEBuffer 4 contained 50 mM potassium acetate, 20 mM Tris-acetate, 10 mM magnesium acetate and 1 mM dithiothreitol (pH 7.9 at 25°C).

2.4.1.2 Luria-Bertani (LB) medium

20 g LB-broth (corresponding 10 g bacto-trypon, 5 g bacto-yeast extract, 10 g NaCl, pH 7.0; Invitrogen, Karlsruhe, Germany) were solved in 1 l ddH_2O and autoclaved.

2.4.1.3 LB-agar

1 l LB medium was supplemented with 15 g bacto-agar (BDBiosciences Difco, Heidelberg, Germany) and autoclaved.

2.4.1.4 DNA preparation buffers

DNA preparation buffers were purchased from Qiagen (Hilden, Germany).

2.4.1.4.1 Resuspensionbuffer P1

Resuspensionbuffer P1 contained 50 mM Tris-HCl pH 8.0, 10 mM EDTA and 100 μg/ml RNAse A.

2.4.1.4.2 Lysisbuffer P2

Lysisbuffer P2 contained 200 mM NaOH and 1 % (w/v) SDS.

2.4.1.4.3 Neutralizationbuffer P3

Neutralizationbuffer P3 contained 3 M potassiumacetate pH 5,5.

2.4.1.4.4 Equilibrationbuffer QBT

Equilibrationbuffer QBT contained 750 mM NaCl, 50 mM MOPS pH 7.0, 15 % isopropanol and 0,15 % triton X-100.

2.4.1.4.5 Washbuffer QC

Washbuffer QC contained 1 M NaCl, 50 mM MOPS pH 7.0 and 15 % isopropanol.

2.4.1.4.6   Elutionbuffer QF

Elutionbuffer QF contained 1.25 mM NaCl, 50 mM Tris-HCl pH 8.5 and 15 % isopropanol.

2.4.1.5   Sequencing and PCR primers

DNA oligonucleotides used as primers for sequencing and PCR are listed with their sequences and annealing temperatures (T_{AN}).

Primer	sequence	T_{AN}
D1	5'-GCTAGATGTCCTGACTGTCC-3'	58°C
D2	5'-CCAGTAGCCCAGGTTGCATA-3'	58°C
Dneo	5'-TATGGCGCGCCATCGATCTC-3'	58°C
M13rev	5'-TTCACACAGGAAACAGCTATGACC-3'	55°C
ME18Sfw	5'-CTTCTGCTCTAAAAGCTGCG-3'	55°C
ME18Srev	5'-CGACCTGCAGCTCGAGCA-3'	60°C
SP6	5'-ATTTAGGTGACACTATAGAATA-3'	50°C
T3	5'-AATTAACCCTCACTAAAGGG-3'	55°C
T7	5'-GTAATACGACTCACTATAGGGC-3'	55°C
Tie1fw	5'-CGAAGGGATGGGAGAGAGAGC-3'	58°C
Tie1rev	5'-TGACGCTATGACGACGACGAT-3'	58°C

2.4.1.6   Vectors

The following vectors were used in this present work:

pBS-SK . . . .   Stratagene, Amsterdam, The Netherlands

pBSII-KS+ . . . .   Stratagene, Amsterdam, The Netherlands

pBSII-SK+ . . . .   Stratagene, Amsterdam, The Netherlands

pT7T3D-Pac . . . . . .   Amersham Biosciences, Freiburg. Germany

pGEM3 . . . .   Promega, Mannheim, Germany

pME18S-FL3 . . . . . .   S. Sugano

pλtriplex2 . . . .   BDBiosciences Clontech, Heidelberg, Germany

pSPORT1 . . . .   Invitrogen, Karlsruhe, Germany

pCMV-SPORT6 . . .   Invitrogen, Karlsruhe, Germany

2.4.1.7 Plasmids

Plasmids which were used in this present study are shown in Table 2.4.1, listing their inserts and vector, as well as the source they were obtained from.

2.4.1.8 Bacterial strains

For molecular cloning techniques, the following bacterial *E. coli* strain XL1-Blue (Stratagene, Amsterdam, The Netherlands) was used.

```
recA1 endA1 gyrA96 thi-1 hsdR17 supE44 relA1 lac [F'proAB
lacIqZDM15 Tn10 (Tet^r)]
```

2.4.2 Molecular DNA cloning techniques

2.4.2.1 Preparation of chemically competent XL1-Blue bacteria

Bacteria of the *E. coli* strain XL1-Blue (Stratagene, Amsterdam, The Netherlands; 2.4.1.8) were prepared to be competent for chemical transformation (see 2.4.2.2). Therefore, 5 ml LB medium containing 12.5 μg/ml tetracycline were inoculated with a single bacterial clone of XL1-Blue and incubated in a shaker over night (250 rpm, 12 – 16 h, 37°C). 400 ml LB medium (12.5 μg/ml tetracycline) were inoculated with 4 ml of this over night culture and grown in a shaker (250 rpm, 37°C) for about 3 hours until optical density at 600 nm wavelength OD_{600nm} was between 0.5 – 0.6. Bacteria were centrifuged (2500 g, 15 min, 4°C) and carefully resuspended in 30 ml TSB (5 % (v/v) DMSO, 10 mM $MgCl_2$, 10 mM $MgSO_4$, 10 % PEG 6000 in LB medium) and incubated for 1 hour on ice. 200 μl aliquots were shock-frozen in liquid nitrogen and stored at -80°C until use.

2.4.2.2 Chemical transformation of competent bacteria

100 μl chemically competent *E. coli*, strain XL1-blue, were thawed on ice. An ice-cold mixture of 20 μl 5× KCM (500 mM KCl, 150 mM $CaCl_2$, 250 mM $MgCl_2$), 79 μl ddH$_2$O and 1 μl DNA solution was added and gently resuspended. The mixture was

plasmid	insert	vector	source	reference
mMIG-pME18S	CXCL9	pME18S	IMAGE:2135986 [a]	[b] [c]
mMIG-pBSII	CXCL9	pBSII-KS+	mMIG-pME18S	[c]
mIP10-pBSII#12	CXCL10	pBSII-KS+	mIP10-pTOPO-108-32 [d]	[e] [c]
mSDF1a-pBSII#21	CXCL12	pBSII-KS+	mSDF1a-pTOPO-82-11[d]	[e] [c]
mMCP1-pBSII#52	CCL2	pBSII-KS+	mMCP1-pTOPO-101-92[d]	[e] [c]
mMIP1a-pBS-SK#16	CCL3	pBS-SK	IMAGE:533862[a]	[e] [c]
mMIP1b-pT7T3D#19	CCL4	pT7T3D-Pac	IMAGE:621095[a]	[b] [e]
mMIP1b-pBSII	CCL4	pBSII	mMIP1b-pT7T3D#19	[c]
mRANTES-pT7T3D#22	CCL5	pT7T3D-Pac	IMAGE:832342[a]	[b] [e] [c]
mRANTES-pBSII	CCL5	pBSII	mRANTES-pT7T3D#22	[c]
mC10-pT7T3D	CCL6	pT7T3D-Pac	IMAGE:1195057[a]	[b] [c]
mC10-pBSII	CCL6	pBSII	mC10-pT7T3D	[c]
mCCL11-pT7T3D	CCL11	pT7T3D	IMAGE:1054858[a]	[b]
mCCL11-pBSII	CCL11	pBSII	mCCL11-pT7T3D	
mELC-pT7T3D	CCL19	pT7T3D-Pac	IMAGE:832043[a]	[b] [c]
mELC-pBSII	CCL19	pBSII-KS+	mELC-pT7T3D	[c]
m6CKine-pT7T3D#1	CCL21	pT7T3D-Pac	IMAGE:389013[a]	[b] [e] [c]
m6CKine-pBSII	CCL21	pBSII-KS+	m6CKine-pT7T3D#1	[c]
mABCD1-pT7T3D#5	CCL22	pT7T3D-Pac	IMAGE:619257[a]	[b] [e] [c]
mABCD1-pBSII	CCL22	pBSII	mABCD1-pT7T3D#5	[c]
mLT-pT7T3D	XCL1	pT7T3D-Pac	IMAGE:576815[a]	[b] [c]
mLT-pBSII	XCL1	pBSII-KS+	pLT-pT7T3D	[c]
mFKN-pT7T3D	CX3CL1	pT7T3D-Pac	IMAGE:1230315[a]	[b]
mFKN-pBSII	CX3CL1	pBSII	mFKN-pT7T3D	
mCXCR3-pT7T3D	CXCR3	pT7T3D-Pac	IMAGE:3820689[a]	[b]
mCXCR3-pBSII	CXCR3	pBSII-KS+	mCXCR3-pT7T3D	
mCCR7-pT7T3D	CCR7	pT7T3D-Pac	IMAGE:53342[a]	[b] [c]
mCCR7-pBSII	CCR7	pBSII-KS+	mCCR7-pT7T3D	[c]
mCCR11-pT7T3D	CCR11	pT7T3D-Pac	IMAGE:51130[a]	[b]
mCCR11-pBSII	CCR11	pBSII-KS+	mCCR11-pT7T3D	
mDuffy-pT7T3D	DARC	pT7T3D-Pac	IMAGE:718084[a]	[b]
mDuffy-pBSIID	DARC	pBSII-KS+	mDuffy-pT7T3D	
mD6-pT7T3D#9	D6	pT7T3D-Pac	IMAGE:3385312[a]	[b]
mD6-pBSII#7	D6	pBSII-KS+	mD6-pT7T3D-Pac#9	
mflk1ecII	VEGFR2	pGEM3	[f]	[c] [g]

[a] cDNA EST clones were obtained from the rzpd (Deutsches Ressourcenzentrum für Genomforschung GmbH, Berlin, Germany, http://www.rzpd.de).

[b] Lennon et al. (1996)

[c] Alt et al. (2002)

[d] Kindly provided by Hellmut Augustin, Freiburg, Germany.

[e] Alt (1999)

[f] Kindly provided by Georg Breier, Bad Nauheim, Germany.

[g] Millauer et al. (1993)

Table 2.4.1: Plasmids are listed with their inserts, vector backbones, their sources and references.

incubated (20 min, 0°C) and heat-shocked (10 min, RT). 1 ml prewarmed (37°C) LB medium was added and bacteria were shaked for 1 hour at 37°C to allow development of antibiotic resistance. 20 μl and 200 μl bacteria suspension were equally distributed on LB-agar plates containing 100 μg/ml ampicillin (Roche, Mannheim, Germany) and incubated (14 – 16 h, 37°C). Single colonies were picked and grown in 5 ml LB medium containing 50 μg/ml ampicillin (14 – 16 h, 37°C). These cultures were analyzed by DNA mini preparation (see 2.4.2.3) and used for DNA midi preparations (see 2.4.2.4).

2.4.2.3   DNA mini preparation

5 ml LB medium containing 50 μg/ml ampicillin were inoculated with a single bacterial clone and grown overnight for 12 – 16 hours. 1.5 ml of this suspension were centrifuged (13000 rpm, 5 min, RT) and pellets were resuspended in 300 μl resuspensionbuffer P1 (Qiagen, Hilden, Germany) by vortexing. Bacteria were lysed by addition of 300 μl lysis buffer P2, mixed gently and incubated (3 min, RT). Lysis was stopped by addition of 300 μl neutralization buffer P3, mixed gently and incubated (15 min, 0°C). Subsequently, cell debris and genomic DNA was removed by centrifugation (13000 rpm, 30 min, 4°C). 800 μl supernatant were mixed with 560 μl isopropanol and centrifuged again (13000 rpm, 30 min, 4°C). DNA pellet was washed twice in 70 % ethanol, air-dried and resuspended in 100 μl ddH$_2$O. DNA concentration was measured by photometry (see 2.4.2.9) and purity was checked by agarose gel electrophoresis (see 2.4.2.6).

2.4.2.4   DNA midi preparation

Plasmid DNA was prepared using the Qiagen plasmid midi kit modified from the suppliers protocol. Therefore, 50 ml LB medium containing 50 μg/ml ampicillin were inoculated with with a single bacterial clone and grown over night for 12 – 16 hours. Bacterial suspension was centrifuged (4400 g, 15 min, RT). The bacterial pellet was thoroughly resuspended in 4 ml resuspensionbuffer P1. 4 ml lysisbuffer P2 were added, gently mixed by inversion and incubated (5 min, RT). 4 ml neutralizationbuffer P3 were added and mixed gently to stop the lysis and then incubated on ice (15 min, 0°C). The mixture was centrifuged to pellet cell trash and genomic DNA (4400 g, 30 min, 4°C). Meanwhile, a fluted filter was mounted on top of an affinity-

chromatography column (Qiagen-tip 100) and 4 ml equilibrationbuffer QBT1 were applied to wet the filter and equilibrate the column. Centrifugation supernatant was applied to the filter and allowed to flow through the column by gravity. Column was washed twice with 10 ml washingbuffer QC. DNA was eluted with 5 ml elution-buffer QF. Eluate was supplemented with 3.5 ml isopropanol at room temperature to precipitate DNA and centrifuged (4400 g, 30 min, RT). Pellet was resuspended in 1 ml 70 % ethanol, transferred to a 1.5 ml microcentrifuge column, washed twice (13000 rpm, 5 min, 4°C) and air-dried. Dried DNA was redissolved in either ddH$_2$O or 10 mM Tris HCl pH 8.5. DNA concentration and purity was measured photometrically (see 2.4.2.9). Additionally, purity was checked by agarose gel electrophoresis (see 2.4.2.6).

2.4.2.5   DNA digestion by restriction endonucleases

2.4.2.5.1   Qualititative digestion

DNA fragments were identified by digestion with restriction endonucleases (New England Biolabs, Schwalbach, Germany; MBI Fermentas, St. Leon-Rot, Germany). Therefore, 500 ng DNA were incubated with 3 – 5 units enzyme in 10 μl buffer (see 2.4.1.1) for 2 hours at 37°C according to the manufacturer's protocol. Then, DNA was analyzed by agarose gel electrophoresis (see 2.4.2.6).

2.4.2.5.2   Quantitative digestion

Preparation of DNA fragments for subcloning was done by digestion of 5 mg DNA with 20 units enzyme in 50 μl buffer for 2 hours at 37°C according to the manufacturer's protocol. DNA fragments were immediately separated by agarose gel electrophoresis (see 2.4.2.6) and extracted (see 2.4.2.7).

2.4.2.6   Agarose gel electrophoresis

DNA fragments were separated by horizontal agarose gel electrophoresis. 1 % agarose (Cambrex; Biozym, Hamburg, Germany) was solved in 0.5 % TBE buffer (45 mM Tris, 45 mM boric acid, 1 mM EDTA) by boiling. Solution was cooled down to 55°C and 0.5 μg/ml ethidium bromide were added. Gel was casted in a tray, combs were immediately added to prepare slots for application of DNA samples and removed after the gel was solidified. The gel was placed in a gel chamber

containing 0.5 % TBE buffer. Probes were supplemented with 5× loading buffer (30 % (v/v) glycerol, 25 % (w/v) bromphenol blue, 0,25 % (w/v) xylenxyanol) and applied to the slots. As a size marker, a DNA mixture was used (1-kb-ladder; Invitrogen, Karlsruhe, Germany). Gels were run at 10 V per centimeter gel length for 30 – 60 minutes. Then, DNA was visualized by ethidium bromide excitation with UV light (λ=312 nm) and a picture was taken using a videocamera and printed on thermal paper. Preparative gels were run at lower voltages and higher durations.

2.4.2.7 DNA agarose gel extraction

DNA was extracted from agarose gels using the QIAquick gel extraction kit (Qiagen, Hilden, Germany). Therefore, DNA fragments were excised from agarose gel using a clean, sharp scalpel. Subsequently, they were weighed, 3 volumes buffer QX1 (recipe not provided by the manufacturer) were added and incubated for 10 min at 50°C while mixing regularly. One volume isopropanol was added, probes were applied to QIAquick spin columns and centrifuged (13000 rpm, 1 min, RT). Columns were washed with 750 μl washing buffer PE (recipe not provided by the manufacturer) and centrifuged twice (13000 rpm, 1 min, RT). Afterwards, columns were incubated with 30 μl ddH$_2$O for 1 min and DNA was eluted by centrifugation (13000 rpm, 1 min, RT).

2.4.2.8 DNA fragment ligation

Ligation of compatible DNA fragments was done using the λ-phage T4 DNA ligase (Roche, Mannheim, Germany). 100 ng vector DNA fragment were incubated with a 5- to 10-fold molar excess of the integrating fragment in 10 μl 1× T4 ligase buffer (660 mM Tris-HCl, 50 mM MgCl$_2$, 10 mM dithiothreitol (DTT), 10 mM ATP, pH 7.5). Incubation was done on thawing ice over night, so that probes slowly warmed up to room temperature. The next day, bacteria were transformed with this DNA (see 2.4.2.2).

2.4.2.9 Photometric nucleic acid concentration measurement

Nucleic acids absorb UV light at $\lambda = 260$nm, while proteins have their absorption maximum at $\lambda = 280$nm. Therefore, DNA and RNA concentrations c_{DNA} / c_{RNA} can be determined photometricly by UV light absorbance (A$_{260}$) at $\lambda = 260\ nm$ if

diluted by factor DF in TE buffer (10 mM Tris pH 8.0, 1 mM EDTA) according to
the following formulas:

$$c_{\text{DNA}} = 50\frac{\text{ng}}{\mu\text{l}} \times \text{DF} \times \text{A}$$

$$c_{\text{RNA}} = 47\frac{\text{ng}}{\mu\text{l}} \times \text{DF} \times \text{A}$$

Absorbance ratio $\lambda_{260}/\lambda_{280}$ indicates purity of the preparation and should range
between 1.8 and 2.0.

2.4.2.10   DNA sequence analysis

Sequencing of plasmid DNA was performed modified as described (Sanger et al.,
1977). Therefore, 200 – 400 ng plasmid DNA were incubated with 2 μl BigDye
Terminator v3.0 Cycle Sequencing Ready Reaction Kit Premix (Applied Biosys-
tems, Darmstadt, Germany) and 1 μl of a respective sequencing primer (10 μM; see
2.4.1.5). Sequencing reaction was done in a Gene Amp PCR System 9700 (Applied
Biosystems, Darmstadt, Germany) as follows:

$$
\left.
\begin{array}{ll}
96°\text{C} & 5\text{min} \\
96°\text{C} & 10\text{sec} \\
\text{T}_{\text{AN}} & 4\text{min} \\
4°\text{C} & \infty
\end{array}
\right\} \text{25 cycles}
$$

After reaction, 10 μl ddH$_2$O were added and dye terminators were removed
using the QIAgen DyeEx Kit according to the manufacturer's instructions. In brief,
Qiagen gel filtration columns were gently vortexed, opened and centrifuged (750 g,
3 min, RT). Sequencing reaction mixes were carefully applied to the middle of the
gel bed and centrifuged (750 g, 3 min, RT). Eluates were collected and measured
by an in-house service facility using a 96-capillary sequencer ABI Prism 3700 DNA
Analyzer (Applied Biosystems, Darmstadt, Germany).

2.4.3   Subtractive suppression hybridization

Brain microvessel preparation of mice afflicted with EAE and healthy littermates
as well as cell samples of encephalitogenic and non-encephalitogenic T cells were
created in this present work. From these materials, Bioserve Biotechnologies Ltd.

(Laurel, MD, USA) created cDNA libraries cloning libraries, expression libraries and subtractive suppression hybridization libraries.

2.4.4 High-throughput DNA mini preparation and sequencing

Screening of cDNA libraries was essentially done by DNA mini preparations (see 2.4.2.3) and sequencing (see 2.4.2.10) as described. However, preparations were performed in a 96-well plate format using the silicagel-membrane based QIAprep 96 turbo Miniprep Kit (Qiagen, Hilden, Germany) in a high-throughput approach according to the manufacturer's instructions.

In detail, LB-agar was boiled in a microwave oven, cooled down to 55°C in a water bath and supplemented with 10 μg/ml ampicillin. Furthermore, 1 mM IPTG and 50 μg/ml X-gal were added for blue-white selection. 150 mm plates were casted under sterile conditions, dried for 2 hours and stored protected from light at 4°C.

A small amount of frozen bacterial suspension was scratched out of the storage tube without thawing. The storage tube was immediately stored at -80°C again. The small amount of bacterial suspension was thawed on ice and its volume was checked, diluted and plated on dried LB-agar plates in different concentrations. Plates were incubated (12 – 16 h, 37°C). White clones were picked and 1.3 ml LB medium containing 50 μg/ml ampicillin were inoculated in a 96-well masterblock (Greiner, Nürtingen, Germany). The block was sealed using a porous membrane (Qiagen, Hilden, Germany) and incubated for 20 – 24 hours. Blocks were covered with adhesive tape and bacteria were harvested by centrifugation (1500 g, 5 min, RT). Adhesive tape was carefully stripped off and supernatant was removed by quickly inverting the block and then firmly drying it on a paper towel. 250 μl buffer P1 were added per well, the block was sealed with adhesive tape and vortexed to resuspend bacteria. Tape was removed and 250 μl buffer P2 were added per well. Block was sealed again, gently inverted 5 times and incubated (5 min, RT). Tape was removed and lysis was stopped by addition of 350 μl N3 buffer, sealing and gently inverting 5 times. Tape was removed and lysates were applied to a TurboFilter plate being placed on top of a QIAprep plate in a QIAvac96 vacuum holder. 200 mbar vacuum were applied using a vacuum regulator. Thereby, lysates

were filtered through the TurboFilter to remove cell debris and DNA was bound on the QIAprep plate. The vacuum holder was slowly ventilated and the TurboFilter discarded. The QIAprep plate was washed twice with 900 μl PE and bottom outlets were carefully dried on a towel paper. Plate was dried for 10 minutes at 600 – 750 mbar. 100 μl ddH$_2$O were applied per well, incubated for 1 minute, DNA was eluted into 96-well plates and stored at -20°C.

For sequencing, 5 μl DNA solution were supplemented with 1 μl M13rev primer and 2 μl BigDye premix exactly as described (see 2.4.2.10). After sequencing reaction was done, 10 μl ddH$_2$O were added. Unincorporated dye terminators were removed by gel filtration using the DyeEx 96 kit (Qiagen, Hilden, Germany). Therefore, DyeEx 96 plate were unsealed and dehydrated by centrifugation in a Sigma Centrifuge 4K15C using a Qiagen rotor (2500 rpm, 3 min, RT). The DyeEx plate was placed on an elution plate and the sequencing reactions were carefully applied to the middle of the gel-bed surfaces. DNA was eluted by centrifugation (2500 rpm, 3 min, RT) and stored on ice. Sequencing was performed by an in-house service facility using an ABI Prism 3700 DNA Analyzer (Applied Biosystems, Darmstadt, Germany).

2.4.5 Genotyping by polymerase chain reaction

DNA was prepared from tail-biopsies of DARC knockout mice and analyzed by polymerase chain reaction (PCR) to identify the genotype of these mice as follows.

2.4.5.1 DNA extraction from mouse tissue

Tails of at least 14 day old mice were cut with hot sterile scissors by the animal caretakers. Tail biopsies were then lysed for 4 – 12 hours at 55°C in 300 μl ready-to-use lysis buffer (50 mM KCl, 1.5 mM MgCl$_2$, 10 mM Tris-HCl pH 8.3, 0.45 % NP-40, 0.45 % Tween 20) supplemented with 4 μl proteinase K (20 mg/ml; Merck, Darmstadt, Germany). After complete lysis, proteinase K was heat-inactivated (20 min, 95°C). DNA solution was either stored at -20°C or used directly for PCR analysis.

2.4.5.2 Analytic polymerase chain reaction

DNA was analyzed by two separate PCR reactions. One of them used primer D1 specific for the wildtype DARC allele exon 1 and primer D2 complementary to wild-type DARC allele exon 2, thereby creating a 400-bp PCR product in DARC wildtype mice. In DARC knockout mice, exon 1 had been been deleted and replaced by a DNA sequence containing a neomycin resistance gene. Therefore, usage of primer Dneo and D2 creates a 300 bp PCR product in DARC knockout mice. Additionally, tie-1 specific primers were added as a control (see 2.4.1.5).

Identification of DNA segments was done in 20 μl analytical PCR reactions. Therefore, 19 μl PCR reaction mix (2 μl 10$\times$ PCR buffer, 1.2 μl 25 mM MgCl$_2$, 0.4 μl 10 mM dNTPs, 0.13 μl 100 μM primer 1, 0.13 μl 100 μM primer 2, 0.13 μl 100 μM primer 3, 0.13 μl 100 μM primer 4, 0.2 μl Taq-polymerase (5 U/μl; Promega, Madison, WI, USA), 14.68 μl ddH$_2$O) were supplemented with 1 μl DNA probe (approximately 500 ng genomic mouse DNA or 1 pg plasmid DNA) and PCR was performed in a Gene Amp PCR System 9700 (Applied Biosystems, Darmstadt, Germany) under the following conditions:

Initial denaturing	94°C	4 min
Denaturing	94°C	30 sec
Hybridization		45 sec
Elongation	72°C	60 sec
Final elongation	72°C	5 min
	4°C	∞

35 cycles (for Denaturing, Hybridization, Elongation)

Reaction products were analyzed by agarose gel electrophoresis (see 2.4.2.6).

2.4.6 Molecular RNA preparation and analysis

2.4.6.1 Silicagel membrane RNA preparation

Tissue samples were prepared as described (see 2.1.4.1) and washed three times in ice-cold PBS. RNA was prepared using the RNeasy kit (Qiagen, Hilden, Germany) according to the manufacturer's protocol. Samples were resuspended in 600 μl buffer RLT (recipe not provided by the manufacturer) supplemented with 1 % β-ME. Tissue was homogenized by passing the lysate 20 times through a 0.6 mm needle

fitted to a syringe and stored at -80°C until further processing.

Probes were thawed and centrifuged (13000 rpm, 3 min, RT). Supernatant was transferred to a new vial and 600 μl 70 % ethanol were added and mixed well by pipetting. Sample was applied to an RNeasy mini spin column in successive 700 μl aliquots and centrifuged (13000 rpm, 15 s, RT). Column was washed by addition of 700 μl buffer RW1 (recipe not provided by the manufacturer) and centrifugation (13000 rpm, 15 s, RT) as well as addition of 500 μl RPE (recipe not provided by the manufacturer) and centrifugation (13000 rpm, 15 s, RT). Then column was washed again with 500 μl RPE and centrifuged thoroughly to dry the RNeasy membrane (13000 rpm, 2 min, RT). RNeasy column was transferred to a new collection tube and eluated twice with 30 μl ddH$_2$O. RNA concentration was measured (see 2.4.2.9) and RNA analyzed by agarose gel electrophoresis (see 2.4.6.3).

2.4.6.2   Poly-A RNA preparation

Tissue samples were prepared as described (see 2.1.4.1) and washed three times with ice-cold PBS. They were transferred to 50 ml centrifugation tubes, shock-frozen in liquid nitrogen and stored at -80°C. 4 ml solution D (4 M guanidine thiocyanate, 25 mM sodiumcitrate, 100 mM β-mercaptoethanol, 0.5 % lauroylsarcosine, 0.1 % antifoam A) were directly applied and the frozen material was dispersed using an Ultra-Turrax T25 (IKA Labortechnik, Staufen, Germany), with speed setting blue/red (about 80 %) for 30 seconds. Subsequently, 0.4 ml 2 M sodiumacetate pH 4.0, 4 ml phenol and 0.8 ml chloroform were added. Mixture was vortexed for 20 seconds and incubated on ice (15 min, 0°C). Suspensions were transferred to a 30 ml Corex-tube and centrifuged (8000 rpm, 15 min, 4°C). Supernatant was supplemented with 7 ml isopropanol and 1 μl tRNA (50 μg/μl) for 12 – 16 hours at -20°C. RNA was spun down (5000 rpm, 15 min, 4°C) and air-dried. Optionally, total RNA was dissolved in 100 μl ddH$_2$O.

Alternatively, poly-A RNA could be prepared as follows. Total RNA pellet was dissolved in 5 ml ice-cold STE (0.1 M NaCl, 20 mM Tris pH 7.4, 10 mM EDTA pH 8.0) and 450 μl 5 M NaCl were added. Meanwhile, 1 g oligo dT cellulose (Roche, Mannheim, Germany) was resuspended in loading buffer (0.4 M NaCl, 20 mM Tris pH 7.4, 10 mM EDTA pH 8.0, 0.2 % SDS) and shaked gently (30 min, RT). 3 ml oligo dT cellulose suspension were added to the total RNA solution and shaked

gently (3 h – O/N, RT). Suspension was centrifuged (2000 rpm, 5 min, RT), washed with 10 ml loading buffer (3 × 3 min, RT) and centrifuged (2000 rpm, 5 min, RT). Oligo dT cellulose was washed with oligo dT washing buffer (0.1 M NaCl, 10 mM Tris pH 7.4, 20 mM EDTA pH 8.0, 0.2 % SDS) (2 × 3 min) and centrifuged (2000 rpm, 5 min, RT). Oligo dT cellulose was resuspended in 6 ml oligo dT washing buffer and applied to a column. Poly-A-RNA was eluted with 5 × 1 ml elution buffer (1 mM Tris pH 7.4, 1 mM EDTA pH 8.0, 0.2 % SDS) into a Corex-tube. 200 μl were stored for concentration measurement (see 2.4.2.9). Poly-A-RNA was precipitated by addition of 1 μl tRNA (50 μg/μl) and 880 μl 2 M sodiumacetate pH 4.5. After shaking, 12 ml 100 % ethanol were added, shaked again and stored at -20°C over night. RNA was pelleted by centrifugation (8000 rpm, 45 min, 4°C), resuspended in depc-H_2O (1 l ddH_2O thoroughly mixed with 200 μl depc, incubated for at least 1 hour and autoclaved) to a final concentration of 0.5 μg/μl and stored at -80°C.

For reuse, oligo dT cellulose was incubated with 0.1 N sodiumhydroxide (30 min, RT) and washed three times with loading buffer. pH was checked and if it was no longer basic, oligo dT cellulose was stored at 4°C for reuse up to 3 times.

2.4.6.3 RNA formaldehyde gel electrophoresis

Denaturing formaldehyde gels were used to analyze RNA preparations. Therefore, 0.4 g agarose were solved in 40 ml ddH_2O by boiling and then cooled down to 60°C in a water bath. 1 ml 50× MOPS buffer (1 M MOPS, 0.25 M sodiumacetate, 0.05 M EDTA pH 7.0; stored light-protected at 4°C) and 8.5 ml freshly prepared formaldehyde (37 %) were added and gel was casted using combs to prepare probe slots. After gel was solidified, combs were removed, gel was put into the gel chamber and running buffer (5 ml 50× MOPS, 41.25 ml formaldehyde (37 %), 250 ml ddH_2O) was added. Each RNA sample was supplemented with 30 μl RNA loading buffer (20 μl formamid, 7 μl formaldehyde, 1 μl 50× MOPS, 2 μl saturated bromphenol blue solution) to a maximum volume of 50 μl, mixed well, heated (5 min, 70°C), chilled on ice and loaded onto the gel. Gel was run with constant voltage (10 V/cm gellength), stained with SYBR gold (Molecular Probes; MoBiTec, Göttingen, Germany) nucleic acid stain solution (diluted 10000-fold in 10 mM Tris, 1 mM EDTA pH 8.0) for 20 minutes and photographed using a SYBR Gold gel stain photographic filter (Molecular Probes; MoBiTec, Göttingen, Germany).

2.4.7   Gene array analysis

Tissue samples were prepared and shock-frozen in this present work (see 2.1.4.1) and then were sent to Mrs. Kristina Duvefelt at Astra-Zeneca (Södertälje, Sweden), who prepared RNA, applied it to a gene array and identified regulated genes as described below. Resulting data were subsequently analyzed in this present work.

2.4.7.1   RNA preparation

mRNA was prepared at Astra-Zeneca from approximately 10 mg microvessels (wet weight) with a Dynabeads mRNA direct kit (Dynal, Oslo, Norway) according to the manufacturer's protocol.

2.4.7.2   Gene array

Subsequently, RNA was processed at Astra-Zeneca to be applied to an Affymetrix Mu6500 GeneChip array set (Affymetrix, Santa Clara, CA, USA) according to manufacturer's instructions as follows. Briefly, 75 % of the mRNA obtained were used for cDNA synthesis with a SUPERSCRIPT choice system (Invitrogen, Carlsbad, CA, USA) using a T7-dT24 primer for first strand synthesis. From this cDNA, cRNA was synthesized using a MEGAscript kit (Ambion, Huntingdon, UK) and biotinylated CTP and UTP nucleotides (Enzo, New York, NY, USA). 15 μg cRNA were fragmented in fragmentation buffer (40 mM Tris/acetate pH 8.1, 100 mM potassiumacetate, and 30 mM magnesiumacetate) by heating (35 min, 94°C) prior to hybridization. 12 μg of fragmented cRNA, control cRNA and grid alignment oligonucleotide were hybridized to each array of the Mu6500 GeneChip Array Set in a GeneChip hybridization oven (60 rpm, 16 h, 45°C). Optionally, arrays were washed and stained with streptavidin-phycoerythrin conjugate (Molecular Probes, Eugene, OR, USA) in an Affymetrix fluidics station 400. Fluorescent signals were detected by a gene array scanner (Hewlett Packard, Palo Alto, CA, USA). Signal intensity of each gene present on the chips was calculated by Genechip Software (Affymetrix, Santa Clara, CA, USA) and thereby quantitative gene expression levels were obtained. Signal intensity was scaled to a single value, 150, for all probes on a chip to allow comparison of samples.

Fold changes were calculated comparing the data of a main sample and a control

sample. Changes smaller than 2-fold over baseline had to be considered as background variability according to the manufacturer. Presence of each individual gene was scored by Affymetrix data analysis software. Regarding this score, an increase in expression of an individual gene was only considered significant if this individual gene was scored positive in the analyzed sample. Accordingly, a decrease in gene expression was only considered significant if this individual gene was scored present in the control sample. All probe sets with the suffixes _g, _f and _s for which duplicate probe sets exist, were omitted.

2.4.7.3 Data analysis

In this present work, regulated genes were analyzed and sorted into functional groups using NetAffx Analysis Center (Liu et al., 2003) applying respective Mu11K gene chip probe set identifiers to the respective Mu6500 chip probes according to the manufacturer. This analysis was supplemented by homology comparisons as well as literature searches.

2.5 Biochemistry

2.5.1 Preparation of protein samples from animal tissue

Protein samples were prepared from different animal tissues. Therefore, animals were sacrificed, tissues were prepared, washed in ice-cold PBS and 10 times homogenized on ice in a Dounce homogenizer (Kontes Glass, Vineland, NJ, USA) containing either RIPA buffer (120 mM NaCl, 50 mM Tris pH 8.0, 1 % NP40, 0.5 % sodium deoxycholate, 0.1 % SDS) or RIPAU buffer (6 M urea in RIPA buffer). Buffers had been supplemented with protease inhibitors just before use (1 μg/ml aprotinin, 1 μg/ml leupeptin, 1 μg/ml pepstatin, 1 mM PMSF). Lysates were centrifuged (13000 rpm, 1 h, 4°C) and pellets were discarded. Protein concentrations of lysates were measured (see 2.5.2) and lysates analyzed.

2.5.2 Bicinchoninic acid (BCA) protein assay

This assay modified from Smith et al. (1985) was used to quantify protein concentrations utilizing alkaline reduction of cupric ions to cuprous ions by proteins and

subsequent chelation and color development. Most detergents do not interfere with this assay. In detail, a dilution series of a BSA calibration standard solutions (1000, 500, 250, 125, 62.5 and 31.25 μg/ml) was prepared. 10 μl of diluted calibration standard, tenfold and fiftyfold diluted protein-containing sample as well as 10 μl ddH$_2$O as a blank value were added in duplicates to a 96-well plate. Protein determination reagent was freshly prepared by mixing 50 volumes bicinchoninic acid (BCA) solution (Sigma, Deisenhofen, Germany) with 1 volume 4 % coppersulfate-pentahydrate. 200 μl protein determination reagent were applied per well, plates were covered with a lid, incubated (30 min, 37°C), cooled down to room temperature and absorbance A$_{560}$ at $\lambda = 560$nm was measured. Blank values were subtracted, a calibration plot prepared and protein sample concentration determined by interpolation.

2.5.3 Polyacrylamide gel electrophoresis (PAGE)

Separation of small proteins ranging from $5 - 20$ kDa by electrophoresis was achieved using a Tris-Tricine Buffer system modified as described (Schagger and von Jagow, 1987). A 10 % separating gel was cast and covered with butanol until it was polymerized. Butanol was removed and a stacking gel overlaid, using a comb to prepare slots for probe application. The following solutions were used per two 6×8 cm gels:

	separating gel		stacking gel	
48 % acrylamide / 1.5 % bisacrylamide	2440	μl	480	μl
3 M Tris-HCl / 0.3 %SDS pH 8.45	4000	μl	1488	μl
ddH$_2$O	5960	μl	3032	μl
10 % APS	60	μl	30	μl
TEMED	12	μl	6	μl

After polymerization, combs were removed and slots were rinsed with ddH$_2$O once. Gels were set up in an electrophoresis apparatus (Peqlab, Erlangen, Germany). The upper chamber was filled with cathode buffer (0.1 M Tris, 0.1 M Tricine, 0.1 % SDS, pH 8.25; no correction of pH necessary, should be 8.25) and slots were carefully washed again with cathode buffer using a syringe. Then, the lower chamber was filled with anode buffer (0.2 M Tris-HCl pH 8.9). Protein samples were prepared as follows. 75 μg tissue lysate or 25 ng recombinant protein were supplemented with $4\times$ sample buffer (4 % SDS, 12 % glycerol, 50 mM Tris, 2 % β-mercaptoethanol,

0.01 % Serva Blue G, pH 6.8) in a total volume of 50 μl. Samples were heated (2 min, 95°C) and applied to the slots. Gels were run with 30 V until the samples left the stacking gel, then they were run with 100 V for 4 – 5 hours. Gels were either stained with Coomassie Blue (see 2.5.4) or proteins were blotted on a membrane (see 2.5.5) for further analysis (see 2.5.6).

2.5.4   Coomassie staining of SDS-gels

To visualize proteins on polyacrylamide gels, they were washed once with destaining solution (45 % (v/v) methanol, 10 % (v/v) acetic acid, 45 % (v/v) ddH$_2$O) and stained in staining solution (0.05 % Coomassie Brilliant Blue in destaining solution) for 12 – 16 hours. Then, gels were destained in destaining solution until specific proteins bands became visible. Gels were dried for two hours at 80°C using a Gel Dryer Model 583 (Bio-Rad, Munich, Germany).

2.5.5   Semi-dry electroblot

After protein separation on polyacrylamide gel, proteins were electroblotted onto nitrocellulose (0.2 μm; Schleicher & Schuell, Einbeck, Germany) or polyvinylidene difluoride membranes (PVDF; 0.45 μm; Millipore, Schwalbach, Germany) using a semi-dry transfer system. Therefore, 8 sheets of filter paper (Schleicher & Schuell, Einbeck, Germany) as well as a blotting membrane were cut slightly larger than the gel containing proteins. PVDF membranes were wet with methanol for 3 seconds and then washed with ddH$_2$O for about 1 – 2 minutes until the membrane no longer floated on the water surface. Filter papers and the membrane were thoroughly soaked with semi-dry blotting buffer (48 mM Tris, 39 mM glycine, 1.3 mM SDS, 20 % methanol). Four filter papers with the transfer membrane being placed on top of it were put onto the anode unit of a semi-dry transfer cell (Trans-Blot SD; Bio-Rad, Munich, Germany). The gel was taken out of the electrophoresis unit, washed in semi-dry blotting buffer, put onto the transfer membrane and covered by four filter papers. Care had to be taken to avoid air bubbles in between gel, transfer membrane or filter papers. The cathode unit was put on top of the transfer stack and proteins were transferred at constant current (1 mA / cm^2, 1 hour).

2.5.6 Immunoblotting (western blotting)

After electrophoretic transfer of proteins on a retentive membrane, unspecific protein binding sites on the membrane were blocked with 5 % (w/v) low-fat milk powder in TBST (20 mM Tris-HCl pH 7.6, 50 mM NaCl, 1 % (v/v) Tween 20) for 12 – 16 hours. Subsequently, first antibody (10 μg/ml in 5 % low-fat milk powder in TBST) was applied (2 h, RT). Blots were washed in TBST (3 × 7 min, RT) and a biotinylated secondary antibody was applied (see 2.3.1.3; 2 h, RT). In the meanwhile, a streptavidin-biotin-horseradish peroxidase (SA/biotin/HRP) complex was prepared (StreptABComplex/HRP kit; DakoCytomation, Hamburg, Germany) by mixing 1 μl streptavidin solution, 1 μl biotinylated-HRP solution and 10 ml Tris-HCl pH 8.0. Blots were washed (3 × 7 min), the SA/biotin/HRP solution was applied (1 hour, RT) and blots were washed again (3 × 7 min). Antigens were visualized by chemoluminescence applying the SuperSignal Reagent Kit (Pierce; Bonn, Germany) for 10 minutes followed by exposure to a photosensitive film (Hyperfilm ECL; Amersham Biosciences, Freiburg, Germany) and its development and fixation (M35 X-OMAT Developer; Kodak, Stuttgart, Germany).

2.5.7 Proteomics

Proteomic analysis was done in cooperation with Dr. Bosse Franzén at Astra-Zeneca (Södertälje, Sweden). Tissue samples were prepared and shock-frozen in this present work. Subsequently, they were sent to Astra-Zeneca and by them separated by 2-dimensional gel electrophoresis. Spots of interest were identified by mass spectrometry.

2.5.7.1 2-dimensional (2D) gel electrophoresis and image analysis

Unless otherwise stated, electrophoresis-grade chemicals were used (Genomic Solutions, Chelmsford, MA, USA).

Frozen microvessels were lysed by addition of 20 μl lysis buffer (8 M urea, 0.5 % (v/v) NP-40, 2 % (w/v) CHAPS, 0.3 % (w/v) DTT, 0.5 % (v/v) IPG buffer 3-10 NL and 0.02 % BPB) per mg (wet weight) lysate. Lysates were mixed vigorously for 2 hours and remaining insoluble material was removed by centrifugation (15000 rpm, 15 min). Protein concentration was determined with a modified Bradford method

(Bio-Rad, Hercules, CA, USA; Bradford (1976)) and 150 μg protein per sample were applied to isoelectric focusing (IEF).

First-dimension IEF: Samples were diluted to a final volume of 350 μl lysis buffer and applied to IPG-Phor sample trays (Amersham Biosciences, Uppsala, Sweden). Immobiline DryStrips (18 cm pH 3 – 10 NL) were processed under a layer of Drystrip cover fluid at 20°C according to the manufacturer's instructions. Focusing was performed in 5 steps: 30 V for 12 h (rehydration step), 500 V for 1 h, gradient up to 2000V during 2 h, gradient up to 8000V during 1 h and finally 8000 V for 5 h to reach a total of 48.6 kVh (all steps at 50 mA/strip). After IEF, cover fluid was poured off and DryStrips were equilibrated while shaking gently (2 × 10 min). First equilibration was performed in 30 % (w/v) glycerol, 6 M urea, 2 % SDS, 50 mM Tris-HCl pH 8.8, 65 mM DTT and a trace of BPB as tracking dye. Second equilibration was done in the same solution, besides DTT being replaced by 260 mM iodoacetamide (St. Louis, MO, USA; Gorg et al. (1995)).

Second-dimension SDS-PAGE: Equilibrated strips were sealed at the top of the second-dimension polyacrylamidegel (12 % T, 2.1 % C) with 0.6 % agarose (FMC BioProducts, Rockland, ME, USA) in SDS running buffer. Electrophoresis was performed in the IsoDalt tank (Hoefer, San Francisco, CA, USA) until the tracking dye reached the anodic end of the gels (100 V, approximately 18 h). Ten gels were run in parallel.

Staining of gels: SYPRO Ruby staining was performed according to the manufacturer (Molecular Probes, Eugene, OR, USA) with minor modifications. Autostainers (Amersham Biotechnologies, Uppsala, Sweden) were used in order to obtain maximal reproducibility of staining intensities.

Image analysis: A cooled CCD camera-based instrument, Fluor-S MultiImager (Bio-Rad, Hercules, CA, USA) was used to image SYPRO Ruby-stained gels. Raw scans were processed using the 2D software PDQuest (v6.1.0; Bio-Rad, Hercules, CA, USA). Spots were detected according to the manufacturer's instructions. Spot patterns of different gels were matched so that each spot was given a unique identification number (SSP). Resolved proteins were individually quantified and normalized to the total intensity of detected spots in each gel. The average intensities of resolved spots were compared by statistical and quantitative analysis using the PDQuest software (Mann-Whitney non-parametric test, $p < 0.05$; t-test, $p < 0.05$) to

find spots that differed quantitatively between controls and main groups.

2.5.7.2   Identification of proteins by mass spectrometry

2.5.7.2.1   In-gel digestion and peptide extraction

Protein spots of interest were cut out of stained wet gels using a scalpel. Gel pieces were placed in 0.5 ml microreaction tubes which had been washed with ethanol and in-gel digested according to the procedure described by the mass spectrometry facility of the UCSF (University of San Fransisco, San Francisco, CA, USA) with some modifications:

Step 1: Gel pieces were washed with water, incubated for 30 minutes and all liquid was removed. Step 2: 25 mM bicarbonate (NH_4HCO_3) pH 8.0 was added and incubated for 10 minutes. An equal volume of CH_3CN was added and incubated for another 10 minutes. Then step 2 was repeated. Step 3: Just enough CH_3CN was added to cover the gel pieces. After shrinking of the gel pieces, liquid was removed. Step 4: Gel pieces were dried in a SpeedVac vacuum evaporator for 30 min. Step 5: Approximately 10 μl freshly prepared and chilled digestion solution containing 10 ng/μl trypsin (Promega, Madison, WI, USA) in 25 mM NH_4HCO_3, enough to cover the gel pieces, were added and incubated (30 min, RT). Step 6: 15 μl of 25 mM NH_4HCO_3 pH 8.0 buffer were added and incubated overnight at 37°C. Step 7: Finally, peptides were extracted by addition of 25 μl 1 % formic acid and incubation for 1 hour.

2.5.7.2.2   Matrix assisted laser desorption/ionization time-of-flight mass spectrometry

1 – 2 μl peptide extracts were mixed with the same volume of α-cyano-4-hydroxycinnamic acid solution (10 mg/ml; Hewlett-Packard, Böblingen, Germany) and mixtures were spotted onto a MALDI target (Micromass, Manchester, UK). Internal mass calibration was achieved by use of trypsin autodigestion products (842.51 Da and 2211.11 Da). External calibrants were added in a 1 : 2 mixture of Hewlett-Packard α-cyano-4-hydroxycinnamic acid solution (10 mg/ml) and 1 % formic acid containing 50 – 100 fmol/μl each of human bradykinin ([M+H]+ 1060.5691), angiotensin I ([M+H]+ 1296.685), renin ([M+H]+ 1759.9395), human ACTH clip 18–39 ([M+H]+2465.199) and β-amyloid 1–28 ([M+H]+ 3263.511).

MALDI-TOF-MS analysis was performed using a Micromass TofSpec 2E (Manchester, UK) in reflectron mode.

2.5.7.2.3   Nano-electrospray ionization tandem mass spectrometry

Trypsin digest peptides were extracted and desalted with a small bed of Poros R20 (Applied Biosystems, Foster City, CA, USA) which had been prepared in a gel load tip. Bed was prewashed with 50 % acetonitrile containing 1 % formic acid, followed by 1 % formic acid before sample loading. 10 μl of peptide mixture were applied on the Poros R20 bed, washed with 10 μl of 0.1 % formic acid and peptides were eluted with 5 μl of 50 % acetonitrile containing 1 % formic acid into a borosilicate nanospray capillary needle (Protana, Denmark) for subsequent MS/MS analysis. The mass spectrometer used therefore was a hybrid instrument Q-ToF 2 (Micromass, Manchester, UK) and was calibrated with fragment ions of [Glu1]-fibrinopeptide.

2.5.7.2.4   Database searching

SWISS-PROT / TrEMBL database searches using the Mascot peptide mass fingerprinting search programs (Matrix Science, London, UK) identified the proteins. Peptide mass fingerprinting criteria for positive identification were as follows; (i) hit should score relevant by the Mascot algorithm; (ii) a minimum of four matching peptides should be found; (iii) no less than 50 % of the measured masses should match the theoretical fragments. If the isotopic pattern of the measured peptide masses was clearly atypical, or could be attributed to known artifacts or to adjacent, identified proteins, measured peptide masses could be excluded. Two or more MS/MS sequences were required for identification by MS/MS, unless supporting peptide mass fingerprinting data were accessible. Theoretical Mr/pI values of matching candidates were compared with calculated values obtained from the 2D electrophoresis gels.

Chapter 3

Results

3.1 Expression and functional involvement of chemokines in lymphocyte recruitment across the endothelial BBB

Involvement of chemokines in recruiting lymphocytes across the endothelial blood-brain barrier during EAE requires their presence at the luminal surface of the endothelial blood-brain barrier. Therefore, they need to be either expressed by endothelial cells themselves or would have to be actively transported from the CNS parenchyma across the endothelial BBB to the luminal surface of the endothelial cells by a yet unknown mechanism. Chemokine expression can only be investigated by *in situ* hybridization.

3.1.1 Preparation of chemokine cDNA clones

Some cDNA clones which were required to detect murine chemokine and receptor mRNA expression by *in situ* hybridization had been obtained and subcloned in an earlier study (Table 2.4.1). Additional cDNA clones of murine chemokines and receptors were obtained as follows. Sequences were obtained by ENTREZ database search (http://www.ncbi.nlm.nih.gov/entrez) and checked against the complete primary mouse cDNA database using the Basic Local Alignment Search Tool (BLAST) algorithm (http://www.ncbi.nlm.nih.gov/BLAST/) to obtain the longest published cDNA sequence of a given gene. Mouse expressed sequence tag (EST) database

was searched for these sequences by BLAST to identify publicly available cDNA clones. The longest cDNA containing the full proteincoding sequence was chosen and ordered from rzpd (Deutsches Ressourcenzentrum für Genomforschung GmbH, Berlin, Germany, http://www.rzpd.de). Thereby, cDNA clones for the chemokines CXCL9, CCL6, CCL11, CCL19, XCL1; the chemokine receptors CXCR3, CCR7, CCR11, CX3CL1 and the receptor D6 were obtained in this present study (Table 2.4.1).

These potential clones were ordered, streaked on LB agar plates containing 100 μg/ml ampicillin, incubated (12 – 16 hours, 37°C) and 3 – 6 single colonies were investigated by DNA mini preparation and restriction analysis (Figure 3.1.1 and Figure 3.1.2) to exclude possible contaminations. Subsequently, clones were sequenced and analyzed by DNAstar (DNAstar Inc. Madison, WI, USA) to identify correct cDNA inserts.

Probes for *in situ* hybridization have to be created by *in vitro* transcription using T3, T7 or SP6 RNA polymerases. To create RNA probes from either direction, plasmids containing cDNA clones for *in situ* hybridization need to have a promoter site for two different RNA polymerases. It turned out in this present study, that there are significant differences in promoter activity between different plasmids. Especially the pT7T3D-Pac plasmid, which was used to create EST cDNA libraries, has a very low efficiency T7 promoter site, while the promoter sites in pBSII-KS+ have a very good efficiency. Therefore, *in situ* hybridization probe inserts were subcloned into pBSII-KS+ (Figure 3.1.1 and Figure 3.1.2).

3.1.2 Functional expression of the lymphoid chemokines CCL19 and CCL21 at the blood-brain barrier

For chemokines to be involved in recruitment of T cells or monocytes across the endothelial BBB, they need to be present at the luminal surface of the endothelial cells. Thus, they need to be either expressed by the endothelial cells themselves or would have to be actively transported from the CNS parenchyma across the endothelial blood-brain barrier to the luminal surface of the endothelial cells. Searching for chemokines being expressed at the endothelial BBB, *in situ* hybridizations for a large panel of chemokines were performed on brain and spinal cord sections of SJL/N
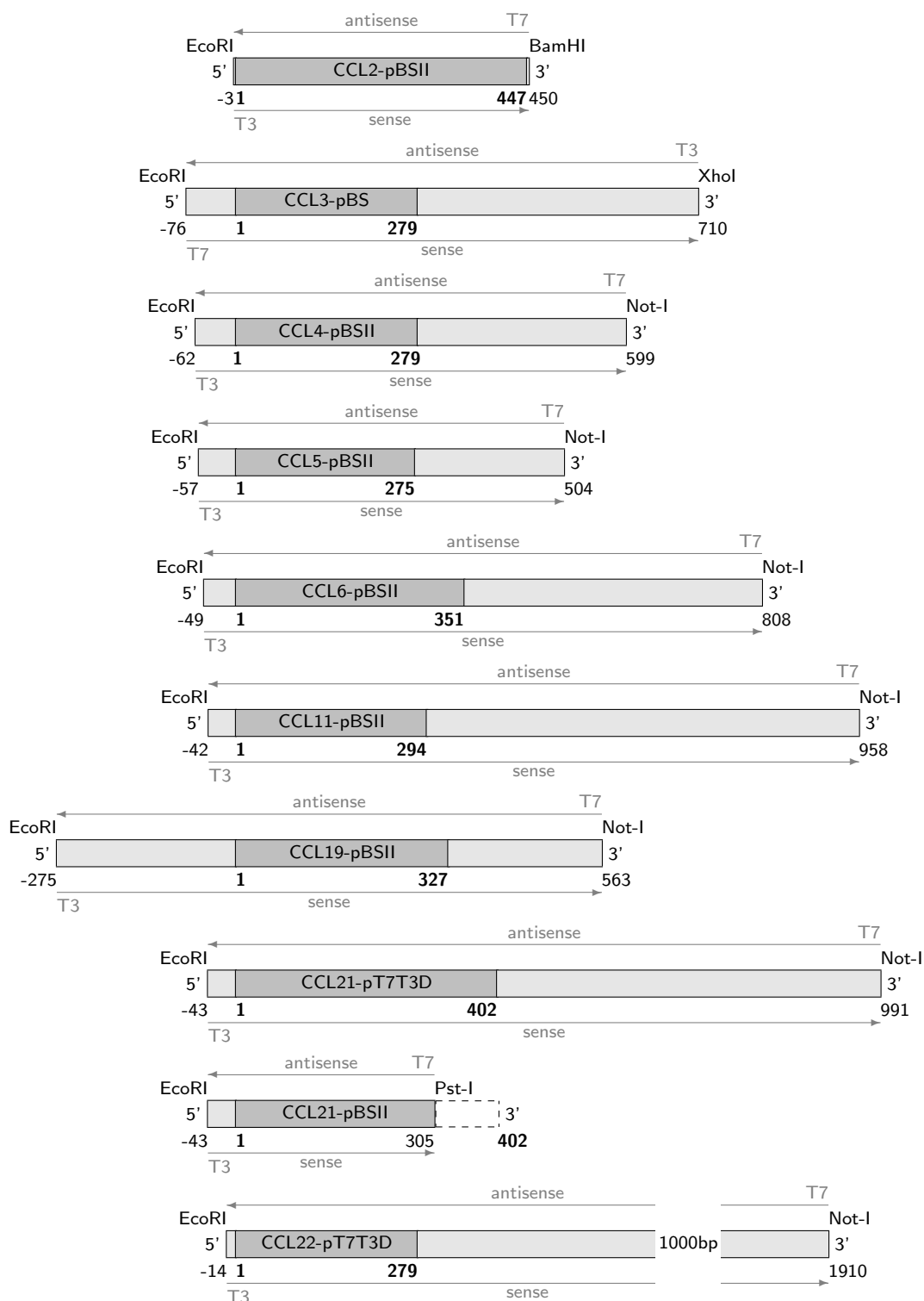
Figure 3.1.1: cDNA inserts of plasmids encoding CC chemokines are shown. Coding sequences are marked with bold numbers. Lengths of inserts are approximated by sequencing results up to the named restriction sites, possibly including adapter sequences used for cloning. Additionally, restriction sites and RNA polymerases used for creation of antisense and sense probes for *in situ* hybridization are listed.
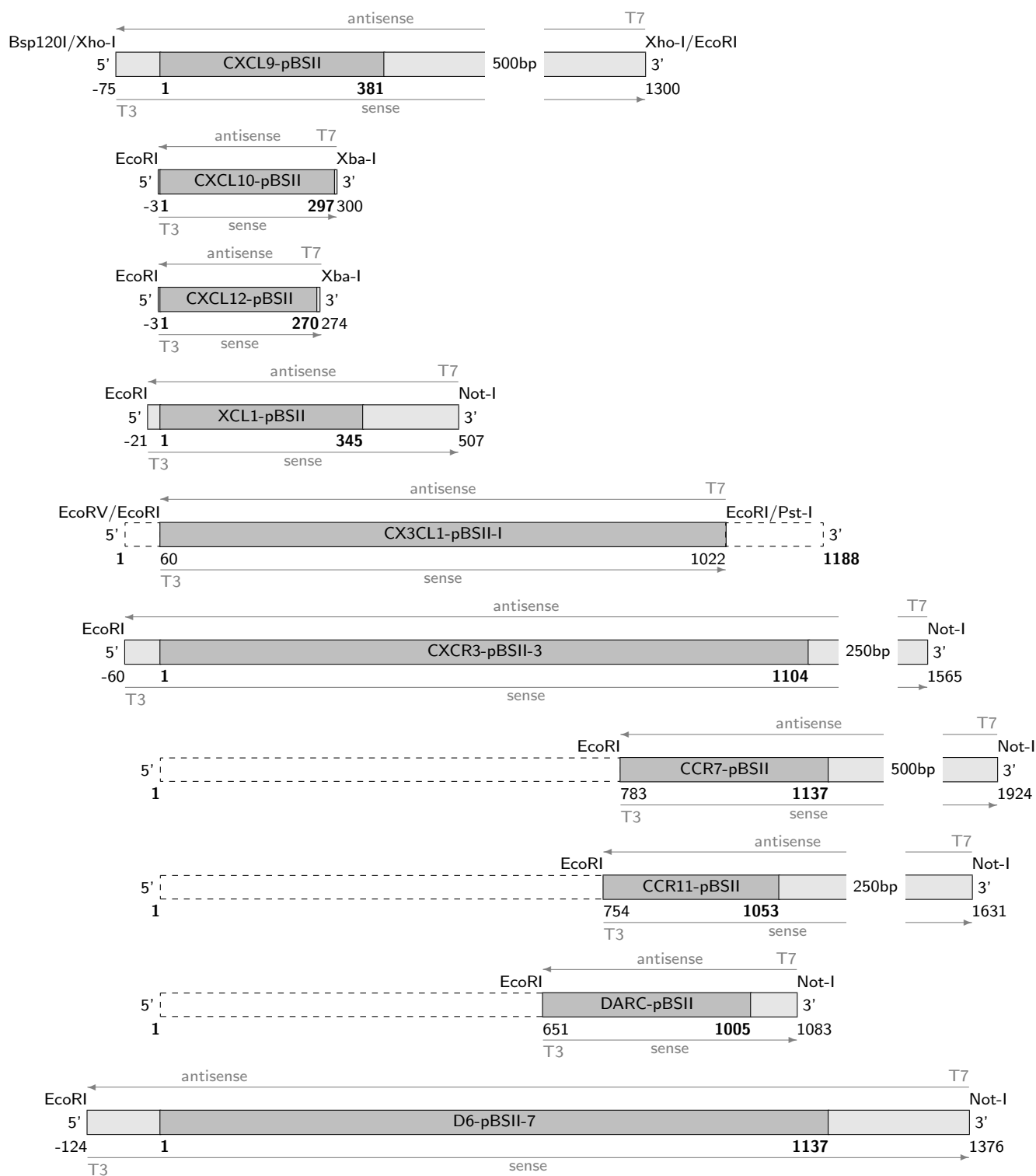
Figure 3.1.2: cDNA inserts of plasmids encoding CXC chemokines and chemokine receptors are shown. Coding sequences are marked with bold numbers. Lengths of inserts are approximated by sequencing results up to the named restriction sites, possibly including adapter sequences used for cloning. Additionally, restriction sites and RNA polymerases used for creation of antisense and sense probes for *in situ* hybridization are listed.

	brain		spinal cord	
	inflamm. cells	endoth. cells	inflamm. cells	endoth. cells
CXCL9 (MIG)	++	-	++	-
CXCL10 (IP-10)	++	-	++	-
CXCL12 (SDF-1)^a	+	-	+	-
CCL2 (MCP-1)	+	-	++	-
CCL3 (MIP-1α)	+	-	++	-
CCL4 (MIP-1γ)	+	-	++	-
CCL5 (RANTES)	+	-	++	-
CCL6 (C10)	++	-	++	-
CCL19 (ELC)	-	++	-	++
CCL21 (SLC)	-	++	-	++
CCL22 (MDC)	+	-	+	-
XCL1(Lymphotactin)	-	-	-	-

^{a}Expression was detected in choroid plexus and in brain parenchymal cells not spatially correlated to inflammatory cuffs.

Table 3.1.1: Semiquantitative analysis of the expression of chemokine mRNA during EAE. Semiquantitative analysis was performed by counting the total number of inflammatory cuffs per section in relation to the number of inflammatory cuffs with specific *in situ* hybridization signals. Results were divided into three groups: ++, >50 % of the infiltrates show positive cells; +, < 50 % of the infiltrates show positive signals; -, no detectable hybridization signal. (Reproduced with permission from Alt et al., 2002).

mice, afflicted with EAE and of healthy SJL/N mice as a control (Figure 3.1.1 and Figure 3.1.2). These results were taken together with the results from an earlier study (Alt, 1999) and semiquantitatively analyzed (Table 3.1.1).

Besides CCL19 and CXCL12, expression of chemokine mRNA was not detectable in brain and spinal cord sections of healthy SJL/N mice by *in situ* hybridization. While CXCL12 was detected within the choroid plexus, in astrocytes or microglial cells scattered throughout the CNS parenchyma and in some rare perivascular cells (Figure 3.1.3), expression of CCL19 was localized to cerebral venules as shown by a hybridization signal exactly resembling expression of the endothelial cell-specific VEGF receptor 2 / flk-1 (Figure 3.1.4).

During EAE, expression of the lymphoid chemokine CCL19 was tremendously upregulated and thereby detected in almost all venules which were surrounded by inflammatory cuffs (Table 3.1.1 and Figure 3.1.5). Moreover, expression of another
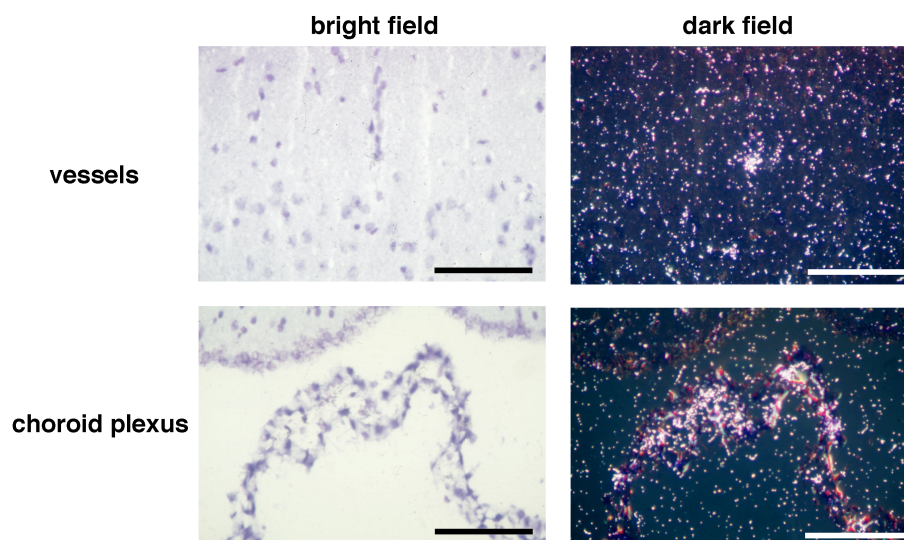
bright field	dark field

vessels

choroid plexus

Figure 3.1.3: *In situ* hybridization analysis of CXCL12 mRNA expression in the healthy brain of an SJL/N mouse is shown. A specific hybridization signal for CXCL12 can be localized to CNS parenchymal cells of healthy SJL/N mice with the CXCL21 antisense probe, Additionally, CXCL12 expression can be detected in the choroid plexus. Sections are counterstained with toluidine blue. Bright and dark field illumination are shown. Bar =100 μm.

lymphoid chemokine CCL21/SLC was observed to be induced in almost all venules surrounded by perivascular infiltrates in brain and spinal cord sections of mice afflicted with active EAE. Expression of the common receptor for both chemokines, CCR7, could be detected in a subpopulation of cells present within inflammatory cuffs (Figure 3.1.5).

As expression of CCL19 and CCL21 has been described in lymph nodes before (Cyster, 1999; Luther et al., 2000), *in situ* hybridization was performed for both chemokines on frozen sections of lymph nodes as a control for CNS expression of CCL19 and CCL21. Thereby, CCL19 expression was detected in stromal cells located in the T cell zones of peripheral lymph nodes which had been derived from healthy SJL/N mice (Figure 3.1.5). Additionally, expression of CCL21 mRNA could be specifically detected in lymph node high endothelial venules (HEV) at levels which were comparable to those found in inflamed venules in the CNS of mice afflicted with EAE (Figure 3.1.5). In addition, CCR7 expression was observed in a number of lymph node parenchymal cells (Figure 3.1.5).

Induction of no other chemokine investigated in this present study could be detected in BBB endothelial cells during EAE (Table 3.1.1). Rather, expression of these additionally expressed cells was observed within the brain or spinal cord
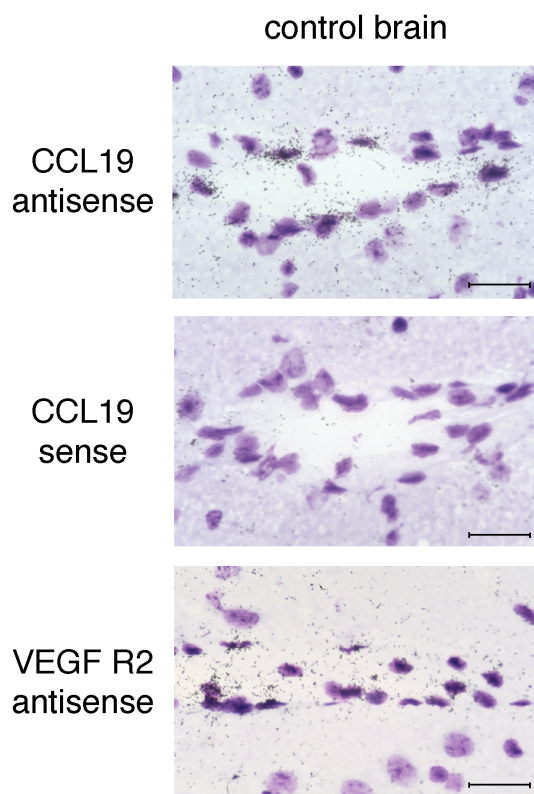
control brain

Figure 3.1.4: *In situ* hybridization analysis of CCL19 mRNA expression in the healthy brain of an SJL/N mouse is shown. A hybridization signal for CCL19 can be localized to venules of the CNS of healthy SJL/N mice with the CCL19 antisense probe, whereas no hybridization signal is seen with the CCL19 sense control probe. The endothelial cell specific hybridization signal for VEGF-receptor-2 mRNA is shown for comparison. Sections are counterstained with toluidine blue. Bar = 20 μm. (Reproduced with permission from Alt et al., 2002).

parenchyma, either in cells localized within inflammatory cuffs or alternatively in astrocytes or microglial cells in no spatial relation to the distribution of cellular infiltrates (Table 3.1.1). The expression pattern of CXCL12/SDF-1 in the CNS during EAE was not distinguishable from its expression pattern in the healthy CNS. Finally, expression of XCL1/lymphotactin could not be detected in brain or spinal cords of mice afflicted with EAE.

Therefore, in contrast to the expression of the inflammatory chemokines like CXCL9, CXCL10, CCL2, CCL3, CCL4, CCL5, CCL6 and CCL22, which were only observed in cells within the CNS parenchyma, constitutive expression of the lymphoid chemokine CCL19 and inducible expression of the lymphoid chemokine CCL21 could be detected in CNS venules. Additionally, expression of their common receptor, CCR7 in infiltrating cells during EAE implies a possible involvement of
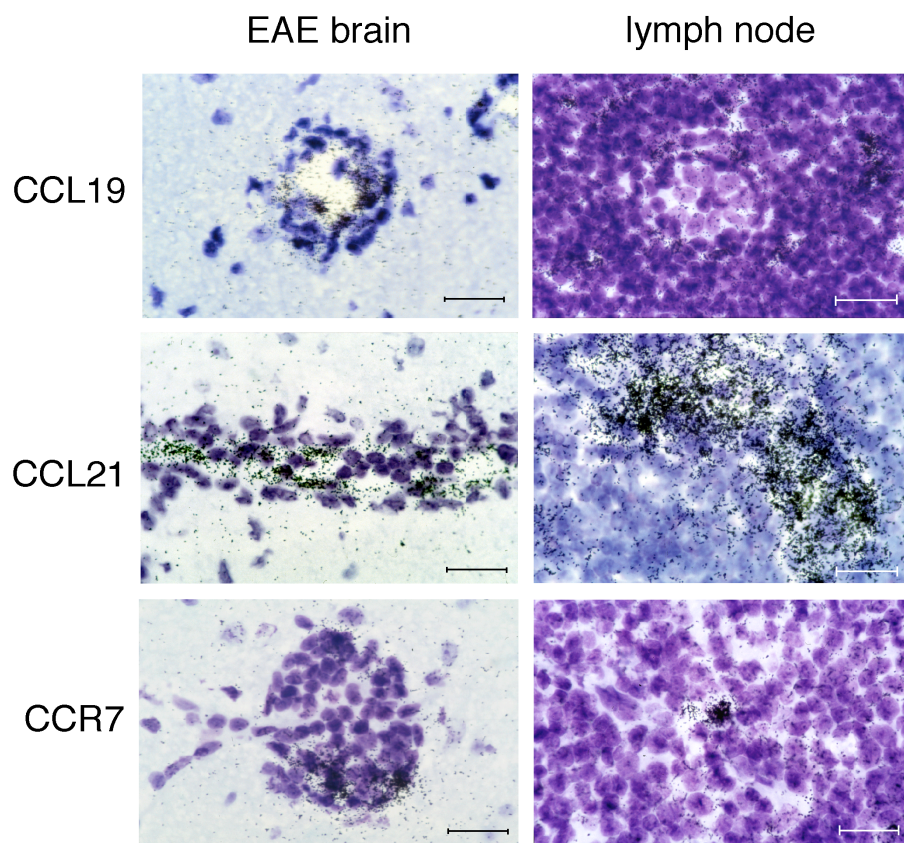
	EAE brain	lymph node
CCL19		
CCL21		
CCR7		

Figure 3.1.5: CCL19 and CCL21 are expressed at the inflamed BBB. *In situ* hybridization analysis for CCL19, CCL21 and their common receptor CCR7 in the brain of an SJL/N mouse afflicted with EAE (day 14, clinical score 2/3) and in a peripheral lymph node derived from a healthy SJL/N mouse is shown. A specific hybridization signal for CCL19 and CCL21 mRNA can be localized to inflamed vessels surrounded by inflammatory cells, whereas a hybridization signal for CCR7 mRNA can be localized to individual cells present within the inflammatory cuff. Control *in situ* hybridization for both lymphoid chemokines and their receptor on peripheral lymph nodes demonstrates their known expression within the lymph node parenchyma (CCL19, CCR7) and in high endothelial venules (CCL21). Sections are counterstained with toluidine blue. Bar = 20 μm. (Reproduced with permission from Alt et al., 2002).

these chemokine/receptor pairs in recruitment of inflammatory cells across the BBB into the CNS parenchyma.

3.1.3 CCL19 and CCL21 are present in inflammatory cuffs in the CNS of mice afflicted with EAE

After having detected expression of CCL19 and CCL21 in blood-brain barrier endothelial cells, the question arose if these two proteins are really present at the endothelial blood-brain barrier. Therefore, immunohistochemistry was performed
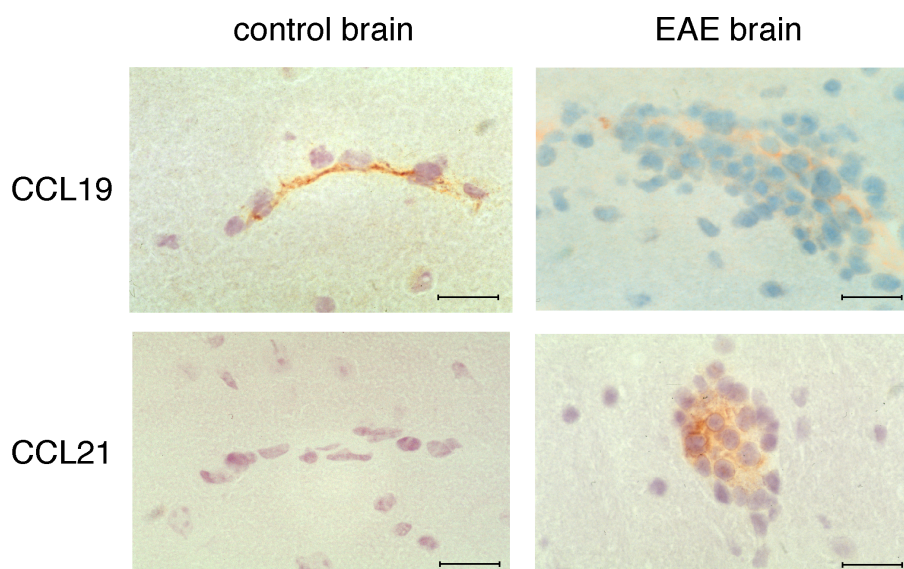
Figure 3.1.6: Detection of CCL19 and CCL21 on the protein level in healthy and EAE brain. In healthy brain, immunostaining for CCL19 but not CCL21 can be demonstrated on a subpopulation of venules throughout the brain. In EAE, immunostaining for both chemokines can be detected within inflammatory cuffs. Identical staining with several control sera showed no background staining (data not shown). Immunoperoxidase staining with hematoxyline counterstain. Bar = 20 μm. (Reproduced with permission from Alt et al., 2002).

on brain sections of mice afflicted with EAE and healthy littermates to localize CCL19 and CCL21 proteins in the CNS of SJL/N mice. Consistent with the mRNA expression pattern detected in the CNS of healthy SJL/N mice, a specific immunostaining for CCL19 could be observed on a small subpopulation of venules, while CCL21 could not be detected in the healthy CNS (Figure 3.1.6). However, during EAE, immunostaining was observed within perivascular infiltrates for both lymphoid chemokines, CCL19 and CCL21 (Figure 3.1.6). This staining was mostly diffuse but strictly limited to inflammatory cuffs. This suggests that both lymphoid chemokines CCL19 and CCL21 might either be released into the perivascular space by the BBB endothelial cells or might be additionally detected on inflammatory cells bound to their specific receptors.

3.1.4   Quantification of CCL19 and CCL21 in whole brain lysate of mice afflicted with EAE

Next we asked if CCL19 and CCL21 protein expression changes can be quantified in the brain of mice afflicted with EAE in comparison to healthy untreated control
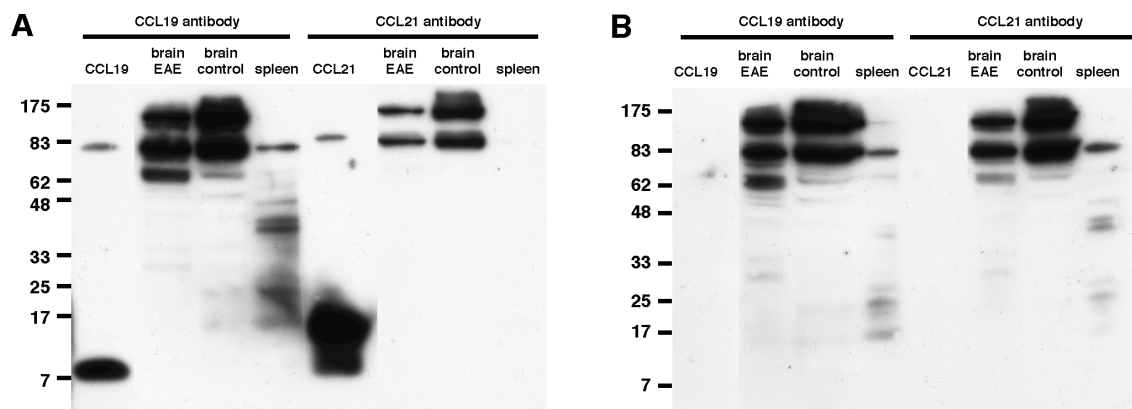
Figure 3.1.7: A: Immunoblot of whole brain lysates with CCL19 and CCL21 antisera (AF880 and AF457) on PVDF membranes. Recombinant CCL19 and CCL21 could be detected. However, neither of these two chemokines could be detected in either brain or spleen lysates. B: Immunoblot without primary antibodies shows unspecific binding of the secondary antibody.

mice. Therefore, lysates were prepared from whole brains of SJL/N mice afflicted with EAE and of healthy SJL/N mice. Furthermore, lysates were prepared from spleens or lymph nodes of Balb/C mice, where CCL19 and CCL21 expression has been described before. As chemokines are known to strongly bind to extracellular matrix proteins, RIPA buffer containing anionic, cationic and neutral detergents was used to create tissue lysates. Protein concentrations were determined by bicinchoninic acid (BCA) assay. About 200 μg protein lysate were loaded per midi gel lane and separated by Tris-Tricine buffered SDS-PAGE. As a control, 60 ng recombinant chemokine (R&D, Wiesbaden, Germany) were loaded. Proteins were electroblotted on PVDF membranes. By immunoblot using either goat-anti-CCL19 antiserum (AF880; see 2.3.1.2) or goat-anti-CCL21 antiserum (AF457; see 2.3.1.2) and a biotinylated donkey-anti-goat IgG second stage antibody, which was visualized by chemiluminescence, recombinant CCL19 or CCL21 could be detected (Figure 3.1.7). However, although the secondary antibody alone did result in unspecific binding, neither CCL19 nor CCL21 could be detected in any lysate (Figure 3.1.7). To allow detection of CCL19 or CCL21 in the lysates, several modifications of the protocol were undertaken. RIPA buffer containing 6 M urea was used for better denaturation during lysate preparation to make sure that no chemokines remained bound to extracellular matrix components, however, without success. Recombinant CCL19 or CCL21, which had been added to the tissue lysates as a control, could be detected as expected and were neither masked nor bound to other lysate proteins.

Lysates were blotted alternatively on nitrocellulose or PVDF membranes, to test if CCL19 or CCL21 preferably bound to either of these two membranes. PVDF membranes appeared to result in slightly better control protein detection, however, nothing was detected in any lysate (data not shown). Different primary antibodies recognizing CCL21 (rabbit-anti-CCL21; Peprotech, London, UK; 4B1, kindly provided by Martin Dorf, Boston, MA, USA) were tested but did not allow detection of the recombinant protein (data not shown). Alternate secondary antiserum (rabbit-anti-goat; Vector; Linaris, Wertheim, Germany) did not allow detection of the protein in lysates and provided even more unspecific signals (data not shown). Therefore, CCL19 and CCL21 were not detectable by immunoblot in brain or spleen lysates with the currently available antibodies.

3.1.5   CCR7 and CXCR3 are present on encephalitogenic T lymphocytes

While CCR7 is the common receptor of CCL19 and CCL21, it has been described by one research group, that mouse CCL21 does additionally bind and signal via the CXC chemokine receptor CXCR3 (Soto et al., 1998). Therefore, immunohistochemical stainings of cytospin preparations of encephalitogenic T lymphoblasts were performed to investigate the presence of CCR7 and CXCR3. By this, specific staining for both chemokine receptors, CCR7 and CXCR3 could be detected (Figure 3.1.8). This strongly suggests that CCL19 and CCL21 can bind to their specific receptors on encephalitogenic T lymphoblasts.

3.1.6   Encephalitogenic T lymphocytes express L-selectin *in vivo*

In contrast to other observations, that effector memory T lymphocytes do not express CCR7 and L-selectin (Sallusto et al., 2000), freshly restimulated encephalitogenic T lymphoblasts did express CCR7, however, L-selectin surface expression could not be detected by flow cytometry. Therefore, the questions arose, whether they represent a new group of T cells and if they may express L-selectin *in vivo*. To analyze this, freshly restimulated SJLB.PLP6 T lymphoblasts were labeled with Cell Tracker Green (CTrG) and injected into SJL/N mice. After 48 and 72 hours, single
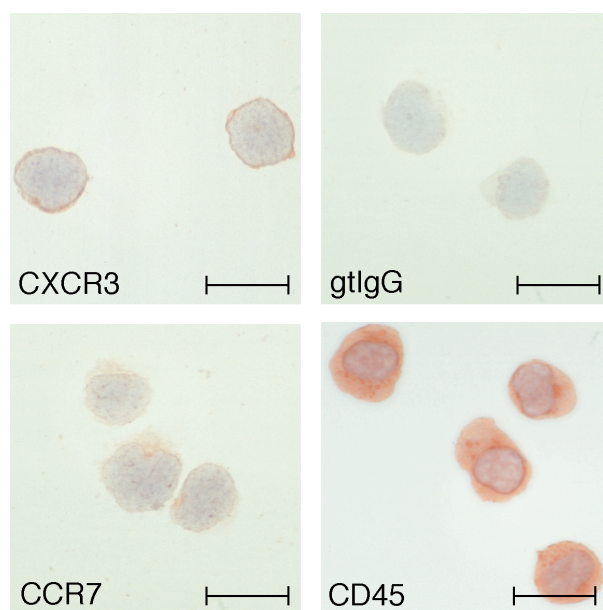
Figure 3.1.8: CCR7 and CXCR3 are present on encephalitogenic T cell blasts. Immunostaining for CCR7 and CXCR3 on cytospin preparations of SJL.PLP6 are shown. After fixation with acetone, T cells were stained with purified goat anti CCR7 and purified goat anti-mouse CXCR3. The apparent intracellular staining for CCR7 is partially explained by the fact that the antibody is directed against the intracellular C terminus. Staining for CD45 is shown as positive control, and staining with irrelevant goat IgG as a negative control. Both chemokine receptors can be detected on encephalitogenic T lymphoblasts. Immunoperoxidase staining with hematoxyline counterstain. Bar = 20 μm. (Reproduced with permission from Alt et al., 2002).

cell suspensions were prepared from spleens, blood samples, mesenteric and peripheral (mixture of axillary, inguinal and popliteal) lymph nodes. These cells were stained with Mel 14 and phycoerythrin-conjugated secondary antibody to detect L-selectin surface expression. Cells were analyzed by flow cytometry, scattergating for lymphocytes and gated for green fluorescent cells (Figure 3.1.9A).

CTrG-labeled T lymphoblasts had been cultured in parallel *in vitro* for flow cytometer calibration to be able to find the CTrG stained cell *in vitro*. After 48 hours, 99.6 % of these SJLB.PLP6 cells stained positive for CTrG, however, they did not express L-selectin (Figure 3.1.9B). 0.3 % of the splenocytes, 0.1 % of the mesenteric lymphocytes and 0.7 % of the peripheral lymphocytes stained positive for CTrG, while blood samples did not contain enough cells for analysis. L-selectin expression of these freshly prepared cells was increased (Figure 3.1.9B).

After 72 hours, 99.9 % of the *in vitro* cultured SJLB.PLP6 remained positive for CTrG, while L-selectin surface expression was not detectable (Figure 3.1.9B).
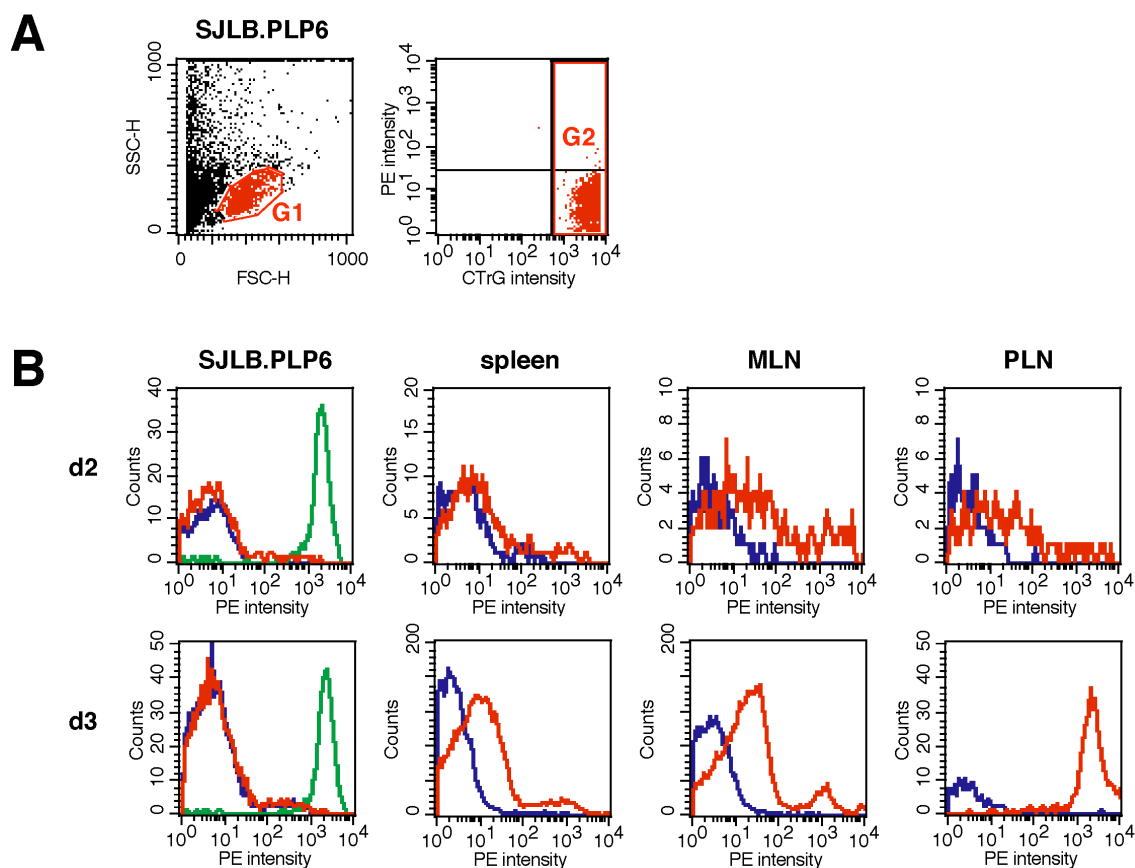
Figure 3.1.9: L-selectin expression of CTrG labeled encephalitogenic T lymphoblasts *in vivo*. SJLB.PLP6 lymphoblasts were labeled with CTrG directly after restimulation and intravenously injected into SJL/N mice. In parallel, a small subset of labeled cells was cultured *in vitro*. After 48 and 72 hours, splenocytes, mesenteric lymphocytes and peripheral lymphocytes were prepared and stained with Mel-14, an antibody directed against murine L-selectin. A: Cells were scattergated for lymphocytes (G1) and for green fluorescent cells (G2). B: In comparison to *in vitro* cultured SJLB.PLP6 T lymphocytes, L-selectin expression is increased in splenocytes, mesenteric lymph node cells (MLN) and peripheral lymph node cells (PLN) after 2 or 3 days *in vivo*. 9B5 negative control stained cells are shown in blue, M1/9 positive control stained cells are shown in green and Mel-14 stained cells are shown in red. 1 of 2 independent experiments is shown.

However, numbers of CTrG positive cells of freshly prepared lymph node cells were increased (splenocytes 4.4 %, mesenteric lymphocytes 2.6 %, peripheral lymphocytes 3.4 %). Additionally, there were distinct L-selectin expressing populations detectable in spleen and mesenteric lymph nodes and a very prominent population in the peripheral lymph nodes (Figure 3.1.9B). Therefore we concluded, that encephalitogenic T lymphoblasts can reexpress L-selectin *in vivo*, while losing it *in vitro*.

3.1.7 Encephalitogenic T lymphocytes specifically chemotax towards CCL19 and CCL21

Next we asked, whether encephalitogenic T cells can specifically chemotax towards CCL19 and CCL21 in a two-chamber system *in vitro* (see 2.1.6). Already in the absence of either chemokine, encephalitogenic T lymphocytes spontaneously migrated across fibronectin-coated filters into the lower chamber of the two-chamber system (Figure 3.1.10).

Addition of increasing concentrations of either CCL19 or CCL21 to the lower chambers did significantly increase the number of migrating T lymphocytes. Migration was concentration dependent, with CCL19 having its effect at concentrations of 1 ng/ml and CCL21 at 10 ng/ml. Interestingly, only chemotaxis towards CCL19 but not CCL21 reached a plateau level. Simultaneous presence of both chemokines in the lower chamber did not increase the chemotactic efficacy (Figure 3.1.11). CCL19 or CCL21 induced chemotaxis of towards CCL19 or CCL21 was comparable to that observed for lymphocytes which had been freshly isolated from lymph nodes (Figure 3.1.10). As pretreatment of either chemokine with a respective blocking antibody reduced the chemotaxis rate of autoaggressive T lymphocytes to background levels, migration was specifically induced by the investigated chemokines (Figure 3.1.10). Additionally, increased migration towards both chemokines required intact $G_{\alpha i}$-protein signaling of the T lymphocytes, as pretreatment with PTX but not with MTX reduced migration to background levels irrespective of chemokine concentrations (Figure 3.1.10). Therefore, CCL19 and CCL21 specifically induced G-protein-dependent chemotaxis of encephalitogenic T cells *in vitro*.

3.1.8 Transmigration of encephalitogenic T cells towards chemokines

The next question was, whether encephalitogenic T cells transmigrate across brain endothelioma cell lines towards chemokines in a concentration dependent manner. To answer this question, bEnd5 cells were seeded onto two-chamber filter inserts and grown for two days until confluency. Then, chemokines were added to the lower chamber and encephalitogenic T cells, which were untreated or pretreated with either PTX or MTX, were added to the upper chamber. Cells were incubated
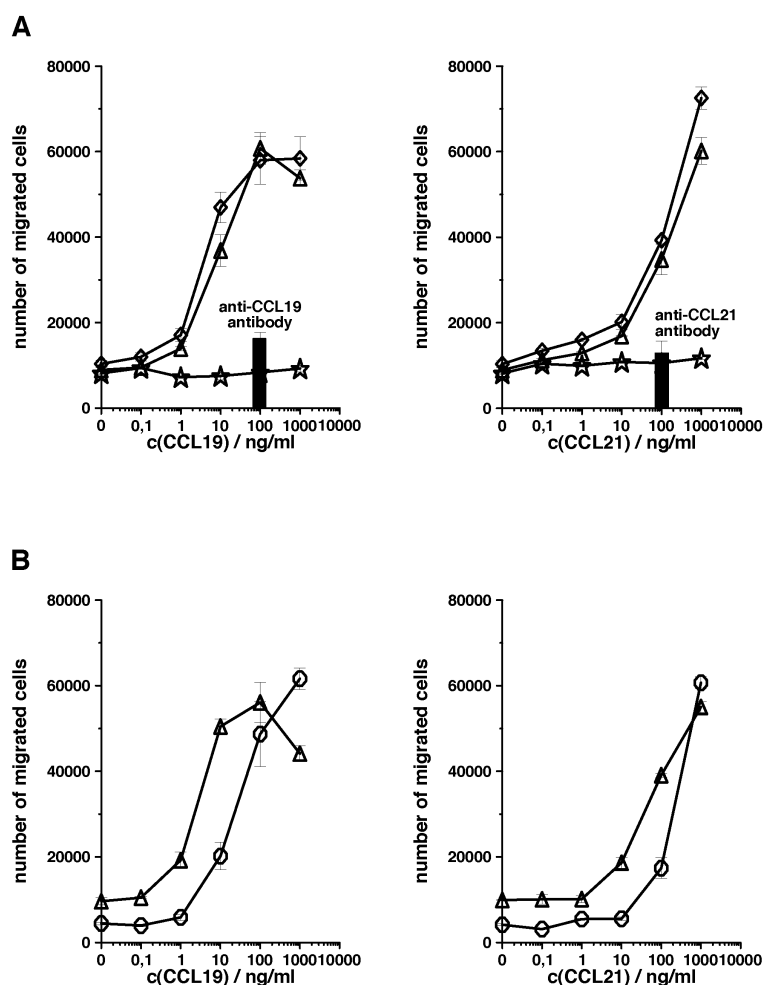
Figure 3.1.10: Encephalitogenic T cells specifically chemotax towards CCL19 and CCL21. (A) Migration of SJL.PLP6 across fibronectin-coated Transwell filters is shown. SJL.PLP6 migrated in a concentration-dependent manner towards CCL19 or CCL21 (triangles). Migration could be specifically reduced to spontaneous migration levels by pretreatment of the chemokine with its respective blocking antibody (bars; 50 μg/ml). Pretreatment of SJL.PLP6 with pertussis toxin (PTX) (stars) but not mutated PTX (MTX; diamonds) abrogated the directed migration to the level of spontaneous migration. MTX (PTX-9K/129G) had been kindly provided by R. Rappuoli, Chiron SpA, Siena, Italy (Pizza et al., 1989). (B) Comparison of chemotaxis of encephalitogenic T cells (triangles) and lymphocytes (circles) freshly isolated from lymph nodes is shown. Encephalitogenic T cells demonstrate increased migration towards CCL19 and CCL21 at lower concentrations compared to increased migration of lymph node lymphocytes. (Reproduced with permission from Alt et al., 2002).

Figure 3.1.11: Combination of CCL19, CCL21 and CXCL12 does not increase specific chemotactic efficacy of encephalitogenic T cells as shown by comparison of chemotactic response to either single chemokines (open symbols) or combinations of two chemokines (filled symbols). One representative experiments shows specific chemotaxis of encephalitogenic T cells towards CCL19 (open tri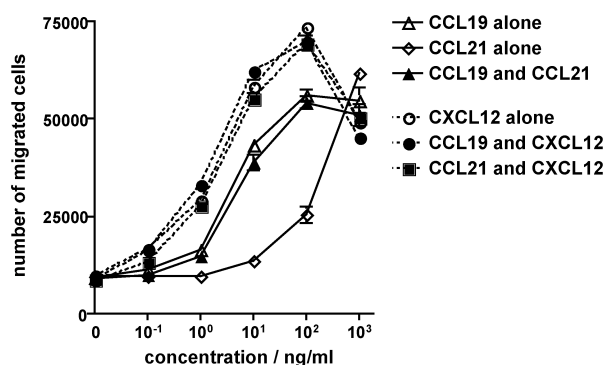angles) and CCL21 (open diamonds), while combination of these two chemokines (filled triangles) does not increase chemotaxis but rather resembles the chemotactic response towards CCL19 (n=2). Additionally, preliminary data of one experiment show that neither combined application of CCL19/CXCL12 (filled circles) nor CCL21/CXCL12 (filled quadrangles) result in increased chemotaxis as compared to CXCL12 alone (empty circles).
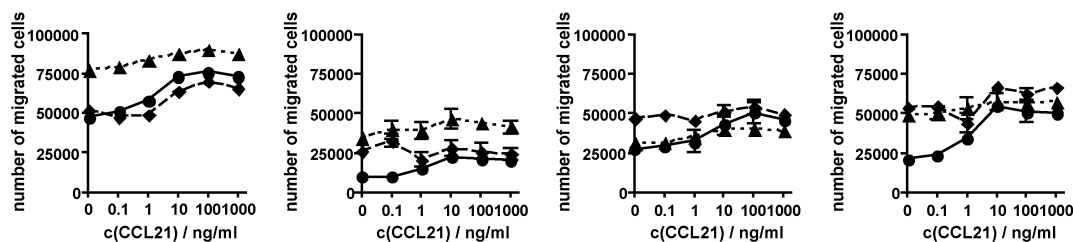
Figure 3.1.12: Transmigration of encephalitogenic T cells across bEnd5 cells towards CCL21. Four independent experiments showing numbers of SJLB.PLP6 lymphocytes at day 2 after restimulation transmigrating across TNFα–stimulated bEnd5 endothelioma cell monolayers towards increasing concentrations of CCL21 (circles, solid lines). As a comparison, T lymphocytes had been pretreated with either PTX (triangles, dotted lines) to block chemokine receptor signaling as well as MTX (diamonds, dashed lines) as a control.

for four hours and migrated cells were counted using a CASY TT Cell Counter (Figure 3.1.12). Untreated cells showed a dose-dependent migration towards the chemokine, which could be inhibited by blocking chemokine receptor signaling with PTX treatment. However, although PTX treatment blocked the dose dependent migration towards each chemokine, it surprisingly resulted in increased baseline migration of the encephalitogenic T cells, suggesting a haptotactic effect of PTX.

Even more surprisingly, MTX pretreatment of T cells, which was used as a negative control and should not have had any effect, did in fact increase the baseline levels of T cell migration in the majority of the experiments. Furthermore, additional factors may be important in this experimental setup. I. e., chemokines may be expressed by bEnd5 endothelioma cells themselves, which was not measured. Taken together, these experiments have to be considered inconclusive.

3.1.9   Reduced binding of encephalitogenic T lymphocytes to inflamed brain venules *in vitro*

In order to get more direct evidence of CCL19 and CCL21 to be functionally involved in adhesion strengthening of encephalitogenic T lymphocytes to CNS venules, modified Stamper-Woodruff-binding assays were performed on unfixed frozen sections of EAE brains (Stamper and Woodruff, 1976; Steffen et al., 1994). Thereby, selective binding of encephalitogenic T lymphocytes to inflamed venules exposed in frozen sections of EAE brains was observed (Figure 3.1.13A). General inhibition of chemokine receptor signaling by pretreatment of T lymphocytes with PTX or specific functional deletion of CCR7 and CXCR3 by desensitization with high doses of CCL19 and CCL21 significantly reduced the number of firmly adhering T lymphocytes on inflamed venules in EAE brains (Figure 3.1.13). Alternatively, the number of T lymphocytes firmly adhering to cerebral vessels of EAE brains was reduced by pretreatment of frozen sections with blocking antisera directed against CCL19 and CCL21. Therefore, functional binding of the lymphoid chemokines CCL19 and CCL21 to their respective receptor(s) participates in adhesion strengthening induction of encephalitogenic T lymphocytes to inflamed venules located in EAE brains *in vitro*.

3.1.10   Functional involvement of CCL19 and CCL21 in lymphocyte recruitment across the endothelial BBB *in vivo*

Next we asked, if we can prove functional involvement of CCL19 and CCL21 in lymphocyte recruitment across the endothelial BBB *in vivo*. Therefore, encephalitogenic T lymphoblasts SJLB.PLP7 were stained with Cell Tracker Orange (CTrO)
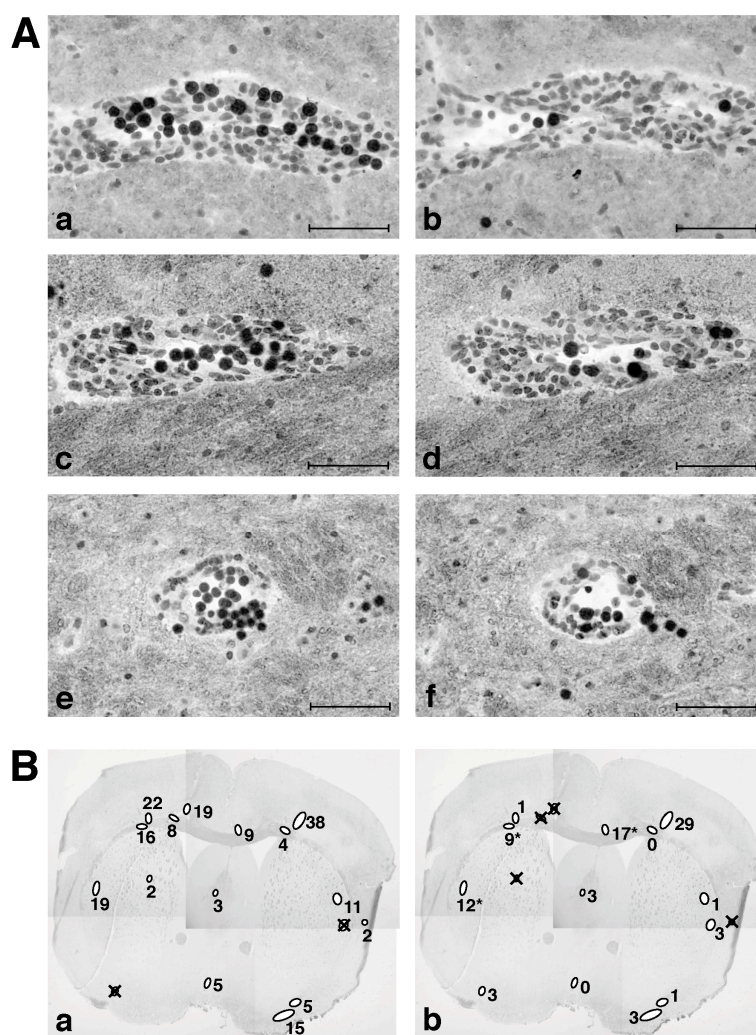
Figure 3.1.13: A: CCL19 and CCL21 are involved in adhesion strengthening of encephalitogenic T cells to inflamed vessels in EAE brain. Adhesion of the encephalitogenic T cells to inflamed venules exposed in serial frozen sections of EAE brains is shown for each condition. Pretreatment of T lymphocytes with PTX significantly reduced the number of firmly adhering T cells (a: control, 26 bound T cells; b: PTX-pretreated T cells, 3 bound T cells) as did desensitization of T lymphocytes with CCL19 and CCL21 (c: control, 15 bound T cells; d: desensitized T cells, 8 bound T cells). Also blocking CCL19 and CCL21 interfered with adhesion strengthening of T cells (e: control, 23 bound T cells; f: in presence of blocking antibodies, 8 bound T cells). Toluidine blue counterstain. Bar = 50 μm. (Reproduced with permission from Alt et al., 2002). B: A representative experiment shows adhesion of PTX pretreated (a) and untreated (b) encephalitogenic T cells to inflamed venules exposed in serial frozen sections of EAE brains. Pretreatment of T lymphocytes with PTX significantly reduced the number of firmly adhering T cells which was counted for serial sections. Inflamed venules which could not be analyzed due to tissue quality are marked with an X, while numbers of T cells which aggregated with each other were marked with an asterix. In both cases, these results were excluded. Toluidine blue counterstain.
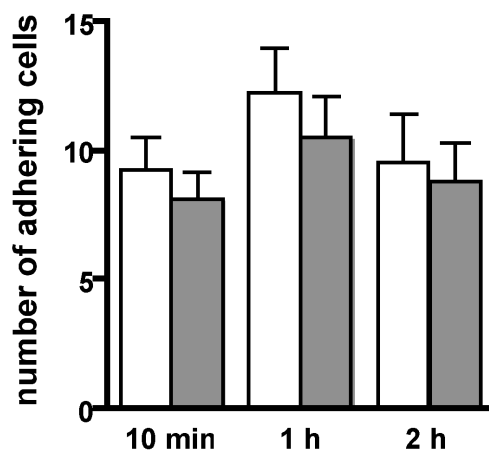
Figure 3.1.14: Firm adhesion of encephalitogenic T lymphoblasts after CCL19 desensitization as analyzed by intravital fluorescence videomicroscopy in SJL/N mice (n = 2). Desensitization with CCL19 reduces firmly adhering SJLB.PLP7 T lymphoblasts as compared to mock-treated T lymphoblasts *in vivo*.

and optionally pretreated with a high concentration of CCL19 to desensitize CCR7 by receptor internalization. Dr. Peter Vajkoczy (Klinikum Mannheim, University of Heidelberg) prepared a catheter in the right common carotid artery of SJL/N mice and opened the spine and dura mater to be able to watch the spinal cord. He injected FITC-dextrane into the right carotid artery to visualize the vascular system. Subsequently, CTrO labeled encephalitogenic T cells were injected and interaction with spinal cord microvasculature was followed. The following analysis was performed in this present work. Lymphoblasts adhering to spinal cord venules were counted 10 min, 1 hour and 2 hours after injection. Comparison of CCL19- and mock-pretreated T lymphoblasts revealed a slightly reduced firm adhesion of encephalitogenic T lymphoblasts to spinal cord microvessels (Figure 3.1.14). Although this preliminary experiment proposes functional involvement of CCL19 in lymphocyte recruitment across the endothelial BBB *in vivo*, the results has to be considered not significant. Additional studies are required to obtain final proof.

3.2 Gene and protein expression profiling of cerebral microvessels in EAE

3.2.1 Gene chip analysis of cerebral microvessels

In order to identify new genes being involved in lymphocyte recruitment from the bloodstream across the endothelial BBB into the brain parenchyma, in this present work cerebral microvessels were isolated from two different mouse strains afflicted with EAE as well as age and strain-matched healthy mice (see 2.1.4.1.2).

These microvessel preparations were shock-frozen and sent to Mrs. Kristina Duvefelt (Astra-Zeneca, Södertälje, Sweden), who performed the following experiments: 0.25 mg mRNA was obtained from 10 mg cerebral microvessels (wet weight) isolated from 12 C57Bl/6 mice afflicted with EAE (day 12 post immunization, mean disease score 0.5 ± 0.1) and 0.60 mg mRNA were isolated from 10 mg cerebral microvessels (wet weight) of 9 SJL mice afflicted with EAE (day 14 p.I., mean clinical disease score 2.8 ± 1.2). In both cases, control preparations were done from respective numbers of age and strain-matched healthy mice. Oligonucleotide microarrays representing 6500 murine genes and ESTs were used to investigate gene expression profiles of cerebral microvessels isolated from two different mouse strains afflicted with EAE and compared to gene expression profiles obtained for cerebral microvessels isolated from age and strain-matched healthy mice.

In this present thesis, 2-fold expression changes were considered to be significant, according to the manufacturer. 238 regulated genes were found in tissue samples derived from C57Bl/6 mice, 139 genes were upregulated and 99 genes were downregulated. In cerebral microvessels derived from SJL mice 177 regulated genes were found, 134 of which were upregulated and 43 downregulated. These regulated genes were evaluated and sorted into functional clusters. When comparing both gene array profiles 128 of the genes regulated in each model were found to be regulated in cerebral microvessel preparations derived from both EAE models, while 288 genes were found in preparations from either EAE model (Figure 3.2.1). Thus, common but also uniquely regulated gene expression was defined in the present approach. Genes coding for proteins involved in different cellular and molecular processes were found and great care was taken to functionally group them into 26 different sub-
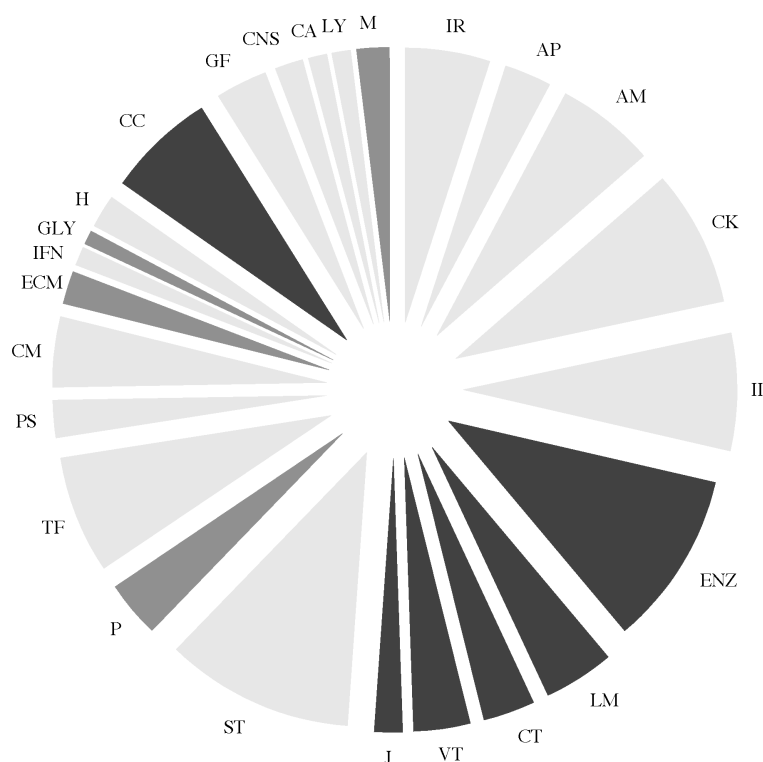
Figure 3.2.1: Cluster Analysis of Microarrays. 288 genes were found to be regulated in either C57Bl/6 or SJL mice during EAE and sorted into different functional groups. Groups which were mainly upregulated are shown in white, genes which were mainly downregulated are shown in black and groups of genes with similar numbers of upregulated and downregulated genes are shown in gray. About one quarter of the regulated genes was involved in immune responses: immune receptors (IR), antigen presentation (AP), adhesion molecules and their modification (AM), cytokines, chemokines and receptors (CK) and innate immunity (II). Another quarter of molecules was involved in general metabolism and transport mechanisms: enzymes and metabolism (ENZ), lipid metabolism (LM), channels and transporters (CT), vesicular transport, secretory pathways and membrane traffic (VT), junctional and cell-cell contact molecules (J). A third quarter of genes was involved in regulatory processes: signal transduction (ST), phosphatases (P), transcription factors and nuclear proteins (TF) and protein synthesis (PS). The last quarter consisted of genes involved in different functions like cytoskeletal molecules (CM), extracellular matrix (ECM), type I interferon regulated molecules (IFN), glycosylation enzymes (GLY), hormones, mediators and receptors (H), cell cycle, cell growth, cell survival and apoptosis (CC), growth factors, receptors and related molecules (GF), CNS-related molecules (CNS), coagulation (CA), lysosomal proteins (LY) and miscellaneous (M).

groups (Table 3.2.1). Besides these previously described genes, 11 genes of unknown function had been found, which require further investigation (Table 3.2.1: U).

Table 3.2.1: Genes which were up- or downregulated at least 2-fold according to the non-antibody-enhanced gene array in cerebral microvessels of EAE afflicted C57Bl/6 (MOG-induced EAE) and SJL/N (PLP-induced EAE) mice are listed. Genes are grouped by function of their geneproducts and listed alphabetically. Within each group genes regulated in both EAE models are listed first. Respective gene accession numbers and fold change values in either mouse strain are shown. Data for gene regulation detected only by antibody-enhanced gene array are not included except a given gene was found to be regulated in both EAE models including these values. Values obtained only by antibody-enhanced gene array are marked with an asterix.

acc. no.	name	MOG	PLP
adhesion molecules and their modification (AM)			
X14951	β2-integrin	7.1	7.9
M68903	β7-integrin	2.6	3.9
L32812	CD157 antigen	4.1	6.7*
X17501	CD48 antigen	4.3	3.2
Z16078	CD53 antigen	2.9	3.2
X97227	CD53 antigen	3.2	3.0
X14943	contactin 1	-3.8	-3.2
M31585	intercellular adhesion molecule-1	2.0	2.7
M25324	L-selectin	7.7*	2.4
X68273	macrosialin	5.2	7.0*
M87861	P-selectin	3.0	3.1*
X91144	P-selectin glycoprotein ligand 1	4.4	5.0
W08454	transmembrane 4 superfamily member 8, pending	-2.3	-2.1*
M87862	E-selectin	7.0	
D26483	transmembrane 4 superfamily member 2	-5.0	
Y00023	CD2 antigen		5.3
AA028405	intercellular adhesion molecule-2		-4.3
AA124859	intercellular adhesion molecule-2		-4.0
L15429	transmembrane 4 superfamily member 1		-2.2
antigen presentation (AP)			
V01527	class II antigen, I-A-beta	3.8	5.5
K01923	histocompatibility 2, class II antigen A, alpha	12.8*	7.3
U35323	histocompatibility 2, class II, locus Mb1	2.5*	2.7
M57890	histocompatibility 2, complement component factor B	21.6	7.1
X00496	Ia-associated invariant chain	3.6	3.5
M55637	transporter 1, ATP-binding cassette, sub-family B (MDR/TAP)	3.1	

Table 3.2.1: Regulated genes during EAE in cerebral microvessels of C57Bl/6 and SJL/N mice

acc. no.	name	MOG	PLP
X00702	histocompatibility 2, class II antigen E beta		4.2
X62743	histocompatibility 2, class II, locus Mb1		5.9
X62742	histocompatibility 2, class II, locus Mb1		7.2
cell cycle, cell growth, cell survival and apoptosis(CC)			
L16462	B-cell leukemia/lymphoma 2 related protein A1a	2.6	13.5
U09507	cyclin-dependent kinase inhibitor 1A (P21)	2.3	3.2
X59846	growth arrest specific gene 6	-2.0	-4.1
X82786	Ki-67 antigen	5.4*	3.5
X70398	P311	-2.8	-6.8
AA059662	protease, serine, 11 (Igf binding)	-2.9	-3.9
M90397	B-cell leukemia/lymphoma 3	11.1	
M64292	B-cell translocation gene 2	2.1	
U22399	cyclin-dependent kinase inhibitor 1C (P57)	-2.1	
X67644	immediate early response 3	6.5	
M93310	metallothionein-III	-2.8	
X83570	neuronatin	-2.2	
D49429	RAD21 homolog (S. pombe)	-2.3	
X92665	ubiquitin-conjugating enzyme E2E 1	-2.7	
M64279	B lymphoma Mo-MLV insertion region 1		-2.6
L49433	baculoviral IAP repeat-containing 3		2.3
M83749	cyclin D2		-2.4
X54149	growth arrest and DNA-damage-inducible 45 β		4.1
channels and transporters (CT)			
M92378	gamma-aminobutyric acid (GABA-A) transporter 1	-5.0	-2.3*
L02914	aquaporin 1	-3.3	
X61433	ATPase, Na+/K+ transporting, beta 1 polypeptide	-2.4	
M14757	ATP-binding cassette, sub-family B (MDR/TAP), member 1B	3.2	
AA145535	FXYD domain-containing ion transport regulator 1	-2.1	
J04036	solute carrier family 4 (anion exchanger), member 2	-5.5	
U20372	voltage-dependent calcium channel $\beta 3$ subunit	-3.3	
AA109109	transient receptor potential cation channel, subfamily C, member 2		-2.2
U69135	uncoupling protein 2, mitochondrial		2.7
CNS-related molecules (CNS)			
X72230	5-hydroxytryptamine (serotonin) receptor 2C	-3.0	
X59520	cholecystokinin	-4.8	
U51908	neurotensin receptor 2	-6.2	

Table 3.2.1: Regulated genes during EAE in cerebral microvessels of C57Bl/6 and SJL/N mice

acc. no.	name	MOG	PLP
M37335	proteolipid protein	-5.2	
U57324	presenilin 2		2.8
coagulation (CA)			
M16238	fibrinogen-like protein 2	2.6	3.4
W70579	coagulation factor X		2.7
J03520	tissue plasminogen activator		2.9
cytokines, chemokines and receptors (CK)			
D17292	adrenomedullin receptor	5.5	2.1
X80992	bone morphogenetic protein 6	-2.8	-2.7*
M19681	CCL2	2.7	4.8
U02298	CCL5	5.8	11.3
M58004	CCL6	11.5	6.4
X70058	CCL7	6.4	4.3
U15209	CCL9	7.4	20.1
J04596	CXCL1	5.8	4.1*
M86829	CXCL10	2.2	2.8
M34815	CXCL9	5.6	8.2
M58288	G-CSF receptor	12.5	6.0
M64404	interleukin-1 receptor antagonist	2.0*	3.6
M15131	interleukin-1β	12.0	9.8
M83649	tumor necrosis factor receptor superfamily member 6	2.6	2.8
U77630	adrenomedullin	8.4	
U56819	CCR2	7.8	
M20658	CD121a antigen	2.2	
M27960	CD124 antigen	2.6	
U21795	CD132 antigen	2.0	
X57796	tumor necrosis factor receptor superfamily member 1a	2.4	
M59378	tumor necrosis factor receptor superfamily member 1b	2.2	
X57413	transforming growth factor β 2		-2.7
U06950	tumor necrosis factor		4.1
cytoskeletal molecules (CM)			
AA106190	calmodulin-like 4	-18.5	-3.0*
X54511	capping protein (actin filament), gelsolin-like	2.9	2.0
M90316	lymphocyte specific 1	3.3	4.1
D00208	S100 calcium binding protein A4	2.8	3.3
X66449	S100 calcium binding protein A6 (calcyclin)	2.2	3.1
X87966	S100 calcium binding protein A8 (calgranulin A)	29.8	17.5

Table 3.2.1: Regulated genes during EAE in cerebral microvessels of C57Bl/6 and SJL/N mice

acc. no.	name	MOG	PLP
M83219	S100 calcium binding protein A9 (calgranulin B)	25.1	13.8
AA097087	kinesin family member 5B	-2.4	
D37837	lymphocyte cytosolic protein 1	3.3	
L22144	S100 beta	-4.8	
X60671	villin 2	-2.8	
AA153569	centrin 2		-2.3
enzymes and metabolism (ENZ)			
M22679	alcohol dehydrogenase 1	-3.5	-2.6
K00811	carbonic anhydrase 2	-6.3	-2.2
U37091	carbonic anhydrase 4	-3.4	-3.2
U49350	cytidine 5'-triphosphate synthase	3.8	2.5*
AA028501	cytochrome c oxidase, subunit VIIIh	-13.3	-3.5
AA028501	cytochrome c oxidase, subunit VIIIh	-4.4	-3.5
AA028501	cytochrome c oxidase, subunit VIIIh	-4.3	-3.1
U44389	hydroxyprostaglandin dehydrogenase 15 (NAD)	-5.3	-11.9*
U51805	liver arginase 1	11.8	5.7
D44464	uridine phosphorylase	5.4	2.6*
X75129	Xanthine dehydrogenase	4.0	2.7
U12791	3-hydroxy-3-methylglutaryl-coenzyme A synthase 2	-2.8	
W09791	aldolase 3, C isoform	-4.2	
W53351	aldolase 3, C isoform	-9.6	
U49430	ceruloplasmin	2.8	
M74149	creatine kinase, brain	-3.6	
W16151	diazepam binding inhibitor	-2.4	
M61215	ferrochelatase	-2.2	
Z11911	glucose-6-phosphate dehydrogenase X-linked	6.3	
U24428	glutathione S-transferase, mu 5	-2.8	
X51905	lactate dehydrogenase 2, B chain	-4.6	
U27195	leukotriene C4 synthase	-2.8	
M36084	malate dehydrogenase, soluble	-2.3	
J02652	malic enzyme, supernatant	-3.6	
U35646	puromycin-sensitive aminopeptidase	-3.0	
W81960	sulfotransferase family 1A, phenol-preferring, member 1	2.2	
D26123	carbonyl reductase 2		-3.7
L25069	catalase 1		-2.3
U36993	cytochrome P450, 7b1		4.6
U09816	GM2 ganglioside activator protein		2.3

Table 3.2.1: Regulated genes during EAE in cerebral microvessels of C57Bl/6 and SJL/N mice

acc. no.	name	MOG	PLP
U29947	mannosidase 2, alpha B1		5.1
Z14986	S-adenosylmethionine decarboxylase 1		-2.2
L10244	spermidine/spermine N1-acetyl transferase		2.4
extracellular matrix (ECM)			
X66976	collagen 8 alpha 1 chain	-3.0	-2.8*
M28312	tissue inhibitor of metalloproteinase 1	4.0*	6.1
L19932	transforming growth factor, beta induced, 68 kDa	6.2	7.4
X94322	cartilage derived retinoic acid sensitive protein	-3.4	
L33416	extracellular matrix protein 1		2.0
L02918	procollagen, type V, alpha 2		-3.2
glycosylation enzymes (GLY)			
X73523	sialyltransferase 4A (beta-galactosidase alpha-2,3-sialyltransferase)	2.6	
W36875	sialyltransferase 9 (CMP-NeuAc:lactosylceramide alpha-2,3-sialyltransferase)	-3.5	
growth factors, receptors and related molecules (GF)			
L05439	insulin-like growth factor binding protein 2	-3.0	
X81582	insulin-like growth factor binding protein 4	14.7	
X81584	insulin-like growth factor binding protein 6	3.3	
L40459	latent transforming growth factor beta binding protein 3	-2.6	
U59230	nel-like 2 homolog (chicken)	192.1	
X96793	placental growth factor	2.6	
W29430	serine protease inhibitor, Kunitz type 2	-3.3	
M70641	connective tissue growth factor		3.7
W16389	latent transforming growth factor beta binding protein4		-3.9
AA106674	latent transforming growth factor beta binding protein4		-3.6
hormones, mediators and receptors (H)			
AA002750	arachidonate 5-lipoxygenase activating protein	2.1	3.7
W83564	arachidonate 5-lipoxygenase activating protein	18.8	8.7
L13593	prolactin receptor	-5.0	-5.7
X07751	c-erbA alpha2 (thyroid hormone receptor)	-2.5	
M88242	cyclooxygenase 2	3.2	
W20990	thyroid hormone receptor alpha (Thra)	-2.5	
X04418	prolactin		6.6
immune receptors (IR)			
M34510	CD14 antigen	23.2	18.2
X02339	CD3δ antigen	6.8	8.6

Table 3.2.1: Regulated genes during EAE in cerebral microvessels of C57Bl/6 and SJL/N mice

acc. no.	name	MOG	PLP
M14343	CD45 antigen	3.1	4.3
M31314	Fc gamma receptor I	5.2	4.5
M63284	Fc gamma receptor IIb	16.8	15.4
W41745	Fc receptor, IgE, high affinity I, gamma polypeptide	2.9	3.7
U05265	gp49B	11.3	8.3
W75007	antigen identified by monoclonal antibody MRC OX-2	2.9	
V00802	immunoglobulin kappa chain variable 28 (V28)	3.3	
J00475	Ig germline alpha-chain gene C-switch region		20.2
M80423	IgK chain gene, C-region		17.0
V00802	immunoglobulin kappa chain variable 28 (V28)		5.0
M26053	T-cell receptor germline beta-chain gene constant region (CT)		2.5
M12379	Thy-1.2 glycoprotein		3.8
innate immunity (II)			
X94353	cathelin-like protein	2.5	6.2
X58861	complement component 1, q subcomponent, alpha polypeptide	2.9	5.5
M22531	complement component 1, q subcomponent, beta polypeptide	3.5	4.3
X66295	complement component 1, q subcomponent, c polypeptide	2.2	4.4
J00369	complement component 3	11.0	22.8
M96827	haptoglobin	7.0	3.6
J03298	lactotransferrin	5.5	3.9
X16834	lectin, galactose binding, soluble 3	2.5	4.0
M21050	lysozyme M	3.4	5.7
L20315	macrophage expressed gene 1	5.0	13.9
W13166	neutrophil gelatinase-associated lipocalin	28.7	2.2
L37297	neutrophilic granule protein	5.4	8.3
X86374	peptidoglycan recognition protein	3.5	3.4
U73004	secretory leukocyte protease inhibitor	9.3	6.7
X03505	serum amyloid A 3	16.5	20.6
M17790	serum amyloid A 4	14.0*	13.3
M17440	complement component 4, a subcomponent	2.3	
X04072	granzyme B	5.8	
X99347	lipopolysaccharide binding protein	-3.1	
M64085	serine (or cysteine) proteinase inhibitor, clade A, member 3G	3.0	
junctional and cell-cell contact molecules (J)			
Z70023	Connexin-30	-3.7*	-2.7
W97077	cadherin 13	5.5	
U19582	claudin-11	-5.8	

Table 3.2.1: Regulated genes during EAE in cerebral microvessels of C57Bl/6 and SJL/N mice

acc. no.	name	MOG	PLP
U49185	occludin	-2.1	
M90364	beta-catenin		-2.9
lipid metabolism (LM)			
W55620	apolipoprotein D	2.9	3.0*
U04827	brain fatty acid-binding protein	-8.0	-2.2*
Z22216	apolipoprotein C-II	6.2	
AA036067	apolipoprotein E	-5.2	
X14961	fatty acid binding protein 3, muscle and heart	-5.4	
M21285	stearoyl-Coenzyme A desaturase 1	-3.7	
M26270	stearoyl-Coenzyme A desaturase 2	-2.3	
U06670	very low density lipoprotein receptor	-6.5	
AA016431	fatty acid binding protein 5		2.7
M60847	lipoprotein lipase		5.7
U34277	phospholipase A2 group VII (platelet-activating factor acetylhydrolase, plasma)		7.1
U37226	phospholipid transfer protein		-2.4
lysosomal proteins (LY)			
AA146437	cathepsin S	3.6	10.8
AA089333	cathepsin S	5.2	10.2
AA106931	interferon gamma inducible protein 30	2.3	3.4
U29539	retinoic acid-inducible E3 protein	2.5	4.3
phosphatases (P)			
M99054	acid phosphatase type 5	43.2*	4.4
J02980	alkaline phosphatase 2, liver	-2.5*	-12.0
X61940	dual specificity phosphatase 1	2.2	3.4
AA016397	ectonucleotide pyrophosphatase/phosphodiesterase 2	-7.8	-2.7
AA059550	ectonucleotide pyrophosphatase/phosphodiesterase 2	-5.7	-2.7
AA116737	protein phosphatase 1, regulatory (inhibitor) subunit 1A	-4.0	-2.5*
M68902	SHP-1	3.3	5.5
L43371	hydrogen peroxide inducible protein 53	-2.7	
U24700	protein tyrosine phosphatase, non-receptor type 1	2.4	
M90388	protein tyrosine phosphatase, non-receptor type 8		3.0
X58289	protein tyrosine phosphatase, receptor type, B		-2.1
signal transduction (ST)			
U70622	endothelial differentiation, lysophosphatidic acid G-protein-coupled receptor, 2	-3.0	-2.4
X84797	hematopoietic cell specific Lyn substrate 1	3.1	3.6*

Table 3.2.1: Regulated genes during EAE in cerebral microvessels of C57Bl/6 and SJL/N mice

acc. no.	name	MOG	PLP
J03023	hematopoietic cell kinase	5.5	8.0
U20159	lymphocyte cytosolic protein 2	3.2	4.1
U15635	SAM domain and HD domain, 1	2.7	2.4
M64086	serine (or cysteine) proteinase inhibitor, clade A, member 3N	4.2	2.8
M12056	tyrosine protein kinase p56-tck	4.4	4.1
L04538	amyloid beta (A4) precursor-like protein 1	-3.2	
M69260	annexin A1	2.4	
D87117	discs, large homolog 3 (Drosophila)	-2.3	
U28728	embryonal Fyn-associated substrate	-6.3	
AA028742	guanine nucleotide binding protein (G protein), gamma transducin activity polypeptide 2	2.6	
AA153021	guanylate nucleotide binding protein 2	2.7	
X15373	inositol 1,4,5-triphosphate receptor 1	-2.7	
AA166439	kinase interacting protein 2	-2.8	
M57696	lynB	2.6	
D86176	phosphatidylinositol-4-phosphate 5-kinase, type 1 alpha	-2.6	
M94632	PKCζ	-2.6	
X17320	Purkinje cell protein 4	-10.1	
AA104043	raf-related oncogene	-3.4	
X53247	RAS-related C3 botulinum substrate 2	2.3	
U06924	signal transducer and activator of transcription 1	4.0	
U08378	signal transducer and activator of transcription 3	2.0	
W15802	similar to Serine/threonine-protein kinase pim-3	2.4	
Z46299	sperm autoantigenic protein 17	-2.4	
U15636	T-cell specific GTPase	2.2	
AA106492	cyclic AMP-dependent protein kinase A regulatory subunit 1A		41.3
U36220	FK506 binding protein 5 (51 kDa)		2.8
AA163272	FK506 binding protein 9		-3.1
X61399	MARCKS-like protein		3.0
Z49877	spleen tyrosine kinase		3.9
W46019	tyrosine 3-monooxygenase/tryptophan 5-monooxygenase activation protein, theta polypeptide		-2.2
transcription factors and nuclear proteins (TF)			
U29762	albumin gene D-Box binding protein gene	2.5	-10.9
X62600	CCAAT/enhancer binding protein (C/EBP), beta	5.9	6.3
X61800	CCAAT/enhancer binding protein (C/EBP), delta	7.4	3.4
V00727	c-fos	5.1	4.6

Table 3.2.1: Regulated genes during EAE in cerebral microvessels of C57Bl/6 and SJL/N mice

acc. no.	name	MOG	PLP
X01023	c-myc	2.9	2.7*
X07414	excision repair cross-complementing rodent repair deficiency, complementation group 1	2.2*	3.1
AA050733	glucocorticoid-induced leucine zipper	3.1	2.1*
AA097366	glucocorticoid-induced leucine zipper	3.7	3.0
Z46757	high mobility group box 2	2.5	2.7
J03236	junB	12.9	9.0
U19118	activating transcription factor 3	5.1	
AA051446	cerebellar degeneration-related 2	-5.8	
J03482	H1 histone family, member 2	-2.5	
X75018	inhibitor of DNA binding 4	-3.2	
X62648	small nuclear ribonucleoprotein N	-15.1	
U31967	SRY-box containing gene 2	-7.9	
W82793	topoisomerase (DNA) III beta	-2.9	
AA016424	X-box binding protein 1	2.7	
U63133	c-fos		8.0
J04179	high mobility group AT-hook 1		3.7
U70662	Kruppel-like factor 4 (gut)		2.0
protein synthesis (PS)			
M55561	ribosomal protein L7	4.3	5.7
AA153342	carbon catabolite repression 4 homolog (S. cerevisiae)	-2.3	
M22432	eukaryotic translation elongation factor 1 alpha 1	2.3	
U50631	heat-responsive protein 12	-3.4	
U48363	nascent polypeptide-associated complex alpha polypeptide	-2.1	
D78135	cold inducible RNA binding protein		2.2
type 1 interferon regulated molecules (IFN)			
U19119	interferon inducible protein 1	2.8	
AA145371	interferon stimulated gene 12	2.1	
X56602	interferon-stimulated protein (15 kDa)		-2.2
vesicular transport, secretory pathways and membrane traffic (VT)			
W13196	caveolin, caveolae protein, 22 kDa	-2.2*	-2.1
M64782	folate receptor 1 (adult)	-8.7	-2.1*
AA138226	clathrin, light polypeptide (Lcb)	3.2	
D38613	complexin II	-2.3	
U02982	secretogranin III	-14.8	
U58887	SH3 domain protein 2 C2	-2.8	
D83206	vesicular membrane protein p24	-4.9	

Table 3.2.1: Regulated genes during EAE in cerebral microvessels of C57Bl/6 and SJL/N mice

acc. no.	name	MOG	PLP
L38971	integral membrane protein 2A		-2.6
D13003	reticulocalbin		-2.8
miscellaneous (M)			
X15592	cytotoxic T lymphocyte-associated protein 2 beta	3.3	3.6
U69488	G7e protein (G7e-pending)	7.8	6.9
AA031158	brain abundant, membrane attached signal protein 1	-2.2	
M29325	L1Md-9 repetitive sequence (EXTRACTED 3'UTR)	-2.5	
U17259	neuron specific gene family member 2	-3.3	
X52622	IN gene for the integrase of an endogenous retrovirus		3.9
unknown (U)			
AA153032	hypothetical protein 4930422C14	2.9	3.9*
W29508	interferon induced transmembrane protein 2 like	24.4	3.8
W77701	similar to human acylphosphatase 1, erythrocyte (common) type (ACYP1)	-2.1*	-2.9
AA013976	from neonate thymus, retrovirus related endonuclease	2.3	
AA138866	hypothetical protein MGC47046 / similar to human polymerase (RNA) II (DNA directed) polypeptide B, 140kDa	2.4	
AA062342	similar to human/rat RAB28, member RAS oncogene family	-4.2	
AA124453	similar to rat interferon-inducible protein 16	7.0	
W50088	"predicted" sequence		-2.1
W13739	similar to human dimerization cofactor of hepatocyte nuclear factor 1 (HNF1) from muscle (DCOHM)		-2.4
W10459	similar to rat ATP synthase, H+ transporting, mitochondrial F1 complex, epsilon subunit (Atp5e)		-2.2
AA120109	similar to rat-IFI271 / rat-ERG2		-3.0

Supporting the current concept of EAE as a model for chronic inflammatory demyelinating diseases of the CNS with an autoimmune pathogenesis, gene array analysis resulted in the upregulation of genes coding for molecules involved in adaptive immune functions such as immune cell activation or antigen presentation ("immune receptors", "antigen presentation"; Table 3.2.1) or leukocyte recruitment ("adhesion molecules and their modification" and "cytokines, chemokines and receptors"). Increased expression of the intercellular adhesion molecule-1 (ICAM-1) was validated by *in situ* hybridization and immunohistochemistry with both approaches, demonstrating increased expression of ICAM-1 mRNA and protein in inflamed cere-
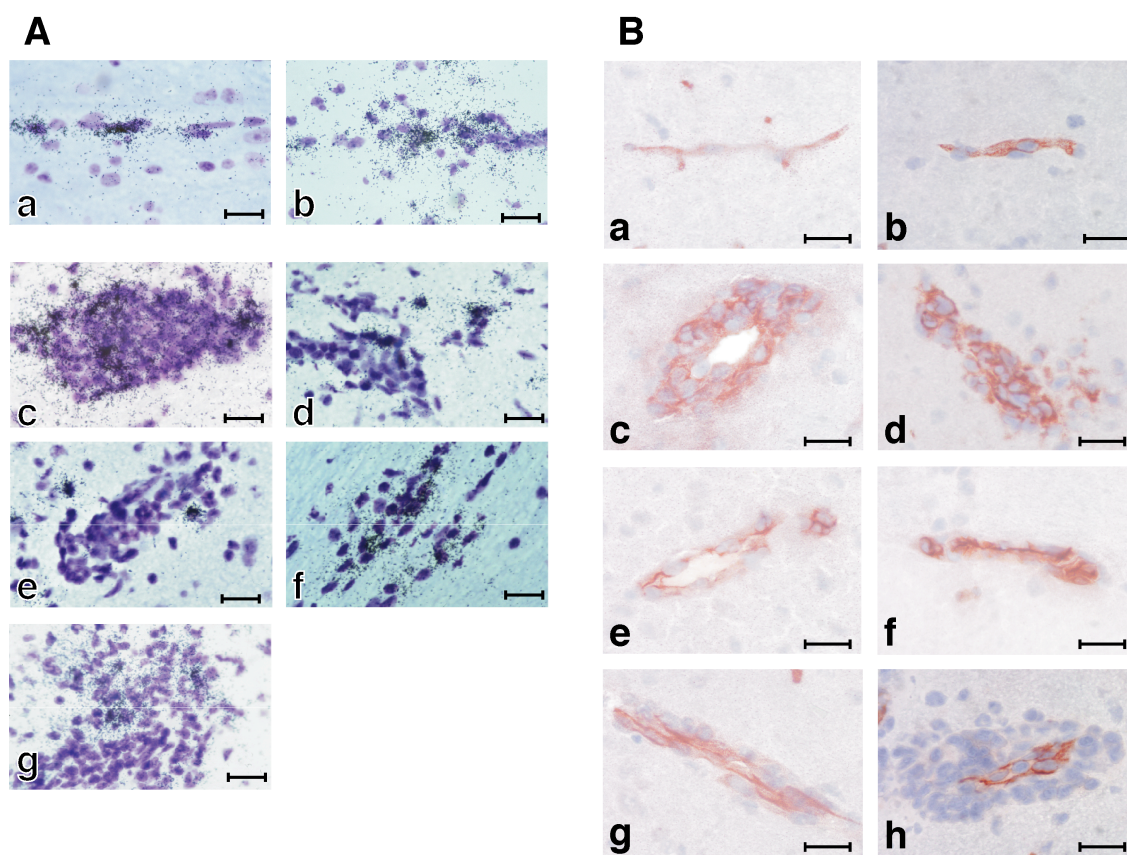
Figure 3.2.2: A: *In situ* hybridization analysis of ICAM-1, CCL2, CCL5, CCL6, CXCL9 and CXCL10 mRNA expression in brain of a healthy SJL mouse (a) and SJL mice afflicted with acute EAE (b) – (g) is shown. ICAM-1 mRNA was detected (a) and (b), as well as mRNA of inflammatory chemokines CXCL9 (c), CXCL10 (d), CCL2 (e), CCL5 (f) and CCL6 (g). Vessels (a) or vessels surrounded by inflammatory cuffs are shown (b) – (g). Toluidine blue counterstain. Bar = 20 μm. B: Presence of ICAM-1 (a) – (d) and ICAM-2 (e) – (f) in vessels of healthy brain, (a), (b), (e) and (f), or vessels surrounded by inflammatory cuffs in diseased brain (c), (d), (g) and (h) are shown. This was done in either C57Bl/6 (a), (c), (e) and (g), or SJL/N mice (b), (d), (f) and (h). Immunoperoxidase staining with hematoxyline counterstain. Bar = 20 μm.

bral venules in brains of mice afflicted with EAE when compared to healthy controls (Table 3.2.1: AM; Figure 3.2.2). Also, increased expression of inflammatory chemokines CCL2, CCL5, CCL6, CXCL9 and CXCL10 observed in the oligonucleotide microarray analysis could be confirmed by means of *in situ* hybridization (Table 3.2.1: CK, Figure 3.2.2), with undetectable expression in brains of healthy mice (data not shown), but a strong induction of their expression in close vicinity to inflamed cerebral venules surrounded by inflammatory cuffs in EAE brains (Figure 3.2.2). Additionally, we found T cell specific genes encoding CD3δ or the T cell receptor (TCR) β chain as well as macrophage specific genes i. e. coding for

CD14 (Table 3.2.1: IR), or genes coding for leukocyte adhesion receptors such as β_2-integrin or L-selectin (Table 3.2.1: AM) in our screen.

Regulation of endothelial cell specific genes was detected, which was demonstrated by the finding that gene expression for caveolin was found to be downregulated in both EAE models (Ikezu et al., 1998). Furthermore, in the SJL mouse EAE model but not in the C57Bl/6 model, downregulation of intercellular adhesion molecule-2 (ICAM-2) mRNA was detected by gene array analysis (Table 3.2.1: AM) although ICAM-2 is also present on T lymphocytes. Immunohistochemistry demonstrated endothelial cell specific staining for ICAM-2, however, failed to distinguish between different protein expression levels of ICAM-2 at cerebral microvessels in healthy or EAE brains (Figure 3.2.2). E-selectin expression was not found to be induced in the microarray screen in the SJL mouse, while P-selectin induction could only be observed after antibody amplification of the signals. In contrast upregulation of E- and P-selectin was observed in the MOG-induced EAE model in the C57Bl/6 mouse. CD53 was found to be upregulated during EAE in this present study (Table 3.2.1: AM). Upregulation of 16 genes coding for molecules involved in innate immunity in both EAE models was detected, i. e. complement component C3 was found to be upregulated by 11- or even 22-fold in MOG-induced versus PLP-induced EAE respectively.

The largest groups of genes regulated at the level of cerebral microvessels based on the gene array analysis were found to code for enzymes involved in general cell metabolism ("enzymes and metabolism") and in lipid metabolism with expression of most genes in both groups being downregulated during EAE. This was accompanied by a reduced gene expression for ion channels as well as genes coding for proteins involved in vesicular transport, secretory pathways, membrane traffic mechanisms and cell-cell-contact proteins (Table 3.2.1).

Furthermore altered expression levels of genes coding for "signaling molecules", "phosphatases", "transcription factors and nuclear proteins", "protein synthesis" were found in both models with a tendency to upregulation of gene expression within these groups (Table 3.2.1). One of the most prominently regulated genes was found to be the gene coding for the transcription factor JunB with 12-fold and 9-fold upregulation in the C57Bl/6- and SJL-model respectively (Table 3.2.1: TF).

Changes of gene expression as detected with the oligonucleotide microarrays
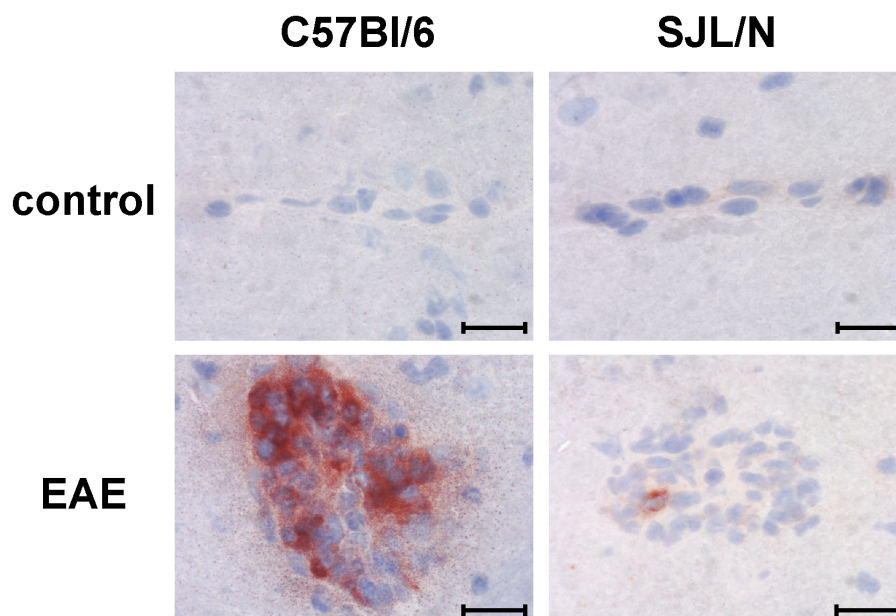
Figure 3.2.3: Inflammation of Gr-1 expressing cells can be observed during EAE in C57Bl/6 mice (day 17 after induction of disease, clinical disease score 1) but hardly in SJL/N mice (day 14 after induction of disease, clinical disease score 2). Immunoperoxidase staining with hematoxyline counterstain. Bar = 20 μm.

were extended to genes coding for cytoskeletal or extracellular matrix proteins (Table 3.2.1), underlining changes in tissue architecture at the BBB during EAE beyond the protein level. Additionally arachidonate 5 lipoxygenase activating protein (ALOX5AP) and cyclooxygenase-2 (Cox-2) were upregulated (Table 3.2.1: H). Also, altered gene expression of extracellular matrix proteins was found in both EAE models as for example tissue inhibitors of matrix metalloproteases (TIMP-1; Table 3.2.1: ECM) was found to be upregulated in both EAE models.

Furthermore, genes coding for type 1 interferon regulated proteins, namely interferon inducible protein 1 (IFI1), interferon stimulated gene 12 (ISG12) and interferon-stimulated protein 15 kDa (ISG15) were found to be upregulated in both EAE models (Table 3.2.1: IFN). Altered gene expression of beta-galactosidase alpha-2,3-sialyltransferase 4A (SiaT4A) and CMP-NeuAc:lactosylceramide alpha-2,3-sialyltransferase (SiaT9), also known as ganglioside GM3 synthase, was detected in mRNA in cerebral microvessels in the MOG EAE model but not in the PLP EAE model (Table 3.2.1: GLY). Additionally, difference in granulocyte recruitment during EAE in C57Bl/6 and SJL/N mice can be observed (Figure 3.2.3). The question arose, whether regulation of SiaT4A does result in altered glycosylation during
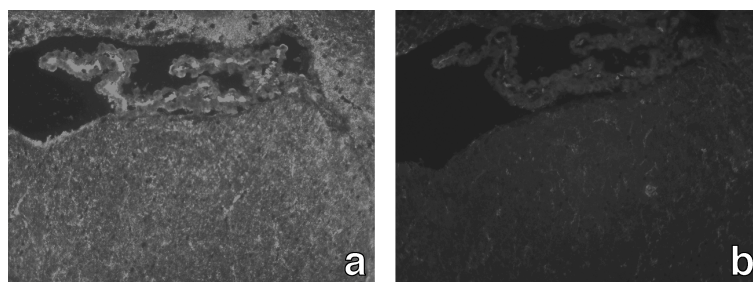
Figure 3.2.4: MALII binding on choroid plexus and vessels of EAE afflicted C57Bl/6 mouse brain (a). Binding is largely prevented by pretreating sections for 2 hours with sialidase (b). Shown is 1 preliminary experiment.

EAE pathogenesis. *Maackia amurensis* lectin II (MALII) has been described to bind preferably to the glycosylation product of SiaT4A, (α-2,3)-sialylgalactose residues and additionally bind to (α-2,6)-sialylgalactose residues. Therefore, MALII binding to brain sections of C57Bl/6 mice afflicted with EAE (day 20 after induction of disease, clinical disease score 3) was investigated. Preliminary results showed binding of MALII to brain vessels and choroid plexus of C57Bl/6 mice afflicted with EAE (Figure 3.2.4). Binding could be partially prevented by pretreating the sections with *Clostridium perfringens*-derived sialidase, which preferably digests (α-2,3)-sialylgalactose residues, according to the manufacturer (Figure 3.2.4). However, this pretreatment could not totally abolish lectin binding. Furthermore, sialidase pretreatment seemed to unmask additional binding sites (data not shown). Therefore, care has to be taken considering these preliminary results. In an alternate approach, (α-2,3)-sialylgalactose residues were detected by flow cytometry on brain-derived *in vitro* cultured bEnd5 endothelioma cells (Figure 3.2.5). Preliminary results show MALII binding, suggesting bEnd5 endothelioma cells to possess (α-2,3)-sialylgalactose residues, weak *Sambucus nigra* lectin binding, suggesting (α-2,6)-sialylgalactose residues as well as *Griffonia simplicifolia* lectin I binding, suggesting bEnd5 endothelioma cells to express α-galactose residues (see Figure 3.2.5).

3.2.2   Subtractive suppression hybridization analysis of cerebral microvessels

While gene array analysis allows to detect regulation of known genes, unknown genes which are not present on the array are missed. Alternatively, subtractive suppression
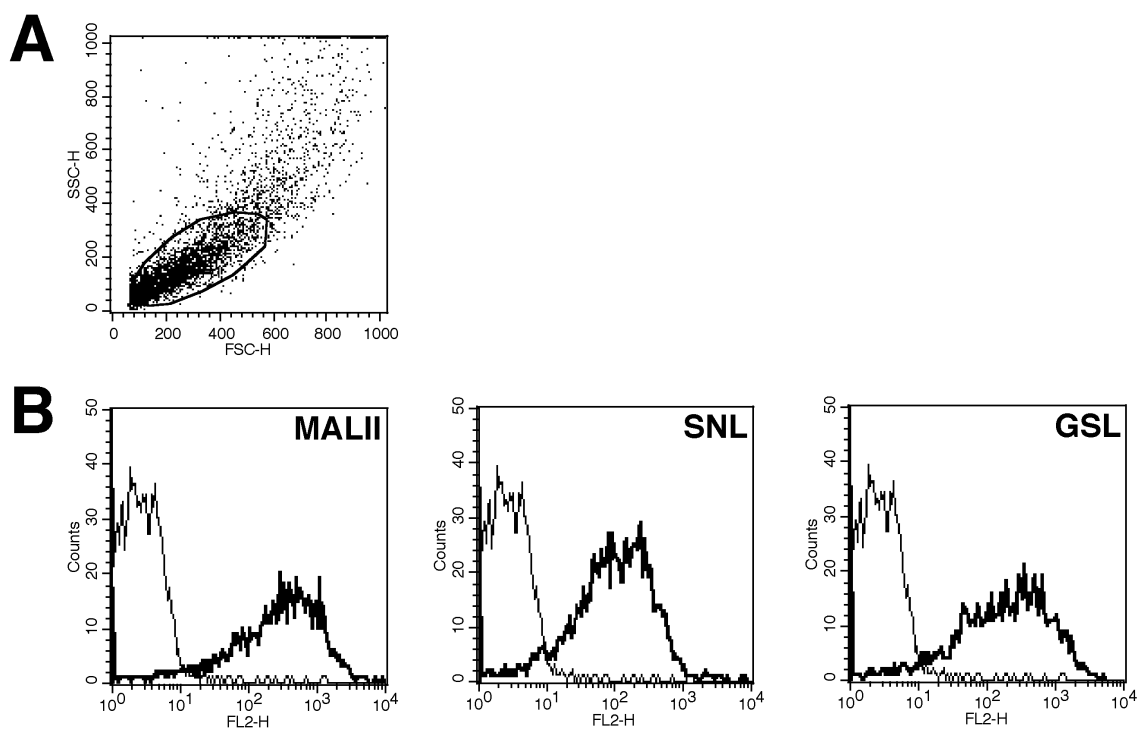
Figure 3.2.5: Lectin binding to bEnd5 endothelioma cell lines. Binding of *Maackia amurensis* lectin II (MALII), *Sambucus nigra* lectin and *Griffonia simplicifolia* lectin (GSL) on bEnd5 endothelioma cell lines as detected by flow cytometry. (A) Endothelial cells were scattergated. (B) Overlays for MALII, SNL and GSL show surface staining on bEnd5 endothelioma line cells (thick line) in comparison to no lectin (thin line).

hybridization (SSH) with subsequent high-throughput sequencing allows identification of so far unknown genes possibly being involved in lymphocyte recruitment across the endothelial blood-brain barrier during EAE.

First we asked, whether separation of cerebral microvessel by mechanic homogenization with a Dounce homogenizer (see 2.1.4.1.2) or by enzymatic digestion (see 2.1.4.1.1) resulted in higher quality of RNA. For the first preparation, 10 age-matched B6C3F1 mice were sacrificed, brains taken out, cerebellums and meninges were removed. Cerebrums were homogenized with two scalpels and digested with collagenase type II for 30 minutes at 37°C. Digestion mix was diluted in ice-cold buffer A, centrifuged and the pellet was applied to BSA gradient centrifugation, thereby separating microvessels from myelin components. Microvessels were carefully resuspended, shock-frozen in liquid nitrogen and stored at -80°C . For the second preparation, 10 age-matched B6C3F1 mice were sacrificed, brains were taken out, cerebellums and meninges removed. Brains were homogenized using a
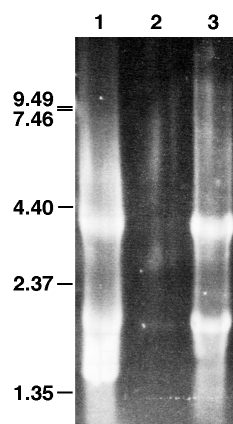
Figure 3.2.6: Comparison of RNA yield resulting from enzymatic (1) and mechanic (2) microvessel preparations showed a high quality and quantity of total RNA in the enzymatic preparation, while the mechanic preparation hardly resulted in any RNA. A control RNA preparation was added (3), which had been kindly provided by Dr. Rüdiger Arnold and Dr. Friedemann Kiefer.

Dounce homogenizer with a large clearance pestle and filtered over a 180 μm nylon mesh. Flow through was homogenized using a small clearance pestle and microvessels which got stuck on a 63μm nylon mesh were collected, shock-frozen in liquid nitrogen and stored at -80°C. Total RNA was prepared from frozen microvessel preparations without thawing the samples as described (see 2.4.6.2). Equal volumes of both samples were compared by RNA agarose gel electrophoresis (see 2.4.6.3). The first preparation by enzymatic digestion resulted in a high RNA yield, while the second preparation by mechanic separation resulted in a much lower RNA yield (Figure 3.2.6). Therefore, the enzymatic digestion was the method of choice to prepare cerebral microvessels for subsequent RNA preparation.

For the microvessel preparation, SJL/N mice were immunized on two subsequent days subcutaneously, and 3×10^9 heat inactivated organisms of *Bordetella pertussis* were injected on day 1 and day 3 after immunization intravenously with the help of Irene Küchenmeister. 125 mice which had a clear onset of disease resulting in a disease score of $1-3$ were sacrificed from day $11-16$ after immunization. In parallel, 120 untreated age-matched control mice were sacrificed. Cerebral microvessels were prepared as described by enzymatic digestion of about 20 brains per batch, shock-frozen in liquid nitrogen and stored at -80°C. Meninges were removed with the help of Irene Küchenmeister, Katharine Ling, Monika Rieschel and Veronika Schmidt. Once all preparations and control preparations were performed, samples

library	vector	number	created
standard brain microvessels, EAE #13	pSPORT1	1.3×10^7	01/10/2001
standard brain microvessels, EAE #14	pCMV-SPORT6	3.8×10^7	01/10/2001
standard brain microvessels, control, #2	pλtriplex2	3.5×10^6	12/11/2001
standard brain microvessels, control, #3	pλtriplex2	3.6×10^6	12/11/2001
subtraction brain microvessels, EAE – control, #1	pBSII-SK+	3.2×10^6 [a]	11/01/2001
subtraction brain microvessels, EAE – control, #5.1	pBSII-SK+	1.6×10^4 [a]	01/10/2001
subtraction brain microvessels, EAE – control, #5.2	pBSII-SK+	6.0×10^4 [a]	01/25/2001
subtraction brain microvessels, control – EAE, #2	pBSII-SK+	3.2×10^6 [a]	11/01/2001
SMART subtraction brain microvessels, EAE – control, #7.1	pBSII-SK+	4.8×10^4 [a]	01/10/2001
SMART subtraction brain microvessels, EAE – control, #7.2	pBSII-SK+	8.0×10^4 [a]	01/25/2001

[a]Numbers refer to clones which scored negative after blue-white selection and therefore have lost their β-galactosidase activity due to cDNA fragment integration.

Table 3.2.2: cDNA libraries of cerebral microvessels were created from 125 mice afflicted with EAE (day 11 – 14 after immunization, clinical score 1 – 3) as well as 120 healthy age-matched control mice in cloning and expression vectors. Additionally, subtractive and SMART subtracted libraries were created.

were sent to Bioserve Biotechnologies Ltd. (Laurel, MD, USA), where the libraries were created by Robert Skurla. The following libraries were obtained and analyzed by us (Table 3.2.2).

To identify genes, which were regulated during EAE in cerebral microvessels, the library "subtraction brain microvessels, EAE – control, #1" was analyzed in this present thesis by high-throughput sequencing. Therefore, 10 μl frozen glycerol stock were scratched off and diluted in 1000 μl LB medium. Immediately, 100 μl diluted bacterial suspension, containing about 540 clones, were plated per 150 mm LB agar plate containing ampicillin as well as X-Gal and IPTG for selection and grown over night. 375 unstained clones, which had no β-galactosidase activity, were used to inoculate LB medium (40 μg/ml ampicillin), grown over night and DNA was prepared using the QIAprep 96 turbo miniprep kit. DNA preparations were sequenced unidirectional using the M13rev primer, dye terminators were removed and sequencing reactions were measured by an in-house service facility.

Sequence data files were analyzed using the GCG software package v10.2 (Genetics Computer Group (GCG), Madison, WI, USA), which was located on a server at the Gesellschaft für Wissenschaftliche Datenverarbeitung, Göttingen (gwdg; Göttingen, Germany). Sequence data files were transferred to this server and subsequently compared with the non-redundant gene bank database by use of the fol-

lowing shellscript, which had been written in this present thesis:

```
\#!/usr/local/bin/bash
\# automated blast-searches for several files


for query in 'ls | grep .seq'
do
echo "Starting to process \$query ..."
reformat -default -monitor \$query
echo "\$query reformatted!"
blast2 -IN2=gb\_nt -DBN -EXP=10 -LIS=10 -OUT=\${\rmfamily \\
        \{ }query\%.seq{\rmfamily \} }.blastn -BEG=141 -END=380 \$query
echo "\$query done!"
done
```

This script automatically reformats each sequence file to be readable by the GCG software, and then does a BLAST comparison of the nucleotides 141 – 380 with the non-redundant gene bank database gb-nt, thereby omitting sequenced vector backbone DNA. In case of short insert cDNA, this approach did result in preferably recognizing the vector DNA. In these cases, this vector DNA had to be excluded by additional manual BLAST comparisons. Of the 375 clones analyzed, 188 could be identified (see 3.2.3), while 7 clones contained repetitive elements, 15 contained only vector sequences and maybe very short inserts. 165 clones could not be identified by sequencing. Adhesion molecules, immune receptors, innate immunity related molecules and MHCII molecules were detected, which allude to leukocyte contaminations in the microvessel preparation, as experienced in the gene array analysis as well. However, cytoskeletal proteins may refer to alterations of endothelial cells, as well as possible modifications to the extracellular matrix and cell-cell contacts. Interestingly, Duffy antigen / receptor for chemokines (DARC) and three more serpentine receptors were found to be upregulated. As chemokine receptors are serpentine receptors, these molecules are of particular interest as possible chemokine receptors. Additionally, 28 sequences referred to unknown genes, either being as EST clones or genomic sequences in the gene bank database.

Table 3.2.3: Genes enriched in cerebral microvessel preparations during EAE as detected by SSH are listed in different functional groups. Internal clone numbers, gene bank accession numbers and gene names are listed together with the first and last nucleotide of the respective clone as compared to the listed gene bank entry.

acc. no.	name	start – stop	clone no.
adhesion molecules and their modification			
19852057	clone cDSL-Z6 Down syndrome cell adhesion molecule-like protein	242 – 71	185
9910157	C-type (calcium dependent, carbohydrate recognition domain) lectin, superfamily member 10	10 – 233	25
antigen presentation			
13540710	histocompatibility 2, class II antigen A, alpha	36 – 122	216
3169659	histocompatibility 2, class II antigen A, alpha	364 – 594	102
6996918	histocompatibility 2, complement component factor B	276 – 37	35
	ditto	281 – 446	316
	ditto	282 – 57	124
	ditto	323 – 481	83
	ditto	1656 – 1889	9
	ditto	1656 – 1889	290
	ditto	1656 – 1889	21
	ditto	1656 – 1682	319
	ditto	1656 – 1859	48
	ditto	1692 – 1726	72
	ditto	2013 – 1774	187
	ditto	2278 – 2041	103
	ditto	2292 – 2069	100
	ditto	2304 – 2065	73
	ditto	2306 – 2068	113
20878874	Ia-associated invariant chain (Ii)	165 – 57	174
	ditto	251 – 436	81
	ditto	436 – 258	5
	ditto	436 – 247	112
2555188	Major Histocompatibility Locus class II region	120289 – 120468	14
199449	MHC class II H2-IA-alpha (d haplotype)	1 – 133	136
	ditto	1 – 133	159
	ditto	14 – 133	170
199465	MHC class II H2-IA-alpha (s haplotype)	40 – 8	196
199489	MHC class II H2-IA-beta (s haplotype)	194 – 1	285

Table 3.2.3: Enriched genes in cerebral microvessel preparations during EAE as detected by SSH

acc. no.	name	start – stop	clone no.
cell cycle, cell growth, cell survival and apoptosis			
12963604	apoptosis-associated speck-like protein containing a CARD	206 – 403	186
6753597	defender against cell death 1 (Dad1)	79 – 260	115
2522268	EAT/MCL-1	1531 – 1391	50
12659133	melanoma antigen family D1	1193 – 1100	62
3860228	neuronal apoptosis inhibitory protein 2	1576 – 1789	133
	ditto	1583 – 1698	157
20894856	ras association (RalGDS/AF-6) domain family 1	224 – 64	184
20885862	retinoblastoma-like 2	4130 – 3902	125
6755567	schlafen 1	1661 – 1456	189
3983149	schlafen 2	190 – 1	168
5932000	similar to: Serf1 protein, survival of motor neuron protein, neuronal apoptosis inhibitory protein-rs6, and neuronal apoptosis inhibitory protein-rs3	59026 – 58974	137
6678284	telomerase associated protein-1	5452 – 5527	16
channels and transporters			
7657517	ATP-binding cassette, sub-family E (OABP), member 1	987 – 1220	106
6678735	lactotransferrin	769 – 538	275
6755565	solute carrier family 9 (sodium/hydrogen exchanger), isoform 3 regulator 1	1718 – 1868	122
coagulation			
2664219	coagulation factor X	1163 – 925	162
cytokines, chemokines and receptors			
20910320	chitinase 3-like 1	775 – 537	130
	ditto	776 – 975	182
	ditto	803 – 975	40
	ditto	1216 – 1146	289
6753415	chitinase 3-like 3	178 – 328	155
	ditto	404 – 166	191
	ditto	419 – 228	47
	ditto	422 – 182	160
	ditto	424 – 190	1
	ditto	426 – 585	68
	ditto	585 – 420	181
6753629	Duffy blood group	6 – 54	243

Table 3.2.3: Enriched genes in cerebral microvessel preparations during EAE as detected by SSH

acc. no.	name	start –	stop	clone no.
6754313	interferon gamma inducing factor binding protein	535 –	393	59
	ditto	573 –	393	288
6754329	interleukin 1 receptor, type II	438 –	518	265
	ditto	440 –	679	108
	ditto	470 –	656	94
7305180	interleukin 2 receptor, gamma chain	710 –	850	188
	ditto	850 –	663	90
3153815	oncostatin M specific receptor	2062 –	2237	252
cytoskeletal molecules				
6671508	actin, beta, cytoplasmic	1265 –	1166	175
2252815	Axin	1643 –	1755	312
21361132	MAP/microtubule affinity-regulating kinase 3 (homo sapiens)	615 –	732	127
2443283	motor domain of KIF6	102 –	13	29
6679384	plastin 2, L	178 –	378	70
	ditto	1830 –	1676	204
21687243	RAN GTPase activating protein 1	2148 –	2381	117
13161248	sad1-unc84-like protein	661 –	885	31
20899777	tubulin, beta 5	35 –	184	241
	ditto	722 –	922	55
enzymes and metabolism				
7106254	arginase 1, liver	620 –	514	358
20342361	enolase 1, alpha non-neuron	1 –	170	96
204490	glutathione S-transferase (rat)	134 –	17	63
12642663	glycine N-methyltransferase	3234 –	3384	82
2388721	liver carnitine palmitoyltransferase I	3885 –	4109	144
18426808	Niemann Pick type C2	1 –	31	32
extracellular matrix				
20848653	fibronectin 1	2436 –	2288	78
	ditto	2955 –	3137	163
20888218	similar to putative dipeptidase (LOC244632)	793 –	907	110
6678320	transforming growth factor, beta induced, 68 kDa	2496 –	2261	13
G protein coupled receptors				
7707356	CD97 antigen	2139 –	2371	280
14249165	Homo sapiens seven transmembrane domain protein (NIFIE14)	394 –	593	277
22095024	vomeronasal 1 receptor, A2	3261 –	3301	295

Table 3.2.3: Enriched genes in cerebral microvessel preparations during EAE as detected by SSH

acc. no.	name	start –	stop	clone no.
glycosylation enzymes				
6754683	mannoside acetylglucosaminyltransferase 1	1410 –	1533	30
growth factors and related molecules				
2547133	neuropilin-2(a5), alternatively spliced	40 –	5	46
immune receptors				
6753331	CD14 antigen	39 –	200	166
	ditto	196 –	1	19
	ditto	556 –	768	43
	ditto	767 –	538	17
14719423	CD52 antigen	22 –	167	154
6941603	gp49A	3973 –	4204	107
195552	Ig nonexpressed rearranged heavy-chain V-region (V-J), clone 264	61 –	109	264
1806127	IgG2c gene for immunoglobulin constant heavy chain, allele Igh-1	934 –	1113	92
	ditto	1506 –	1700	56
13540502	immunoglobulin superfamily, member 6	1 –	209	180
	ditto	13 –	234	132
	ditto	240 –	13	183
11096337	lymphocyte antigen 116	739 –	500	169
6754581	lymphocyte antigen 6 complex, locus C	2489 –	2462	193
6754583	lymphocyte antigen 6 complex, locus D	395 –	156	28
	ditto	642 –	403	109
6678747	lymphocyte antigen 6 complex, locus E	15 –	167	45
198927	lymphocyte differentiation antigen Ly-6C.2	32 –	265	165
	ditto	611 –	372	291
54826	rearranged immunoglobulin gamma 2b heavy chain	1006 –	1197	138
1199649	thymic shared antigen-1	742 –	705	33
innate immunity				
6753471	cathelin-like protein	361 –	528	22
	ditto	420 –	259	292
	ditto	493 –	353	190
	ditto	500 –	367	10
192278	complement component C3, alpha and beta subunits	4451 –	4684	121
1209751	gp91phox	1275 –	1174	131
8850218	haptoglobin	14 –	229	88
	ditto	15 –	230	116

Table 3.2.3: Enriched genes in cerebral microvessel preparations during EAE as detected by SSH

acc. no.	name	start −	stop	clone no.
	ditto	246 −	52	140
	ditto	246 −	136	336
	ditto	246 −	60	80
20824061	lipocalin 2	1 −	78	229
	ditto	191 −	1	150
	ditto	192 −	1	172
	ditto	249 −	412	148
20983337	properdin factor complement	912 −	992	254
20858952	serine protease inhibitor 2-1	717 −	533	104
20859248	similar to serine protease inhibitor 2-2 (LOC238393)	74 −	1	101
	ditto	1015 −	1254	126
lysosomal proteins				
21450788	cathepsin D	1 −	150	139
2746722	cathepsin S precursor	652 −	472	64
1439569	cystatin B	611 −	482	171
11345387	lysosomal thiol reductase precursor	675 −	747	215
signal transduction				
16418422	guanylate binding protein 4 (H. sapiens)	188 −	149	281
6382003	ionized calcium binding adapter molecule 1	233 −	21	37
458709	signal transducer and activator of transcription	1176 −	1414	53
13992531	suppression of tumorigenicity 5 gene, L27a gene and Kiaa0298 gene	125308 −	125249	274
20864092	tumor protein D52	833 −	938	147
54813	tyrosine protein kinase p56-tck	1594 −	1372	76
transcription factors and nuclear proteins				
9800524	GTF2IRD1 and CYLN2	197331 −	197300	98
19168506	MAIL gene for molecule possessing ankyrin-repeats induced by lipopolysaccharide, exons 3 to 14	2190 −	2429	276
22137804	modulator recognition factor 2	167 −	406	192
20344706	signal transducer and activator of transcription 2	1261 −	1355	2
18860912	SKI-interacting protein (homo sapiens)	967 −	814	118
7305600	TXK tyrosine kinase	868 −	1094	75
1261918	45S pre rRNA gene	0 −	0	85
protein synthesis				
194026	heat-shock protein 84	908 −	1137	158
198642	ribosomal protein L19	1 −	198	156
1938405	ribosomal protein S11	106 −	2	34

Table 3.2.3: Enriched genes in cerebral microvessel preparations during EAE as detected by SSH

acc. no.	name	start – stop	clone no.
12963510	ribosomal protein S19	156 – 354	27
13592066	ribosomal protein S9 (rattus norvegicus)	613 – 522	97
20866310	similar to 60S ribosomal protein L21 (LOC216390)	513 – 317	179
20825378	similar to RNA binding motif protein 3 (LOC226497)	546 – 665	128
7710041	IQ motif containing GTPase activating protein 1	1137 – 954	153
miscellaneous			
20886552	proteasome (prosome, macropain) 26S subunit, non-ATPase, 7	513 – 748	279
3930524	sex-determination protein homolog Fem1a	3498 – 3615	142
20899569	similar to viral envelope protein G7e	2763 – 2732	79
20820998	ubiquitin A-52 residue ribosomal protein fusion product 1	6 – 245	3
6941889	ubiquitin-specific processing protease	2918 – 2994	177
12841057	10 day old male pancreas cDNA, RIKEN full-length enriched library, clone:1810013K23:homolog to E1-LIKE PROTEIN	10 – 153	87
unknown			
12841677	10 day old male pancreas cDNA, RIKEN full-length enriched library, clone:1810054D07:homolog to HYPOTHETICAL 65.8 KDA PROTEIN (FRAGMENT)	195 – 58	167
26084120	12 days embryo embryonic body between diaphragm region and neck cDNA, RIKEN full-length enriched library, clone:9430022I10 product:unknown EST	357 – 891	111
26329388	adult male cecum cDNA, RIKEN full-length enriched library, clone:9130222K18 product:hypothetical eukaryotic thiol (cysteine) proteases active site containing protein	2286 – 2428	60
12832925	adult male kidney cDNA, RIKEN full-length enriched library, clone:0610031L02:unclassifiable transcript	190 – 83	99
12857810	adult male medulla oblongata cDNA, RIKEN full-length enriched library, clone:6330419P03:unclassifiable transcript	1467 – 1282	7
12857460	adult male thymus cDNA, RIKEN full-length enriched library, clone:5830427D03:unclassifiable	951 – 766	129

Table 3.2.3: Enriched genes in cerebral microvessel preparations during EAE as detected by SSH

acc. no.	name	start –	stop	clone no.
12857556	adult male thymus cDNA, RIKEN full-length enriched library, clone:5830460E08:unclassifiable transcript	166 –	19	249
16303564	BAC clone RP11-510H11 from 2 (homo sapiens)	191008 –	190990	355
19387740	chromosome 15, clone RP11-184D12 (homo sapiens)	152197 –	152220	120
22203334	chromosome 2 clone RP24-394D4	154315 –	154264	321
22138544	chromosome 3 clone RP24-545E4	64174 –	64156	6
3287367	chromosome 6 BAC-284H12 (Research Genetics mouse BAC library)	122370 –	122556	20
18463962	clone 33L10 alpha globin gene cluster	16749 –	16988	173
20072138	clone IMAGE:1328913	27 –	206	8
18605613	clone MGC:27898 IMAGE:3499319	1707 –	1565	145
19353356	clone MGC:35713 IMAGE:4973059	103 –	1	74
19909475	clone RP23-3D14, complete sequence	18744 –	18894	15
1673296	DNA (homo sapiens)	25 –	58	250
14422212	DNA sequence from clone RP21-544J17 on chromosome 5	65593 –	65766	58
18855252	DNA sequence from clone RP23-209G11 on chromosome 13	3946 –	3964	11
20798989	DNA sequence from clone RP23-317F9 on chromosome 11	214268 –	214247	66
18070910	DNA sequence from clone RP23-319B15 on chromosome 11	24599 –	24447	26
16307419	MAP kinase-interacting serine/threonine kinase 2, clone MGC:5881 IMAGE:3257646	2963 –	2853	151
20161859	Oryza sativa (japonica cultivar-group) genomic DNA, chromosome 1, BAC clone:B1139B11	90883 –	90904	266
2653780	peptidase homolog (homo sapiens)	27 –	9	247
18043719	RIKEN cDNA 1600014C10 gene, clone MGC:29915 IMAGE:5123719	960 –	874	114

Applying these two different techniques, gene array analysis as well as SSH with subsequent high-throughput sequencing HTS to microvessel preparations, allowed identification of genes being regulated during EAE in SJL/N mice by two different methods. By application of these two techniques, 13 genes were identified in parallel (Table 3.2.4). All of these 13 genes had been identified by SSH/HTS and by gene

array analysis to be upregulated. Thus, there were no contradictory results and both techniques can be considered complementary.

3.2.3 Proteomic analysis of cerebral microvessels

In this present work, cerebral microvessels from EAE afflicted SJL mice were prepared as described (see 2.1.4.1.2) and shock-frozen.

Frozen materials were further investigated by Dr. Bosse Franzén at Astra-Zeneca (Södertälje, Sweden) as follows. 150 μg protein lysate were obtained from 5 mg cerebral microvessels (wet weight) isolated from 5 SJL mice afflicted with EAE (day 16 post immunization, mean disease score 1.0 ± 0.6) and 200 μg protein lysate were isolated from 9 mg cerebral microvessels (wet weight) of 8 SJL mice afflicted with EAE (day 13 p. i., mean clinical disease score 1.1 ± 1.2). In both cases, control preparations were done from at least five age and strain-matched healthy mice. These preparations were applied to 2D gel electrophoresis and protein sample spots that differed between EAE and healthy controls were identified by mass spectrometry (Figure 3.2.7). The proteomics approach allowed to identify 6 differentially

acc. no.	name	fold change.	clone no.
J00369	complement component 3	22.8	121
M34510	CD14 antigen	18.2	17, 19, 43, 166
AA146437	cathepsin S	10.8	64
AA089333	cathepsin S	10.2	64
L19932	transforming growth factor, beta induced, 68 kDa	7.4	13
K01923	histocompatibility 2, class II antigen A, alpha	7.3	102, 216
M57890	histocompatibility 2, complement component factor B	7.1	35
U69488	G7e protein (G7e-pending)	6.9	79
X94353	cathelin-like protein	6.2	10, 22, 190, 292
U51805	liver arginase 1	5.7	358
M12056	tyrosine protein kinase p56-tck	4.1	76
M96827	haptoglobin	3.6	80, 88, 116, 140, 336
X00496	Ia-associated invariant chain	3.5	5, 81, 112, 174
W70579	coagulation factor X	2.7	162
U06924	signal transducer and activator of transcription 1	4.0[a]	53

[a] Expression change during EAE in C57Bl/6 mice.

Table 3.2.4: Differentially regulated genes during EAE as detected by gene array analysis and SSH. Accession numbers of genes which have been detected to be regulated during EAE in SJL/N mice by gene array analysis and found in the cDNA library which had been created by SSH. Respective clone numbers are listed.
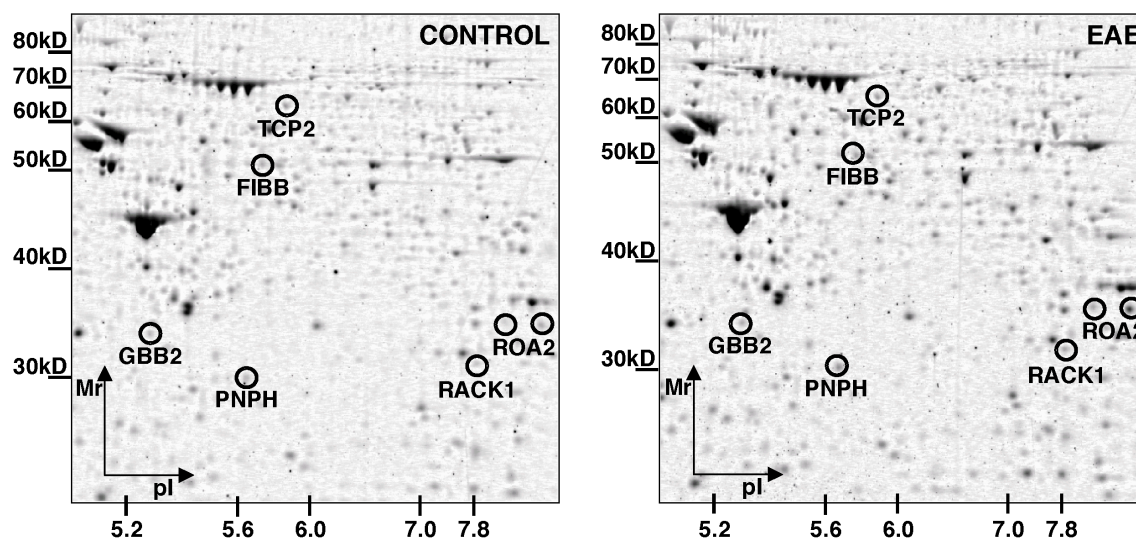
Figure 3.2.7: 2D gel electrophoresis maps showing identified proteins of cerebral microvessels from EAE afflicted and healthy SJL mice. Comparative SYPRO Ruby-stained gels of cerebral microvessel preparations of mice afflicted with EAE and healthy controls are shown. Protein sample spots, expression levels of which were detected by PDQuest software to be reproducibly altered during EAE, are marked. Protein identifiers as determined by mass spectrometry are added.

expressed proteins, whereby genes of 5 of these proteins were found to be represented on the Affymetrix chip (Table 3.2.5). Only one of them, fibroleukin was found to be significantly upregulated in both, the proteomics and oligonucleotide microarray screen (Table 3.2.5). While purine nucleosid phosphorylase was detected to be not transcriptionally regulated, regulation of receptor of activated protein kinase C 1 (RACK-1), tailless complex polypeptide 1B and transducin beta chain 2 correlated with their transcriptional regulation, as corresponding genes and proteins were either both upregulated or both downregulated. However, according to the manufacturer, these results could not be considered significant (Table 3.2.5). Thus, no contradictory results comparing gene and protein expression level changes were found and both techniques can be considered complementary. Upregulated protein expression was detected for an acidic and basic variant of heterogeneous nuclear ribonucleoprotein (hnRNP) A2/B1, which was not represented on the Affymetrix chip. Confirmation of these results by immunohistochemistry using polyclonal antisera against RACK-1, GBB2 or hnRNP (Santa Cruz, Heidelberg, Germany) did unfortunately not reveal any conclusive results.

		proteomics			gene array	
SSP	fold change	MALDI / Q-TOF	acc. no.	name	acc. no.	fold change
4621	+3.9	FIBB	P14480	rat fibroleukin precursor / fibrinogen like protein 2	M16238	+3.4
8309	+2.4	ROA2	O88569	mouse heterogeneous nuclear ribonucleoprotein A2/B1	not on array	
8301	+1.6	ROA2	O88569	mouse heterogeneous nuclear ribonucleoprotein A2/B1	not on array	
4202	+1.8	PNPH	P23492	mouse purine nucleosid phosphorylase	X56548	±1.0
7208	+1.6	GBLP	P25388	human guanine nucleotide-binding protein beta subunit like protein 12.3 / receptor of activated protein kinase C 1	W78338 X75313 AA089264	+1.1 +1.2 +1.3
4708	−1.45	TCP	P11983	tailless complex polypeptide 1B	D90344	−1.1
2306	−1.45	GBB2	P54312	guanine nucleotide-binding protein G(I)/G(S)/G(T) beta subunit 2 / transducin beta chain 2	W41722	−1.2

Table 3.2.5: Protein expression analysis: Identities of altered protein expression during EAE in cerebral microvessels of SJL mice. 7 sample spots (SSP) were detected to be either up- or downregulated and identified by MALDI or Q-TOF. Protein database accession numbers (acc. no.) and gene names are listed. Additionally, gene accession numbers (acc. no.) of corresponding genes represented on the Affymetrix Mu6500 gene array are shown together with the detected transcriptional changes.

3.3 Gene expression profiling of encephalitogenic T cells

PLP-specific T cell lines established from SJL/N mice are referred to as encephalitogenic or non-encephalitogenic depending on their ability to transfer clinical EAE into naïve syngeneic recipients. Independent of this capability, encephalitogenic and non-encephalitogenic T cells do neither differ in antigen specificity nor does comparison of adhesion molecule and cytokine expression patterns of encephalitogenic T cell lines reveal any difference. Additionally, encephalitogenic T cells lines lose their encephalitogenicity after several *in vitro* restimulation steps with their specific

antigen. Therefore, the question arose, what molecular differences are crucial for encephalitogenicity of T lymphoblasts.

3.3.1   Gene array analysis of encephalitogenic T cells

Differences in gene expression between encephalitogenic and non-encephalitogenic T lymphoblasts were assessed by gene array analysis of 8×10^6 encephalitogenic T lymphoblasts SJLB.PLP7 in comparison to 8×10^6 non-encephalitogenic T lymphoblasts SJLB.PLP3. Freshly restimulated T lymphoblasts were separated by density gradient centrifugation, thoroughly washed, frozen and sent to Mrs. Kristina Duvefelt (Astra-Zeneca, Södertälje, Sweden).

At Astra-Zeneca, gene array analysis was performed as follows: Two gene arrays analyzed the expression of encephalitogenic T cells, while two arrays analyzed the expression of non-encephalitogenic T cells, thereby resulting in four different comparisons. Additionally, all arrays were amplified with streptavidin, thereby resulting in another 4 different comparisons.

In this present thesis, further analysis was performed. Genes were scored to be regulated, if they were positive in at least all 4 streptavidin-amplified comparisons. Thereby, 73 regulated genes were found, of which 36 were up- and 37 were downregulated each (Table 3.3.1).

Adhesion molecule expression was hardly different. Cytokine and cytokine receptor expression overall appeared to be lower in encephalitogenic T cells as compared to the non-encephalitogenic T cells. Cytoskeletal molecules as well as extracellular RNA expression was altered. Furthermore, mRNA levels of 4 so far unknown genes were partially highly increased in encephalitogenic T cells as compared to the non-encephalitogenic cells and may result in relevant differences. However, more detailed analysis is required to elucidate the function of these molecules in lymphocyte recruitment into the CNS.

Table 3.3.1: Altered mRNA levels in encephalitogenic vs. non-encephalitogenic T cells which were at least least 3-fold increased in 4 non-streptavidin-phycoerythrin enhanced gene arrays are listed. If genes were detected to be altered in 4 streptavidin-phycoerythrin enhanced arrays, but not in all 4 non-enhanced arrays, fold-changes (f. c.) are marked with an asterix.

acc. no.	name	f. c.
adhesion molecules and their modification		
W98255	CD81 antigen	3.7
cell cycle, cell growth, cell survival and apoptosis		
W41072	cell division cycle 34 homolog (S. cerevisiae)	4.1
AA110061	cell division cycle 6 homolog (S. cerevisiae)	10.9
AA021788	death-associated kinase 3	13.3*
X54149	growth arrest and DNA-damage-inducible 45 beta	-3.7
L41495	serine/threonine protein kinase pim-2	-3.5*
channels and transporters		
AA153484	ATPase, Ca++ transporting, cardiac muscle, slow twitch 2	60.0
AA117973	ATPase, Na+/K+ transporting, alpha 1 polypeptide	6.6
AA032860	ATP-binding cassette, sub-family F (GCN20), member 2	6.8
X57349	transferrin receptor	4.5
cytokines, chemokines and receptors		
U28404	CCR1	-7.2
D87757	chitinase 3-like 3	-4.7
X53798	CXCL2	-9.9
W62918	Epstein-Barr virus induced gene 3	3.1*
X03019	granulocyte-macrophage colony stimulating factor	4.2
X64534	IL-3 receptor alpha chain	-4.4
D13695	interleukin 1 receptor-like 1	-4.7
J03783	interleukin 6	-6.9
X59769	interleukin-1 receptor type 2	-3.2
M37897	interleukin-10	-7.1
U64199	interleukin-12 receptor beta2	3.3
M25892	interleukin-4	-6.6
cytoskeletal molecules		
AA015415	kinesin 2	9.9
AA059763	tubulin beta 2	4.7
AA152515	actinin alpha 2	-17.4
AA137524	calcium binding protein P22	53.3
enzymes and metabolism		
W41963	acetyl-Coenzyme A synthetase 2 (ADP forming)	8.9
Y08135	acid sphingomyelinase-like phosphodiesterase 3a	-4.4*

Table 3.3.1: Altered mRNA levels in encephalitogenic vs. non-encephalitogenic T cells

acc. no.	name	f. c.
W33415	ATP citrate lyase	3.7*
AA073296	ATP CITRATE-LYASE	3.2*
M69109	indoleamine 2,3-dioxygenase	4.0*
M63445	methylenetetrahydrofolate dehydrogenase (NAD+ dependent), methenyltetrahrofolate cyclohydrolase	-4.5
extracellular matrix		
M16238	fibrinogen-like protein 2	-4.7
X16490	plasminogen activator inhibitor 2	-7.7*
X70296	protease-nexin 1	4.9
L19932	transforming growth factor, beta induced	-7.5
growth factors, receptors and related molecules		
L41352	schwannoma-derived growth factor	-5.8
immune receptors		
X05719	cytotoxic T-lymphocyte-associated protein 4	-3.3
innate immunity		
U73004	secretory leukocyte protease inhibitor	-7.1
X03505	serum amyloid A 3	-4.8
X04072	granzyme B	-4.1
peroxisomal proteins		
W66916	peroxisomal farnesylated protein	13.1*
phosphatases		
W34891	protein phosphatase 1G (formerly 2C), magnesium-dependent, gamma isoform	4.0*
U35368	protein tyrosine phosphatase, receptor type, E	-7.1
protein biosynthesis		
AA104940	arginyl-tRNA synthetase	5.3*
W13693	DnaJ (Hsp40) homolog, subfamily A, member 4	18.7
AA109180	eukaryotic translation initiation factor 2B, subunit 5 epsilon	4.3*
W51433	heat shock protein 1 alpha	3.3
U44940	quaking type I	-3.6
AA067335	tumor rejection antigen gp96	4.4
signal transduction		
W77226	ADP-ribosylation-like 3	5.0*
X12616	c-fes	-41.0
D13759	mitogen activated protein kinase kinase kinase 8	-6.0
transcription factors and nuclear proteins		

Table 3.3.1: Altered mRNA levels in encephalitogenic vs. non-encephalitogenic T cells

acc. no.	name	f. c.
X62600	CCAAT/enhancer binding protein beta	-4.0
U63133	c-fos oncogene	-57.5
V00727	c-fos oncogene	-5.5
X67083	chop-10 mRNA	-80.7
AA104319	damage specific DNA binding protein 1	4.0
AA166139	damage specific DNA binding protein 1	4.0
J03482	histone H1c	-3.2*
U20532	nuclear, factor, erythroid derived 2, like 2	-3.7
W50655	nucleosome assembly protein 1-like 4	3.8
D14636	runt related transcription factor 2	-3.6
J00424	tetradecanoyl phorbol acetate induced sequence 7	-4.7
W08822	zinc finger protein 289	3.5*
M58691	zinc finger protein 36	-3.7
miscellaneous		
AA153021	guanylate nucleotide binding protein 2	5.4
M21050	lysozyme	-14.6
U60593	N-myc downstream regulated-like 1	-4.0
unknown		
AA170375	hypothetical protein MGC6725	4.1
AA027669	RIKEN cDNA 2410044K02 gene	23.6
AA008547	RIKEN cDNA 9130211I03 gene	3.5
W91360	RIKEN cDNA 9130221H12 gene	12.3

3.3.2   Subtractive-suppression hybridization analysis of encephalitogenic T cells

The next question was, whether additional genes have altered RNA levels in encephalitogenic T lymphoblasts as compared to non-encephalitogenic T lymphoblasts, especially genes which were not represented on the Affymetrix Mu6500 gene array. To identify such genes, 5.0×10^7 freshly restimulated encephalitogenic T lymphoblasts (line SJLB.PLP6, 5th *in vitro* restimulation) and 4.2×10^7 freshly restimulated non-encephalitogenic T lymphoblasts (line SJLB.PLP3, 6th *in vitro* restimulation) were shock-frozen and sent to Bioserve Biotechnologies Ltd. (Laurel, MD, USA).

name	vector	number	creation date
standard T cell, non-enc.	pSPORT1	1.2×10^7	08/29/2001
standard T cell, non-enc.	pCMV-SPORT6	3.9×10^7	11/31/2001
standard T cell, non-enc., #15	pCMV-SPORT6	1.4×10^6	02/08/2001
standard T cell, enc., #16	pSPORT1	2.6×10^6	01/10/2001
standard T cell, enc., #17	pCMV-SPORT6	8.3×10^6	01/10/2001
subtraction T cell, enc. – non-enc, #3	pBSII-SK+	4.9×10^6 [a]	11/01/2001
subtraction T cell, enc. – non-enc, #10.1	pBSII-SK+	1.6×10^4 [a]	01/10/2001
subtraction T cell, enc. – non-enc, #10.2	pBSII-SK+	2.3×10^5 [a]	02/08/2001
subtraction T cell, non-enc. – enc, #4	pBSII-SK+	3.2×10^6 [a]	11/01/2001
subtraction T cell, non-enc. – enc, #11	pBSII-SK+	4.0×10^4 [a]	01/10/2001

Table 3.3.2: Standard cloning and expression cDNA libraries were created from freshly restimulated encephalitogenic T lymphoblasts (line SJLB.PLP6, 5th restimulation) and non-encephalitogenic T lymphoblasts (SJLB.PLP3 6th restimulation). Cloning libraries were used to create subtractive T cell libraries.

At Bioserve, standard cloning cDNA libraries, expression cDNA libraries as well as SSH libraries were created (Table 3.3.2).

In this present thesis, preliminary analysis of the library "subtraction T cell, enc. – non-enc, #10.1" was performed. Therefore, frozen clones of the library "subtraction T cell, enc. – non-enc, #10.1" were scratched off the frozen stock solution, diluted in LB medium containing 50 μg/ml ampicillin, plated on LB agar plates containing ampicillin and X-Gal/IPTG for selection and grown over night. White clones were inoculated in LB agar (50 μg/ml ampicillin), grown over night, plasmid DNA was prepared and 18 clones were sequenced using an M13rev primer. Sequencing results were compared to the non-redundant gene bank database and results are shown in Table 3.3.3. Comparing the gene array analysis and SSH/HTS did not reveal any gene being detected by both techniques.

acc. no.	name	start – end	clone no.
5295972	chaperonin containing TCP-1 zeta-2 subunit	544 – 1201	9
5295972	chaperonin containing TCP-1 zeta-2 subunit	544 – 1202	16
3057136	epsilon-sarcoglycan	1443 – 953	17
33859481	eukaryotic translation elongation factor 2	15 – 640	7
33859481	eukaryotic translation elongation factor 2	15 – 667	10
33859481	eukaryotic translation elongation factor 2	2603 – 2979	15
33859481	eukaryotic translation elongation factor 2	3070 – 2716	18
21410869	hook homolog 1 (Drosophila)	1765 – 1948	13
21410869	hook homolog 1 (Drosophila)	2603 – 2979	12
1469399	T cell death associated gene 51	5 – 24	6
1469399	T cell death associated gene 51	1765 – 1949	2
1644303	calcitonin[a]	5882 – 5863	5
17467265	lyst[a]	97 – 75	5

[a]Clone no. 5 did not allow identification of a distinct gene, but rather two different genes.

Table 3.3.3: Genes being expressed at higher mRNA levels in encephalitogenic T lymphoblasts in comparison to non-encephalitogenic T lymphoblasts as detected by SSH and subsequent plasmid DNA preparation of library "subtraction T cell, enc. – non-enc, #10.1". Shown are internal clone numbers as well as the homolog sequences as defined by BLAST algorithm analysis with their respective starting and ending points.

3.4   Involvement of DARC in leukocyte recruitment across the endothelial blood-brain barrier

3.4.1   Expression of DARC during EAE

As described earlier, DARC mRNA levels were found to be increased during EAE in brain microvessel preparations, as detected by SSH. This supported earlier findings, which showed upregulation of DARC in inflamed cerebral vessels during EAE by *in situ* hybridization (Alt, 1999). Thus, DARC mRNA expression was induced in BBB endothelial cells themselves during EAE. So we asked, if DARC is involved in chemokine transcytosis from the CNS parenchyma across the endothelial BBB to the luminal surface of the endothelial cells, and if it thereby affects lymphocyte recruitment into the CNS.
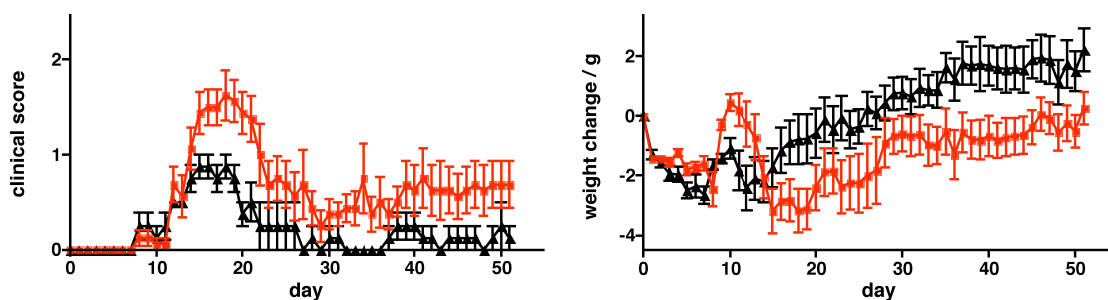
Figure 3.4.1: Active EAE in C57Bl/6 wildtype and DARC-deficient mice was induced with MOG$^{35-55}$. Clinical score and weight change was measured daily. In knockout mice (n = 8; gray quadrangles), disease onset was delayed as compared to wildtype mice (n = 4; black triangles), however disease was more severe in DARC-deficient mice. One representative experiment is shown (n = 3).

3.4.2 Experimental autoimmune encephalomyelitis in DARC-deficient mice

Focusing on the functional role of DARC mRNA induction during EAE pathogenesis, the question arose, if DARC is involved in lymphocyte recruitment across the endothelial BBB. This question was approached by investigation of DARC-deficient mice, which had been created by Dawson et al. (Dawson et al., 2000) and were kindly provided by Antal Rot (Novartis, Vienna, Austria). These knockout animals were backcrossed into the C57Bl/6 background for 8 generations to obtain mice susceptible for EAE. After four generations of backcrossing, initial EAE experiments were performed by immunization with MOG$^{35-55}$ in CFA (see 2.2.1.2; Figure 3.4.1). These preliminary experiments revealed a delayed disease onset, but a more severe disease course in DARC-deficient mice, as compared to untreated littermates (Figure 3.4.1). Next, possible differences in both groups regarding the expression of endothelial cell specific molecules (Figure 3.4.2B), adhesion and junctional molecules (Figure 3.4.2C) as well as the composition of inflammatory cells (Figure 3.4.2D) were investigated by immunohistochemistry. No significant differences could be defined.

To perform transfer EAE experiments, MOG-specific T cell lines had to be established from C57Bl/6 mice. Therefore, primary T cells were prepared from lymph nodes and spleens of C57Bl/6 mice (Harlan-Winkelmann, Borchen, Germany) 15 days after immunization with MOG in CFA. Primary culture of splenocytes derived from these mice did specifically proliferate in presence of MOG$^{35-55}$ as com-
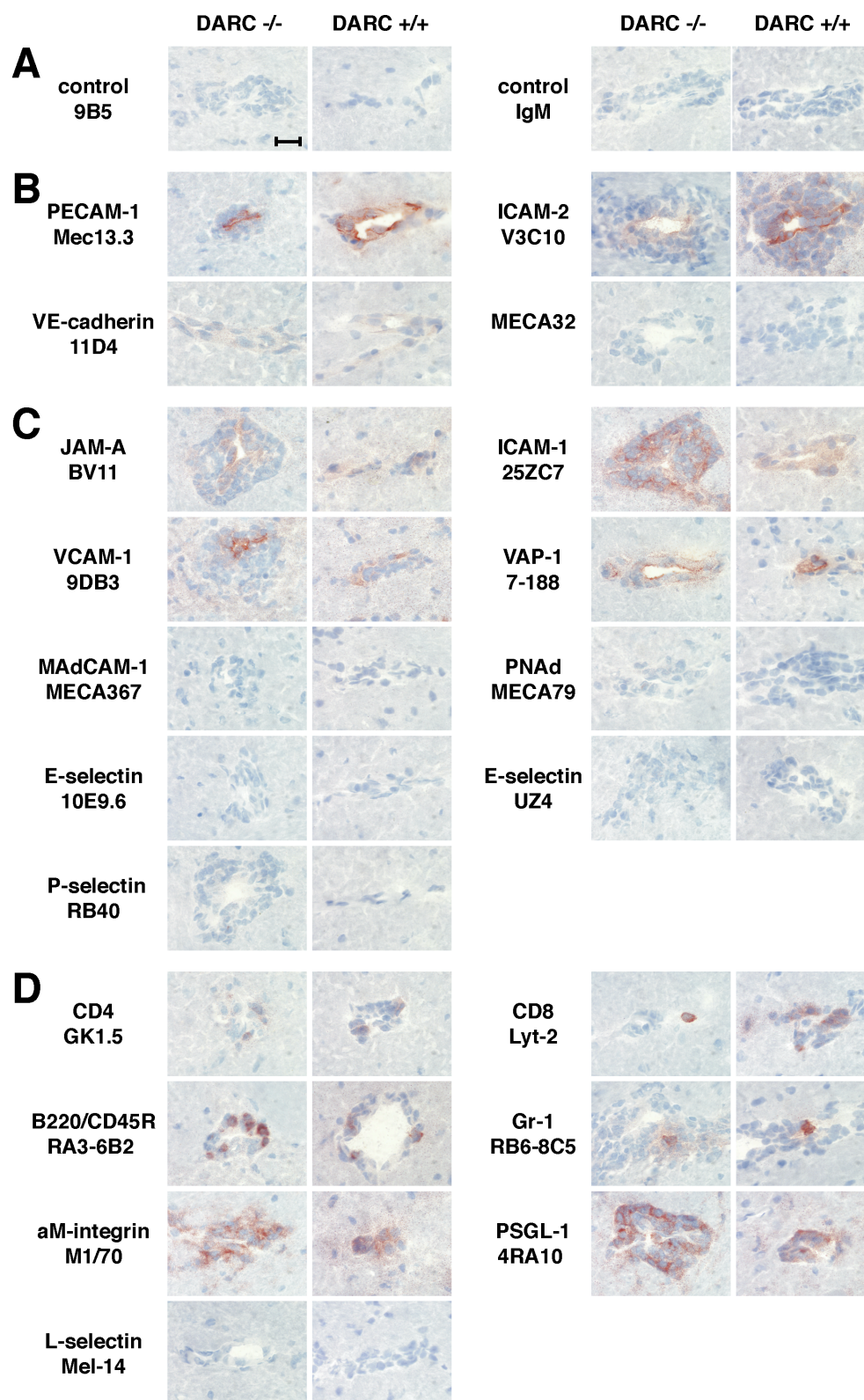
Figure 3.4.2: Surface molecule expression is compared by immunohistochemistry in mouse brain at day 23 after DARC-deficient -/- (clinical disease score 2) and C57Bl/6 wildtype +/+ (clinical disease score 0.25). Control stainings are shown (A). No significant difference in expression of endothelial cell markers (B), adhesion and junctional molecules (C) or leukocyte surface molecules (D) could be detected. Immunoperoxidase staining with hematoxyline counterstain. Bar = 20 μm.
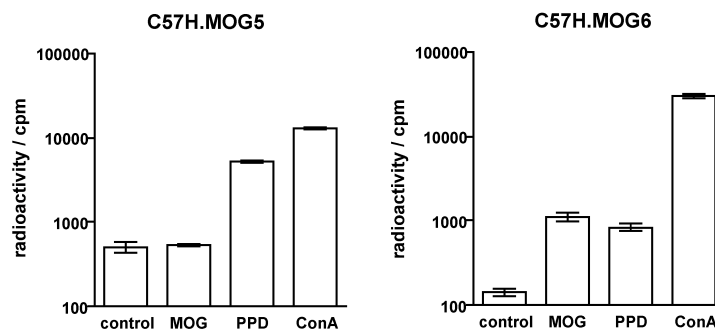
Figure 3.4.3: Proliferation of C57H.MOG T lymphocyte lines C57H.MOG5 (prepared from popliteal and inguinal lymphocytes) and C57H.MOG6 (prepared from spleens) in response to different antigens as measured by 3H-dT incorporation. MOG^{35-55} resulted in a specific response of C57H.MOG6 splenocytes, but not C57.MOG5 lymphocytes as compared to baseline levels. PPD resulted in an antigen-specific proliferation in both cell lines. Proliferation was as well be stimulated by treatment of T cells with ConA.

pared to baseline levels, while primary inguinal and popliteal lymphocytes showed less specific proliferation (see Figure 3.4.3). Additionally, proliferation in response to purified protein derivate (PPD) of *Mycobacterium tuberculosis* was measured. As to be expected due to the immunization procedure with CFA, which contained inactivated *Mycobacterium tuberculosis*, proliferation in response to PPD was high. However, the time constraints of this dissertation prevented from accomplishing these transfer EAE experiments.

3.4.3 Endothelioma cell lines lacking DARC

To elucidate a possible function of DARC *in vitro*, i. e. by adhesion and transmigration experiments, DARC-deficient endothelioma cell lines would be of great help and were to be established. Therefore, brains and additionally lungs, where a modified immune response had been described before in DARC-deficient mice (Dawson et al., 2000; Luo et al., 2000, 2003), were prepared from 2 – 7 day old newborn DARC-deficient mice, cut into small pieces with two scalpels and digested with collagenase type II. Microvessel fragments were separated by BSA density gradient centrifugation and plated on collagen-coated tissue culture dishes over night. Cells were retrovirally transduced with the polyoma middle T oncogene (pymT), which preferably transforms endothelial cells. Transformed endothelial cells are currently cultured to obtain pure cell lines (Figure 3.4.4).

luEndD10   **bEndD4**   **bEndD5**   **bEndD7**
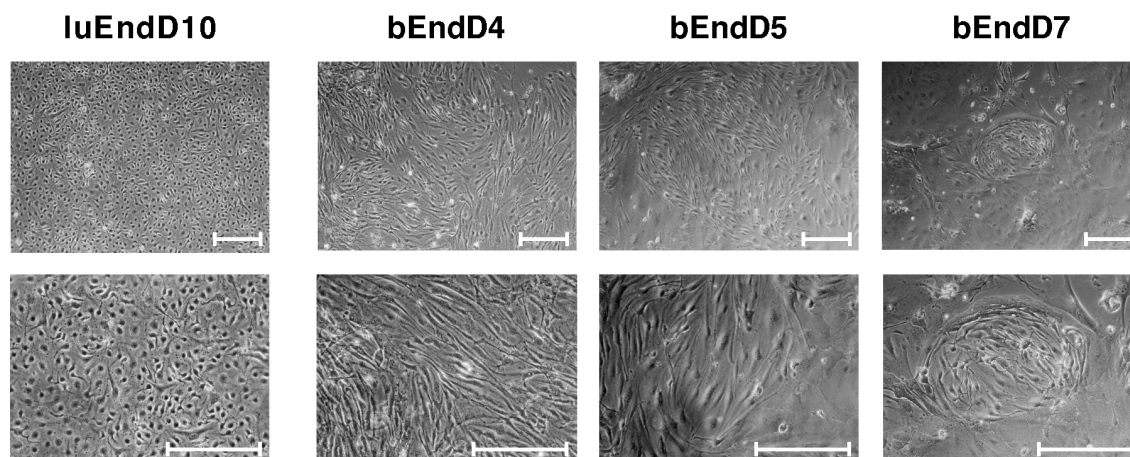
Figure 3.4.4: DARC-deficient endothelioma cell lines are shown by phase contrast microscopy. Lung-derived luEndD10 form a nice monolayer, while brain-derived bEndD4, bEndD5 and bEndD7 are forming islands in-between fibroblasts and are crowding other cell types out. Bar = 250 μm.
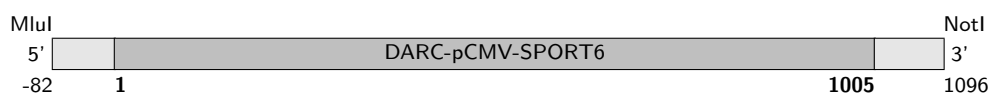
Figure 3.4.5: Full-length DARC cDNA sequence

In parallel, a full-length cDNA-DARC EST clone IRAKp961L2217 was obtained from rzpd (Deutsches Ressourcenzentrum für Genomforschung GmbH, Berlin, Germany, http://www.rzpd.de) and sequenced (Figure 3.4.5). This cDNA contains the full length DARC cDNA and will be used to reconstitute DARC expression in the DARC deficient endothelioma cells. Comparing the interaction of encephalitogenic T cells and DARC-deficient vs. DARC-reconstituted endothelioma cell lines *in vitro* by means of adhesion or transmigration assays will hopefully provide further insight into the function of DARC in lymphocyte recruitment.

Chapter 4

Discussion

4.1   Functional expression of CCL19 and CCL21 at the endothelial BBB

Chemokines are suggested to be crucially involved in the successful recruitment of encephalitogenic T cells across the BBB by the requirement for signaling via G-protein-coupled, PTX-sensitive receptors on encephalitogenic T cells to firmly arrest on BBB endothelium *in vivo* and to successfully transfer EAE (Vajkoczy et al., 2001; Alt et al., 2002). Therefore, we hypothesized that chemokines mediating the G-protein-dependent arrest of encephalitogenic T cells within CNS microvessels *in vivo* should be produced by the BBB endothelium itself.

Searching for chemokines expressed by BBB endothelium, *in situ* hybridizations were performed on brain and spinal cord sections of SJL/N mice afflicted with EAE and of healthy littermates. Out of 12 chemokines investigated, none of the inflammatory chemokines was found to be induced at the BBB during EAE. In contrast, constitutive expression of the lymphoid chemokine CCL19 was detected in CNS venules of healthy animals and its upregulation in inflamed venules in the CNS of mice afflicted with EAE was observed. Additionally, expression of the lymphoid chemokine CCL21, which was not detected to be expressed at the healthy BBB, was induced in inflamed CNS venules during EAE. CCR7, the common receptor for CCL19 and CCL21 as well as the alternative CCL21 receptor, CXCR3, were found on encephalitogenic T lymphoblasts which specifically chemotaxed towards both chemokines in a concentration-dependent manner comparable to naïve lym-

phocytes *in vitro*. Additionally, binding assays on frozen sections of EAE brains demonstrated a functional involvement of CCL19 and CCL21 in adhesion strengthening of encephalitogenic T lymphocytes to inflamed venules in the brain. Thus, the lymphoid chemokines CCL19 and CCL21 are functionally expressed at the BBB and might, therefore, be critically involved in the initiation and chronic maintenance of CNS inflammation during EAE.

Chemokines have been implicated in the pathogenesis of EAE before, as CNS expression of high levels of a diversity of inflammatory chemokines like CCL2, CCL3, CCL5 and CXCL10 was observed in tight temporal correlation to disease onset, as well as in tight spatial correlation to the appearance of inflammatory infiltrates around CNS venules (reviewed in Karpus and Ransohoff, 1998). In agreement with the *in situ* hybridization studies in this present thesis, previous studies demonstrated that the major producing source for CXCL10 and CCL2 was astrocytes (Ransohoff et al., 1993) and for CCL3, CCL4, CCL5 and CCL6 was both astrocytes and mononuclear cells within perivascular cuffs (Miyagishi et al., 1997; Asensio et al., 1999). Additionally, in this study similar expression patterns for CXCL9 and CCL22 were found. It is important to note that the major cellular sources for inflammatory chemokines detected during EAE were located "behind" the BBB.

Functional evidence for the involvement of CNS chemokines in the pathogenesis of EAE resulted from *in vivo* neutralization studies where blocking antibodies directed against CCL2 or CCL3 inhibited onset of EAE or ameliorated chronic EAE, respectively (Kennedy et al., 1998). Furthermore, antibodies against CXCL10 were shown to interfere with the development of EAE transferred with encephalitogenic T cells (Fife et al., 2001). CNS specific expression of CCL6 was shown to induce leukocyte infiltration into the CNS (Asensio et al., 1999). In contrast, absence of CCL2 was shown to lead to amelioration of EAE, while absence of its receptor CCR2 inhibits onset of the disease (Fife et al., 2000; Izikson et al., 2000; Huang et al., 2001). Lack of CCR1, which is a receptor for both CCL5 and CCL7, has been described to result in less severe EAE (Rottman et al., 2000), while absence of CCR5, which is an additional receptor for CCL5 was shown to have no influence EAE pathogenesis (Tran et al., 2000). This suggests that lack of CCR5 can be compensated by CCL5 binding to CCR1, while lack of CCR1 results in lack of CCL5 and CCL7 binding which cannot be compensated. While mice lacking CXCR2 and CXCR3, which are

receptors for CXCL1, CXCL9 and CXCL10, have been generated, a potential effect of the absence of these receptors during EAE has not been reported yet. Mice lacking the receptors for CCL6 and CCL9 do not exist, as these receptors are currently still unknown.

In contrast to microvessels elsewhere, the highly specialized endothelium of the BBB forms a physical barrier between the bloodstream and CNS parenchyma, hindering paracellular or transcellular diffusion of chemokines across the BBB by the complex tight junctions between the BBB endothelial cells and the lack of pinocytotic activity of the BBB endothelium, respectively. Consequently, the obvious question arose, how chemokines produced within the CNS parenchyma could possibly attract lymphocytes in the bloodstream from which they are separated by the BBB. Transport of chemokines from the abluminal to the luminal surface of endothelial cells *in vivo* has so far only been observed in dermal microvessels (Middleton et al., 1997) and in HEV of peripheral lymph nodes (Baekkevold et al., 2001). Although the inflammatory chemokines CCL2 and CCL3 can bind to the abluminal side of freshly isolated human brain microvessels *in vitro* (Andjelkovic et al., 1999; Andjelkovic and Pachter, 2000), it remains to be demonstrated whether these chemokines can be transported across the endothelial BBB *in vivo* and subsequently induce G-protein-dependent leukocyte arrest on the luminal surface of the BBB endothelium under shear.

CCL19 and CCL21 are structurally related chemokines referred to as lymphoid chemokines, because they are constitutively expressed within secondary lymphoid tissue (summarized in Cyster, 1999; Moser and Loetscher, 2001). There, they regulate the homing of lymphocytes into the lymph nodes as well as the formation of secondary lymphoid tissue by acting via their common receptor CCR7, as demonstrated in a mutant mouse, the plt (paucity of lymph node T cells) mouse, lacking detectable levels of both CCL19 and CCL21 expression (Nakano et al., 1997; Gunn et al., 1999) and in CCR7-deficient mice (Forster et al., 1999). This is further supported by the observation that T lymphocyte homing from blood into lymphoid tissues by triggering their integrin-mediated arrest on the HEV is regulated by CCR7 and its ligand CCL21 *in vivo* (Warnock et al., 2000).

Constitutive expression outside of secondary lymphoid tissues, has only been demonstrated for CCL21, but not for CCL19 in tertiary lymphatic endothelium.

Inducible expression of CCL19 and CCL21 outside of secondary lymphatic tissue
has been observed during experimental autoimmune diabetes (Hjelmstrom et al.,
2000) and rheumatoid arthritis (Takemura et al., 2001) in spatial and temporal
correlation to the formation of tertiary lymphoid tissue in the respective target
organs. In EAE, development of tertiary lymphatic tissue has not been observed
within the CNS. However, induction of the cytokines TNF-α and lymphotoxin-α,
which have been shown in lymphoid tissue to maintain the constitutive expression
of CCL19 and CCL21 (Ngo et al., 1999), are induced in the CNS during EAE
(Issazadeh et al., 1995; Juedes et al., 2000) and could therefore be responsible for
the expression of both chemokines at the BBB.

EAE can only be transferred by freshly activated, autoantigen-specific CD4$^+$
T lymphoblasts, usually from the T_H1 subset, but not by resting T lymphocytes,
which is suggested to be due to their ability to access the CNS (Wekerle et al.,
1986; Hickey et al., 1991). Surface expression of chemokine receptors on T cells has
been reported to be regulated such that, upon activation, T cells lose lymphoid-
organ homing receptors like L-selectin and CCR7 while gaining expression of other
subsets of adhesion molecules or chemokine receptors, enabling efficient immuno-
surveillance of non-lymphoid tissues for injury and infection (Butcher et al., 1999).
In human peripheral blood, activated / memory T cells have been divided into two
subpopulations according to their CCR7 expression. While CCR7-negative T cells
were defined as effector / memory T cells producing large amounts of inflammatory
cytokines, CCR7-positive T cells lacking profound cytokine production showed sur-
face expression of L-selectin and were referred to as central memory T cells, which
could possibly account for those activated / memory T cells able to migrate to lymph
nodes (Sallusto et al., 2000). However, it has been recently described, that this con-
cept does not hold absolutely true in the murine system, suggesting a more complex
network there (Bjorkdahl et al., 2003). Encephalitogenic T cells are maximally ac-
tivated effector / memory T cells at the time point of their injection and produce
high amounts of pro-inflammatory cytokines, however, despite their positive stain-
ing for CCR7, they lack surface expression of L-selectin at that stage (Laschinger
and Engelhardt, 2000). Thus, it seems that these *in vitro* cultured encephalitogenic
T cells can either not be grouped into any of these previously described phenotypes
or the absence of L-selectin is a result of the *in vitro* culture, as these cells express

L-selectin after *in vivo* culture. The chemokines and chemokine receptors involved in the homing of effector / memory T lymphocytes into non-lymphoid tissue during immunosurveillance have not been well characterized. At a first glance it appears surprising that encephalitogenic T cells should use the lymphoid chemokines CCL19 and CCL21 expressed at the BBB and their common receptor CCR7 to specifically migrate into the CNS. However, it was demonstrated that T lymphoblasts require high-affinity α_4-integrin to be captured on VCAM-1 expressed by CNS microvessels under flow *in vivo* (Vajkoczy et al., 2001). While α_4-integrin-mediated capture of T cells was independent of G-protein-signaling, subsequent α_4-integrin-mediated adhesion strengthening required G-protein-mediated signals *in situ*. In this thesis, binding assays performed on frozen sections of EAE brains provided more proof for functional involvement of CCL19 and CCL21 in adhesion strengthening of encephalitogenic T lymphocytes to inflamed venules in the brain *in vitro*, which was further emphasized by preliminary results, which were obtained by intravital microscopy *in vivo*, showing a slight reduction of firmly adhering encephalitogenic T cells after functional inhibition of CCR7. Therefore, it is tempting to speculate that captured T cells can bind CCL19 or CCL21, which via CCR7 triggers an increase in α_4-integrin avidity. Subsequently, this may lead to the adhesion strengthening of encephalitogenic T cells on VCAM-1 in CNS venules and their transmigration via LFA-1 as observed previously *in vivo* (Vajkoczy et al., 2001; Laschinger et al., 2002). In contrast, naïve T lymphocytes are unlikely to see the lymphoid chemokines present on BBB endothelium, as they lack high-affinity α_4-integrin which is required to stop within CNS venules. Furthermore, while L-selectin mediated T cell tethering and rolling is a prerequisite for CCR7 engagement of CCL19 and CCL21 in HEV, there are no L-selectin ligands described to be expressed on BBB endothelium. However, new L-selectin ligands have been shown within lymphoid endothelial cells (M'Rini et al., 2003; van Zante et al., 2003) and their potential expression by BBB endothelial cells has not been analyzed yet. Vice versa, encephalitogenic T cells lacking L-selectin would rather home to the immunoprivileged CNS than to peripheral lymph nodes as they lack luminal expression of VCAM-1 on their HEV. However, one can imagine that L-selectin ligands might be induced on the inflamed BBB later during chronic inflammatory disease. This might then allow lymphocytes, which usually home to secondary lymphoid tissues, to migrate into the CNS, thereby maintaining chronic

CNS inflammation.

In this present thesis, functional involvement of CCL19 and CCL21 in adhesion strengthening of encephalitogenic T lymphocytes was demonstrated by binding assays on frozen brain sections of mice afflicted with EAE *in vitro*. Moderate inhibitory effects observed after functional inhibition of CCR7 by intravital fluorescence videomicroscopy in spinal cord of healthy mice supported these findings *in vivo*, however, they had to be considered as not significant. Therefore, these preliminary results have to be considered inconclusive at present, however, they suggest involvement of additional, potentially unknown chemokines to be involved in lymphocyte recruitment across the endothelial BBB into the immunoprivileged CNS.

In summary, these findings suggest an additional function for the lymphoid chemokines CCL19 and CCL21 besides regulating lymphocyte homing to secondary lymphoid tissue. Due to their functional expression at the BBB, they might be involved in the migration of activated effector T lymphocytes across the healthy BBB into the immunoprivileged CNS and in the recruitment of mononuclear cells across the inflamed BBB during chronic autoimmune disease. However, the moderate effect observed by functional inhibition of these chemokines suggests additional, potentially new, chemokines, receptors as well as unknown molecules to be involved in this process. These were to be identified by gene array, SSH and proteomics approaches in this present thesis.

4.2 Gene and protein profiling of cerebral microvessels

Oligonucleotide microarrays representing 6500 murine genes and ESTs were used in collaboration with Astra-Zeneca (Södertälje, Sweden) to investigate gene expression profiles of cerebral microvessels isolated from two different mouse strains afflicted with EAE in comparison to gene expression profiles obtained for cerebral microvessels isolated from age and strain-matched healthy mice. Regulated genes were found in tissue samples derived from either C57Bl/6 or SJL mice to be up- or downregulated. When comparing both gene array profiles, genes were found to be regulated in cerebral microvessel preparations derived from either both or only one EAE model.

Thus, we were able to define genes commonly regulated in both EAE models, but also genes specifically regulated in either model. Genes coding for proteins involved in different cellular and molecular processes were found and great care was taken to functionally sort them into different subgroups.

Supporting the current concept of EAE as a model for chronic inflammatory demyelinating diseases of the CNS with an autoimmune pathogenesis, gene array analysis detected the upregulation of genes coding for molecules involved in adaptive immune functions such as immune cell activation or antigen presentation ("immune receptors", "antigen presentation") or leukocyte recruitment ("adhesion molecules and their modification" and "cytokines, chemokines and receptors"). Increased expression of the intercellular adhesion molecule-1 (ICAM-1), previously suggested to be involved in EAE pathogenesis (Archelos et al., 1993) was validated by *in situ* hybridization and immunohistochemistry, with both approaches demonstrating increased expression of ICAM-1 mRNA and protein in inflamed cerebral venules in brains of mice afflicted with EAE, when compared to healthy controls. Also, increased expression of inflammatory chemokines CCL2, CCL5, CCL6, CXCL9 and CXCL10 were observed in the oligonucleotide microarray analysis and could be confirmed by means of *in situ* hybridization, with undetectable expression in brains of healthy mice, but a strong induction of their expression in close vicinity to inflamed cerebral venules surrounded by inflammatory cuffs in EAE brains. Thus, not only endothelial cell expressed genes, but also genes which were upregulated in inflammatory cells located in close proximity to the cerebral microvessels were identified by gene expression profiling. This was confirmed by our findings that T cell specific genes encoding CD3δ or the T cell receptor (TCR) β chain as well as macrophage specific genes, i. e. the gene encoding CD14, or genes coding for leukocyte adhesion receptors, such as β_2-integrin or L-selectin, were found in our screen. Hence, gene expression comparison of cerebral microvessels from healthy and EAE brains only allowed to separate the inflamed compartment, but did not allow the complete separation of cerebral microvessels from inflammatory cells, microglial cells, pericytes and astrocytic endfeet. Thus, localization of the expression of regulated genes needs to be confirmed by *in situ* hybridization or immunohistochemistry.

Despite our finding that increased gene expression of chemokines did not necessarily localize to the inflamed endothelial cells proper, but was rather detected

in close vicinity to inflamed cerebral microvessels, functional importance for the chemokines described in this present study in the inflamed microvascular compartment during EAE has been demonstrated before (see 4.1).

This study did detect the regulation of endothelial cell specific genes, which is demonstrated by the finding that gene expression for caveolin-1 was also found to be downregulated during both EAE models (Ikezu et al., 1998). Furthermore, in the SJL mouse EAE model but not in the C57Bl/6 model, downregulation of intercellular adhesion molecule-2 (ICAM-2) mRNA was detected by gene array analysis although ICAM-2 is also present on T lymphocytes. Immunohistochemistry demonstrated endothelial cell specific staining for ICAM-2, however, failed to distinguish between different protein expression levels of ICAM-2 at cerebral microvessels in healthy or EAE brains. Supporting our previous observations of the lack of expression and functional involvement of the endothelial E- and P-selectin in EAE pathogenesis in the SJL mouse (Engelhardt et al., 1997), we did not find any E-selectin induction in the microarray screen in this model. P-selectin induction could only be observed after antibody amplification of the signals suggesting that this might also be derived from low levels of mRNA present in platelets. In contrast upregulation of E- and P-selectin was observed in the MOG-induced EAE model in the C57Bl/6 mouse supporting a possible involvement of endothelial selectins in neutrophil recruitment into the CNS, which are detectable in this but not in the SJL EAE model.

CD53 was found to be upregulated during EAE in this present study as well as by others (Ibrahim et al., 2001; Carmody et al., 2002). Interestingly, CD53 has been described to coimmunoprecipitate with $\alpha_4\beta_1$-integrin (Mannion et al., 1996), which is involved in EAE pathogenesis (Engelhardt et al., 1998; Vajkoczy et al., 2001).

Upregulation of genes coding for molecules involved in innate immunity in both EAE models underlines the involvement of the innate immune system in the autoimmune pathogenesis especially at the level of the BBB. In our present study, complement component C3 was found to be upregulated by 11 or even 22-fold in MOG- induced versus PLP-induced EAE respectively, whereas a previous study comparing gene expression in entire spinal cord tissue during EAE found upregulation of C3 to be only 3- to 4-fold (Ibrahim et al., 2001). It should be noted that C3 was found to be amongst the susceptibility genes for EAE in linkage studies

and mice lacking complement are resistant to EAE (Davoust et al., 1999; Ibrahim et al., 2001). Thus complement activation at the level of cerebral vessels is of major importance in EAE pathogenesis.

The largest groups of genes regulated at the level of cerebral microvessels based on the gene array analysis were found to code for enzymes involved in general cell metabolism ("enzymes and metabolism") and in lipid metabolism with expression of most genes in both groups being downregulated during EAE. This was accompanied by a reduced gene expression for ion channels as well as genes coding for proteins involved in vesicular transport, secretory pathways, membrane traffic mechanisms and cell-cell-contact proteins, suggesting that breakdown of the BBB during EAE is accompanied by a reduced gene expression for those molecules otherwise responsible for the maintenance of a functional BBB.

Furthermore altered expression levels of genes coding for "signaling molecules", "phosphatases", "transcription factors and nuclear proteins", "protein synthesis" were found in both models with a tendency to upregulation of gene expression within these groups. One of the most prominently regulated genes was found to be the gene coding for the transcription factor JunB with 12-fold and 9-fold upregulation in the C57Bl/6- and SJL- model respectively. Whereas loss of JunB *in vivo* was shown to have severe consequences already during placentation (Schorpp-Kistner et al., 1999) overexpression of JunB *in vivo* did not lead to an apparent phenotype with exception to the CD4$^+$ T cell population where JunB expression was shown to be essential (Schorpp-Kistner et al., 1999). A recent study demonstrated that JunB expression has to be tightly adjusted in CD4$^+$ T cells to ensure proper cell function (Hartenstein et al., 2002). Thus, as speculated, before a dysbalance of $T_H 1$ versus $T_H 2$ response might be critically involved in EAE pathogenesis. Interestingly, upregulation of JunB was not reported by Ibrahim et al. (Ibrahim et al., 2001), who performed a similar microarray study from spinal cord preparations derived from C57Bl/6 mice afflicted with EAE. In contrast, a 6.02-fold upregulation of JunB was observed during acute EAE in spinal cord preparations of Lewis rats and subsequently downregulated to 0.41-fold after recovery of the mice for at least 5 days (Carmody et al., 2002).

Changes of gene expression as detected with the oligonucleotide microarrays were extended to genes coding for cytoskeletal or extracellular matrix proteins, underlining changes in tissue architecture at the BBB during EAE beyond the protein

level. This extends previous findings that cytoskeletal changes are required within
cerebral endothelial cells in order to allow inflammatory cell recruitment across the
BBB (Etienne-Manneville et al., 2000). Additionally, upregulation of arachidonate
5 lipoxygenase activating protein (ALOX5AP) and cyclooxygenase-2 (Cox-2) sug-
gests increase in prostaglandin metabolism, which may result in alterations of the
vascular tone and blood flow. Increased Cox-2 expression has been described in
rat endothelium during EAE, while increased Cox-1 expression was localized to
macrophages/microglial cells (Deininger and Schluesener, 1999). As we did not
detect regulation of Cox-1 in this present work, this underlines that we detected
upregulated genes in endothelial cells or closely related inflammatory cells. Also, al-
tered gene expression of extracellular matrix proteins found in both EAE models at
the vascular level emphasizes that molecular alterations in the BBB basal membrane
favoring inflammatory cell recruitment and BBB breakdown are not simply a con-
sequence of loss of certain extracellular matrix proteins due to enzymatic digestion,
but might additionally be influenced by reduced gene expression in cerebral endothe-
lial cells. Interestingly, tissue inhibitors of matrix metalloproteases (TIMP-1) was
found to be upregulated in both EAE models, suggesting that repair mechanisms
might be activated in parallel.

Additionally, genes coding for type 1 interferon regulated proteins, namely in-
terferon inducible protein 1 (IFI1), interferon stimulated gene 12 (ISG12) and
interferon-stimulated protein 15 kDa (ISG15) were found to be upregulated in both
EAE models. While not much is known about IFI1, neuroprotective functions of
ISG12 during viral infections have been shown (Labrada et al., 2002). ISG15 is
also known as ubiquitin cross reactive protein (UCRP) and has been described to
have ubiquitin-like functions by conjugating to other intracellular proteins (Loeb
and Haas, 1992). Recently, its involvement in JAK/STAT signaling has been sug-
gested (Malakhova et al., 2003; Malakhov et al., 2003). Such signaling events might
be involved in protective effects on the BBB, which have been described for human
recombinant interferon β-1a in chicken (Nico et al., 2000). As Type I interferon
stimulated genes have been suggested to be crucial players in viral infections of the
CNS (Akwa et al., 1998), our observations suggest that similar mechanisms are in-
volved in viral and autoimmune induced inflammation. This is supported by the
recent finding that systemic lack of interferon-β (IFN-β) leads to increased severity

of EAE (Teige et al., 2003).

Regarding individual genes of which expression was differentially regulated comparing both EAE models, we considered the increased gene expression of beta-galactosidase alpha-2,3-sialyltransferase 4A (SiaT4A) mRNA in cerebral microvessels in the MOG EAE model but not in the PLP EAE model as potentially interesting. As neutrophils lacking beta-galactosidase alpha-2,3-sialyltransferase 4C (SiaT4C) have been described to show reduced E- and P-selectin mediated rolling *in vitro* (Ellies et al., 2002) and neutrophil infiltration is observed in MOG induced EAE in C57Bl/6 mice but not in PLP induced EAE in SJL/N mice, SiaT4A might be a potential regulator of neutrophil recruitment across the BBB. Another sialyltransferase, CMP-NeuAc:lactosylceramide alpha-2,3-sialyltransferase (SiaT9), also known as ganglioside GM3 synthase, was found to be selectively downregulated in the MOG EAE model. High GM3 synthase activity has been described in bovine brain microvascular endothelial cells (Kanda et al., 1997). Involvement of GM3 in modifying growth factor receptor functions has been suggested, as described by inhibition of FGF receptor and FGF internalization in BHK cells as well as EGF-dependent growth in A431 and KB cells (reviewed by Hakomori, 2000). Additionally, there have been reports that low doses of GM3 may enhance activity of the fibronectin receptor $\alpha_5\beta_1$-integrin while high doses result in inhibition of $\alpha_5\beta_1$-integrin activity in reconstituted membranes (reviewed by Hakomori, 2000). Furthermore, GM3-dependent B16 melanoma cell adhesion to LacCer, Gb4 or Gg3 coated plates has been reported (reviewed by Hakomori, 2000). Therefore, as variations in GM3 expression have been described to result in altered cell-cell interactions, maybe partially due to altered integrin activity, GM3 synthase may modify constitutively expressed surface molecules, i. e. adhesion molecules at the BBB endothelium. This might alter leukocyte adhesion and thereby leukocyte infiltration into the CNS.

While the gene array approach allowed highly sensitive identification of genes, which were regulated in cerebral microvessels during EAE pathogenesis, it was limited to genes being presented on the chip and regulated more than 2-fold. A totally different approach, SSH enriches genes, which are increased in one versus another tissue sample. These genes can subsequently be identified by cloning and DNA sequencing, which allows identification of so far unknown genes. Multiple copies of one given gene may result from more abundantly expressed genes. Hence, the clone

number of a given gene does not correlate with its functional relevance, as high and low level expressed genes may be very important. Comparing the results from these different approaches, 13 genes were identified to be enriched by SSH/HTS, which had as well been detected to be upregulated by gene array analysis, while no contradictory results were observed. On a first glance, the number of genes identified by both techniques in parallel was astonishingly low. To be able to predict this number, one would have to assume that each gene is randomly and independently identified by either gene array analysis or SSH/HTS, which is not the case. Nevertheless, under this prerequisites, the following could be calculated: As 134 upregulated genes were detected by gene array analysis in cerebral microvessels during EAE and the gene array represented about 20 % of the mouse genome, assumably 670 genes should have been regulated in total. SSH/HTS allowed identification of approximately 100 regulated genes, which represents about 15 % of 670 genes that had been regulated in total. Therefore, 15 % of the 130 genes being identified by gene array analysis, 20 genes, should have been identified by both approaches in parallel, so that the actual number of 13 genes should be less surprising and these two different techniques have to be considered rather complementary than confirmative.

Although a different cerebral microvessel preparation method was used for the SSH/HTS approach, as compared to the gene array analysis, mRNA derived from inflammatory cells was contained in this preparation as well, as we found enrichment of the macrophage-specific immune receptor gene CD14 and the T cell-specific immune receptor CD52 / CAMPATH-1. Nevertheless, humanized antibodies directed against CD52 have been described to result in T cell depletion, thereby ameliorating MS pathogenesis, while unfortunate side effects cause carbimazole-responsive autoimmune hyperthyroidism (Coles et al., 1999). Thus, although we found non-endothelial cell specific genes, these are of high functional importance for EAE pathogenesis. Additionally, gp49A has been detected by SSH/HTS to be differentially expressed. This gene has been identified before to be an either mast cells or NK-cells expressed glycoprotein (Katz et al., 1989; Arm et al., 1991; Rojo et al., 1997), which delivers inhibitory signals into the cells. Involvement of mast cells and NK cells in EAE pathogenesis (Secor et al., 2000; Jahng et al., 2001) and multiple sclerosis (reviewed in Zappulla et al., 2002) has been described before. Transfer of bone marrow-derived mast cell into mast cell-deficient W/W^v mice did not restore

mast cells within the CNS, lymph nodes and heart; but reconstituted mice exhibited an EAE disease course equivalent to that induced in wild-type mice (Tanzola et al., 2003). Thus, mast cells outside the CNS may influence EAE. However, the absence of mast cells within the lymphoid system and the CNS may have more general effects, so that the potential role of mast cells located within the CNS during EAE pathogenesis remains to be solved.

Regarding leukocyte recruitment into the CNS, additional adhesion molecules were identified to be differentially expressed in cerebral microvessel preparation during EAE pathogenesis. Down syndrome cell adhesion molecule-like protein 1 (DSCAML1) was detected to be enriched during EAE pathogenesis. While this molecule has been suggested to be involved in axonal guidance during neural development and homophilic adhesion (Agarwala et al., 2001), a potential function in leukocyte recruitment across the endothelial BBB requires more detailed analysis. Furthermore, C-type lectin, superfamily member 10 (CLECSF10) / dectin-2 (Ariizumi et al., 2000; Okazaki et al., 2002) has been identified to be enriched in the cerebral microvessel compartment during EAE pathogenesis. Dectin-2 was described as undetectable in healthy brain and to be specifically expressed in dendritic cells (DC), while not being expressed by other hematopoietic cell types (Ariizumi et al., 2000), however, expression within the brain of mice afflicted with EAE has not been analyzed yet. Therefore, further analysis is required to elucidate potential involvement of dectin-2 in recruitment of i. e. dendritic cells in EAE pathogenesis.

Besides adhesion molecules, we found chitinase 3-like 1 (Chi3l1) and chitinase 3-like 3 (Chi3l3) to be enriched in cerebral microvessel preparations during EAE pathogenesis. As another chitinase-family member had been described as exhibiting chemotactic properties and some homology to the chemokine family (Owhashi et al., 2000), Chi3l1 and Chi3l3 might be involved in leukocyte recruitment. Further studies suggested involvement of Chi3l1 in another autoimmune disease, rheumatoid arthritis and in tissue remodeling (Volck et al., 1998) or mitogenic signaling processes via mitogen-activated protein kinase and the protein kinase B (AKT) (Recklies et al., 2002).

The Duffy antigen / receptor for chemokines (DARC) was identified by SSH/HTS to be enriched during EAE pathogenesis in cerebral microvessels. This matches our previous finding showing DARC upregulation in cerebral endothelial cells during

EAE pathogenesis by *in situ* hybridization (Alt, 1999) and will be discussed in more detail (see 4.4). Besides DARC, three additional serpentine receptors were found to be enriched in cerebral microvessel preparations during EAE pathogenesis. Increased expression of one of them, CD97, has been described in MS lesions in T lymphocytes, macrophages and microglial cells, while its ligand, CD55 was expressed by endothelial cells. The two other receptors, one of them related to *Homo sapiens* seven transmembrane domain protein (NIFIE14) and vomeronasal 1 receptor, A2 (V1RA2) require detailed analysis, as their functional role has not been described yet.

Two enriched genes might be involved in junctional integrity. One of them, axin, had been originally identified as a negative regulator of wnt-signaling pathways (Zeng et al., 1997), while additionally interacting with β-catenin (Ikeda et al., 1998). Furthermore, IQ motif containing GTPase activating protein 1 (IQGAP1) has been suggested to be involved in E-cadherin – β-catenin interactions during murine preimplantation development (Natale and Watson, 2002). Therefore, both genes could potentially be involved in modifying junctional properties during EAE pathogenesis.

Another very interesting finding was enrichment of neuropilin-2 (NP-2) in cerebral microvessel preparations during EAE pathogenesis. NPs are cell surface glycoproteins with short cytoplasmic tails. They bind semaphorins, which are involved in axonal guidance during neural development, as well as several vascular endothelial growth factor (VEGF) family members (reviewed in Matsumoto and Claesson-Welsh, 2001; Neufeld et al., 2002). NPs are non-signaling coreceptors for semaphorins and require the presence of signal transducing receptors of the plexin family to mediate their effects. NP-2 expression in lymphatic vessels has been shown, while additionally NP-2–deficiency in mice results in severe reduction or complete absence of lymphatic vessels during embryonic development, suggesting an important role in lymphatic development (Yuan et al., 2002). As there are no lymphatic vessels present within the CNS, several questions arise regarding the function of NP-2 in the brain during EAE pathogenesis: Is expression of NP-2 accompanied by induction of additional lymphatic endothelial cell marker molecules, potentially due to edema formation during the disease? Does this result in a modified, rather lymphatic phenotype of vascular endothelium in the CNS during EAE? Are known

interaction partners of NP-2, i. e. plexins, semaphorins, PlGF or distinct VEGF-isoforms, present at the CNS endothelium to interact with NP-2, and might this result in a so far unknown function of these interactions?

After having found differentially expressed genes in cerebral microvessels during EAE pathogenesis, a proteomics approach allowed to identify 6 differentially expressed proteins, of which 5 were found to be represented on the Affymetrix chip. However, only one of them, fibroleukin was significantly upregulated in both, the proteomics and oligonucleotide microarray screen. Such a low correlation between protein and gene expression profiling has been described before (Anderson and Seilhamer, 1997; Gygi et al., 1999; Chen et al., 2002) and may result from several technical problems: On the one hand, gene expression changes smaller than 2-fold have to be considered not significant according to the manufacturer, nevertheless, they may result in significant protein level changes detectable by proteomics. On the other hand, proteomics approaches may have missed expression changes of very small or very large, hydrophobic or secreted proteins, which may have been lost during the tissue preparation. I. e. chemokines may have been lost during the tissue preparation and are too small to be reliably quantified by the 2D-gelelectrophoresis. Therefore, both techniques have to be considered rather complementary than confirmative.

We found strong upregulation of fibroleukin / fgl2, expression of which has been described before in human endothelial, intestinal, trophoblast and cytotoxic T cells and to be inducible in macrophages / monocytes (Liu et al., 2003). While acting as an immune coagulant due to its prothrombinase activity (Parr et al., 1995), soluble fgl2 has been described recently to suppress T cell and dendritic cell proliferation and to polarize T cells towards a T_H2 profile (Chan et al., 2003). This underlines our gene array results, which suggest an important role of T_H1 / T_H2 equilibrium in EAE pathogenesis. Additionally, upregulated protein expression of an acidic and basic variant of heterogeneous nuclear ribonucleoprotein A2/B1, both involved in RNA processing, was detected, suggesting modulatory effects on translation of other proteins in inflamed cerebral microvessels during EAE. Another protein identified to be upregulated was purine nucleosid phosphorylase (PNP) / inosine phosphorylase, deficiency of which has been described to result in T cell depletion, while B cell function remains mostly intact (Stoop et al., 1977). Also, guanine nucleotide-binding

protein subunit-like protein 12.3 / receptor of activated protein kinase C 1 (RACK-1) could be identified to be upregulated. Involvement of RACK-1 in integrin mediated adhesion, protrusion and chemotactic cell migration has been described *in vitro* (Cox et al., 2003). Considering its multiple functional domains, RACK-1 might act as a scaffolding protein, which is underlined by observations demonstrating its interaction with other WD40 domain containing proteins, i. e. G-protein β subunits (Dell et al., 2002). The additionally observed downregulation of the WD40 domain containing guanine nucleotide binding protein beta subunit 2 (GBB2) suggests that modifications in RACK-1 scaffolding with different other proteins might either play a potential role in lymphocyte migration across the endothelial BBB or in endothelial cells allowing lymphocytes to transmigrate. Along the same lines, the observed upregulation of tailless complex polypeptide 1 (TCP-1), a chaperon suggested to be involved in the folding of actin and tubulin, points to increased actin remodeling in inflamed cerebral microvessels during EAE.

In conclusion, all three techniques allowed to discover new molecules which are regulated in the cerebral microvessel compartment during EAE providing new insight into the disease pathogenesis and raising the exciting possibility to target new molecules for the therapy of human inflammatory demyelinating diseases of the CNS.

4.3 Gene expression profiling of encephalitogenic T cells

PLP-specific T cell lines established from SJL/N mice are referred to as either encephalitogenic or non-encephalitogenic depending on their ability to transfer clinical EAE into naïve syngeneic recipients. While some T cell lines are never encephalitogenic, others lose their encephalitogenicity after several *in vitro* restimulation steps. The question by what molecular means this functional difference is caused has been addressed in our laboratory and by others before. Different cytokine and α_4-integrin expression have been suggested to be critically involved in encephalitogenicity (Tokuchi et al., 1990; Baron et al., 1993; Kuchroo et al., 1993). However, such results were never observed when comparing encephalitogenic vs. non-encephalitogenic T cell lines in our laboratory (Engelhardt et al., unpublished data). Thus, we applied molecular screening techniques to analyze potential differences.

Comparing encephalitogenic with non-encephalitogenic T lymphoblasts by gene array analysis, only few molecules being possibly directly involved in leukocyte recruitment were altered. While there was a decent number of cytokines, chemokines and their receptors mostly decreased in encephalitogenic T cells as compared to non-encephalitogenic T cells, only one adhesion related molecule was regulated, CD81. CD81 belongs to the tetraspanin family, which has been described to regulate α_4-integrin mediated adhesion strengthening under shear (Feigelson et al., 2003). As α_4-integrin involvement in recruitment of encephalitogenic T lymphoblasts across the endothelial BBB has been shown in our laboratory *in vivo* (Vajkoczy et al., 2001), this strongly suggests an important role of CD81 in lymphocyte recruitment.

Cytoskeleton related proteins are predominantly increased in encephalitogenic versus non-encephalitogenic T lymphoblasts, of which calcium binding protein p22 is the most prominent regulated one. Involvement of this gene in directed vesicular transport and association with the microtubular cytoskeleton has been described (Barroso et al., 1996; Timm et al., 1999), suggesting a possible role in motility and thereby transmigration of lymphocytes across vascular walls. Thus, encephalitogenic T lymphoblasts might be more motile than non-encephalitogenic T lymphoblasts.

Furthermore, there were significant differences in genes being involved in signal transduction and transcription. The proto-oncogene and receptor tyrosine kinase c-fes was decreased in encephalitogenic versus non-encephalitogenic T cell lines. As c-fes has been shown to be involved in IL-4 mediated signaling events (Izuhara et al., 1996), one might suggests, that non-encephalitogenic T cells have been shifted towards a T_H2 specific immune response. Although T_H2 lymphoblasts are able to induce EAE as well (Lafaille et al., 1997), such a T_H1 / T_H2 dysbalance might result in loss of encephalitogenicity. Additionally, strongly decreased c-fos in encephalitogenic versus non-encephalitogenic T lymphoblasts has been observed in this present thesis. c-fos overexpression has been described to result in increased collagenase-1 expression by T cells (Gack et al., 1994). This would suggest decreased collagenase-1 expression, which has to be considered inconclusive at present. Another transcription related gene, chop-10, was massively decreased in encephalitogenic versus non-encephalitogenic T cells. As chop-10 binds to leucine zipper type transcription factors, but lacks DNA binding properties, it may function as a negative regulator of other transcription factors (Ron and Habener, 1992). How-

ever, its role in T cell function has not been described yet. Another significant difference in signaling events might result from the fact, that we detected highly increased amounts of ATPase-2 A2 (ATP2A2) / sarcoplasmic/endoplasmic reticulum Ca^{2+}-activated adenosine triphosphatase 2 / SERCA-2 in encephalitogenic versus non-encephalitogenic T cells, which maintains the intracellular Ca^{2+} stores. Reduced activity of this transporter may therefore result in reduced Ca^{2+} signaling events.

Besides these regulated genes, genes being upregulated in encephalitogenic versus non-encephalitogenic T cells were identified by SSH and subsequent sequencing. The most interesting one was hook homolog 1, which has been described as a linker of the microtubular manchette and flagellum to cellular structures in spermatozoa, suggesting a possible role in T lymphoblast diapedesis across the endothelial BBB (Mendoza-Lujambio et al., 2002).

Taken together, these two approaches allowed to discover molecules differentially expressed in encephalitogenic versus non-encephalitogenic T lymphoblasts, thereby being of potentially high relevance for encephalitogenic T lymphoblast function and proposing new target molecules for treatment of inflammatory demyelinating diseases of the CNS.

4.4   Involvement of DARC in T cell recruitment into the CNS during EAE pathogenesis

In this present thesis, the Duffy Antigen / Receptor for Chemokines (DARC), which is a blood group antigen presented on erythrocytes, was detected by SSH/HTS to be upregulated in cerebral microvessel preparations during EAE. This nicely confirms our previous *in situ* observations, that DARC is induced in cerebral venules during clinical EAE (Alt, 1999). DARC expression has been described before in kidney, lung, spleen and thyroid endothelial cells (Hadley et al., 1994; Peiper et al., 1995; Chaudhuri et al., 1997) and in Purkinje cells within the brain parenchyma (Horuk et al., 1996), while expression in brain endothelial cells has not been reported yet. Nevertheless, DARC involvement has been suggested in autoimmune responses, such as crescentic glomerulonephritis and rheumatoid arthritis (Segerer et al., 2000; Patterson et al., 2002), while two studies with DARC-deficient mice described its

involvement during inflammatory responses *in vivo* (Dawson et al., 2000; Luo et al., 2000, 2003).

Regarding the functional role of DARC, it has been proposed to fulfill one or multiple different tasks: On the one hand, endothelial cell expressed DARC may be involved in chemokine transcytosis to and presentation at the luminal surface of endothelial cells (reviewed in Middleton et al., 2002). On the other hand, erythrocyte expressed DARC may remove chemokines from the bloodstream ("sink") (Dawson et al., 2000). This local "sink" function might have to be extended by a systemic "reservoir" function, as it has been described, that DARC delays the disappearance of systemically administered chemokines from the blood plasma, thereby maintaining plasma chemokine concentrations (Fukuma et al., 2003).

In this present thesis, EAE in DARC-deficient mice resulted in a delayed onset of disease, while clinical severity of the disease was increased as compared to wild type mice. These surprising results allow different explanations. First of all, experiments were performed in mice which had been backcrossed into the C57Bl/6 background for only 4 generations. However, as wildtype littermates were used as a control, it is unlikely that diversity in genetic background influences the experiments. Rather, lack of DARC expression on endothelial cells and erythrocytes results in beneficial and detrimental effects, antagonizing each other. Hence, we would like to suggest the following: Initial recruitment of T lymphoblasts mediated by CCL19 is unaffected by DARC absence, as CCL19 has been described not to bind to DARC (Kashiwazaki et al., 2003). Subsequently, inflammatory chemokines which are produced within the CNS parenchyma cannot be transported across the endothelial BBB to be presented at the luminal surface. Thus, onset of disease is delayed. However, after onset of disease and breakdown of the endothelial BBB, inflammatory chemokines might diffuse across the leaky BBB and reach reach the luminal surface of the endothelial cells. Due to the absence of DARC on erythrocytes, chemokines are not removed and therefore, increased amounts of secondary inflammatory cells are attracted to the CNS, resulting in more severe clinical symptoms. To distinguish these different effects, bone marrow chimeras will have to be established, which possess either DARC-deficient endothelial cells or erythrocytes.

4.5 Model for chemokine involvement in lymphocyte recruitment into the CNS

In conclusion, we would like to suggest the model shown in Figure 4.5.1.
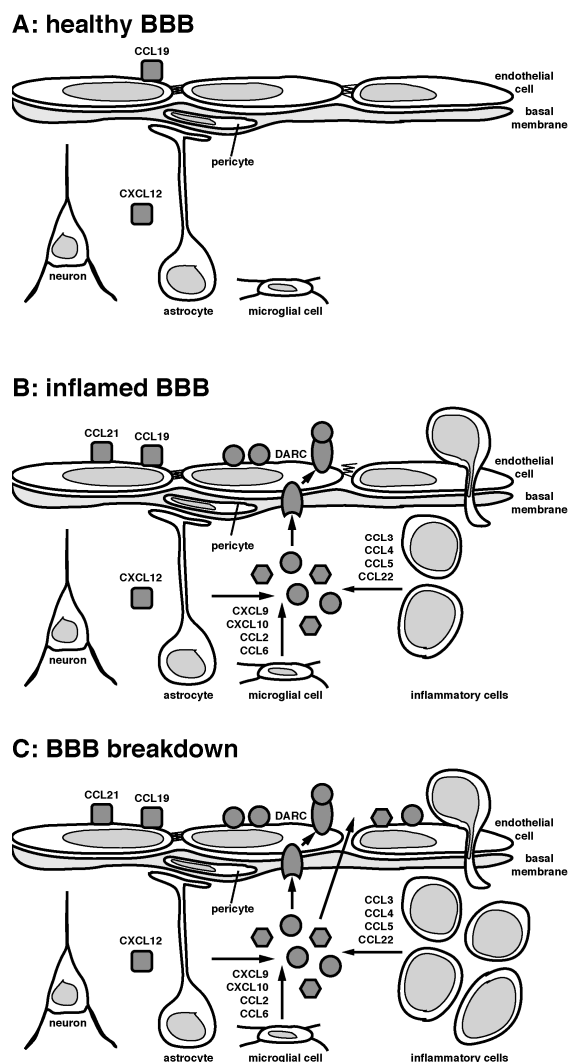
Figure 4.5.1: Model showing the potential involvement of lymphoid (quadrangles), inflammatory DARC-binding (circles) and non-DARC-binding (hexagons) chemokines in lymphocyte recruitment into the CNS. A: At the healthy BBB, initial T lymphoblast recruitment is mediated by CCL19, which is presented on the luminal surface of endothelial cells, while CXCL12 is expressed by astrocytes but cannot pass the endothelial BBB. B: During inflammation, CCL21 expression is induced in endothelial cells, so it is presented on the luminal surface and directly affects lymphocyte recruitment into the CNS. Induced expression of DARC allows transport of a distinct inflammatory chemokines, which are expressed within the brain parenchyma, across the endothelial BBB to the luminal surface. Further effector functions are fulfilled by chemokines located within the CNS. C: During severe inflammation and after BBB breakdown, additional chemokines can reach the luminal surface of the endothelial cells and further increase CNS inflammation.

A Bibliography

M. Adelmann, J. Wood, I. Benzel, P. Fiori, H. Lassmann, J. M. Matthieu, M. V. Gardinier, K. Dornmair, and C. Linington. The N-terminal domain of the myelin oligodendrocyte glycoprotein (MOG) induces acute demyelinating experimental autoimmune encephalomyelitis in the Lewis rat. *J Neuroimmunol*, 63(1):17–27, 1995.

K. L. Agarwala, S. Ganesh, Y. Tsutsumi, T. Suzuki, K. Amano, and K. Yamakawa. Cloning and functional characterization of DSCAML1, a novel DSCAM-like cell adhesion molecule that mediates homophilic intercellular adhesion. *Biochem Biophys Res Commun*, 285(3):760–72, 2001.

Y. Akwa, D. E. Hassett, M. L. Eloranta, K. Sandberg, E. Masliah, H. Powell, J. L. Whitton, F. E. Bloom, and I. L. Campbell. Transgenic expression of IFN-alpha in the central nervous system of mice protects against lethal neurotropic viral infection but induces inflammation and neurodegeneration. *J Immunol*, 161(9): 5016–26, 1998.

C. Alt. Die Rolle von Chemokinen bei der Rekrutierung von T-Lymphozyten über die endotheliale Blut-Hirn Schranke. Diploma, Philipps Universität, Marburg, 1999.

C. Alt, M. Laschinger, and B. Engelhardt. Functional expression of the lymphoid chemokines CCL19 (ELC) and CCL 21 (SLC) at the blood-brain barrier suggests their involvement in G-protein-dependent lymphocyte recruitment into the central nervous system during experimental autoimmune encephalomyelitis. *Eur J Immunol*, 32(8):2133–44, 2002.

L. Anderson and J. Seilhamer. A comparison of selected mRNA and protein abundances in human liver. *Electrophoresis*, 18(3-4):533–7, 1997.

A. V. Andjelkovic and J. S. Pachter. Characterization of binding sites for chemokines MCP-1 and MIP-1alpha on human brain microvessels. *J Neurochem*, 75(5):1898–906, 2000.

A. V. Andjelkovic, D. D. Spencer, and J. S. Pachter. Visualization of chemokine binding sites on human brain microvessels. *J Cell Biol*, 145(2):403–12, 1999.

J. J. Archelos, S. Jung, M. Maurer, M. Schmied, H. Lassmann, T. Tamatani, M. Miyasaka, K. V. Toyka, and H. P. Hartung. Inhibition of experimental autoimmune encephalomyelitis by an antibody to the intercellular adhesion molecule ICAM-1. *Ann Neurol*, 34(2):145–54, 1993.

K. Ariizumi, G. L. Shen, S. Shikano, 3rd Ritter, R., P. Zukas, D. Edelbaum, A. Morita, and A. Takashima. Cloning of a second dendritic cell-associated C-type lectin (dectin-2) and its alternatively spliced isoforms. *J Biol Chem*, 275(16): 11957–63, 2000.

J. P. Arm, M. F. Gurish, D. S. Reynolds, H. C. Scott, C. S. Gartner, K. F. Austen, and H. R. Katz. Molecular cloning of gp49, a cell-surface antigen that is preferentially expressed by mouse mast cell progenitors and is a new member of the immunoglobulin superfamily. *J Biol Chem*, 266(24):15966–73, 1991.

V. C. Asensio, S. Lassmann, A. Pagenstecher, S. C. Steffensen, S. J. Henriksen, and I. L. Campbell. C10 is a novel chemokine expressed in experimental inflammatory demyelinating disorders that promotes recruitment of macrophages to the central nervous system. *Am J Pathol*, 154(4):1181–91, 1999.

E. S. Baekkevold, T. Yamanaka, R. T. Palframan, H. S. Carlsen, F. P. Reinholt, U. H. von Andrian, P. Brandtzaeg, and G. Haraldsen. The CCR7 ligand ELC (CCL19) is transcytosed in high endothelial venules and mediates T cell recruitment. *J Exp Med*, 193(9):1105–12, 2001.

E. T. Baldwin, I. T. Weber, R. St Charles, J. C. Xuan, E. Appella, M. Yamada, K. Matsushima, B. F. Edwards, G. M. Clore, A. M. Gronenborn, and A. Wlodawer. Crystal structure of interleukin 8: symbiosis of NMR and crystallography. *Proc Natl Acad Sci U S A*, 88(2):502–506, Jan 1991.

G. Bardi, M. Lipp, M. Baggiolini, and P. Loetscher. The T cell chemokine receptor CCR7 is internalized on stimulation with ELC, but not with SLC. *Eur J Immunol*, 31(11):3291–7, 2001.

J. L. Baron, J. A. Madri, N. H. Ruddle, G. Hashim, and Jr. Janeway, C. A. Surface expression of alpha 4 integrin by CD4 T cells is required for their entry into brain parenchyma. *J Exp Med*, 177(1):57–68, 1993.

M. R. Barroso, K. K. Bernd, N. D. DeWitt, A. Chang, K. Mills, and E. S. Sztul. A novel Ca2+-binding protein, p22, is required for constitutive membrane traffic. *J Biol Chem*, 271(17):10183–7, 1996.

J. F. Bazan, K. B. Bacon, G. Hardiman, W. Wang, K. Soo, D. Rossi, D. R. Greaves, A. Zlotnik, and T. J. Schall. A new class of membrane-bound chemokine with a CX3C motif. *Nature*, 385(6617):640–644, Feb 1997.

R. W. Beck, P. A. Cleary, Jr. Anderson, M. M., J. L. Keltner, W. T. Shults, D. I. Kaufman, E. G. Buckley, J. J. Corbett, M. J. Kupersmith, N. R. Miller, P. J. Savino, R. Guy, J. D. Trobe, J. A. McCrary, Smith C. H., G. A. Chrousos, H. S. Thompson, Katz B. J., Brodsky M. C., J. A. Goodwin, and et al. A randomized, controlled trial of corticosteroids in the treatment of acute optic neuritis. The Optic Neuritis Study Group. *N Engl J Med*, 326(9):581–8, 1992.

A. Ben-Nun, H. Wekerle, and I. R. Cohen. The rapid isolation of clonable antigen-specific T lymphocyte lines capable of mediating autoimmune encephalomyelitis. *Eur J Immunol*, 11(3):195–199, Mar 1981.

M. S. Berger, D. D. Taub, A. Orlofsky, T. R. Kleyman, B. Coupaye-Gerard, D. Eisner, and S. A. Cohen. The chemokine C10: immunological and functional analysis of the sequence encoded by the novel second exon. *Cytokine*, 8(6):439–447, Jun 1996.

O. Bjorkdahl, K. A. Barber, S. J. Brett, M. G. Daly, C. Plumpton, N. A. Elshourbagy, J. P. Tite, and L. L. Thomsen. Characterization of CC-chemokine receptor 7 expression on murine T cells in lymphoid tissues. *Immunology*, 110(2): 170–9, 2003.

C. C. Bleul, M. Farzan, H. Choe, C. Parolin, I. Clark-Lewis, J. Sodroski, and T. A. Springer. The lymphocyte chemoattractant SDF-1 is a ligand for LESTR/fusin and blocks HIV-1 entry. *Nature*, 382(6594):829–833, Aug 1996.

R. Bosse and D. Vestweber. Only simultaneous blocking of the L- and P-selectin completely inhibits neutrophil migration into mouse peritoneum. *Eur J Immunol*, 24(12):3019–24, 1994.

W. Boyle. An extension of the 51Cr-release assay for the estimation of mouse cytotoxins. *Transplantation*, 6(6):761–4, 1968.

M. M. Bradford. A rapid and sensitive method for the quantitation of microgram quantities of protein utilizing the principle of protein-dye binding. *Anal Biochem*, 72:248–54, 1976.

M. J. Briskin, L. M. McEvoy, and E. C. Butcher. MAdCAM-1 has homology to immunoglobulin and mucin-like adhesion receptors and to IgA1. *Nature*, 363 (6428):461–4, 1993.

S. D. Burrows, M. L. Doyle, K. P. Murphy, S. G. Franklin, J. R. White, I. Brooks, D. E. McNulty, M. O. Scott, J. R. Knutson, D. Porter, P. R. Young, and P. Hensley. Determination of the monomer-dimer equilibrium of interleukin-8 reveals it is a monomer at physiological concentrations. *Biochemistry*, 33(43):12741–12745, Nov 1994.

E. C. Butcher. Leukocyte-endothelial cell recognition: three (or more) steps to specificity and diversity. *Cell*, 67(6):1033–6, 1991.

E. C. Butcher, M. Williams, K. Youngman, L. Rott, and M. Briskin. Lymphocyte trafficking and regional immunity. *Adv Immunol*, 72:209–53, 1999.

R. J. Carmody, B. Hilliard, K. Maguschak, L. A. Chodosh, and Y. H. Chen. Genomic scale profiling of autoimmune inflammation in the central nervous system: the nervous response to inflammation. *J Neuroimmunol*, 133(1-2):95–107, 2002.

M. W. Carr, R. Alon, and T. A. Springer. The C-C chemokine MCP-1 differentially modulates the avidity of beta 1 and beta 2 integrins on T lymphocytes. *Immunity*, 4(2):179–187, Feb 1996.

M. W. Carr, S. J. Roth, E. Luther, S. S. Rose, and T. A. Springer. Monocyte chemoattractant protein 1 acts as a T-lymphocyte chemoattractant. *Proc Natl Acad Sci U S A*, 91(9):3652–3656, Apr 1994.

R. Cecchelli, B. Dehouck, L. Descamps, L. Fenart, V. V. Buee-Scherrer, C. Duhem, S. Lundquist, M. Rentfel, G. Torpier, and M. P. Dehouck. In vitro model for evaluating drug transport across the blood-brain barrier. *Adv Drug Deliv Rev*, 36 (2-3):165–178, 1999.

C. W. Chan, L. S. Kay, R. G. Khadaroo, M. W. Chan, S. Lakatoo, K. J. Young, L. Zhang, R. M. Gorczynski, M. Cattral, O. Rotstein, and G. A. Levy. Soluble fibrinogen-like protein 2/fibroleukin exhibits immunosuppressive properties: suppressing T cell proliferation and inhibiting maturation of bone marrow-derived dendritic cells. *J Immunol*, 170(8):4036–44, 2003.

A. Chaudhuri, S. Nielsen, M. L. Elkjaer, V. Zbrzezna, F. Fang, and A. O. Pogo. Detection of Duffy antigen in the plasma membranes and caveolae of vascular endothelial and epithelial cells of nonerythroid organs. *Blood*, 89(2):701–12, 1997.

G. Chen, T. G. Gharib, C. C. Huang, J. M. Taylor, D. E. Misek, S. L. Kardia, T. J. Giordano, M. D. Iannettoni, M. B. Orringer, S. M. Hanash, and D. G. Beer. Discordant protein and mRNA expression in lung adenocarcinomas. *Mol Cell Proteomics*, 1(4):304–13, 2002.

G. M. Clore, E. Appella, M. Yamada, K. Matsushima, and A. M. Gronenborn. Three-dimensional structure of interleukin 8 in solution. *Biochemistry*, 29(7): 1689–1696, Feb 1990.

R. L. Coffman. Surface antigen expression and immunoglobulin gene rearrangement during mouse pre-B cell development. *Immunol Rev*, 69:5–23, 1982.

A. J. Coles, M. Wing, S. Smith, F. Coraddu, S. Greer, C. Taylor, A. Weetman, G. Hale, V. K. Chatterjee, H. Waldmann, and A. Compston. Pulsed monoclonal antibody treatment and autoimmune thyroid disease in multiple sclerosis. *Lancet*, 354(9191):1691–5, 1999.

E. A. Cox, D. Bennin, A. T. Doan, T. O'Toole, and A. Huttenlocher. RACK1

regulates integrin-mediated adhesion, protrusion, and chemotactic cell migration via its Src-binding site. *Mol Biol Cell*, 14(2):658–69, 2003.

C. Crone and S. P. Olesen. Electrical resistance of brain microvascular endothelium. *Brain Res*, 241(1):49–55, Jun 1982.

J. C. Cruveilhier. *Anatomie pathologique du corps humain.* Bailliere, Paris, 1830 – 1842.

J. G. Cyster. Chemokines and cell migration in secondary lymphoid organs. *Science*, 286(5447):2098–102, 1999.

P. A. D'Amore and M. Klagsbrun. Endothelial cell mitogens derived from retina and hypothalamus: biochemical and biological similarities. *J Cell Biol*, 99(4 Pt 1):1545–9, 1984.

N. Davoust, S. Nataf, R. Reiman, M. V. Holers, I. L. Campbell, and S. R. Barnum. Central nervous system-targeted expression of the complement inhibitor sCrry prevents experimental allergic encephalomyelitis. *J Immunol*, 163(12):6551–6, 1999.

T. C. Dawson, A. B. Lentsch, Z. Wang, J. E. Cowhig, A. Rot, N. Maeda, and S. C. Peiper. Exaggerated response to endotoxin in mice lacking the Duffy antigen/receptor for chemokines (DARC). *Blood*, 96(5):1681–4, 2000.

M. H. Deininger and H. J. Schluesener. Cyclooxygenases-1 and -2 are differentially localized to microglia and endothelium in rat EAE and glioma. *J Neuroimmunol*, 95(1-2):202–8, 1999.

A. Del Maschio, A. De Luigi, I. Martin-Padura, M. Brockhaus, T. Bartfai, P. Fruscella, L. Adorini, G. Martino, R. Furlan, M. G. De Simoni, and E. Dejana. Leukocyte recruitment in the cerebrospinal fluid of mice with experimental meningitis is inhibited by an antibody to junctional adhesion molecule (JAM). *J Exp Med*, 190(9):1351–6, 1999.

E. J. Dell, J. Connor, S. Chen, E. G. Stebbins, N. P. Skiba, D. Mochly-Rosen, and H. E. Hamm. The betagamma subunit of heterotrimeric G proteins interacts with RACK1 and two other WD repeat proteins. *J Biol Chem*, 277(51):49888–95, 2002.

P. Ehrlich. Über die Beziehung chemischer Constitution, Vertheilung, und phar-makologischer Wirkung. In *Gesammelte Arbeiten zur Immunitätsforschung.* Berlin, 1904.

L. G. Ellies, M. Sperandio, G. H. Underhill, J. Yousif, M. Smith, J. J. Priatel, G. S. Kansas, K. Ley, and J. D. Marth. Sialyltransferase specificity in selectin ligand formation. *Blood*, 100(10):3618–25, 2002.

B. Engelhardt, M. Laschinger, M. Schulz, U. Samulowitz, D. Vestweber, and G. Hoch. The development of experimental autoimmune encephalomyelitis in the mouse requires alpha4-integrin but not alpha4beta7-integrin. *J Clin Invest*, 102(12):2096–2105, Dec 1998.

B. Engelhardt, D. Vestweber, R. Hallmann, and M. Schulz. E- and P-selectin are not involved in the recruitment of inflammatory cells across the blood-brain barrier in experimental autoimmune encephalomyelitis. *Blood*, 90(11):4459–4472, Dec 1997.

S. Etienne-Manneville, J. B. Manneville, P. Adamson, B. Wilbourn, J. Greenwood, and P. O. Couraud. ICAM-1-coupled cytoskeletal rearrangements and transendothelial lymphocyte migration involve intracellular calcium signaling in brain endothelial cell lines. *J Immunol*, 165(6):3375–83, 2000.

T. J. Fahey, K. J. Tracey, P. Tekamp-Olson, L. S. Cousens, W. G. Jones, G. T. Shires, A. Cerami, and B. Sherry. Macrophage inflammatory protein 1 modulates macrophage function. *J Immunol*, 148(9):2764–2769, May 1992.

J. M. Farber. A macrophage mRNA selectively induced by gamma-interferon encodes a member of the platelet factor 4 family of cytokines. *Proc Natl Acad Sci U S A*, 87(14):5238–42, 1990.

S. W. Feigelson, V. Grabovsky, R. Shamri, S. Levy, and R. Alon. The CD81 tetraspanin facilitates instantaneous leukocyte VLA-4 adhesion strengthening to VCAM-1 under shear flow T. *J Biol Chem*, 2003.

B. T. Fife, G. B. Huffnagle, W. A. Kuziel, and W. J. Karpus. CC chemokine receptor 2 is critical for induction of experimental autoimmune encephalomyelitis. *J Exp Med*, 192(6):899–905, 2000.

B. T. Fife, K. J. Kennedy, M. C. Paniagua, N. W. Lukacs, S. L. Kunkel, A. D. Luster, and W. J. Karpus. CXCL10 (IFN-gamma-inducible protein-10) control of encephalitogenic CD4+ T cell accumulation in the central nervous system during experimental autoimmune encephalomyelitis. *J Immunol*, 166(12):7617–24, 2001.

T. J. Fleming, M. L. Fleming, and T. R. Malek. Selective expression of Ly-6G on myeloid lineage cells in mouse bone marrow. RB6-8C5 mAb to granulocyte-differentiation antigen (Gr-1) detects members of the Ly-6 family. *J Immunol*, 151(5):2399–408, 1993.

R. Forster, A. Schubel, D. Breitfeld, E. Kremmer, I. Renner-Muller, E. Wolf, and M. Lipp. CCR7 coordinates the primary immune response by establishing functional microenvironments in secondary lymphoid organs. *Cell*, 99(1):23–33, 1999.

N. Fukuma, N. Akimitsu, H. Hamamoto, H. Kusuhara, Y. Sugiyama, and K. Sekimizu. A role of the Duffy antigen for the maintenance of plasma chemokine concentrations. *Biochem Biophys Res Commun*, 303(1):137–9, 2003.

S. Gack, R. Vallon, J. Schaper, U. Ruther, and P. Angel. Phenotypic alterations in fos-transgenic mice correlate with changes in Fos/Jun-dependent collagenase type I expression. Regulation of mouse metalloproteinases by carcinogens, tumor promoters, cAMP, and Fos oncoprotein. *J Biol Chem*, 269(14):10363–9, 1994.

W. M. Gallatin, I. L. Weissman, and E. C. Butcher. A cell-surface molecule involved in organ-specific homing of lymphocytes. *Nature*, 304(5921):30–4, 1983.

A. Z. Ge and E. C. Butcher. Cloning and expression of a cDNA encoding mouse endoglin, an endothelial cell TGF-beta ligand. *Gene*, 138(1-2):201–6, 1994.

R. Godiska, D. Chantry, G. N. Dietsch, and P. W. Gray. Chemokine expression in murine experimental allergic encephalomyelitis. *J Neuroimmunol*, 58(2):167–176, May 1995.

R. Godiska, D. Chantry, C. J. Raport, S. Sozzani, P. Allavena, D. Leviten, A. Mantovani, and P. W. Gray. Human macrophage-derived chemokine (MDC), a novel chemoattractant for monocytes, monocyte-derived dendritic cells, and natural killer cells. *J Exp Med*, 185(9):1595–604, 1997.

E. E. Goldmann. Vitalfärbung am Zentralnervensystem. *Abhandlungen der Königlich-Preussischen Akademie der Wissenschaften: Physikalalisch-Mathematische Classe*, 1:1–60, 1913.

A. Gorg, G. Boguth, C. Obermaier, A. Posch, and W. Weiss. Two-dimensional polyacrylamide gel electrophoresis with immobilized pH gradients in the first dimension (IPG-Dalt): the state of the art and the controversy of vertical versus horizontal systems. *Electrophoresis*, 16(7):1079–86, 1995.

U. Gotsch, E. Borges, R. Bosse, E. Boggemeyer, M. Simon, H. Mossmann, and D. Vestweber. VE-cadherin antibody accelerates neutrophil recruitment in vivo. *J Cell Sci*, 110 (Pt 5):583–8, 1997.

D. E. Griffin, B. Levine, W. R. Tyor, and D. N. Irani. The immune response in viral encephalitis. *Semin Immunol*, 4(2):111–9, 1992.

D. A. Griffiths-Johnson, P. D. Collins, A. G. Rossi, P. J. Jose, and T. J. Williams. The chemokine, eotaxin, activates guinea-pig eosinophils in vitro and causes their accumulation into the lung in vivo. *Biochem Biophys Res Commun*, 197(3):1167–72, 1993.

M. D. Gunn, S. Kyuwa, C. Tam, T. Kakiuchi, A. Matsuzawa, L. T. Williams, and H. Nakano. Mice lacking expression of secondary lymphoid organ chemokine have defects in lymphocyte homing and dendritic cell localization. *J Exp Med*, 189(3): 451–60, 1999.

M. D. Gunn, K. Tangemann, C. Tam, J. G. Cyster, S. D. Rosen, and L. T. Williams. A chemokine expressed in lymphoid high endothelial venules promotes the adhesion and chemotaxis of naive T lymphocytes. *Proc Natl Acad Sci U S A*, 95(1): 258–263, Jan 1998.

S. P. Gygi, Y. Rochon, B. R. Franza, and R. Aebersold. Correlation between protein and mRNA abundance in yeast. *Mol Cell Biol*, 19(3):1720–30, 1999.

T. J. Hadley, Z. H. Lu, K. Wasniowska, A. W. Martin, S. C. Peiper, J. Hesselgesser, and R. Horuk. Postcapillary venule endothelial cells in kidney express a multispecific chemokine receptor that is structurally and functionally identical to the

erythroid isoform, which is the Duffy blood group antigen. *J Clin Invest*, 94(3): 985–91, 1994.

M. Hahne, R. H. Wenger, D. Vestweber, and P. J. Nielsen. The heat-stable antigen can alter very late antigen 4-mediated adhesion. *J Exp Med*, 179(4):1391–5, 1994.

S. Hakomori. Traveling for the glycosphingolipid path. *Glycoconj J*, 17(7-9):627–47, 2000.

R. Hallmann, D. N. Mayer, E. L. Berg, R. Broermann, and E. C. Butcher. Novel mouse endothelial cell surface marker is suppressed during differentiation of the blood brain barrier. *Dev Dyn*, 202(4):325–32, 1995.

A. Hamann and P. Jonas. Lymphocyte migration in vivo: the mouse model. In Lefkovits I., editor, *Immunology Methods Manual*, pages 1333–41. Academic Press, London, 1997.

M. Hammel, G. Weitz-Schmidt, A. Krause, T. Moll, D. Vestweber, H. G. Zerwes, and R. Hallmann. Species-specific and conserved epitopes on mouse and human E-selectin important for leukocyte adhesion. *Exp Cell Res*, 269(2):266–74, 2001.

B. Hartenstein, S. Teurich, J. Hess, J. Schenkel, M. Schorpp-Kistner, and P. Angel. Th2 cell-specific cytokine expression and allergen-induced airway inflammation depend on JunB. *Embo J*, 21(23):6321–9, 2002.

W. F. Hickey, B. L. Hsu, and H. Kimura. T-lymphocyte entry into the central nervous system. *J Neurosci Res*, 28(2):254–60, 1991.

W. F. Hickey and H. Kimura. Perivascular microglial cells of the CNS are bone marrow-derived and present antigen in vivo. *Science*, 239(4837):290–2, 1988.

P. Hjelmstrom, J. Fjell, T. Nakagawa, R. Sacca, C. A. Cuff, and N. H. Ruddle. Lymphoid tissue homing chemokines are expressed in chronic inflammation. *Am J Pathol*, 156(4):1133–8, 2000.

R. Horuk, A. Martin, J. Hesselgesser, T. Hadley, Z. H. Lu, Z. X. Wang, and S. C. Peiper. The Duffy antigen receptor for chemokines: structural analysis and expression in the brain. *J Leukoc Biol*, 59(1):29–38, 1996.

J. C. Houck and C. M. Chang. The purification and characterization of a lymphokine chemotactic for lymphocytes – lymphotactin. *Inflammation*, 2(2):105–13, 1977.

D. R. Huang, J. Wang, P. Kivisakk, B. J. Rollins, and R. M. Ransohoff. Absence of monocyte chemoattractant protein 1 in mice leads to decreased local macrophage recruitment and antigen-specific T helper cell type 1 immune response in experimental autoimmune encephalomyelitis. *J Exp Med*, 193(6):713–26, 2001.

A. L. Hughes and M. Yeager. Coevolution of the mammalian chemokines and their receptors. *Immunogenetics*, 49(2):115–24, 1999.

S. M. Ibrahim, E. Mix, T. Bottcher, D. Koczan, R. Gold, A. Rolfs, and H. J. Thiesen. Gene expression profiling of the nervous system in murine experimental autoimmune encephalomyelitis. *Brain*, 124(Pt 10):1927–38, 2001.

S. Ikeda, S. Kishida, H. Yamamoto, H. Murai, S. Koyama, and A. Kikuchi. Axin, a negative regulator of the Wnt signaling pathway, forms a complex with GSK-3beta and beta-catenin and promotes GSK-3beta-dependent phosphorylation of beta-catenin. *Embo J*, 17(5):1371–84, 1998.

T. Ikezu, H. Ueda, B. D. Trapp, K. Nishiyama, J. F. Sha, D. Volonte, F. Galbiati, A. L. Byrd, G. Bassell, H. Serizawa, W. S. Lane, M. P. Lisanti, and T. Okamoto. Affinity-purification and characterization of caveolins from the brain: differential expression of caveolin-1, -2, and -3 in brain endothelial and astroglial cell types. *Brain Res*, 804(2):177–92, 1998.

S. Issazadeh, A. Ljungdahl, B. Hojeberg, M. Mustafa, and T. Olsson. Cytokine production in the central nervous system of Lewis rats with experimental autoimmune encephalomyelitis: dynamics of mRNA expression for interleukin-10, interleukin-12, cytolysin, tumor necrosis factor alpha and tumor necrosis factor beta. *J Neuroimmunol*, 61(2):205–12, 1995.

L. Izikson, R. S. Klein, I. F. Charo, H. L. Weiner, and A. D. Luster. Resistance to experimental autoimmune encephalomyelitis in mice lacking the CC chemokine receptor (CCR)2. *J Exp Med*, 192(7):1075–80, 2000.

K. Izuhara, R. A. Feldman, P. Greer, and N. Harada. Interleukin-4 induces association of the c-fes proto-oncogene product with phosphatidylinositol-3 kinase. *Blood*, 88(10):3910–8, 1996.

L. D. Jacobs, D. L. Cookfair, R. A. Rudick, R. M. Herndon, J. R. Richert, A. M. Salazar, J. S. Fischer, D. E. Goodkin, C. V. Granger, J. H. Simon, and et al. A phase III trial of intramuscular recombinant interferon beta as treatment for exacerbating-remitting multiple sclerosis: design and conduct of study and baseline characteristics of patients. Multiple Sclerosis Collaborative Research Group (MSCRG). *Mult Scler*, 1(2):118–35, 1995.

A. W. Jahng, I. Maricic, B. Pedersen, N. Burdin, O. Naidenko, M. Kronenberg, Y. Koezuka, and V. Kumar. Activation of natural killer T cells potentiates or prevents experimental autoimmune encephalomyelitis. *J Exp Med*, 194(12):1789–99, 2001.

S. T. Jalkanen, R. F. Bargatze, L. R. Herron, and E. C. Butcher. A lymphoid cell surface glycoprotein involved in endothelial cell recognition and lymphocyte homing in man. *Eur J Immunol*, 16(10):1195–202, 1986.

K. P. Johnson, B. R. Brooks, J. A. Cohen, C. C. Ford, J. Goldstein, R. P. Lisak, L. W. Myers, H. S. Panitch, J. W. Rose, and R. B. Schiffer. Copolymer 1 reduces relapse rate and improves disability in relapsing-remitting multiple sclerosis: results of a phase III multicenter, double-blind placebo-controlled trial. The Copolymer 1 Multiple Sclerosis Study Group. *Neurology*, 45(7):1268–76, 1995.

A. E. Juedes, P. Hjelmstrom, C. M. Bergman, A. L. Neild, and N. H. Ruddle. Kinetics and cellular origin of cytokines in the central nervous system: insight into mechanisms of myelin oligodendrocyte glycoprotein-induced experimental autoimmune encephalomyelitis. *J Immunol*, 164(1):419–26, 2000.

E. A. Kabat, A. Wolf, and A. E. Bezer. The rapid production of acute disseminated encephalomyelitis in rhesus monkey by injection of heterologous and homologous brain tissue. *J Exp Med*, 85:117, 1947.

T. Kanda, T. Ariga, M. Yamawaki, H. Yoshino, X. B. Gu, and R. K. Yu. Glyco-

syltransferase activities in cultured endothelial cells of bovine brain microvascular origin. *Neurochem Res*, 22(4):463–6, 1997.

W. J. Karpus, N. W. Lukacs, B. L. McRae, R. M. Strieter, S. L. Kunkel, and S. D. Miller. An important role for the chemokine macrophage inflammatory protein-1 alpha in the pathogenesis of the T cell-mediated autoimmune disease, experimental autoimmune encephalomyelitis. *J Immunol*, 155(10):5003–5010, Nov 1995.

W. J. Karpus and R. M. Ransohoff. Chemokine regulation of experimental autoimmune encephalomyelitis: temporal and spatial expression patterns govern disease pathogenesis. *J Immunol*, 161(6):2667–71, 1998.

M. Kashiwazaki, T. Tanaka, H. Kanda, Y. Ebisuno, D. Izawa, N. Fukuma, N. Akimitsu, K. Sekimizu, M. Monden, and M. Miyasaka. A high endothelial venule-expressing promiscuous chemokine receptor DARC can bind inflammatory, but not lymphoid, chemokines and is dispensable for lymphocyte homing under physiological conditions. *Int Immunol*, 15(10):1219–27, 2003.

H. R. Katz, A. C. Benson, and K. F. Austen. Activation- and phorbol ester-stimulated phosphorylation of a plasma membrane glycoprotein antigen expressed on mouse IL-3-dependent mast cells and serosal mast cells. *J Immunol*, 142(3): 919–26, 1989.

G. S. Kelner, J. Kennedy, K. B. Bacon, S. Kleyensteuber, D. A. Largaespada, N. A. Jenkins, N. G. Copeland, J. F. Bazan, K. W. Moore, T. J. Schall, and et al. Lymphotactin: a cytokine that represents a new class of chemokine. *Science*, 266 (5189):1395–1399, Nov 1994.

K. J. Kennedy, R. M. Strieter, S. L. Kunkel, N. W. Lukacs, and W. J. Karpus. Acute and relapsing experimental autoimmune encephalomyelitis are regulated by differential expression of the CC chemokines macrophage inflammatory protein-1alpha and monocyte chemotactic protein-1. *J Neuroimmunol*, 92(1-2):98–108, Dec 1998.

F. Kiefer, S. A. Courtneidge, and E. F. Wagner. Oncogenic properties of the middle T antigens of polyomaviruses. *Adv Cancer Res*, 64:125–57, 1994.

E. S. Kleinerman, R. Zicht, P. S. Sarin, R. C. Gallo, and I. J. Fidler. Constitutive production and release of a lymphokine with macrophage-activating factor activity distinct from gamma-interferon by a human T-cell leukemia virus-positive cell line. *Cancer Res*, 44(10):4470–5, 1984.

K. Kojima, T. Berger, H. Lassmann, D. Hinze-Selch, Y. Zhang, J. Gehrmann, K. Reske, H. Wekerle, and C. Linington. Experimental autoimmune panencephalitis and uveoretinitis transferred to the Lewis rat by T lymphocytes specific for the S100 beta molecule, a calcium binding protein of astroglia. *J Exp Med*, 180 (3):817–29, 1994.

V. K. Kuchroo, C. A. Martin, J. M. Greer, S. T. Ju, R. A. Sobel, and M. E. Dorf. Cytokines and adhesion molecules contribute to the ability of myelin proteolipid protein-specific T cell clones to mediate experimental allergic encephalomyelitis. *J Immunol*, 151(8):4371–82, 1993.

P. Kuna, S. R. Reddigari, T. J. Schall, D. Rucinski, M. Y. Viksman, and A. P. Kaplan. RANTES, a monocyte and T lymphocyte chemotactic cytokine releases histamine from human basophils. *J Immunol*, 149(2):636–642, Jul 1992.

R. H. Laatsch, M. W. Kies, S. Gordon, and E. C. Alvord. The encephalitogenic activity of myelin isolated by ultracentrifugation. *J Exp Med*, 115:777, 1962.

L. Labrada, X. H. Liang, W. Zheng, C. Johnston, and B. Levine. Age-dependent resistance to lethal alphavirus encephalitis in mice: analysis of gene expression in the central nervous system and identification of a novel interferon-inducible protective gene, mouse ISG12. *J Virol*, 76(22):11688–703, 2002.

J. J. Lafaille, F. V. Keere, A. L. Hsu, J. L. Baron, W. Haas, C. S. Raine, and S. Tonegawa. Myelin basic protein-specific T helper 2 (Th2) cells cause experimental autoimmune encephalomyelitis in immunodeficient hosts rather than protect them from the disease. *J Exp Med*, 186(2):307–12, 1997.

M. Laschinger and B. Engelhardt. Interaction of alpha4-integrin with VCAM-1 is involved in adhesion of encephalitogenic T cell blasts to brain endothelium but not in their transendothelial migration in vitro. *J Neuroimmunol*, 102(1):32–43, 2000.

M. Laschinger, P. Vajkoczy, and B. Engelhardt. Encephalitogenic T cells use LFA-1 for transendothelial migration but not during capture and initial adhesion strengthening in healthy spinal cord microvessels in vivo. *Eur J Immunol*, 32 (12):3598–606, 2002.

G. Lennon, C. Auffray, M. Polymeropoulos, and M. B. Soares. The I.M.A.G.E. Consortium: an integrated molecular analysis of genomes and their expression. *Genomics*, 33(1):151–2, 1996.

S. Levine. Hyperacute, neutrophilic, and localized forms of experimental allergic encephalomyelitis: a review. *Acta Neuropathol (Berl)*, 28(3):179–189, 1974.

K. Ley and P. Gaehtgens. Endothelial, not hemodynamic, differences are responsible for preferential leukocyte rolling in rat mesenteric venules. *Circ Res*, 69(4):1034–41, 1991.

K. G. Lim, H. C. Wan, P. T. Bozza, M. B. Resnick, D. T. Wong, W. W. Cruikshank, H. Kornfeld, D. M. Center, and P. F. Weller. Human eosinophils elaborate the lymphocyte chemoattractants. IL-16 (lymphocyte chemoattractant factor) and RANTES. *J Immunol*, 156(7):2566–2570, Apr 1996.

P. Lindahl, B. R. Johansson, P. Leveen, and C. Betsholtz. Pericyte loss and microaneurysm formation in PDGF-B-deficient mice. *Science*, 277(5323):242–5, 1997.

C. Linington, T. Berger, L. Perry, S. Weerth, D. Hinze-Selch, Y. Zhang, H. C. Lu, H. Lassmann, and H. Wekerle. T cells specific for the myelin oligodendrocyte glycoprotein mediate an unusual autoimmune inflammatory response in the central nervous system. *Eur J Immunol*, 23(6):1364–72, 1993.

G. Liu, A. E. Loraine, R. Shigeta, M. Cline, J. Cheng, V. Valmeekam, S. Sun, D. Kulp, and M. A. Siani-Rose. NetAffx: Affymetrix probesets and annotations. *Nucleic Acids Res*, 31(1):82–6, 2003.

K. R. Loeb and A. L. Haas. The interferon-inducible 15-kDa ubiquitin homolog conjugates to intracellular proteins. *J Biol Chem*, 267(11):7806–13, 1992.

M. Loetscher, B. Gerber, P. Loetscher, S. A. Jones, L. Piali, I. Clark-Lewis, M. Baggiolini, and B. Moser. Chemokine receptor specific for IP10 and mig: structure,

function, and expression in activated T-lymphocytes. *J Exp Med*, 184(3):963–969, Sep 1996.

H. Luo, A. Chaudhuri, V. Zbrzezna, Y. He, and A. O. Pogo. Deletion of the murine Duffy gene (Dfy) reveals that the Duffy receptor is functionally redundant. *Mol Cell Biol*, 20(9):3097–101, 2000.

H. Luo, A. Chaudhuri, V. Zbrzezna, Y. He, and A. O. Pogo. Author's Correction: Deletion of the murine Duffy gene (Dfy) reveals that the Duffy receptor is functionally redundant. *Mol Cell Biol*, 23(8):3030, 2003.

A. D. Luster, J. C. Unkeless, and J. V. Ravetch. Gamma-interferon transcriptionally regulates an early-response gene containing homology to platelet proteins. *Nature*, 315(6021):672–676, Jun 1985.

S. A. Luther, H. L. Tang, P. L. Hyman, A. G. Farr, and J. G. Cyster. Coexpression of the chemokines ELC and SLC by T zone stromal cells and deletion of the ELC gene in the plt/plt mouse. *Proc Natl Acad Sci U S A*, 97(23):12694–9, 2000.

M. P. Malakhov, K. I. Kim, O. A. Malakhova, B. S. Jacobs, E. C. Borden, and D. E. Zhang. High-throughput immunoblotting. Ubiquitiin-like protein ISG15 modifies key regulators of signal transduction. *J Biol Chem*, 278(19):16608–13, 2003.

O. A. Malakhova, M. Yan, M. P. Malakhov, Y. Yuan, K. J. Ritchie, K. I. Kim, L. F. Peterson, K. Shuai, and D. E. Zhang. Protein ISGylation modulates the JAK-STAT signaling pathway. *Genes Dev*, 17(4):455–60, 2003.

B. A. Mannion, F. Berditchevski, S. K. Kraeft, L. B. Chen, and M. E. Hemler. Transmembrane-4 superfamily proteins CD81 (TAPA-1), CD82, CD63, and CD53 specifically associated with integrin alpha 4 beta 1 (CD49d/CD29). *J Immunol*, 157(5):2039–47, 1996.

D. Markowitz, S. Goff, and A. Bank. A safe packaging line for gene transfer: separating viral genes on two different plasmids. *J Virol*, 62(4):1120–4, 1988.

R. Martin and H. F. McFarland. Immunological aspects of experimental allergic encephalomyelitis and multiple sclerosis. *Crit Rev Clin Lab Sci*, 32(2):121–82, 1995.

T. Matsumoto and L. Claesson-Welsh. VEGF receptor signal transduction. *Sci STKE*, 2001(112):RE21, 2001.

P. B. Medawar. Immunity to homologous grafted skin. III. Fate of skin homografts transplanted to brain, to subcutaneous tissue and to anterior chamber of the eye. *Br J Exp Pathol*, 29(58):69, 1948.

I. Mendoza-Lujambio, P. Burfeind, C. Dixkens, A. Meinhardt, S. Hoyer-Fender, W. Engel, and J. Neesen. The Hook1 gene is non-functional in the abnormal spermatozoon head shape (azh) mutant mouse. *Hum Mol Genet*, 11(14):1647–58, 2002.

J. Middleton, S. Neil, J. Wintle, I. Clark-Lewis, H. Moore, C. Lam, M. Auer, E. Hub, and A. Rot. Transcytosis and surface presentation of IL-8 by venular endothelial cells. *Cell*, 91(3):385–95, 1997.

J. Middleton, A. M. Patterson, L. Gardner, C. Schmutz, and B. A. Ashton. Leukocyte extravasation: chemokine transport and presentation by the endothelium. *Blood*, 100(12):3853–60, 2002.

B. Millauer, S. Wizigmann-Voos, H. Schnurch, R. Martinez, N. P. Moller, W. Risau, and A. Ullrich. High affinity VEGF binding and developmental expression suggest Flk-1 as a major regulator of vasculogenesis and angiogenesis. *Cell*, 72(6):835–46, 1993.

D. H. Miller, O. A. Khan, W. A. Sheremata, L. D. Blumhardt, G. P. Rice, M. A. Libonati, A. J. Willmer-Hulme, C. M. Dalton, K. A. Miszkiel, and P. W. O'Connor. A controlled trial of natalizumab for relapsing multiple sclerosis. *N Engl J Med*, 348(1):15–23, 2003.

R. Miyagishi, S. Kikuchi, C. Takayama, Y. Inoue, and K. Tashiro. Identification of cell types producing RANTES, MIP-1 alpha and MIP-1 beta in rat experimental autoimmune encephalomyelitis by in situ hybridization. *J Neuroimmunol*, 77(1): 17–26, Jul 1997.

K. Morita, M. Furuse, K. Fujimoto, and S. Tsukita. Claudin multigene family encoding four-transmembrane domain protein components of tight junction strands. *Proc Natl Acad Sci U S A*, 96(2):511–6, 1999.

B. Moser, I. Clark-Lewis, R. Zwahlen, and M. Baggiolini. Neutrophil-activating properties of the melanoma growth-stimulatory activity. *J Exp Med*, 171(5):1797–1802, May 1990.

B. Moser and P. Loetscher. Lymphocyte traffic control by chemokines. *Nat Immunol*, 2(2):123–8, 2001.

C. M'Rini, G. Cheng, C. Schweitzer, L. L. Cavanagh, R. T. Palframan, T. R. Mempel, R. A. Warnock, J. B. Lowe, E. J. Quackenbush, and U. H. von Andrian. A novel endothelial L-selectin ligand activity in lymph node medulla that is regulated by alpha(1,3)-fucosyltransferase-IV. *J Exp Med*, 198(9):1301–12, 2003.

H. Nakano, T. Tamura, T. Yoshimoto, H. Yagita, M. Miyasaka, E. C. Butcher, H. Nariuchi, T. Kakiuchi, and A. Matsuzawa. Genetic defect in T lymphocyte-specific homing into peripheral lymph nodes. *Eur J Immunol*, 27(1):215–21, 1997.

D. R. Natale and A. J. Watson. Rac-1 and IQGAP are potential regulators of E-cadherin-catenin interactions during murine preimplantation development. *Gene Expr Patterns*, 2(1-2):17–22, 2002.

G. Neufeld, O. Kessler, and Y. Herzog. The interaction of Neuropilin-1 and Neuropilin-2 with tyrosine-kinase receptors for VEGF. *Adv Exp Med Biol*, 515:81–90, 2002.

V. N. Ngo, H. Korner, M. D. Gunn, K. N. Schmidt, D. S. Riminton, M. D. Cooper, J. L. Browning, J. D. Sedgwick, and J. G. Cyster. Lymphotoxin alpha/beta and tumor necrosis factor are required for stromal cell expression of homing chemokines in B and T cell areas of the spleen. *J Exp Med*, 189(2):403–12, 1999.

V. N. Ngo, H. L. Tang, and J. G. Cyster. Epstein-Barr virus-induced molecule 1 ligand chemokine is expressed by dendritic cells in lymphoid tissues and strongly attracts naive T cells and activated B cells. *J Exp Med*, 188(1):181–91, 1998.

B. Nico, F. Quondamatteo, R. Herken, T. Blumchen, G. Defazio, M. Giorelli, P. Livrea, A. Marzullo, G. Russo, D. Ribatti, and L. Roncali. Interferon beta-1a prevents the effects of lipopolysaccharide on embryonic brain microvessels. *Brain Res Dev Brain Res*, 119(2):231–42, 2000.

T. Nitta, M. Hata, S. Gotoh, Y. Seo, H. Sasaki, N. Hashimoto, M. Furuse, and S. Tsukita. Size-selective loosening of the blood-brain barrier in claudin-5-deficient mice. *J Cell Biol*, 161(3):653–60, 2003.

Y. Okazaki, M. Furuno, T. Kasukawa, J. Adachi, H. Bono, S. Kondo, I. Nikaido, N. Osato, R. Saito, H. Suzuki, I. Yamanaka, H. Kiyosawa, K. Yagi, Y. Tomaru, Y. Hasegawa, A. Nogami, C. Schonbach, T. Gojobori, R. Baldarelli, D. P. Hill, C. Bult, D. A. Hume, J. Quackenbush, L. M. Schriml, A. Kanapin, H. Matsuda, S. Batalov, K. W. Beisel, J. A. Blake, D. Bradt, V. Brusic, C. Chothia, L. E. Corbani, S. Cousins, E. Dalla, T. A. Dragani, C. F. Fletcher, A. Forrest, K. S. Frazer, T. Gaasterland, M. Gariboldi, C. Gissi, A. Godzik, J. Gough, S. Grimmond, S. Gustincich, N. Hirokawa, I. J. Jackson, E. D. Jarvis, A. Kanai, H. Kawaji, Y. Kawasawa, R. M. Kedzierski, B. L. King, A. Konagaya, I. V. Kurochkin, Y. Lee, B. Lenhard, P. A. Lyons, D. R. Maglott, L. Maltais, L. Marchionni, L. McKenzie, H. Miki, T. Nagashima, K. Numata, T. Okido, W. J. Pavan, G. Pertea, G. Pesole, N. Petrovsky, R. Pillai, J. U. Pontius, D. Qi, S. Ramachandran, T. Ravasi, J. C. Reed, D. J. Reed, J. Reid, B. Z. Ring, M. Ringwald, A. Sandelin, C. Schneider, C. A. Semple, M. Setou, K. Shimada, R. Sultana, Y. Takenaka, M. S. Taylor, R. D. Teasdale, M. Tomita, R. Verardo, L. Wagner, C. Wahlestedt, Y. Wang, Y. Watanabe, C. Wells, L. G. Wilming, A. Wynshaw-Boris, M. Yanagisawa, et al. Analysis of the mouse transcriptome based on functional annotation of 60,770 full-length cDNAs. *Nature*, 420(6915):563–73, 2002.

A. Orlofsky, M. S. Berger, and M. B. Prystowsky. Novel expression pattern of a new member of the MIP-1 family of cytokine-like genes. *Cell Regul*, 2(5):403–412, May 1991.

A. Orlofsky, E. Y. Lin, and M. B. Prystowsky. Selective induction of the beta chemokine C10 by IL-4 in mouse macrophages. *J Immunol*, 152(10):5084–91, 1994.

M. Owhashi, H. Arita, and N. Hayai. Identification of a novel eosinophil chemotactic cytokine (ECF-L) as a chitinase family protein. *J Biol Chem*, 275(2):1279–86, 2000.

Y. Pan, C. Lloyd, H. Zhou, S. Dolich, J. Deeds, J. A. Gonzalo, J. Vath, M. Gosselin,

J. Ma, B. Dussault, E. Woolf, G. Alperin, J. Culpepper, J. C. Gutierrez-Ramos, and D. Gearing. Neurotactin, a membrane-anchored chemokine upregulated in brain inflammation. *Nature*, 387(6633):611–617, Jun 1997.

R. L. Parr, L. Fung, J. Reneker, N. Myers-Mason, J. L. Leibowitz, and G. Levy. Association of mouse fibrinogen-like protein with murine hepatitis virus-induced prothrombinase activity. *J Virol*, 69(8):5033–8, 1995.

L. Pasteur. Methode pour prevenir la rage apres morsure. *CR Acad Sci*, 101:765–774, 1885.

P. Y. Paterson. Transfer of allergic encephalomyelitis in rats by means of lymph node cells. *J Exp Med*, 111:119, 1960.

A. M. Patterson, H. Siddall, G. Chamberlain, L. Gardner, and J. Middleton. Expression of the duffy antigen/receptor for chemokines (DARC) by the inflamed synovial endothelium. *J Pathol*, 197(1):108–16, 2002.

S. C. Peiper, Z. X. Wang, K. Neote, A. W. Martin, H. J. Showell, M. J. Conklyn, K. Ogborne, T. J. Hadley, Z. H. Lu, J. Hesselgesser, and et al. The Duffy antigen/receptor for chemokines (DARC) is expressed in endothelial cells of Duffy negative individuals who lack the erythrocyte receptor. *J Exp Med*, 181(4):1311–7, 1995.

G. G. Pendl, C. Robert, M. Steinert, R. Thanos, R. Eytner, E. Borges, M. K. Wild, J. B. Lowe, R. C. Fuhlbrigge, T. S. Kupper, D. Vestweber, and S. Grabbe. Immature mouse dendritic cells enter inflamed tissue, a process that requires E- and P-selectin, but not P-selectin glycoprotein ligand 1. *Blood*, 99(3):946–56, 2002.

M. Pizza, A. Covacci, A. Bartoloni, M. Perugini, L. Nencioni, M. T. De Magistris, L. Villa, D. Nucci, R. Manetti, M. Bugnoli, F. Giovannoni, R. Olivieri, J. T. Barbieri, H. Sato, and R. Rappuoli. Mutants of pertussis toxin suitable for vaccine development. *Science*, 246(4929):497–500, 1989.

C. M. Poser. Notes on the pathogenesis of multiple sclerosis. *Clin Neurosci*, 2(3-4):258–65, 1994.

A. E. Proudfoot, T. M. Handel, Z. Johnson, E. K. Lau, P. LiWang, I. Clark-Lewis, F. Borlat, T. N. Wells, and M. H. Kosco-Vilbois. Glycosaminoglycan binding and oligomerization are essential for the in vivo activity of certain chemokines. *Proc Natl Acad Sci U S A*, 100(4):1885–90, 2003.

K. Rajarathnam, B. D. Sykes, C. M. Kay, B. Dewald, T. Geiser, M. Baggiolini, and I. Clark-Lewis. Neutrophil activation by monomeric interleukin-8. *Science*, 264 (5155):90–92, Apr 1994.

R. M. Ransohoff, T. A. Hamilton, M. Tani, M. H. Stoler, H. E. Shick, J. A. Major, M. L. Estes, D. M. Thomas, and V. K. Tuohy. Astrocyte expression of mRNA encoding cytokines IP-10 and JE/MCP-1 in experimental autoimmune encephalomyelitis. *Faseb J*, 7(6):592–600, 1993.

A. D. Recklies, C. White, and H. Ling. The chitinase 3-like protein human cartilage glycoprotein 39 (HC-gp39) stimulates proliferation of human connective-tissue cells and activates both extracellular signal-regulated kinase- and protein kinase B-mediated signalling pathways. *Biochem J*, 365(Pt 1):119–26, 2002.

T. S. Reese and M. J. Karnovsky. Fine structural localization of a blood-brain barrier to exogenous peroxidase. *J Cell Biol*, 34(1):207–217, Jul 1967.

Y. Reiss, G. Hoch, U. Deutsch, and B. Engelhardt. T cell interaction with ICAM-1-deficient endothelium in vitro: essential role for ICAM-1 and ICAM-2 in transendothelial migration of T cells. *Eur J Immunol*, 28(10):3086–99, 1998.

E. Rieske, M. B. Graeber, W. Tetzlaff, A. Czlonkowska, W. J. Streit, and G. W. Kreutzberg. Microglia and microglia-derived brain macrophages in culture: generation from axotomized rat facial nuclei, identification and characterization in vitro. *Brain Res*, 492(1-2):1–14, Jul 1989.

W. Risau, B. Engelhardt, and H. Wekerle. Immune function of the blood-brain barrier: incomplete presentation of protein (auto-)antigens by rat brain microvascular endothelium in vitro. *J Cell Biol*, 110(5):1757–66, 1990.

W. Risau and H. Wolburg. Development of the blood-brain barrier. *Trends Neurosci*, 13(5):174–178, May 1990.

T. M. Rivers, D. H. Sprunt, and G. P. Berry. Observations on attempts to produce acute disseminated encephalomyelitis in monkeys. *J Exp Med*, 58:39, 1933.

C. Robert, R. C. Fuhlbrigge, J. D. Kieffer, S. Ayehunie, R. O. Hynes, G. Cheng, S. Grabbe, U. H. von Andrian, and T. S. Kupper. Interaction of dendritic cells with skin endothelium: A new perspective on immunosurveillance. *J Exp Med*, 189(4):627–36, 1999.

R. K. Rohnelt, G. Hoch, Y. Reiss, and B. Engelhardt. Immunosurveillance modelled in vitro: naive and memory T cells spontaneously migrate across unstimulated microvascular endothelium. *Int Immunol*, 9(3):435–50, 1997.

S. Rojo, D. N. Burshtyn, E. O. Long, and N. Wagtmann. Type I transmembrane receptor with inhibitory function in mouse mast cells and NK cells. *J Immunol*, 158(1):9–12, 1997.

B. J. Rollins, A. Walz, and M. Baggiolini. Recombinant human MCP-1/JE induces chemotaxis, calcium flux, and the respiratory burst in human monocytes. *Blood*, 78(4):1112–1116, Aug 1991.

D. Ron and J. F. Habener. CHOP, a novel developmentally regulated nuclear protein that dimerizes with transcription factors C/EBP and LAP and functions as a dominant-negative inhibitor of gene transcription. *Genes Dev*, 6(3):439–53, 1992.

D. Rossi and A. Zlotnik. The biology of chemokines and their receptors. *Annu Rev Immunol*, 18:217–42, 2000.

A. Rot, M. Krieger, T. Brunner, S. C. Bischoff, T. J. Schall, and C. A. Dahinden. RANTES and macrophage inflammatory protein 1 alpha induce the migration and activation of normal human eosinophil granulocytes. *J Exp Med*, 176(6): 1489–1495, Dec 1992.

S. J. Roth, M. W. Carr, and T. A. Springer. C-C chemokines, but not the C-X-C chemokines interleukin-8 and interferon-gamma inducible protein-10, stimulate transendothelial chemotaxis of T lymphocytes. *Eur J Immunol*, 25(12):3482–3488, Dec 1995.

J. B. Rottman, A. J. Slavin, R. Silva, H. L. Weiner, C. G. Gerard, and W. W. Hancock. Leukocyte recruitment during onset of experimental allergic encephalomyelitis is CCR1 dependent. *Eur J Immunol*, 30(8):2372–7, 2000.

F. Sallusto, C. R. Mackay, and A. Lanzavecchia. Selective expression of the eotaxin receptor CCR3 by human T helper 2 cells. *Science*, 277(5334):2005–7, 1997.

F. Sallusto, C. R. Mackay, and A. Lanzavecchia. The role of chemokine receptors in primary, effector, and memory immune responses. *Annu Rev Immunol*, 18: 593–620, 2000.

F. Sanger, S. Nicklen, and A. R. Coulson. DNA sequencing with chain-terminating inhibitors. *Proc Natl Acad Sci U S A*, 74(12):5463–7, 1977.

H. Schagger and G. von Jagow. Tricine-sodium dodecyl sulfate-polyacrylamide gel electrophoresis for the separation of proteins in the range from 1 to 100 kDa. *Anal Biochem*, 166(2):368–79, 1987.

T. J. Schall, J. Jongstra, B. J. Dyer, J. Jorgensen, C. Clayberger, M. M. Davis, and A. M. Krensky. A human T cell-specific molecule is a member of a new gene family. *J Immunol*, 141(3):1018–1025, Aug 1988.

C. Schaniel, E. Pardali, F. Sallusto, M. Speletas, C. Ruedl, T. Shimizu, T. Seidl, J. Andersson, F. Melchers, A. G. Rolink, and P. Sideras. Activated murine B lymphocytes and dendritic cells produce a novel CC chemokine which acts selectively on activated T cells. *J Exp Med*, 188(3):451–463, Aug 1998.

C. Schaniel, F. Sallusto, C. Ruedl, P. Sideras, F. Melchers, and A. G. Rolink. Three chemokines with potential functions in T lymphocyte-independent and -dependent B lymphocyte stimulation. *Eur J Immunol*, 29(9):2934–47, 1999a.

C. Schaniel, F. Sallusto, P. Sideras, F. Melchers, and A. G. Rolink. A novel CC chemokine ABCD-1, produced by dendritic cells and activated B cells, exclusively attracts activated T lymphocytes. *Curr Top Microbiol Immunol*, 246:95–101, 1999b.

M. Schorpp-Kistner, Z. Q. Wang, P. Angel, and E. F. Wagner. JunB is essential for mammalian placentation. *Embo J*, 18(4):934–48, 1999.

J. M. Schroder, U. Mrowietz, E. Morita, and E. Christophers. Purification and partial biochemical characterization of a human monocyte-derived, neutrophil-activating peptide that lacks interleukin 1 activity. *J Immunol*, 139(10):3474–83, 1987.

J. M. Schroder, N. L. Persoon, and E. Christophers. Lipopolysaccharide-stimulated human monocytes secrete, apart from neutrophil-activating peptide 1/interleukin 8, a second neutrophil-activating protein. NH2-terminal amino acid sequence identity with melanoma growth stimulatory activity. *J Exp Med*, 171(4):1091–1100, Apr 1990.

V. H. Secor, W. E. Secor, C. A. Gutekunst, and M. A. Brown. Mast cells are essential for early onset and severe disease in a murine model of multiple sclerosis. *J Exp Med*, 191(5):813–22, 2000.

S. Segerer, H. Regele, K. M. Mac, R. Kain, J. P. Cartron, Y. Colin, D. Kerjaschki, and D. Schlondorff. The Duffy antigen receptor for chemokines is up-regulated during acute renal transplant rejection and crescentic glomerulonephritis. *Kidney Int*, 58(4):1546–56, 2000.

B. Sherry, P. Tekamp-Olson, C. Gallegos, D. Bauer, G. Davatelis, S. D. Wolpe, F. Masiarz, D. Coit, and A. Cerami. Resolution of the two components of macrophage inflammatory protein 1, and cloning and characterization of one of those components, macrophage inflammatory protein 1 beta. *J Exp Med*, 168(6): 2251–2259, Dec 1988.

W. A. Sibley, C. R. Bamford, and K. Clark. Clinical viral infections and multiple sclerosis. *Lancet*, 1(8441):1313–5, 1985.

D. E. Sims. The pericyte — a review. *Tissue Cell*, 18(2):153–74, 1986.

J. T. Siveke and A. Hamann. T helper 1 and T helper 2 cells respond differentially to chemokines. *J Immunol*, 160(2):550–554, Jan 1998.

P. K. Smith, R. I. Krohn, G. T. Hermanson, A. K. Mallia, F. H. Gartner, M. D. Provenzano, E. K. Fujimoto, N. M. Goeke, B. J. Olson, and D. C. Klenk. Measurement of protein using bicinchoninic acid. *Anal Biochem*, 150(1):76–85, 1985.

H. Soto, W. Wang, R. M. Strieter, N. G. Copeland, D. J. Gilbert, N. A. Jenkins, J. Hedrick, and A. Zlotnik. The CC chemokine 6Ckine binds the CXC chemokine receptor CXCR3. *Proc Natl Acad Sci U S A*, 95(14):8205–10, 1998.

T. Springer, G. Galfre, D. S. Secher, and C. Milstein. Monoclonal xenogeneic antibodies to murine cell surface antigens: identification of novel leukocyte differentiation antigens. *Eur J Immunol*, 8(8):539–51, 1978.

T. A. Springer. Traffic signals for lymphocyte recirculation and leukocyte emigration: the multistep paradigm. *Cell*, 76(2):301–14, 1994.

Jr. Stamper, H. B. and J. J. Woodruff. Lymphocyte homing into lymph nodes: in vitro demonstration of the selective affinity of recirculating lymphocytes for high-endothelial venules. *J Exp Med*, 144(3):828–33, 1976.

B. J. Steffen, G. Breier, E. C. Butcher, M. Schulz, and B. Engelhardt. ICAM-1, VCAM-1, and MAdCAM-1 are expressed on choroid plexus epithelium but not endothelium and mediate binding of lymphocytes in vitro. *Am J Pathol*, 148(6): 1819–38, 1996.

B. J. Steffen, E. C. Butcher, and B. Engelhardt. Evidence for involvement of ICAM-1 and VCAM-1 in lymphocyte interaction with endothelium in experimental autoimmune encephalomyelitis in the central nervous system in the SJL/J mouse. *Am J Pathol*, 145(1):189–201, Jul 1994.

P. A. Stewart and M. J. Wiley. Developing nervous tissue induces formation of blood-brain barrier characteristics in invading endothelial cells: a study using quail–chick transplantation chimeras. *Dev Biol*, 84(1):183–192, May 1981.

J. W. Stoop, B. J. Zegers, G. F. Hendrickx, L. H. van Heukelom, G. E. Staal, P. K. de Bree, S. K. Wadman, and R. E. Ballieux. Purine nucleoside phosphorylase deficiency associated with selective cellular immunodeficiency. *N Engl J Med*, 296 (12):651–5, 1977.

P. R. Streeter, B. T. Rouse, and E. C. Butcher. Immunohistologic and functional characterization of a vascular addressin involved in lymphocyte homing into peripheral lymph nodes. *J Cell Biol*, 107(5):1853–62, 1988.

J. Takagi, B. M. Petre, T. Walz, and T. A. Springer. Global conformational rearrangements in integrin extracellular domains in outside-in and inside-out signaling. *Cell*, 110(5):599–11, 2002.

S. Takemura, A. Braun, C. Crowson, P. J. Kurtin, R. H. Cofield, W. M. O'Fallon, J. J. Goronzy, and C. M. Weyand. Lymphoid neogenesis in rheumatoid synovitis. *J Immunol*, 167(2):1072–80, 2001.

M. B. Tanzola, M. Robbie-Ryan, C. A. Gutekunst, and M. A. Brown. Mast cells exert effects outside the central nervous system to influence experimental allergic encephalomyelitis disease course. *J Immunol*, 171(8):4385–91, 2003.

K. Tashiro, H. Tada, R. Heilker, M. Shirozu, T. Nakano, and T. Honjo. Signal sequence trap: a cloning strategy for secreted proteins and type I membrane proteins. *Science*, 261(5121):600–603, Jul 1993.

D. D. Taub, A. R. Lloyd, K. Conlon, J. M. Wang, J. R. Ortaldo, A. Harada, K. Matsushima, D. J. Kelvin, and J. J. Oppenheim. Recombinant human interferon-inducible protein 10 is a chemoattractant for human monocytes and T lymphocytes and promotes T cell adhesion to endothelial cells. *J Exp Med*, 177(6): 1809–1814, Jun 1993.

D. D. Taub, T. J. Sayers, C. R. Carter, and J. R. Ortaldo. Alpha and beta chemokines induce NK cell migration and enhance NK-mediated cytolysis. *J Immunol*, 155(8):3877–3888, Oct 1995.

I. Teige, A. Treschow, A. Teige, R. Mattsson, V. Navikas, T. Leanderson, R. Holmdahl, and S. Issazadeh-Navikas. IFN-beta Gene Deletion Leads to Augmented and Chronic Demyelinating Experimental Autoimmune Encephalomyelitis. *J Immunol*, 170(9):4776–84, 2003.

S. Timm, B. Titus, K. Bernd, and M. Barroso. The EF-hand Ca(2+)-binding protein p22 associates with microtubules in an N-myristoylation-dependent manner. *Mol Biol Cell*, 10(10):3473–88, 1999.

F. Tokuchi, M. Nishizawa, J. Nihei, K. Motoyama, K. Nagashima, and T. Tabira. Lymphokine production by encephalitogenic and non-encephalitogenic T-cell

clones reactive to the same antigenic determinant. *J Neuroimmunol*, 30(1):71–9, 1990.

E. H. Tran, W. A. Kuziel, and T. Owens. Induction of experimental autoimmune encephalomyelitis in C57BL/6 mice deficient in either the chemokine macrophage inflammatory protein-1alpha or its CCR5 receptor. *Eur J Immunol*, 30(5):1410–5, 2000.

R. Treisman, U. Novak, J. Favaloro, and R. Kamen. Transformation of rat cells by an altered polyoma virus genome expressing only the middle-T protein. *Nature*, 292(5824):595–600, 1981.

S. Tsukita and M. Furuse. Overcoming barriers in the study of tight junction functions: from occludin to claudin. *Genes Cells*, 3(9):569–573, Sep 1998.

V. K. Tuohy, Z. Lu, R. A. Sobel, R. A. Laursen, and M. B. Lees. Identification of an encephalitogenic determinant of myelin proteolipid protein for SJL mice. *J Immunol*, 142(5):1523–7, 1989.

P. Vajkoczy, M. Laschinger, and B. Engelhardt. Alpha4-integrin-VCAM-1 binding mediates G protein-independent capture of encephalitogenic T cell blasts to CNS white matter microvessels. *J Clin Invest*, 108(4):557–65, 2001.

A. J. Valente, D. T. Graves, C. E. Vialle-Valentin, R. Delgado, and C. J. Schwartz. Purification of a monocyte chemotactic factor secreted by nonhuman primate vascular cells in culture. *Biochemistry*, 27(11):4162–8, 1988.

A. van Zante, J. M. Gauguet, A. Bistrup, D. Tsay, U. H. vn Andrian, and S. D. Rosen. Lymphocyte-HEV interactions in lymph nodes of a sulfotransferase-deficient mouse. *J Exp Med*, 198(9):1289–300, 2003.

A. Vecchi, C. Garlanda, M. G. Lampugnani, M. Resnati, C. Matteucci, A. Stoppacciaro, H. Schnurch, W. Risau, L. Ruco, A. Mantovani, and et al. Monoclonal antibodies specific for endothelial cells of mouse blood vessels. Their application in the identification of adult and embryonic endothelium. *Eur J Cell Biol*, 63(2):247–54, 1994.

B. Volck, P. A. Price, J. S. Johansen, O. Sorensen, T. L. Benfield, H. J. Nielsen, J. Calafat, and N. Borregaard. YKL-40, a mammalian member of the chitinase family, is a matrix protein of specific granules in human neutrophils. *Proc Assoc Am Physicians*, 110(4):351–60, 1998.

U. H. Von Andrian, P. Hansell, J. D. Chambers, E. M. Berger, I. Torres Filho, E. C. Butcher, and K. E. Arfors. L-selectin function is required for beta 2-integrin-mediated neutrophil adhesion at physiological shear rates in vivo. *Am J Physiol*, 263(4 Pt 2):H1034–44, 1992.

E. F. Wagner and W. Risau. Oncogenes in the study of endothelial cell growth and differentiation. *Semin Cancer Biol*, 5(2):137–45, 1994.

A. Walz, P. Peveri, H. Aschauer, and M. Baggiolini. Purification and amino acid sequencing of NAF, a novel neutrophil-activating factor produced by monocytes. *Biochem Biophys Res Commun*, 149(2):755–761, Dec 1987.

R. A. Warnock, S. Askari, E. C. Butcher, and U. H. von Andrian. Molecular mechanisms of lymphocyte homing to peripheral lymph nodes. *J Exp Med*, 187(2): 205–16, 1998.

R. A. Warnock, J. J. Campbell, M. E. Dorf, A. Matsuzawa, L. M. McEvoy, and E. C. Butcher. The role of chemokines in the microenvironmental control of T versus B cell arrest in Peyer's patch high endothelial venules. *J Exp Med*, 191(1): 77–88, 2000.

H. Wekerle, K. Kojima, J. Lannes-Vieira, H. Lassmann, and C. Linington. Animal models. *Ann Neurol*, 36 Suppl:S47–53, 1994.

H. Wekerle, C. Linington, H. Lassmann, and R. Meyermann. Cellular immune reactivity within the CNS. *Trends Neurosci*, 9:271–277, 1986.

D. B. Wilde, P. Marrack, J. Kappler, D. P. Dialynas, and F. W. Fitch. Evidence implicating L3T4 in class II MHC antigen reactivity; monoclonal antibody GK1.5 (anti-L3T4a) blocks class II MHC antigen-specific proliferation, release of lymphokines, and binding by cloned murine helper T lymphocyte lines. *J Immunol*, 131(5):2178–83, 1983.

R. L. Williams, S. A. Courtneidge, and E. F. Wagner. Embryonic lethalities and endothelial tumors in chimeric mice expressing polyoma virus middle T oncogene. *Cell*, 52(1):121–31, 1988.

R. L. Williams, W. Risau, H. G. Zerwes, H. Drexler, A. Aguzzi, and E. F. Wagner. Endothelioma cells expressing the polyoma middle T oncogene induce hemangiomas by host cell recruitment. *Cell*, 57(6):1053–63, 1989.

H. Wolburg, J. Neuhaus, U. Kniesel, B. Krauss, E. M. Schmid, M. Ocalan, C. Farrell, and W. Risau. Modulation of tight junction structure in blood-brain barrier endothelial cells. Effects of tissue culture, second messengers and cocultured astrocytes. *J Cell Sci*, 107 (Pt 5):1347–57, 1994.

H. Wolburg, K. Wolburg-Buchholz, and B. Engelhardt. Involvement of tight junctions during transendothelial migration of mononuclear cells in experimental autoimmune encephalomyelitis. In B. Elger and U. Dirnagl, editors, *Ernst Schering Res. Foundation, Workshop 47*. Springer, Berlin Heidelberg, 2003 - in press -.

H. Wolburg, K. Wolburg-Buchholz, J. Kraus, G. Rascher-Eggstein, S. Liebner, S. Hamm, F. Duffner, E. H. Grote, W. Risau, and B. Engelhardt. Localization of claudin-3 in tight junctions of the blood-brain barrier is selectively lost during experimental autoimmune encephalomyelitis and human glioblastoma multiforme. *Acta Neuropathol (Berl)*, 105(6):586–92, 2003.

S. D. Wolpe, G. Davatelis, B. Sherry, B. Beutler, D. G. Hesse, H. T. Nguyen, L. L. Moldawer, C. F. Nathan, S. F. Lowry, and A. Cerami. Macrophages secrete a novel heparin-binding protein with inflammatory and neutrophil chemokinetic properties. *J Exp Med*, 167(2):570–581, Feb 1988.

H. Xu, J. K. Bickford, E. Luther, C. Carpenito, F. Takei, and T. A. Springer. Characterization of murine intercellular adhesion molecule-2. *J Immunol*, 156 (12):4909–14, 1996.

R. Yoshida, T. Imai, K. Hieshima, J. Kusuda, M. Baba, M. Kitaura, M. Nishimura, M. Kakizaki, H. Nomiyama, and O. Yoshie. Molecular cloning of a novel human CC chemokine EBI1-ligand chemokine that is a specific functional ligand for EBI1, CCR7. *J Biol Chem*, 272(21):13803–9, 1997.

T. Yoshimura, K. Matsushima, J. J. Oppenheim, and E. J. Leonard. Neutrophil chemotactic factor produced by lipopolysaccharide (LPS)-stimulated human blood mononuclear leukocytes: partial characterization and separation from interleukin 1 (IL 1). *J Immunol*, 139(3):788–793, Aug 1987.

L. Yuan, D. Moyon, L. Pardanaud, C. Breant, M. J. Karkkainen, K. Alitalo, and A. Eichmann. Abnormal lymphatic vessel development in neuropilin 2 mutant mice. *Development*, 129(20):4797–806, 2002.

S. S. Zamvil and L. Steinman. The T lymphocyte in experimental allergic encephalomyelitis. *Annu Rev Immunol*, 8:579–621, 1990.

J. P. Zappulla, M. Arock, L. T. Mars, and R. S. Liblau. Mast cells: new targets for multiple sclerosis therapy? *J Neuroimmunol*, 131(1-2):5–20, 2002.

L. Zeng, F. Fagotto, T. Zhang, W. Hsu, T. J. Vasicek, 3rd Perry, W. L., J. J. Lee, S. M. Tilghman, B. M. Gumbiner, and F. Costantini. The mouse Fused locus encodes Axin, an inhibitor of the Wnt signaling pathway that regulates embryonic axis formation. *Cell*, 90(1):181–92, 1997.

A. Zlotnik and O. Yoshie. Chemokines: a new classification system and their role in immunity. *Immunity*, 12(2):121–7, 2000.

B Summary

Migration of autoaggressive T cells across the blood-brain barrier (BBB) is critically involved in the initiation of multiple sclerosis (MS) and its animal model experimental autoimmune encephalomyelitis (EAE). The direct involvement of chemokines in this process was suggested by our recent observation that G-protein-mediated signaling is required to promote adhesion strengthening of encephalitogenic T cells on BBB endothelium *in vivo*. For chemokines to be involved in this process, they have to be either expressed by BBB endothelial cells themselves or would require a yet unknown transport mechanism from the central nervous system (CNS) parenchyma across the endothelial BBB to the luminal surface of the endothelial cells. To search for chemokines expressed by the endothelial BBB itself, *in situ* hybridizations and immunohistochemistry were performed and expression of the lymphoid chemokines CCL19 and CCL21 was found in venules surrounded by inflammatory cells. Their expression was paralleled by the presence of their common receptor CCR7 in inflammatory cells in brain and spinal cord sections of mice afflicted with EAE. Encephalitogenic T cells showed surface expression of CCR7 and the alternative receptor for CCL21, CXCR3. They specifically chemotaxed towards both CCL19 or CCL21 in a concentration dependent and pertussis toxin-sensitive manner comparable to naïve lymphocytes *in vitro*. Functional involvement of CCL19 and CCL21 in adhesion strengthening of encephalitogenic T lymphocytes was demonstrated by binding assays on frozen brain sections of mice afflicted with EAE *in vitro* and preliminary by intravital fluorescence videomicroscopy in spinal cord of healthy mice *in vivo*. The moderate effect observed suggests additional, potentially unknown chemokines to be involved in lymphocyte recruitment across the endothelial BBB into the immunoprivileged CNS. Such chemokines, receptors as well as unknown molecules were identified at the level of the endothelial BBB by oligonucleotide microarrays, subtractive suppression hybridization (SSH) and proteomics. Besides

the upregulation of expected genes and proteins described to be involved in leukocyte recruitment during EAE pathogenesis before, unexpected genes and proteins were identified. The latter included increased Duffy antigen / receptor for chemokines (DARC) expression suggesting its involvement in lymphocyte recruitment during EAE pathogenesis, which was proven as in DARC-deficient mice, disease onset was delayed, while clinical severity was increased. This may be explained by an ambiguous DARC function in EAE pathogenesis. Either endothelial cell expressed DARC "shuttles" chemokines to the luminal surface of the endothelial cells or erythrocyte expressed DARC removes chemokines by its "sink"-like function. This results in either increased or decreased chemokine concentrations accessible to encephalitogenic T lymphoblasts. Their encephalitogenicity was addressed by gene array analysis and SSH of encephalitogenic versus non-encephalitogenic T lymphoblasts identifying 79 differentially expressed genes.

Based on the results obtained during this thesis, we would like to suggest the lymphoid chemokines CCL19 and CCL21 to be critically involved in lymphocyte recruitment across the endothelial BBB during EAE pathogenesis, while the chemokine receptor DARC may provide a "shuttle" mechanism for inflammatory chemokines from the CNS parenchyma across the endothelial BBB to the luminal surface of the endothelial cells during EAE. A large number of additional genes and proteins was identified to be differentially expressed in either endothelial cells or T lymphoblasts pointing to new mechanisms involved in leukocyte trafficking across the BBB.

C Zusammenfassung

Die Wanderung autoaggressiver T-Zellen durch die Blut-Hirn-Schranke (BHS) ist am Ausbruch der Multiplen Sklerose (MS) und ihres Tiermodells, der Experimentellen Autoimmunen Enzephalomyelitis (EAE), entscheidend beteiligt. Unsere kürzlich gemachte Beobachtung, daß G Protein-vermittelte Signale für die Adhäsionsverstärkung enzephalitogener T-Zellen an BHS-Endothel *in vivo* benötigt werden, macht eine direkte Beteiligung von Chemokinen an diesem Vorgang wahrscheinlich. Um direkt an der Lymphozytenrekrutierung beteiligt zu sein, müssen Chemokine entweder von BHS-Endothelzellen exprimiert werden oder sie würden einen bisher unbekannten Transportmechanismus vom Parenchym des Zentralen Nervensystems (ZNS) durch die endotheliale BHS auf die luminale Oberfläche der Endothelzellen benötigen. Von der endothelialen BHS exprimierte Chemokine wurden mit Hilfe von *in situ* Hybridisierungs- und immunhistochemischen Methoden identifiziert, wodurch die Expression der lymphoiden Chemokine CCL19 und CCL21 in Venolen gezeigt wurde, die von inflammatorischen Zellen umgeben waren. Gleichzeitig wurde die Expression ihres gemeinsamen Rezeptors, CCR7, in inflammatorischen Zellen in Gehirn- und Rückenmarkgewebeschnitten an EAE erkrankter Mäuse detektiert. Enzephalitogene T-Zellen wiesen sich durch Oberflächenexpression von CCR7 und des alternativen Rezeptors für CCL21, CXCR3, aus. *In vitro* zeigten sie eine Konzentrations- und Pertussis Toxin-abhängige, chemotaktische Reaktion, die mit der naiver Lymphozyten vergleichbar war. Die funktionelle Beteiligung von CCL19 und CCL21 an der Adhäsionsverstärkung enzephalitogener T-Lymphozyten wurde *in vitro* durch Bindungsversuche auf Gefrierschnitten an EAE erkrankter Mäuse und *in vivo* durch vorläufige Ergebnisse intravitaler Fluoreszenzvideomikroskopie im Rückenmark gesunder Mäuse gezeigt. Die teilweise Hemmung der Bindung enzephalitogener T-Lymphoblasten, die beobachtet wurde, legt die Beteiligung weiterer, möglicherweise

unbekannter Chemokine an der Rekrutierung von Lymphozyten durch die BHS in das immunprivilegierte ZNS nahe. Derartige Chemokine, Rezeptoren, sowie weitere Moleküle wurden in BHS-Endothelzellen mit Hilfe von Oligonukleotid-Mikroarrays, subtraktiver-Unterdrückungshybridisierung und Proteomik Ansätzen identifiziert. Abgesehen von der verstärkten Expression von Genen und Proteinen, deren Einfluß auf die Leukozytenrekrutierung während des Krankheitsverlaufs der EAE bereits gezeigt wurde, wurden weitere Gene und Proteine identifiziert, deren Beteiligung am Krankheitsverlauf der EAE bisher nicht beschrieben war. Zu den letzteren gehörte der Duffy Antigen / Rezeptor für Chemokine (DARC), dessen Beteiligung an der Lymphozytenrekrutierung während des EAE Krankheitsverlaufs daher nahe liegt. Dies wurde mit Hilfe DARC-defizienter Mäuse bewiesen, da deren Krankheitsausbruch verzögert, aber die klinischen Symptome während der EAE verstärkt waren. Dies kann durch eine doppelte Funktion von DARC während des EAE Krankheitsverlaufs erklärt werden. Entweder transportiert auf Endothelzellen exprimiertes DARC Chemokine auf die luminale Seite der Endothelzellen („Pendelverkehr-Funktion") oder auf Erythrozyten exprimiertes DARC entfernt die Chemokine („Abfluß-Funktion"). Somit ergeben sich entweder erhöhte oder gesenkte Chemokinkonzentrationen, die für enzephalitogene T-Lymphozyten zugänglich sind. Deren Enzephalitogenität wurde mit Hilfe von Oligonukleotid-Mikroarrays und subtraktiver-Unterdrückungshybridisierung durch Vergleich enzephalitogener und nicht-enzephalitogener T-Lymphoblasten untersucht, wodurch 79 unterschiedlich exprimierte Gene identifiziert wurden.

Die in dieser Dissertation erhaltenen Ergebnisse legen nahe, daß die lymphoiden Chemokine CCL19 und CCL21 maßgeblich an der Lymphozytenrekrutierung durch die BHS während des EAE Krankheitsverlaufs beteiligt sind, während der Chemokinrezeptor DARC einen Transportmechanismus für inflammatorische Chemokine vom ZNS-Parenchym durch die endotheliale BHS auf die luminale Oberfläche der Endothelzellen während des EAE Krankheitsverlaufs darstellt. Weitere Gene und Proteine, die entweder in Endothelzellen oder T-Lymphoblasten unterschiedlich exprimiert wurden, weisen auf neue Mechanismen während der Leukozytenrekrutierung über die BHS hin.

D List of abbreviations

β-ME .... β-mercaptoethanol

3H-dT .... ^{3}H-deoxy thymidine

aa .... amino acid

ab .... antibody

aEAE .... active experimental autoimmune encephalomyelitis

AEC 3-amino-9-ethyl-carbazol

APC .... antigen presenting cell

ATP .... adenosine triphosphate

BBB .... blood-brain barrier

BCA .... bicinchoninic acid

BLAST ...... basic local alignment search tool

bp .... base pair

BPB .... bromphenol blue

BSA .... bovine serum albumine

CCD .... charged coupled device

cDNA .... copy desoxyribonucleic acid

CFA .... complete Freund's adjuvant

CHAPS .... 3-((3-cholamidopropyl)dimethylammonio)-1-
propanesulfonate

CNS .... central nervous system

CS .... calf serum

ConA .... concanavalin A

ConAS ...... concanavalin A supernatant

CTrG .... Cell Tracker Green

CTrO .... Cell Tracker Orange

CTP . . . .   cytidine triphosphate

depc . . . .   diethylpyrocarbonate

DMEM . . . . . .   Dulbecco's modified eagle medium

DMSO . . . . . .   dimethyl sulfoxide

dATP . . . .   deoxy-adenosine triphosphate

dCTP . . . .   deoxy-cytidine triphosphat

dGTP . . . .   deoxy-guanosine triphosphat

dTTP . . . .   deoxy-thymidine triphosphat

DNA . . . .   desoxyribonucleic acid

dNTPs . . . . . .   mixture of dATP, dCTP, dGTP, dTTP

DC . . . .   dendritic cells

DTT . . . .   dithiotreitol

EAE . . . .   experimental autoimmune encephalomyelitis

EDTA . . . .   ethylen-diamine-tetra-acetic acid

ESI-MS/MS .   electrospray ionization tandem mass spectrometry

EST . . . .   expressed sequence tag

FCS . . . .   fetal calf serum

FITC . . . .   fluorescein isothiocyanate

GFAP . . . .   glial fibrillary acidic protein

GSLI . . . .   *Griffonia simplicifolia* lectin I

GTP . . . .   guanosine triphosphate

HBSS . . . .   Hank's balanced salt solution

HEPES . . . . . .   4-(2-hydroxyethyl)-1-piperazineethanesulfonic acid

HEV . . . .   high endothelial venule

HRP . . . .   horseradish peroxidase

HTS . . . .   high-throughput sequencing

IEF . . . .   isoelectric focusing

IL-2 . . . .   interleukin-2

IPG . . . .   immobilized pH gradient

IPTG . . . .   isopropylthiogalactoside

IU . . . .   International Unit

LB . . . . Luria-Bertani

LPS . . . . lipopolysaccharide

MALII . . . . . . *Maackia amurensis* lectin II

MALDI . . . . . Matrix assisted laser desorption/ionization

MBP . . . . myelin basic protein

MHC . . . . major histocompatibility complex

MOG . . . . myelin oligodendrocytic glycoprotein

MOPS . . . . morpholinopropanesulphonic acid

MTX . . . . mutant pertussis toxin

MS . . . . multiple sclerosis

Mr . . . . molecular weight

mRNA . . . . . . messenger ribonucleic acid

NGS . . . . normal goat serum

NK cell . . . . . . Natural Killer cell

NMS . . . . normal mouse serum

NP . . . . neuropilin

NP40 . . . . nonidet P-40

NRbS . . . . normal rabbit serum

O/N . . . . over night

PAGE . . . . polyacrylamide gel electrophoresis

PBS . . . . phosphate buffered saline

PCI . . . . phenol:chloroform:isoamyl alcohol

PCR . . . . polymerase chain reaction

PE . . . . phycoerythrin

PEG 6000 . . . polyethylene glycol 6000

PFA . . . . paraformaldehyde

pI . . . . isoelectric point

PLP . . . . proteolipid protein

PMSF . . . . phenylmethylsulfonyl fluoride

PPD . . . . purified protein derivate from *Mycobacterium tuberculosis*

PTX . . . . pertussis toxin

pymT . . . .   polyoma middle T oncogene

RIPA . . . .   radio immuno precipitation assay

RPMI . . . .   Roswell Park Memorial Institute

RT . . . .   room temperature

rpm . . . .   rounds per minute

rzpd . . . .   Deutsches Ressourcenzentrum für Genomforschung GmbH,
                       Berlin, Germany

RNA . . . .   ribonucleic acid

SA . . . .   streptavidin

SA/HRP . . . .   streptavidin/horseradish peroxidase

SDS . . . .   sodiumdodecylsulfate

SNL . . . .   *Sambucus nigra* lectin

SSP . . . .   sample spot

Taq . . . .   *Thermophilus aquaticus*

tEAE . . . .   transfer experimental autoimmune encephalomyelitis

TBE . . . .   Tris-borate-EDTA

TESPA 3-aminopropyltriethoxysilane

TNF-α . . . . . .   tumor necrosis factor α

TOF-MS . . . .   time-of-flight mass spectrometry

Tris . . . .   Tris(hydroxymethyl)aminomethane

tRNA . . . .   transfer ribonucleic acid

TJ . . . .   tight junction

UTP . . . .   uraciltriphosphate

UTPαS . . . . . .   uraciltriphosphate-α-S

VEGF . . . .   vascular endothelial growth factor

wt . . . .   wildtype

X-gal 5-bromo-4-chloro-3-indolyl-beta-D-galactopyranoside

E List of figures

F List of tables

G Lebenslauf

	Carsten Alt
Geboren	20. November 1973 in Friedberg/Hessen, Deutschland
Staatsbürgerschaft	deutsch
Familienstand	ledig
Privatanschrift	Feldbergstrasse 5
	61200 Wölfersheim
	Tel.: 0 6036 982488
Dienstanschrift	Max-Planck Institut für Vaskuläre Biologie
	Abteilung für vaskuläre Zellbiologie
	c/o ZMBE
	Von-Esmarch-Strasse 56
	48149 Münster
	Tel.: 0 251 83 57179 (Büro)
	Tel.: 0 251 83 52224 (Labor)
	Fax.: 0 251 83 58616
	E-Mail: alt@mpi-muenster.mpg.de

1980 – 1983	Grundschule Södel
1983 – 1984	Mittelpunktschule Wölfersheim
1984 – 1993	Augustinerschule Friedberg
16.06.1993	Allgemeine Hochschulreife
1993 – 1994	Wehrdienst in Stadtallendorf

1994 – heute	Studium der Humanbiologie an der Philipps-Universität, Marburg
15.10.1996	Vordiplom in Humanbiologie
1998 – 1999	Diplomarbeit am Max-Planck Institut für physiologische und klinische Forschung / W. G. Kerckhoff Institut in Bad Nauheim unter Leitung von Prof. Dr. Werner Risau † / Prof. Dr. Britta Engelhardt
	Thema: "Die Rolle von Chemokinen bei der Rekrutierung von T-Lymphozyten durch die endotheliale Blut-Hirn-Schranke."
30.09.1999	Diplom in Humanbiologie
1999 – heute	Doktorarbeit am Max-Planck Institut für physiologische und klinische Forschung / W. G. Kerckhoff Institut, Bad Nauheim und Max-Planck Institut für vaskuläre Biologie, Münster unter Leitung von Prof. Dr. Werner Risau † / Prof. Dr. Dietmar Vestweber / Prof. Dr. Britta Engelhardt
	Thema: "Die Rolle von Chemokinen bei der Rekrutierung von Leukozyten durch die Blut-Hirn-Schranke."

H Akademische Lehrer

Meine akademischen Lehrer in Marburg waren die Damen und Herren:

Aurich, Beato, Braun, Clauss, Daut, Dressler, Elbel, Elsässer, Engelhardt, Feuser, Fruhstorfer, Garten, Habermehl, Hasilik, Hartmann, Heeg, Kern, Kindl, Kirchner, Klenk, Koolman, Lill, Löffler, Lührmann, Mazumdar, Müeller, Risau, Röhm, Schäfer, Schulz, Schwee, Seitz, Seitz, Steinmetz, Suske, Thomas, Voigt, von Löw, Weihe, Westphal.

I Danksagung

dieser Stelle mein Dank ausgesprochen.

Astra-Zeneca gilt mein Dank für die Unterstützung dieser Arbeit, insbesondere sei die konstruktive Zusammenarbeit mit Maria Anvret, Kristina Duvefelt, Anders Ericsson-Dahlstand, Bosse Franzén und Dan Sunnemark erwähnt.

Ebenso möchte ich mich bei Herrn Dr. Peter Vajkoczy für die gemeinsame Durchführung der intravitalmikroskopischen Versuche bedanken.

Herrn Dr. Urban Deutsch gilt mein Dank dafür, daß er stets ein offenes Ohr für Fragen hatte und mich an seinem schier unbegrenzten molekularbiologischem Wissen teilhaben ließ.

Herrn Dr. Hannes Drexler sei an dieser Stelle mein Dank dafür ausgesprochen, daß er immer bereit war, biochemische Fragen zu diskutieren und half, mögliche Lösungen zu finden.

Bei Herrn Dr. Friedemann Kiefer möchte ich mich für viele ertragreiche Diskussionen bedanken, insbesonders sei hier die Hilfe in RNA-präparativen Fragestellungen erwähnt.

Zu guter Letzt gilt mein Dank meinen Eltern, ohne deren Unterstützung es mir niemals möglich gewesen wäre, diese Arbeit durchzuführen.

J Ehrenwörtliche Erklärung

Ich erkläre ehrenwörtlich, daß ich die dem Fachbereich Medizin Marburg zur Promotionsprüfung eingereichte Arbeit mit dem Titel „Die Rolle von Chemokinen bei der Rekrutierung von Leukozyten durch die Blut-Hirn Schranke" in dem Max-Planck-Institut für klinische und physiologische Forschung / Kerckhoff-Institut, Bad Nauheim unter Leitung von Prof. Dr. Werner Risau † und dem Max-Planck-Institut für vaskuläre Biologie, Münster unter Leitung von Prof. Dr. Dietmar Vestweber mit Unterstützung durch Prof. Dr. Britta Engelhardt ohne sonstige Hilfe selbst durchgeführt und bei der Abfassung der Arbeit keine anderen als die in der Dissertation angeführten Hilfsmittel benutzt habe. Ich habe bisher an keinem in- und ausländischen Medizinischen Fachbereich ein Gesuch um Zulassung zur Promotion eingereicht noch die vorliegende oder eine andere Arbeit als Dissertation vorgelegt. Auszüge aus der vorliegenden Arbeit wurden, bzw. werden wie folgt veröffentlicht:

Original-Publikationen:

Alt, C. & Laschinger, M. & Engelhardt, B., 2002, „Functional expression of the lymphoid chemokines CCL19 (ELC) and CCL 21 (SLC) at the blood-brain barrier suggests their involvement in G-protein-dependent lymphocyte recruitment into the central nervous system during experimental autoimmune encephalomyelitis", Eur. J. Immunol., 32(8), 2133-2144.

Alt, C. & Duvefelt, K. & Franzén, B. & Yang, Y. & Engelhardt, B., 2003, „Gene and protein expression profiling of cerebral microvessels in experimental autoimmune encephalomyelitis in C57Bl/6 and SJL mice", zur Publikation eingereicht.

„Abstract"-Publikationen:

Alt, C. & Engelhardt, B., „Expression of ELC (CCL19) and SLC (CCL21) at the

blood-brain barrier during experimental autoimmune encephalomyelitis suggest their involvement in lymphocyte recruitment into the central nervous system", Immunobiology, 204(1–2), 32, zum Postervortrag ausgewählt auf der 32. Jahrestagung der Deutschen Gesellschaft für Immunologie in Dresden vom 26. – 29. September 2001.

Alt, C. & Engelhardt, B., „Distinct expression patterns of chemokines in the CNS during active experimental autoimmune encephalomyelitis", Immunobiology, 206(1–3), 157, zum Postervortrag ausgewählt auf der 33. Jahrestagung der Deutschen Gesellschaft für Immunologie in Marburg vom 25. – 28. September 2002.

Vorträge und Poster:

Alt, C. & Engelhardt, B., „Involvement of chemokines in the recruitment of T cells across the endothelial blood-brain barrier", präsentiert auf dem 8th Symposium of the Adhesion Workshop / German Society for Immunology in Münster vom 17. – 18. Juli 2000.

Alt, C. & Laschinger, M. & Engelhardt, B., „Expression of the lymphoid chemokines CCL19 (ELC) and CCL21 (SLC) at the blood-brain barrier suggests their involvement in G-protein-dependent lymphocyte recruitment into the CNS during experimental autoimmune encephalomyelitis", präsentiert auf der Gordon Research Conference on Chemotactic Cytokines in South Hadley, MA, USA vom 7. – 12. Juli 2002.

Alt, C. & Duvefelt, K. & Franzen, B. & Engelhardt, B., „Gene and protein expression profiling of blood-brain barrier microvessels during active experimental autoimmune encephalomyelitis in C57Bl/6 and SJL/N mice", zum Postervortrag ausgewählt auf der 5th International Conference of Cerebral Vascular Biology in Amarillo, TX, USA vom 15. – 19. Juni 2003.

Alt, C. & Duvefelt, K. & Franzen, B. & Engelhardt, B., „Gene and protein expression profiling of cerebral microvessels during active experimental autoimmune encephalomyelitis in C57Bl/6 and SJL/N mice", zum Postervortrag ausgewählt auf dem 3rd Symposium on Vascular Biology in Münster vom 08. - 10. Oktober 2003.

Södel, den 10.12.2003   Carsten Alt